USC Viterbi
School of Engineering
Department of Biomedical Engineering

Image Processing and Informatics Laboratory (IPILab)

Annual Progress Report

February 2013

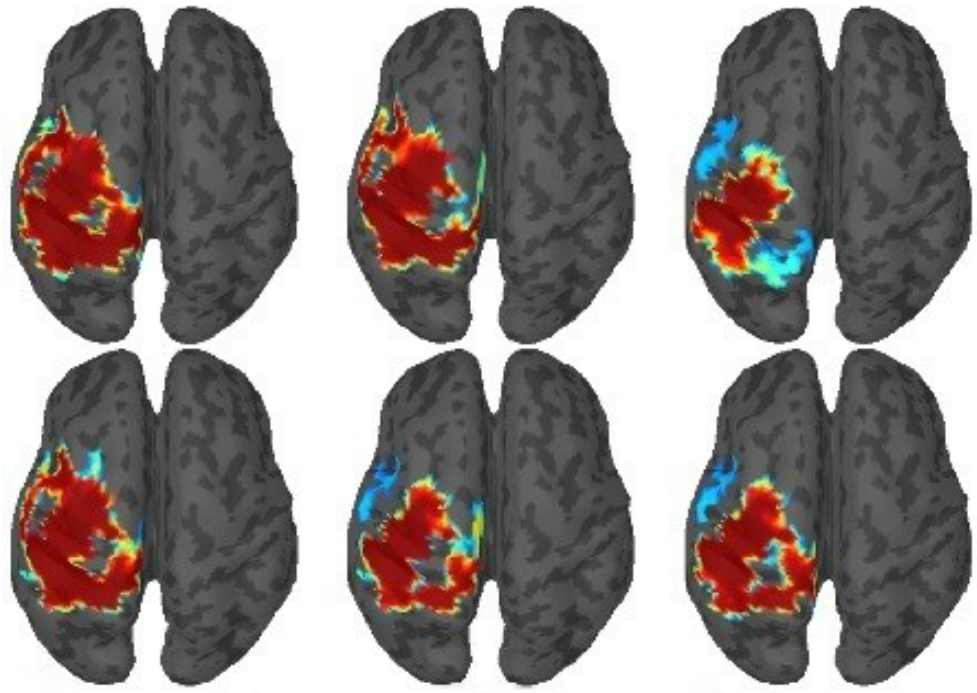

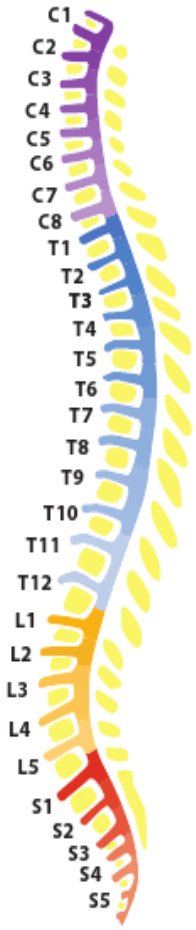

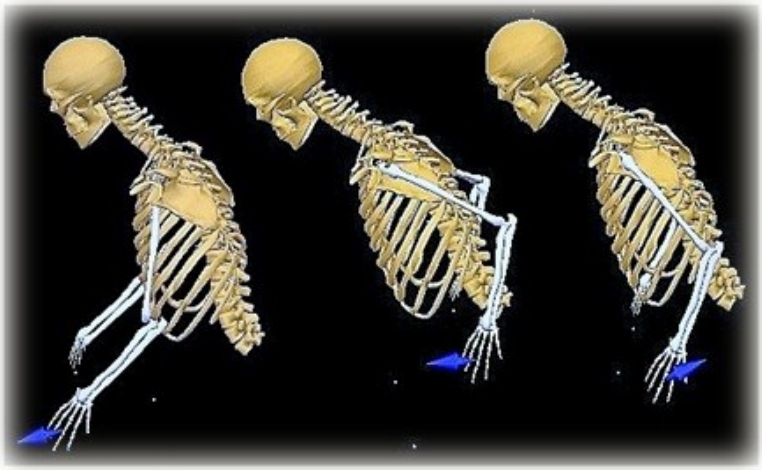

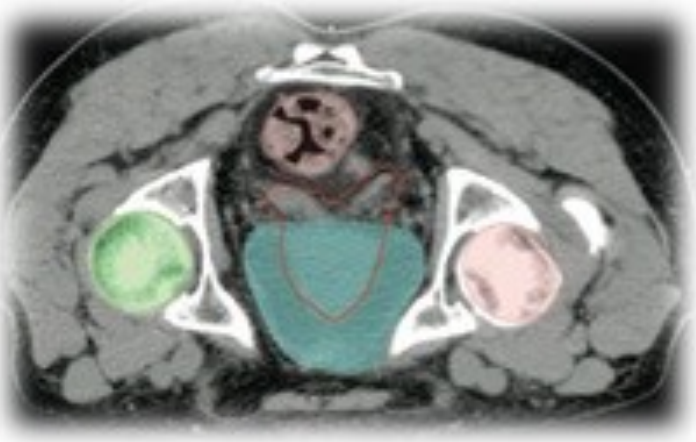

Department of Biomedical Engineering, Viterbi School of Engineering
734 W. Adams Blvd. KER 302, Los Angeles, California 90089-7725, 213-743-1720 (Office), 213-743-2962 (Fax)

DEPARTMENT OF BIOMEDICAL ENGINEERING
VITERBI SCHOOL OF ENGINEERING
UNIVERSITY OF SOUTHERN CALIFORNIA

2013 Annual Report

Image Processing and Informatics Laboratory

734 West Adams Blvd, Los Angeles, CA 90089. Tel: (213) 743-2520 Fax: (213) 743-2962

SUMMARY

The Image Processing and Informatics Laboratory (IPILab), located at the Annenberg Research Park at 734 W. Adams Blvd. in the Kerckhoff Hall near the University Park Campus, continues another year of research and collaboration during these difficult economic times with a challenging transition towards new frontier areas of research in imaging informatics. During this time, IPILab has continued its vision and course to provide a bridge of collaboration between the two schools - Viterbi School of Engineering and the Keck School of Medicine - establishing new collaborations and research funding and hosting visitors interested in Imaging Informatics training and research. Some of the accomplishments and highlights for this year are detailed:

1. Education and Training

One of IPILab's main pillars is providing education and training in imaging informatics research at every level from undergraduate students to working professionals. This last year, the T32 Training Grant from the National Institute of Biomedical Imaging and Bioengineering (NIBIB), National Institutes of Health (NIH), DHHS entitled: "Biomedical Imaging Informatics Training Program" effective September, 1, 2005 – August 31, 2010, totaling about US$1.6 million has come to an end. However, even though the lab has been going through major transitions previous trainees and current lab members continue to receive recognition in national conferences and proceedings papers. Some of the past IPILab trainees milestones include 1) Jorge Documet, PhD who completed his Postdoctoral Fellow and has taken a Software Development position in the Health Informatics industry, 2) Jerry Loo, MD, who is a first year Radiology resident at USC, 3) Jasper Lee, PhD, who also has taken a senior engineering position in the CAD/ Imaging Informatics industry, 4) Anh Le, PhD, who is in her third-year Oncology residency program at the University of Pittsburgh Medical Center (UPMC), and 5) Syed Ashrafulla who graduated from University of Texas and is currently a PhD EE student in the Viterbi School of Engineering and will advance to PhD candidacy this coming Spring.

As usual, summer activities are the height of our academic year for recruiting new young blood into the IPILab for research collaborations. IPILab welcomed two undergraduate research trainees. The USC Summer Undergraduate Research Program continues to fund our efforts to recruit and foster bright young undergraduate students searching for future academic research directions. From the clinical side, IPILab had three additional 4th year USC Medical School students participate in an imaging informatics clinical rotation providing a balanced research environment of future engineers and clinicians. Finally, we had three MS graduate students from the BME program who participated in research training activities and has since found professional positions.

Two former Provost Fellow PhD students Ruchi Deshpande and Ximing Wang as well as former T32 trainee Kevin Ma - all from the BME graduate program - have continued their PhD research with IPILab. A new PhD student Sneha Verma, who received her Master's Degree from Johns Hopkins University, has joined the IPILab in her first year.

2. Research Projects

As previously mentioned, we have continued in our areas of Medical Imaging Informatics research with a transition to new frontier areas of research in addition to previous Radiology-based research: 1) A Multimedia Electronic Patient Record (ePR) framework to manage various types of Image-Assisted (IA) Surgeries; 2) The development of an eFolder System for Multiple Sclerosis Patients; along with new areas including 3) A multimedia ePR system to support the large-scale OPTT-RERC "Rehabilitation Engineering Research Center for Technologies for Successful Aging with Disability" multi-media data; 5) The development of imaging informatics tools for large-scale stroke rehab clinical trials (eg, Interdisciplinary Comprehensive Arm Rehabilitation Evaluations – ICARE); 6) Continued development of data mining of DICOM-RT objects in conventional radiation therapy of prostate cancer patients; 7) An ePR to provide decision support in evaluating does optimization in Stroke Rehabilitation (DOSE); 8) A multi-media system to support VA caregivers of Spinal Cord Injury Patients; and 9) An ePR-based system for Spinal Cord Injury patients for treating pain with Proton Therapy Radiosurgery. We enjoyed a successful RSNA conference in November 2012 with a total of 4 presentations. Some of the research work continues to be supported by extramural finds including NIH, DOE/NIDRR, VA, U.S. Army Medical Research and Materiel Command, and the private industry. We are continuing to transition to areas in Rehabilitative Science and Physical Therapy since multi-media data is utilized in the research field in addition to patient-related imaging informatics data.

3. Industrial Collaborations

In addition to extramural funding, IPILab has continued R & D collaborations with the private industry including but not limited to: Fujifilm, USA in the development of performer observer studies of 3D display for Mammogram Screening.

As described in the Table of Contents, this 2013 Annual Report includes materials related to the IPILab, IPILab R & D plans and current results, selected published and in-press peer-reviewed papers during the year, as well as preprints to appear in the *Proceedings of the International Society for Optical Engineering (SPIE) in Medical Imaging*, Orlando, FL, February 12-14, 2013.

Our research has been supported by:

- NIH/NIBIB Biomedical Imaging Informatics Training Grant T32 EB 00438
- NIH/NINDS/NICHD U01NS05625 (ICARE)
- NIH/NICHD R01HD065438 (DOSE)
- Optimizing Participation Through Technologies (OPTT) - RERC for Successful Aging with Disability, DOE/NIDRR, No. H133E080024
- VA Caregivers Project, VALB/LAREI No. 2135000
- VA SCI HCG IPA No. 54-4508-4361
- DOD/Loma Linda University Subcontract No. W81XWH-11-2-0151
- USC Undergraduate Research Award No. 22-1508-1030
- Fujifilm, USA
- MI^2, USA
- ImageNation, LLC, USA
- SurgMatix, USA

TABLE OF CONTENTS

SELECTED PEER REVIEW REPRINTS

IPILAB ENVIRONMENT AND COLLABORATIONS

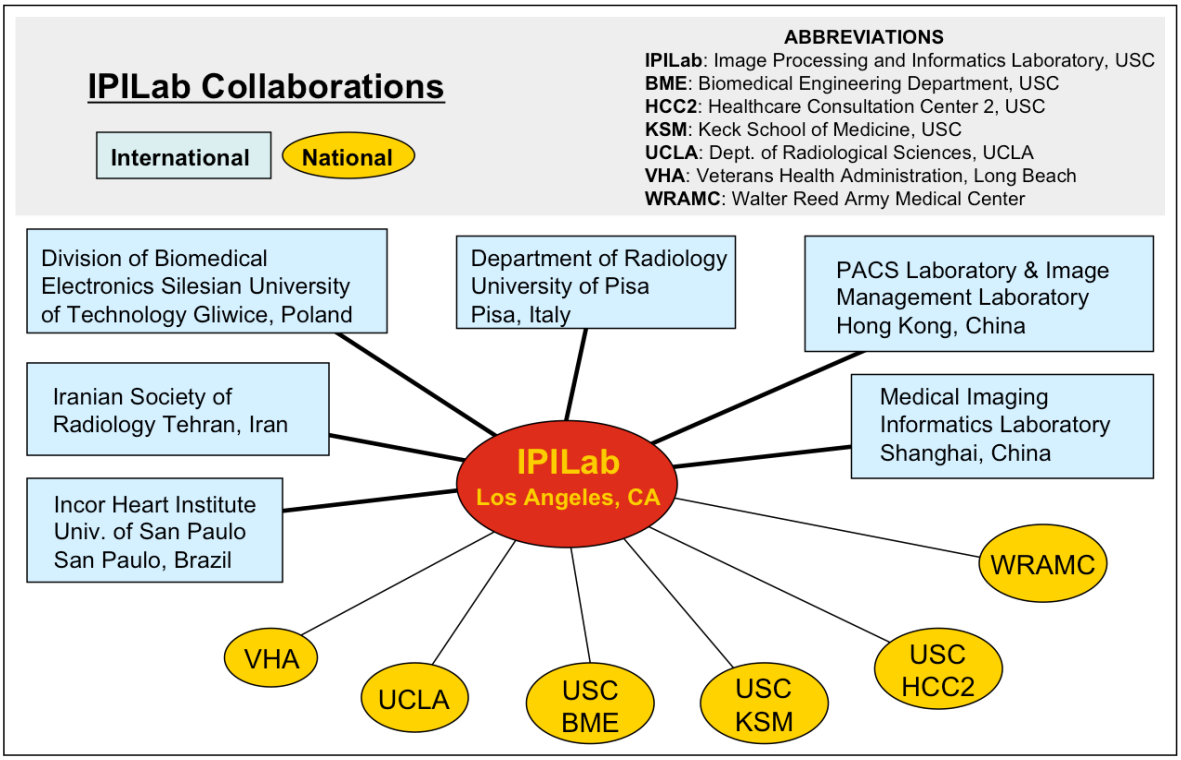

STAFF AND COLLABORATORS

Faculty and Administration	*Academic Collaborators*
Norberto M. Grzywacz, PhD Professor and Chairman, Department of Biomedical Engineering (BME)	**Carolee Winstein, PhD** Professor, Biokinesiology and Physical Therapy
Brent J. Liu, PhD Associate Professor of BME Director, IPILab	**Ewa Pietka, PhD, DSc** Professor, Technical University of Silesia, Poland *Visiting Professor of Radiology*
H.K. Huang, DSc, FRCR (Hon.), FAIMBE Professor Emeritus of Radiology & BME	**Edward V. Grant, MD, FACR** Professor and Chairman, Department of Radiology
James Sayre, PhD Professor of Biostatistics and Radiological Science, UCLA *Consultant*	**Michael Khoo, PhD** Professor of BME, Co-PI, NIBIB Training Grant
Heinz U. Lemke, Professor Technical University Berlin	**Sophia Chun, MD** Chief, SCI at Veterans Health Administration
Jianguo Zhang, PhD Professor, Shanghai Institute of Technical Physics, The Chinese Academy of Science Visiting Professor of Radiology	**James Slater, MD** Radiation Medicine, Loma Linda University
Maria YY Law, MPhil, BRS, PhD Consultant (Medical Imaging and Radiotherapy) Hong Kong Sanatorium and Hospital Professor of Radiation Therapy Tung Wah College, Hong Kong Visiting Associate Professor of Radiology at USC	**Lilyana Amezcua, MD** Assistant Professor of Neurology, Keck Hospital of USC
	Meng Law, MD, MBBS, FRACR Director of Neuroradiology, Keck Hospital of USC
	Alexander Lerner, MD Visiting Assistant Professor of Clinical Radiology, Keck Hospital of USC
	Jorge Documet, PhD Consultant, Senior Software Engineer ,Zynx Health
Postdoctoral and Visiting Fellows	
Paymann Moin, MD Radiologist, Advanced Imaging Center, Valencia, CA	**Richard Lee, MD** Radiology Resident
Anh Le, PhD Oncology Resident, University of Pittsburgh Medical Center	**Jasper Lee, PhD** R&D Manager, SCImage, Los Altos
Ali Maziad, MD Spine Deformity Fellow at Hospital for Special Surgery	**James Fernandez, MD** Radiology Resident
Marco A. Gutierrez, PhD Invited Professor, Heart Institute of University of San Paulo	**Kathleen Garrison, PhD** Associate Post-Doctoral Fellow Department of Psychiatry, Yale University
Graduate Student Assistants	
Kevin Ma, MS	**Sneha Verma, MS**
Ruchi Deshpande, MS	**Nakul Reddy, MD**
Ximing Wang, MS	**Yi Qin, MS**
Syed Ashrafulla, BS	**Longsheng Wang, MS**
Undergraduate Students	
Jeffrey Zhang	**Alyssa Zhou**

IPILAB WEBSITE

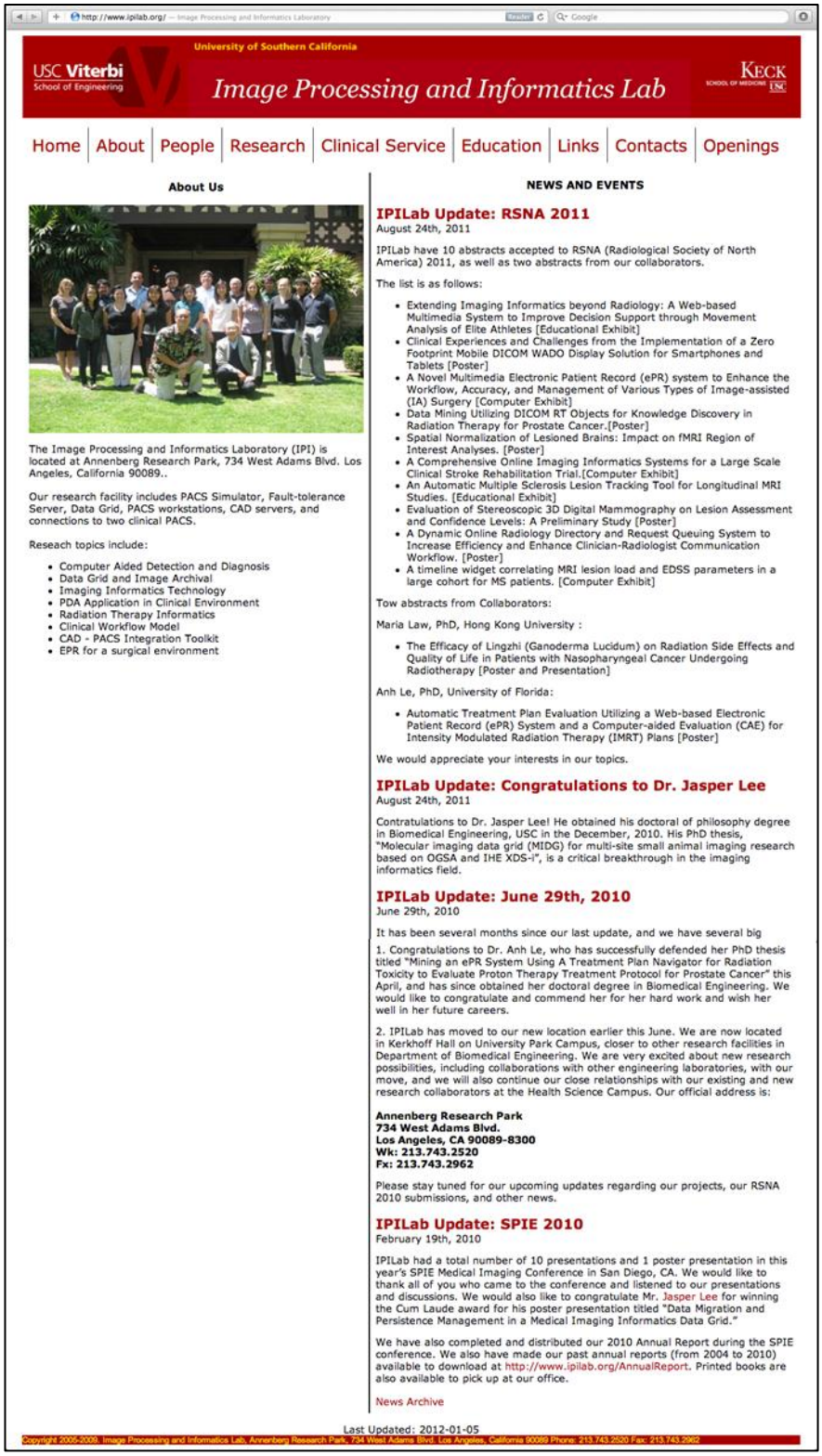

http://www.ipilab.org/ — Image Processing and Informatics Laboratory

University of Southern California

USC Viterbi School of Engineering

Image Processing and Informatics Lab

KECK SCHOOL OF MEDICINE USC

Home | About | People | Research | Clinical Service | Education | Links | Contacts | Openings

About Us

The Image Processing and Informatics Laboratory (IPI) is located at Annenberg Research Park, 734 West Adams Blvd. Los Angeles, California 90089..

Our research facility includes PACS Simulator, Fault-tolerance Server, Data Grid, PACS workstations, CAD servers, and connections to two clinical PACS.

Reseach topics include:

- Computer Aided Detection and Diagnosis
- Data Grid and Image Archival
- Imaging Informatics Technology
- PDA Application in Clinical Environment
- Radiation Therapy Informatics
- Clinical Workflow Model
- CAD - PACS Integration Toolkit
- EPR for a surgical environment

NEWS AND EVENTS

IPILab Update: RSNA 2011
August 24th, 2011

IPILab have 10 abstracts accepted to RSNA (Radiological Society of North America) 2011, as well as two abstracts from our collaborators.

The list is as follows:

- Extending Imaging Informatics beyond Radiology: A Web-based Multimedia System to Improve Decision Support through Movement Analysis of Elite Athletes [Educational Exhibit]
- Clinical Experiences and Challenges from the Implementation of a Zero Footprint Mobile DICOM WADO Display Solution for Smartphones and Tablets [Poster]
- A Novel Multimedia Electronic Patient Record (ePR) system to Enhance the Workflow, Accuracy, and Management of Various Types of Image-assisted (IA) Surgery [Computer Exhibit]
- Data Mining Utilizing DICOM RT Objects for Knowledge Discovery in Radiation Therapy for Prostate Cancer.[Poster]
- Spatial Normalization of Lesioned Brains: Impact on fMRI Region of Interest Analyses. [Poster]
- A Comprehensive Online Imaging Informatics Systems for a Large Scale Clinical Stroke Rehabilitation Trial.[Computer Exhibit]
- An Automatic Multiple Sclerosis Lesion Tracking Tool for Longitudinal MRI Studies. [Educational Exhibit]
- Evaluation of Stereoscopic 3D Digital Mammography on Lesion Assessment and Confidence Levels: A Preliminary Study [Poster]
- A Dynamic Online Radiology Directory and Request Queuing System to Increase Efficiency and Enhance Clinician-Radiologist Communication Workflow. [Poster]
- A timeline widget correlating MRI lesion load and EDSS parameters in a large cohort for MS patients. [Computer Exhibit]

Tow abstracts from Collaborators:

Maria Law, PhD, Hong Kong University :

- The Efficacy of Lingzhi (Ganoderma Lucidum) on Radiation Side Effects and Quality of Life in Patients with Nasopharyngeal Cancer Undergoing Radiotherapy [Poster and Presentation]

Anh Le, PhD, University of Florida:

- Automatic Treatment Plan Evaluation Utilizing a Web-based Electronic Patient Record (ePR) System and a Computer-aided Evaluation (CAE) for Intensity Modulated Radiation Therapy (IMRT) Plans [Poster]

We would appreciate your interests in our topics.

IPILab Update: Congratulations to Dr. Jasper Lee
August 24th, 2011

Contratulations to Dr. Jasper Lee! He obtained his doctoral of philosophy degree in Biomedical Engineering, USC in the December, 2010. His PhD thesis, "Molecular imaging data grid (MIDG) for multi-site small animal imaging research based on OGSA and IHE XDS-i", is a critical breakthrough in the imaging informatics field.

IPILab Update: June 29th, 2010
June 29th, 2010

It has been several months since our last update, and we have several big

1. Congratulations to Dr. Anh Le, who has successfully defended her PhD thesis titled "Mining an ePR System Using A Treatment Plan Navigator for Radiation Toxicity to Evaluate Proton Therapy Treatment Protocol for Prostate Cancer" this April, and has since obtained her doctoral degree in Biomedical Engineering. We would like to congratulate and commend her for her hard work and wish her well in her future careers.

2. IPILab has moved to our new location earlier this June. We are now located in Kerkhoff Hall on University Park Campus, closer to other research facilities in Department of Biomedical Engineering. We are very excited about new research possibilities, including collaborations with other engineering laboratories, with our move, and we will also continue our close relationships with our existing and new research collaborators at the Health Science Campus. Our official address is:

Annenberg Research Park
734 West Adams Blvd.
Los Angeles, CA 90089-8300
Wk: 213.743.2520
Fx: 213.743.2962

Please stay tuned for our upcoming updates regarding our projects, our RSNA 2010 submissions, and other news.

IPILab Update: SPIE 2010
February 19th, 2010

IPILab had a total number of 10 presentations and 1 poster presentation in this year's SPIE Medical Imaging Conference in San Diego, CA. We would like to thank all of you who came to the conference and listened to our presentations and discussions. We would also like to congratulate Mr. Jasper Lee for winning the Cum Laude award for his poster presentation titled "Data Migration and Persistence Management in a Medical Imaging Informatics Data Grid."

We have also completed and distributed our 2010 Annual Report during the SPIE conference. We also have made our past annual reports (from 2004 to 2010) available to download at http://www.ipilab.org/AnnualReport. Printed books are also available to pick up at our office.

News Archive

Last Updated: 2012-01-05

RSNA 2012 PAMPHLET AND POSTERS

LL-INE1263: Extending Imaging Informatics to Rehabilitation Research: A Multimedia Electronic Patient Record System (ePR) for a Randomized Controlled Trial (RCT) of Rehabilitation Dose Optimization after Stroke

X Wang, MS, Los Angeles, CA; C Martinez; Y Qin, MS; S K Verma, MS; H Li; C J Winstein, PhD; et al.

PURPOSE

Imaging studies have been used widely across the healthcare enterprise including imaging-based clinical trials. Currently, clinical trials in rehabilitation usually include a large volume of clinical treatment data, questionnaires, and more recently, imaging studies such as MRI, CT and TMS (transcranial magnetic stimulation). This exhibit aims to demonstrate a web-based multimedia ePR system for data entry and data management of randomized clinical trial. The ePR system also serves as the platform for development of mathematical models for rehabilitation dose optimization.

CONTENT ORGANIZATION

1. Background and challenges encountered in rehabilitation trials.
2. Workflow analysis to demonstrate how the system improves the efficiency of the phase I randomized controlled trial.
3. Demonstration of the system features, including ipad/iphone-based questionnaire data entry, treatment data and laboratory test data recording, imaging data management and sharing, and a web-based zero-footprint DICOM viewer.
4. Graphical user interface of system in mobile devices and PC.

SUMMARY

This exhibit demonstrates an imaging informatics-based multimedia ePR system for RCTs in stroke rehabilitation. The system provides a solution for managing behavioral questionnaires, imaging studies such as MRI, TMS, videos, treatment recording and laboratory test data.

Lakeside Learning Center

Image Processing and Informatics Laboratory

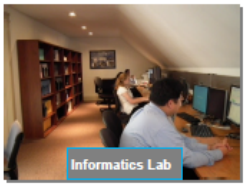

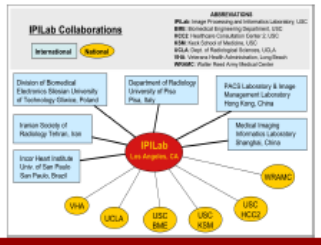

USC Viterbi School of Engineering
734 W Adams Blvd
Los Angeles, CA 90089
Tel: (213) 743 2520
Fax: (213) 743 2962
http://www.ipilab.org

USC University of Southern California

Image Processing and Informatics Laboratory

Department of Biomedical Engineering,
Viterbi School of Engineering

RSNA 2012 Patients First

Education Exhibits & Presentations

November 25 – November 30 2012
McCormick Place, Chicago, Illinois

Keck Medical Center of USC

USC Viterbi School of Engineering
734 W Adams Blvd
Los Angeles, CA 90089
Tel: (213) 743 2520
Fax: (213) 743 2962
http://www.ipilab.org

Faculty and Administration	*Academic Collaborators*
Norberto M. Grzywacz, PhD Professor and Chairman, Department of Biomedical Engineering	**Carolee Winstein, PhD** Professor, Biokinesiology and Physical Therapy
Brent J. Liu, PhD Associate Professor of BME Director, IPILab	**Ewa Pietka, PhD, DSc** Professor, Technical University of Silesia, Poland *Visiting Professor of Radiology*
H.K. Huang, DSc, FRCR (Hon.), FAIBE Professor Emeritus of Radiology & BME	**Edward V. Grant, MD, FACR** Professor and Chairman, Department of Radiology
James Sayre, PhD Professor of Biostatistics and Radiological Science, UCLA *Consultant*	**Michael Khoo, PhD** Professor of BME, Co-PI, NIBIB Training Grant
Cammy Huang, PhD Director of Scientific Outreach, Wallenberg Global Learning Network, Wallenberg Hall, Stanford University *Consultant*	**Sophia Chun, MD** Chief, SCI at Veterans Health Administration
Heinz U. Lemke, Professor Technical University Berlin	**James Slater, MD** Radiation Medicine, Loma Linda University
Angelica Virgen Administrative Manager	**Lilyana Amezcua, MD** Assistant Professor of Neurology, Keck Hospital of USC
Jianguo Zhang, PhD Professor, Shanghai Institute of Technical Physics, The Chinese Academy of Science *Visiting Professor of Radiology*	**Meng Law, MD, MBBS, FRACR** Director of Neuroradiology, Keck Hospital of USC
Maria YY Law, MPhil, BRS, PhD Consultant (Medical Imaging and Radiotherapy) Hong Kong Sanatorium and Hospital *Visiting Associate Professor of Radiology*	**Alexander Lerner, MD** Visiting Assistant Professor of Clinical Radiology, Keck Hospital of USC
	Jorge Documet, PhD Consultant, Senior Software Engineer, Zytrx Health
Postdoctoral and Visiting Fellows	
Paymann Moin, MD Radiologist, Advanced Imaging Center, Valencia, CA	**Marco A. Gutierrez, PhD** Invited Professor, Heart Institute of University of San Paulo
Tao Chan, MD, PhD Asst. Professor, Hong Kong Polytechnic University	**Richard Lee, MD** Radiology Resident
Anh Le, PhD Oncology Resident, University of Pittsburgh Medical Center	**Jasper Lee, PhD** R&D Manager, SCImage, Los Altos
Kathleen Garrison, PhD Associate Post Doctoral Fellow Department of Psychiatry, Yale University	**Ali Maziad, MD** Spine Surgery Fellow at Boston University Medical Center
	James Fernandez, MD Radiology Resident
Graduate Student Assistants	
Kevin Ma, MS **Ruchi Deshpande, MS** **Ximing Wang, BS** **Syed Ashrafulla, BS**	**Sneha Verma, MS** **Nakul Reddy, MD** **Yi Qin, MS** **Longsheng Wang, MS**
Undergraduate Students	
Jeffrey Zhang	**Alyssa Zhou**

LL-INE1239-THB: Development of an Imaging Informatics Infrastructure to Support Collaborative Tools in a Large Scale Phase III Clinical Rehabilitation Trial

X Wang, MS, Los Angeles, CA; B J Liu, PhD; J Mao; N Reddy; H Li; C J Winstein, PhD

BACKGROUND

At RSNA 2011, we demonstrated an imaging informatics system for a large scale stroke clinical rehabilitation trial. With 7 clinical sites across the country and over 500 imaging studies involved, the clinical trial, Interdisciplinary Comprehensive Arm Rehabilitation Evaluation (ICARE), encounters challenges in sharing images and collaborations between different sites. The system presented features: an image uploader, a zero foot-print DICOM viewer with lesion quantifying tools, a studies anonymizer, and forms for collecting quantification result. To further facilitate the multi-site collaboration, we aim to develop a tele-conference plug-in, a web-based publishing platform, and a structured reporting tool for storing rehabilitation information based on the previous system.

EVALUATION

The web-based conference room tool provides a solution for researchers from different sites to hold a tele-conference. Key points in the conference can be logged. The publishing platform allows users to make announcements and publish discussion results. Users can use the platform to discuss research progress, share information, and create meeting agendas. The structured reporting tool utilizes the xml format to store the patient-oriented information, such as image annotations, lesion quantification results, and rehabilitation test data (eg. Fugl-meyer scores, Wolf Motor Function Test). The performance of the new system will be evaluated by 7 clinical sites in ICARE trial.

DISCUSSION

The previous evaluation by ICARE trial expert users has demonstrated that the system improved the efficiency in managing imaging data. However, the collaboration could benefit with additional features. The conference room plug-in enables users to communicate and analyze images at the same time across multiple sites. The structured reporting tool extends the structured reporting concept into the rehabilitation field. Using this tool, the efficiency of generating the subject-based report for the clinical trial is improved.

CONCLUSION

We have developed new functions (a conference room, a publishing platform and a structured reporting tool) based on the previous system to facilitate the multi-site collaboration and enhance the research.

Lakeside Learning Center: 12:15-1:15pm (11/29)

LL-INE1240-SUB: Bridging the gap between post-processing innovations and real-world clinical use: The utilization of an eFolder with embedded IHE workflow profile for MS clinical trials.

K C Ma, Los Angeles, CA; N Reddy; L Amezcua MD; B J Liu, PhD; Ruchi Deshpande, MS; S K Verma, MS

BACKGROUND

Last year at RSNA we presented a multiple sclerosis (MS) eFolder as an integrated imaging-informatics based system to provide several functionalities to both clinical and research environments. The eFolder system combines patients' clinical data, radiological images and computer-aided lesion detection and quantification results to aid in longitudinal tracking, data mining, decision support, and other clinical and research needs. To demonstrate how this system can be integrated in an existing imaging environment such as a large-scale multi-site MS clinical trial, we present a system simulation environment to streamline imaging and clinical data flow with post processing (CAD) steps by following DICOM standards and IHE initiatives. The MS eFolder workflow stores clinical and imaging data, provides CAD post processing algorithm and data storage, and a web-based graphical user interface (GUI) to view clinical trial data and monitor workflow. The integrated system workflow is designed according to IHE post processing workflow profile to further realize MS eFolder's use in a real-world situation.

EVALUATION

The system contains components outlined in the IHE post-processing workflow. The imaging modality simulator sends a set of MRI brain DICOM images containing MS lesions into the eFolder system. The system provides an imaging archive to store the images. The images are then sent to the CAD workstation to perform post-processing, and the completed DICOM-compliant report is then stored in the archive. A web-based GUI is used to query/retrieve and display the imaging data, post-processing results, and patient's data stored in the patient record. The eFolder GUI also monitors data flow of patients' images to ensure delivery of data among each component in the eFolder.

DISCUSSION

We successfully demonstrate using IHE's workflow profile in a real-world clinical environment using an imaging informatics-based MS eFolder. The integrated workflow helps data managing, data mining, viewing and storing imaging and other related data, and perform a quantitative analysis that otherwise not available without post-processing workflow.

CONCLUSION

The MS eFolder provides patient data storage, data management, and quantitative data analysis. The system is integrated with a real-world clinical environment according to the IHE post-processing workflow profile. The success of the integration both demonstrates the usefulness of the eFolder system and provides an example of how to use such system in a real-world situation via IHE guidelines.

Lakeside Learning Center: 12:30-1:30pm (11/05)

LL-INE1267: Challenges and Lessons learned in normalizing pathologic brains in MS and stroke studies with clinical image scanning protocols

K C Ma, Los Angeles, CA; X Wang, MS; N Reddy; B J Liu, PhD

PURPOSE

Brain normalization is a critical step in performing post-processing analysis of brain MRI scans for both clinical and research uses. For lesion identification, quantitative data and location data are key factors in the current medical evaluation process. Brain normalization techniques are developed via carefully-selected training cases under high-resolution scanning protocols. Accuracy of normalization results depends on quality and resolution of the scans. Different scanner manufacturers and protocols also create variability in quality of the scans. Brian normalization becomes difficult to perform for MR studies acquired via traditional clinical scanning protocols because their resolutions are generally larger, and quality of images can sometimes be compromised. In research, brain images scanned via research protocols are costly to obtain, and oftentimes studies are collected retroactively in existing clinical patient database. This study explores applying several different brain normalization techniques to stroke and multiple sclerosis patients' clinical scans. The results of this study aims to teach users how to apply brain normalization to clinical studies, as well as challenges faced in the application and how to overcome those challenges.

CONTENT ORGANIZATION

1. Introduction of lesioned brain studies and importance of brain normalization
2. Application of brain normalization techniques
3. Results from brain normalization methods
4. Challenges and lessons learned in the applications

SUMMARY

Brain normalization is an important step in computer-aided detection and diagnosis (CAD) applications. There are inherent challenges when applying brain normalization techniques to lesioned brains in MRI clinical studies. This study explores different brain normalization techniques and lists all challenges and lessons learned in the process. These results may lead to development or refinement of a brain normalization technique robust enough for use in both clinical and research studies and the challenges associated with multiple variations in imaging scanning protocols.

Lakeside Learning Center

USC

Image Processing and Informatics Lab

Challenges and lessons learned in normalizing pathological brains in MS and stroke studies with clinical image scanning protocols

Kevin Ma, MS[1]; Nakul Reddy, BS[2]; Yi Qin, MS[1]; Longsheng Wang, BS[1], Ximing Wang, MS[1]; Brent Liu, PhD[1]
1 – Department of Biomedical Engineering, Viterbi School of Engineering, University of Southern California, Los Angeles, CA;
2- Keck School of Medicine, University of Southern California, Los Angeles, CA;

INTRODUCTION

Brain normalization is a critical step in performing post-processing analysis of brain MRI scans for both clinical and research uses. For lesion identification, quantitative data and location data are key factors in the current medical evaluation process. Brain normalization techniques are developed via carefully-selected training cases under high-resolution scanning protocols. Accuracy of normalization results depends on quality and resolution of the scans. Different scanner manufacturers and protocols also create variability in quality of the scans. Brain normalization becomes difficult to perform for MR studies acquired via traditional clinical scanning protocols because their resolutions are generally larger, and quality of images can sometimes be compromised. In research, brain images scanned via research protocols are costly to obtain, and oftentimes studies are collected retroactively in existing clinical patient database.

While developing imaging informatics-based electronic patient record (ePR) systems for neurological applications such as multiple sclerosis and stroke rehabilitation, brain lesion profiles become essential in increasing data mining capabilities of such systems. Once brain normalization is completed and brain images are segmented into anatomical subsections, users may, for example ,look up patient studies with lesions located in a particular sub-region, thus making the ePR system more useful in both clinical and research environments.

This study explores applying several different brain normalization techniques to stroke and multiple sclerosis patients' clinical scans.

DATA COLLECTION

For multiple sclerosis studies, 72 pathological imaging studies have been collected retrospectively at USC Academic Medical Center from 2008 to 2012. The studies are brain MR images . The scanning protocol for the clinical studies varies depends on the date and location of when the studies were acquired. The brain MR studies are either 5mm slices with 1.5mm gaps, or 3mm with no gaps.

Stroke studies are collected from a large-scale, 7-site clinical trial network over the continental United States. The brain MR and CT images are scanned via local scanning protocols, and thus are not uniform. The diversity in collected data aims to demonstrate how image data may vary from different sites and illustrate challenges to create a reliable brain normalization technique for the data variances.

METHOD 1: BrainSuite for Subregion Identification

An often-used software package for brain analysis in the research field is BrainSuite. Developed by Laboratory of Neuro Imaging (LONI) at UCLA, BrainSuite (http://www.loni.ucla.edu/Software/BrainSuite) is an open-source software designed for human brain MRI analysis. We started off by evaluating how BrainSuite would perform on our images scanned via clinical protocols, rather than research protocols. Figure 1 shows the brain mask segmentation results on a T1 axial series with default parameters in BrainSuite, and Figure 2 shows the brain mask with manually-adjusted parameters.

In the next step, we completed the cerebrum labeling and the final outcome is computed after topological corrections. Figures 3 and 4 shows the results using BrainSuite.

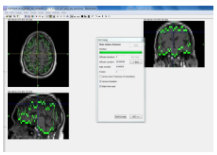

Figure 1
Screenshot of BrainSuite extracting brain mask using default settings on clinical data

Figure 2
Screenshot of BrainSuite extracting brain mask using manually-adjusted settings on clinical data

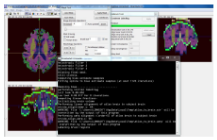

Figure 3
Process and results of cerebrum and subregional labeling

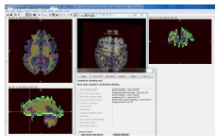

Figure 4
Final result after topological corrections

METHOD 2: BrainSuite with Affine Transform

BrainSuite was able to segment T1 MR brain into subregional labels, thus achieving our original goal of being able to characterize lesion locations in anatomical space. However, the software package itself does not perform spatial warping. Thus, to achieve spatial normalization, we performed affine transform algorithm in MATLAB. We warped the segmented brain matter and label space from BrainSuite and spatially normalized to the Talairach brain template. Figures 5 and 6 displays the results.

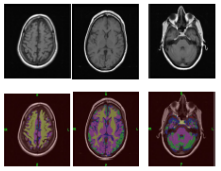

Figure 5
Top row: Original T1 brain images
Bottom row: Segmentation results from BrainSuite

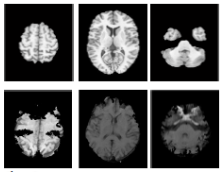

Figure 6
Top row: Talairach template, segmented by BrainSuite
Bottom Row: the same study from figure 5, normalized to Talairach template via affine transformation

METHOD 3: Brain warping using Statistical Parametric Mapping

The third methodology that was investigated is to use the Statistical Parametric Mapping (SPM) package in MATLAB to develop a standalone software to perform spatial warping of the brain to compare normalization results with Method 2.

The normalization feature in the Statistical Parametric Mapping package (version 8), SPM8 (http://www.fil.ion.ucl.ac.uk/spm) was used to coregister T1 MRI images to a template derived from the ICBM/MNI atlas. Then, as per package parameters, nonlinear deformations using a discrete cosine transform basis were applied (in 16 iterations) until a local minimum in the alignment cost function was achieved. The cost function used a normalized mutual information technique (as described in Friston et al). The resulting normalization parameters were applied with Gaussian smoothing and saved in NIFTI format. Figures 7 and 8 displays results from SPM8-based normalization. While Figure 7 shows good normalization results, Figure 8 shows a misalignment in the sagittal view.

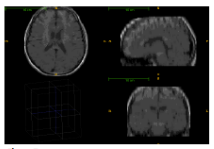

Figure 7
An example of SPM8-based normalization showing good alignment, displayed by ITK-SNAP

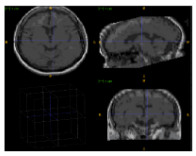

Figure 8
An example of SPM8-based normalization showing misalignment, displayed by ITK-SNAP

CHALLENGES AND CONCLUSIONS

1. Clinical studies usually have fewer slices than research studies which can lead to really low resolution in sagittal and coronal planes after reconstruction from axial planes (Most clinical studies are done in axial planes.). BrainSuite is not designed for segmenting low resolution images. BrainSuite's manual segmentation functions can compensate for bad brain segmentation results. However, it can take 10 minutes to deal with one image which means only segmenting one study may require a few hours to be done. Brain masking using BrainSuite on clinical studies cuts into important brain matter needed for analysis. This led us to believe that BrainSuite is good for case-by-case analysis, but not for an automated analysis of volume of studies we have been collecting.
2. Using MATLAB, either combining with BrainSuite results or using SPM8, produced generally better results than using BrainSuite alone. SPM8-based normalization does not require brain masking and gives more accurate results similar to the affine transform results, however the results of spatial warping distorts image resolution and may affect post-processing analyses, such as identification of MS lesions.
3. Out of the three methods, BrainSuite with affine transform (Method 2) thus far is more automatic and offer the best results, because it includes subreqional segmentation and does not lose too much information in the warping process.
4. Future works of this project include accuracy assessment of our normalization results, to complete analysis on all of the studies we have collected, and to conclude on an automated normalization method integrated into our imaging informatics-based ePR systems.

REFERENCES

1. K.J. Friston, J. Ashburner, C.D. Frith, J.-B. Poline, J.D. Heather, and R.S.J. Frackowiak Spatial Registration and Normalization of Images. Human Brain Mapping 2:165-189(1995)
2. Shattuck DW and Leahy RM (2002) BrainSuite: An Automated Cortical Surface Identification Tool, Medical Image Analysis, 8(2):129-142.
3. Jimmy Shen, "Tools for NIfTI and ANALYZE image" downloaded from http://www.mathworks.com/matlabcentral/fileexchange/8797-tools-for-nifti-and-analyze-image/content/affine.m
4. Paul A. Yushkevich, Joseph Piven, Heather Cody Hazlett, Rachel Gimpel Smith, Sean Ho, James C. Gee, and Guido Gerig. User-guided 3D active contour segmentation of anatomical structures: Significantly improved efficiency and reliability.Neuroimage 2006 Jul 1;31(3):1116-28.

USC

Image Processing and Informatics Laboratory

Bridging the gap between post-processing innovations and real-world clinical use: The utilization of an eFolder with embedded IHE workflow profile for MS clinical trials

Kevin Ma, MS[1]; Ruchi Deshpande, MS[1]; Sneha Verma, BS[1]; Lilyana Amezcua, MD[2]; Brent Liu, PhD[1]

[1]Image Processing and Informatics Lab, Dept. of Biomedical Engineering, Viterbi School of Engineering, USC
[2]Dept. of Neurology, Keck School of Medicine, USC

Overview:

- Multiple Sclerosis eFolder is an imaging informatics based, disease-centric patient information system, combining patient data with imaging and automatic lesion detection and quantification system
- The system can be used for data repository, management, and data mining for large-scale imaging-based clinical trials
- The IHE post-processing workflow profile serves as a guideline for the eFolder's integration and deployment in a clinical environment

Learning Objectives:

- Observe how a web-based eFolder system can manage MS patient data and compute 3-D lesion volumes and profiles
- Observe how users can review patient data in the eFolder system through a web-based system
- Understand how an IHE post-processing integration workflow profile can be utilized by an eFolder system within a clinical environment
- Observe how a status tracking page can track the progress of a study within the IHE workflow

RSNA 2012 Patients First

USC

Image Processing and Informatics Laboratory

IHE Post-processing Workflow Diagram with MS eFolder

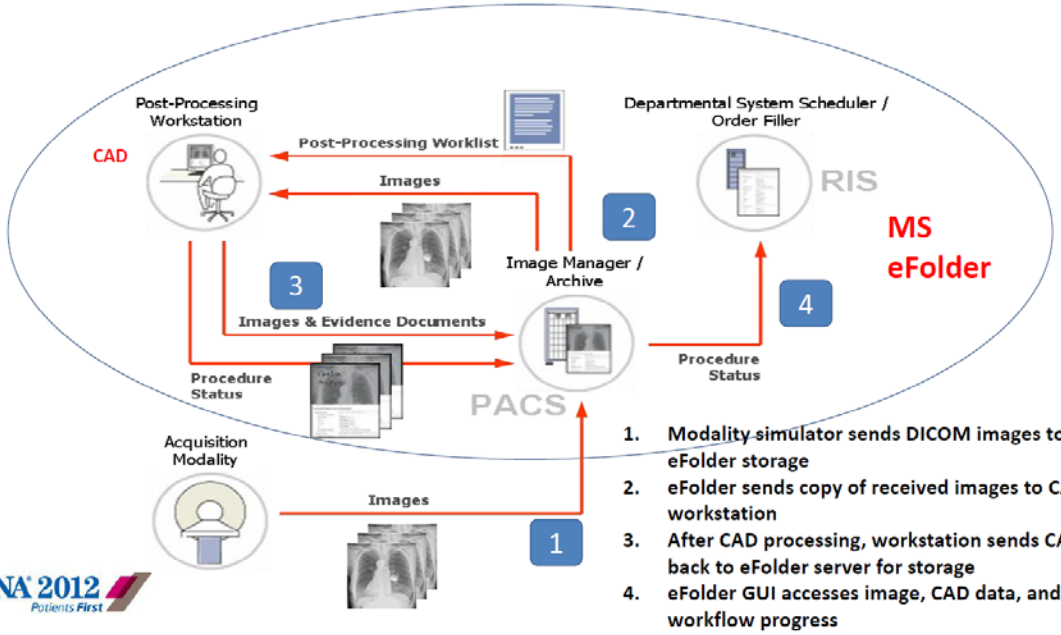

1. Modality simulator sends DICOM images to MS eFolder storage
2. eFolder sends copy of received images to CAD workstation
3. After CAD processing, workstation sends CAD results back to eFolder server for storage
4. eFolder GUI accesses image, CAD data, and monitors workflow progress

RSNA 2012 Patients First

USC

Extending Imaging Informatics to Rehabilitation Research: A Multimedia Electronic Patient Record System (ePR) for a Randomized Controlled Trial (RCT) of Rehabilitation Dose Optimization after Stroke

[1]X Wang, MS; [2]C Martinez, DPT; [1]Y Qin, MS; [1]S K Verma, MS; [1]H Li; [2]C J Winstein, PhD; [1]Brent Liu, PhD

[1] Image Processing and Informatics Lab, Department of Biomedical Engineering, Viterbi School of Engineering, University of Southern California, Los Angeles, CA [2]Biokinesiology and Physical Therapy, University of Southern California, Los Angeles, CA;

USC Viterbi School of Engineering

Background

Imaging studies have been used widely across the healthcare enterprise including imaging-based clinical trials. For example, clinical trials in rehabilitation usually include a large volume of clinical treatment data, questionnaires, and more recently, imaging studies such as MRI, CT and TMS (transcranial magnetic stimulation). This poster aims to present a web-based multimedia ePR system for data entry and data management of a randomized clinical trial – Dose Optimization Stroke Evaluation (DOSE) Clinical Trial.

DOSE Clinical Trial

Stroke is a major cause of adult disability in the United States and Europe. Even though some studies have been conducted with specific patient characteristics, there are few studies that focus on the effects of the dose of therapy as it relates to persistent gains in function and use of the arm and hand. Each patient post stroke has unique impairments and function, it is important to depart from a "one size fits all" approach to rehabilitation.

The objective of the DOSE Clinical Trial is to determine prospectively the optimal dose of therapy that will lead to further improvements of upper extremity use for individual patients who have had a stroke. The trial aims to recruit 60 subjects. Each subject is recruited, enrolled, and randomized into the trial and undergo 10 months of therapy A variety of data will be collected including:

- Rehabilitation evaluation and clinical test data in forms
- MRI studies with DTI
- Transcranial magnetic stimulation (TMS) sensor data

However, there are challenges involved with tracking each participant & collecting their related data in order to develop a tailored computational and predictive statistical model for decision support for an individual patient.

Why Imaging Informatics?

To help DOSE trial overcome these challenges, the imaging informatics approach can be extended to facilitate the DOSE clinical trial managing and analyzing data through the development of an imaging informatics-based ePR system. The system is patient-oriented which integrates the patient's imaging and informatics data into a single location. The leveraged skills and experience gained from Radiology-based imaging informatics include:

- Workflow Analysis
- Database & Data Model Design and Standards (eg, DICOM, HL7, IHE)
- Systems Integration
- Decision Support (eg, Computer Modeling, Knowledge, CAD, GUI Design)

Based on these skills, we have developed an ePR System tailored to the DOSE clinical trial to facilitate the knowledge discovery of optimal dose in stroke rehabilitation for the arm and hand.

Workflow Analysis

As shown in Figure 1, the workflow for each participant of the DOSE clinical trial has three major stages: enrollment, participation and follow-up. In addition to the clinical form data, imaging study data will also be collected. An MRI study with DTI as well as a TMS study will be acquired three times over the course of study participation as follows:

1) During the period of baseline testing but prior to the very first bout of therapy.
2) During the week of Post-Test Bout 3.
3) During the week of the 6 month follow up.

MRI and DTI will be performed on ALL participants, unless the individual is not eligible for MRI. The TMS study will be performed on a subset of TMS-eligible DOSE participants

System Description

As shown in Figure 2, the system is comprised of a database, a file storage system, a web server, a web based graphical user interface, and decision-support tools. The data mining & computational models are still under development. Data flow includes the demographic data, treatment records, screening and evaluation data, MRI studies and TMS data. The system can support PC, laptop and mobile devices or iPad.

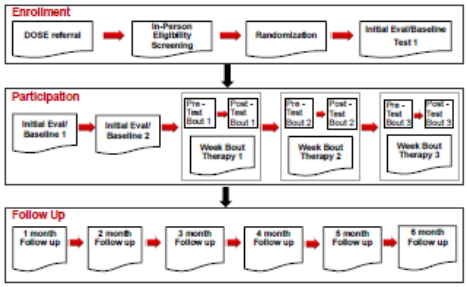

Figure 1 Workflow of the Dose Clinical Trial

User Groups for the System

User access to data within the system is tailored based on the user groups trial workflow and needs

Researcher User Group:
- Blinded from the Evaluation or Treatment Data
- Access only to Screening Data and Review of Data Collected

Evaluator User Group:
- Blinded from Treatment Data and Overall Data Analysis
- Access only to Evaluation Data and Uploading Imaging Studies, TMS Data, and other Sensor Data

Physical Therapist User Group:
- Blinded from Evaluation Data
- Access only to Treatment Data Collection

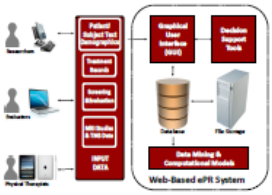

Figure 2 System architecture

System Features

- Screening forms collection
- Screening Decision Support: This tool automatically check all the forms and show a checklist of based on all enrollment requirements.
- Study progress status: The GUI shows the progress of the study.
- Treatment data form. Customized form for collecting treatment data.
- Imaging data uploader. The images uploaded will be parsed, anonymized and linked to the subject ID.
- Web-based Image Viewer with ROI, annotation and measurement tools.
- Database Backup tool. A one-click whole database backup tool, allows data recovery in future.
- Reports preview & generating tools. View online or download excel file of the data collected.

Results

The system has been developed at IPILab, USC and was implemented in the DOSE clinical trial. Figure 3 is a screenshot of the GUI application. The first arrow shows the timeline status with an overview progress of the trial for the specific trial subject. The second arrow shows the forms required in each stage. Figure 4 is an integrated DICOM viewer with measurement tools, ROI tools and annotation tools. The screen shot shows a measurement.

The system is currently used by the DOSE trial team including three user groups. 10 subjects have been enrolled in the trial, and 60 subjects enrollment are expected in the future 3 years. The screening and part of evaluation data of the enrolled subjects have been entered into the system. Therapy data is still in the progress of collecting.

To evaluate the system, we are collecting user's feedback through questionnaires and surveys. Table 1 shows areas of issues we will be focusing. Time improvements will be compared w/ current paper-based workflow.

The time improvement of	Other issues
Screening of a subject	The cost of data storage
Enrollment decision	Reliability of the system
Evaluation of a trial subject	User's suggestion and feedback
Weekly Bout Therapy	System performance
Follow-Up Evaluation	Data recovery
Report Generation	User satisfaction
Retrieving and query the data	Data security

Table 1 Issues considered in the evaluation of the system

Figure 3 Screenshot of the subject treatment status

Figure 4 Web-based Viewer with measurement tools

Conclusion and Future Work

To facilitate a phase I evidence-based clinical trial, we have developed an imaging informatics-based ePR system to support the integration and collection of multimedia data of both clinical information and imaging studies. The system provides a platform for the rapid development of future decision-support tools and predictive computational models to evaluate and predict the effects of therapy dose on recovery outcomes. Figure 5 shows the final concept of the DOSE ePR system. Future work includes developing computational models and decision support tools to provide new patients with a powerful system that can provide the best predicted treatment outcome and plan individually tailored to the specific stroke patient characteristics.

Figure 6 The ultimate dose ePR concept

Acknowledgements

This work is supported by NIH/NICHD R01HD065438

USC University of Southern California

RSNA 2012 Patients First

Image Processing and Informatics Lab

Development of an Imaging Informatics Infrastructure to Support Collaborative Tools in a Large Scale Phase III Clinical Rehabilitation Trial

X Wang, MS[1], Los Angeles, CA; B J Liu, PhD[1]; J Mao MS[1]; N Reddy[1]; H Li[1] ; C J Winstein, PhD[2]

1-Image Processing and Informatics Lab, Department of Biomedical Engineering, Viterbi School of Engineering, University of Southern California, Los Angeles, CA 90089

2-Division of Biokinesiology & Physical Therapy, University of Southern California, Los Angeles, CA 90089

Aim: A web-based system with quantitative measurement tools that can support imaging and informatics related data for evaluation of a large-scale physical therapy clinical trial to improve outpatient therapy for arm paresis after stroke.

Learning Objectives:

- Understand how imaging data can enhance a clinical stroke rehabilitation trial.
- Discover what challenges are met in the large-scale imaging data-related clinical trial.
- Observe how an imaging informatics infrastructure and related tools can support the data sharing and collaboration of seven clinical trial sites.
- Understand how to extend the structure report from radiology to a clinical stroke rehabilitation trial to capture, store and distribute crucial trial outcomes and results.

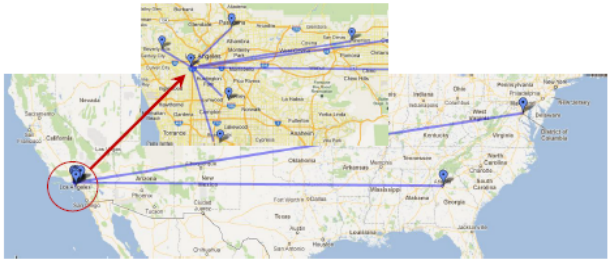

Map of the seven sites involved in the ICARE NIH NCT00871715 Trial

- US National Rehabilitation Hospital, Washington D.C.
- Emory University Center for Rehabilitation Medicine, Atlanta GA
- Cedars-Sinai Medical Center, Los Angeles CA
- Casa Colina Centers for Rehabilitation, Pomona CA
- Huntington Rehabilitation Medicine Associates, Pasadena CA
- Long Beach Memorial Medical Center, Long Beach CA
- Rancho Los Amigos National Rehabilitation Center, Downey CA

USC University of Southern California

RSNA 2012 Patients First

Image Processing and Informatics Lab

Scenario

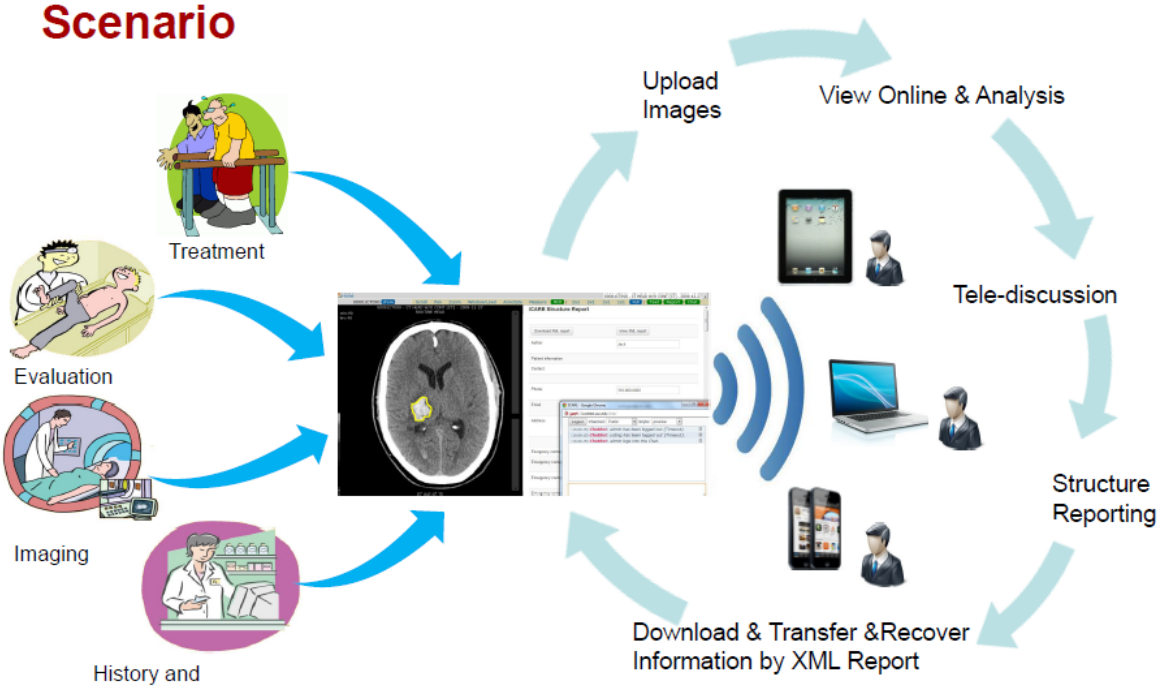

Acknowledgement: This work was supported by USC Provost Fellowship and ICARE NIH NCT00871715

SPIE 2013 PREPRINTS

Role of an imaging informatics-based DICOM-RT cancer registry in evaluating treatment parameters of IMRT for prostate cancer

Ruchi Deshpande[a], Alyssa Zhou[a], Jeffrey Zhang[a], John DeMarco[b], Brent J. Liu[a]
[a]Image Processing and Informatics Laboratory, Department of Biomedical Engineering, University of Southern California, 734 W Adams Blvd, Los Angeles, CA, USA 90089;
[b]Department of Radiation Oncology, University of California Los Angeles, 200 Medical Plaza Drive, Los Angeles, CA

ABSTRACT

Cancer registries are information systems that enable easy and efficient collection, organization and utilization of data related to cancer patients for the purpose of epidemiological research, evidence based medicine and planning of public health policies. Our research focuses on developing a web-based system which incorporates aspects of both cancer registry information systems and medical imaging informatics, in order to provide decision support and quality control in external beam radiation therapy. Integrated within this system is a knowledge base composed of retrospective treatment plan data sets of 42 patients, organized in a systematic fashion to aid query, retrieval and data mining. A major cornerstone of our system is the use of DICOM RT data sets as the building blocks of the database. This offers enormous practical advantages since it establishes a framework that can assimilate data from different treatment planning systems and across institutions by making use of a widely used standard – DICOM. Our system will help clinicians to assess their dose volume constraints for prospective patients. This is done by comparing the anatomical configuration of an incoming patient's tumor and surrounding organs, to that of retrospective patients in the knowledge base. Treatment plans of previous patients with similar anatomical features are retrieved automatically for review by the clinician. The system helps the clinician decide whether his dose/volume constraints for the prospective patient are optimal based on the constraints of the matched retrospective plans. Preliminary results indicate that this small-scale cancer registry could be a powerful decision support tool in radiation therapy treatment planning in IMRT.

Keywords: Cancer Registry, Radiation Therapy, Radiation Oncology, IMRT, Imaging Informatics, Prostate Cancer, DICOM RT

1. INTRODUCTION

Cancer registries are information systems that record diagnostic, treatment and outcomes data associated with cancer patients, mainly for the purpose of epidemiological research and public health policy planning, and may operate either at an institutional, state or national level. Our goal is to draw upon this concept, and add value to it by developing a DICOM-RT-specific system infrastructure for collecting, organizing and mining aggregate RT-related dose-volume data to enable knowledge discovery of existing patterns in dose delivery. The rationale behind this is that Radiation Therapy data objects contain a vast wealth of information that can be mined and analyzed with the ultimate objective of improving the quality of radiation therapy treatment plans and ultimately improving patient outcomes. More specifically, quantifying the relationship between patient anatomy and achievable organ sparing can help predict the most optimal IMRT treatment parameters for future patients.

Currently, most of this data resides in vendor-specific treatment planning systems and the oncology information systems associated with them. The primary utility of these systems is to develop and manage radiotherapy treatment plans. It is difficult to access and work with this data for research purposes since these systems use proprietary formats to store data. Although there are APIs to mobilize the data stored, research tools developed using these APIs become dependent on the TPS and cannot be ported to other treatment planning systems. As a result, a research system that utilizes data from any commercial system should ideally make use of a standard that is easy to work with, recognized and used by major vendors and accepted by the medical community. Most TPS vendors now support export of dose-volume data to DICOM RT [1] [2] objects, which makes DICOM the obvious choice.

To this end, we have developed a web-based, DICOM compliant system that helps in quantifying and ultimately utilizing relationships between patient anatomies and dose distributions for decision support in radiation therapy treatment planning.

1.1 Workflow

In order to design a clinical decision support system, it is essential to analyze the existing workflow of the clinical department and determine where the new system fits in, and how it alters the workflow. Figure 1 shows the operational workflow in Radiation Oncology. Steps of the workflow for the planning stage are outlined below:

- CT Simulation and Portal Image: Generation of the CT images that are used for treatment planning.
- ROI Contouring: All relevant ROIs are contoured slice-by-slice on the TPS.
- Initial Parameters: Selection and placement of fields, adjustment of Multi-Leaf Collimators, etc.
- Dose Grid Computation: The TPS calculates the dose grid.
- Plan Evaluation: Review of Dose Volume Histograms, isodose contours, dose homogeneity, etc.
- Plan Approval: The radiation oncologist either approves or rejects the plan based on the evaluation results
- Re-adjustments and fine-tuning: Further adjustments to resolve inadequacies (if any) found in the evaluation.

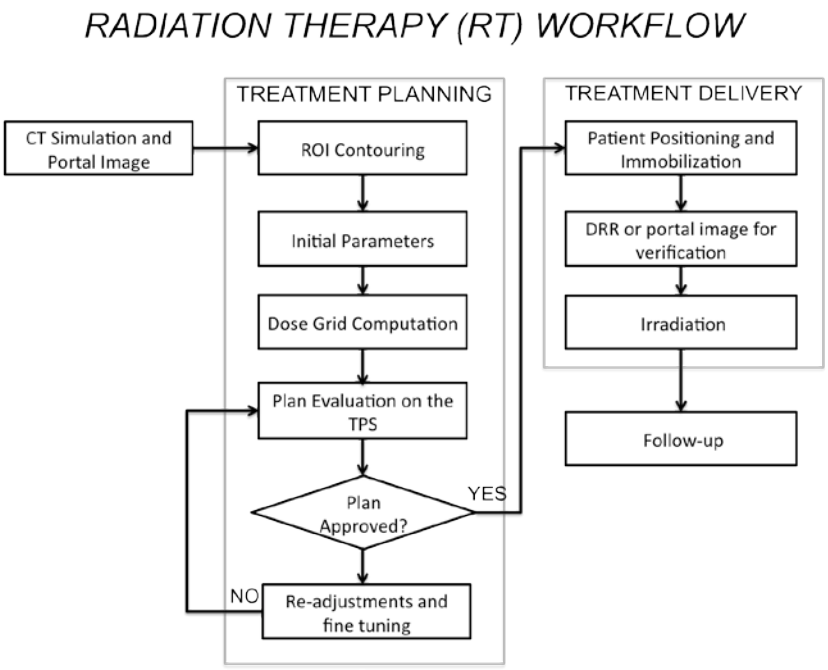

Figure 1. Radiation Therapy Workflow

Usually, the plan evaluation cycle is repeated a few times before finalizing a treatment plan (iterative trial and error methodology). However, there are practical limitations on the number of iterations possible, which may result in a less-than-optimal plan. That in turn, may affect the degree to which vital organs are spared, leading to patient complications, which could have been avoided or at least alleviated in some cases. Therefore, an intelligent system can use retrospective data to eliminate some of the guesswork involved, and optimize the plan evaluation stage by offering intelligent recommendations to the user.

1.2 The Decision Support System

The premise of the decision support system is that the internal anatomical configuration of organs and tumors place constraints of achievable dose distributions. For instance, the closer the bladder is to the tumor, the harder it is to spare

the bladder. On the other hand, even if two patients have tumors that are equidistant from their respective bladders, one of the patients may have a greater degree of overlap between the bladder and tumor, thus making it harder to limit dose to the bladder. Our decision support system enables:

1) Computation of these anatomical features (described in the Methods section).
2) Extraction of relevant dose distribution information to analyze the relationship between these features and achievable lower limits for dose delivery to critical structures.
3) Examine the effect of these anatomical features on dose delivery to the tumor.
4) Quantification of these relationships using mathematical pattern recognition, in order to predict optimal dose constraints for critical organs and the Planning Target Volume (PTV).
5) Develop a ranking system to rate patients according to the level of organ sparing possible on the basis of their anatomy.
6) Use the prediction and ranking tools to customize treatment plans for patients based on their anatomy.

2. METHODS

Careful planning and execution of the design of the decision support system is vital in order to accomplish the functionalities listed in the previous section. The following sections describe the system components and architecture, the data model and the knowledge discovery tools and methods.

2.1 System Architecture

Figure 2 shows the major components of our web-based decision support system. Some important considerations for system design are:

1) DICOM Compliant: The database and system controller should be capable of receiving, storing and processing DICOM data.
2) Web Access: The system should be accessible to users remotely in order to make it portable and easy to use on any client of the user's choice.
3) User Interaction: The end-user should be provided with an easy-to-use interface to avoid the need for direct interaction with the database and computational scripts. This facilitates easy integration of the system into the clinical environment.

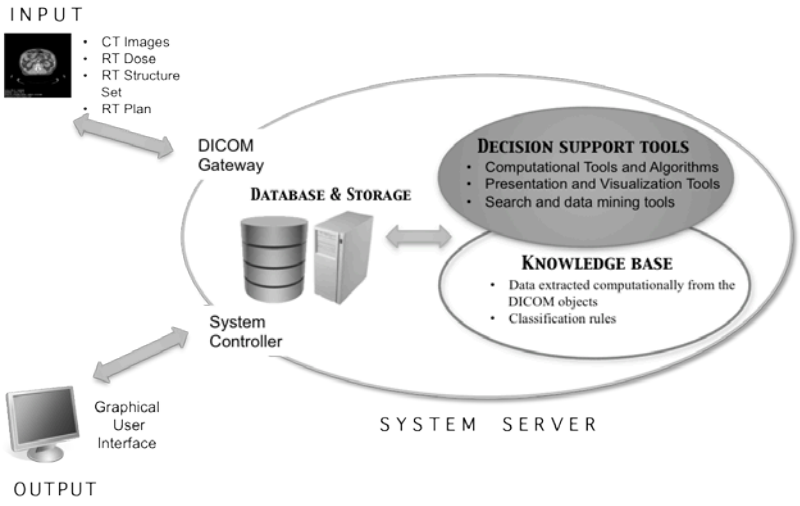

Figure 2. System Component and Architecture diagram

The main components of the system are described below:

1) The DICOM Gateway parses and validates DICOM objects, extracts relevant metadata, records it in the database, creates a file-folder hierarchy for storing the DICOM files, and links objects on the database to their location on the file system. Our DICOM gateway consists of a python script that makes use of the 'Pydicom' library, and can be accessed either through a web page or using DICOM C-Store.

2) The Database stores all relevant metadata associated with various DICOM objects, post processed data derived from DICOM files, user account information, etc. Our system uses MySQL as the database server.

3) The User interacts with the system via the Graphical User Interface (GUI), which includes tools for uploading data, as well as viewing data and results of analysis. This GUI is written using HTML and JavaScript.

4) The Decision Support module currently includes: computational MATLAB scripts that carry out all image processing tasks and can communicate directly with the MySQL database server; data presentation and visualization tools such as a DICOM viewer, contour overlay tool, scripts to generate DVH plots, etc.; and a search application which allows the user to query for specific information.

5) The Knowledge Base consists of information that is intelligently derived from the raw DICOM data. This is a specialized subset of the database, which is physically contained within the database, but is conceptually more specific. For instance, it contains the overlap volume histogram [3][4], which is computed from the DICOM RT Dose, RT Structure Set and CT images.

6) The System Controller acts as the binding link between the database, decision support modules and the Graphical User Interface

2.2 Data Model

The database is the backbone of any informatics system. It stores all the system inputs as well as results of computations. More importantly though, the data model leading up to the actual database lays the foundation for all future applications by ensuring efficient data accessibility. Proper organization and accessibility of data is essential in making the knowledge discovery and data mining tools usable. A good understanding of the structure and the relationship between the principal data elements facilitates proper implementation. The four main types of data objects involved in this system are CT Images, Structure Sets, Dose grids and treatment plans. Figure 3 shows how these objects fit into the DICOM model of the real world. Each object belongs to a DICOM series, which in turn belongs to a study. Each patient may have multiple such studies, and each study may have multiple series.

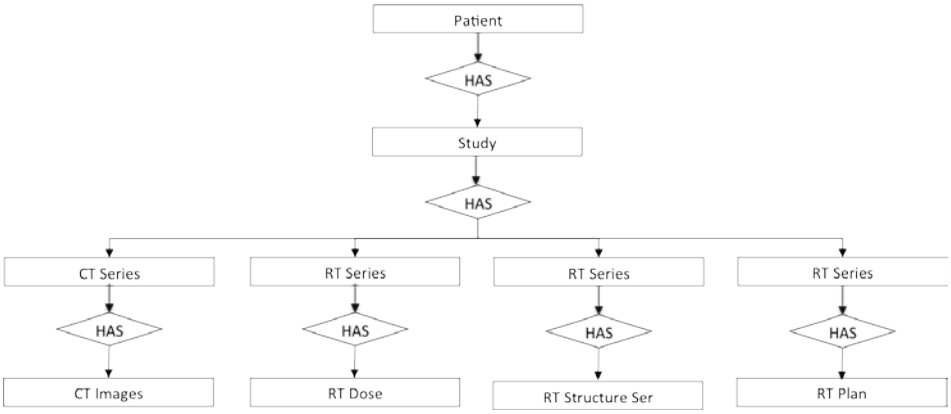

Figure 3. DICOM RT objects in the DICOM data model

The Structure Set object contains information related to certain user-defined regions of interest. For instance, in prostate cancer, the most important ROIs are the rectum, bladder, the prostate and the tumor. All of the information in a Structure Set object is contained within the DICOM header, and as a result, there is no pixel information in these files. Each ROI is assigned a number, and this mapping between the ROI Name and Number is also stored. Each ROI is delineated by ROI Contours, which are stored in the form of coordinates. Each contour is linked to a CT Slice by reference via SOP

Instance UIDs, Study UIDs, etc. However, since the contour points are in the patient-based coordinate system, they need to be converted to a pixel-based system to facilitate registration with the CT slices. Figure 4 shows the internal organization of the DICOM Structure Set object. Each Structure Set may have multiple ROIs defined, and each ROI may have multiple contours, each at a different slice location, with references to associated CT slices.

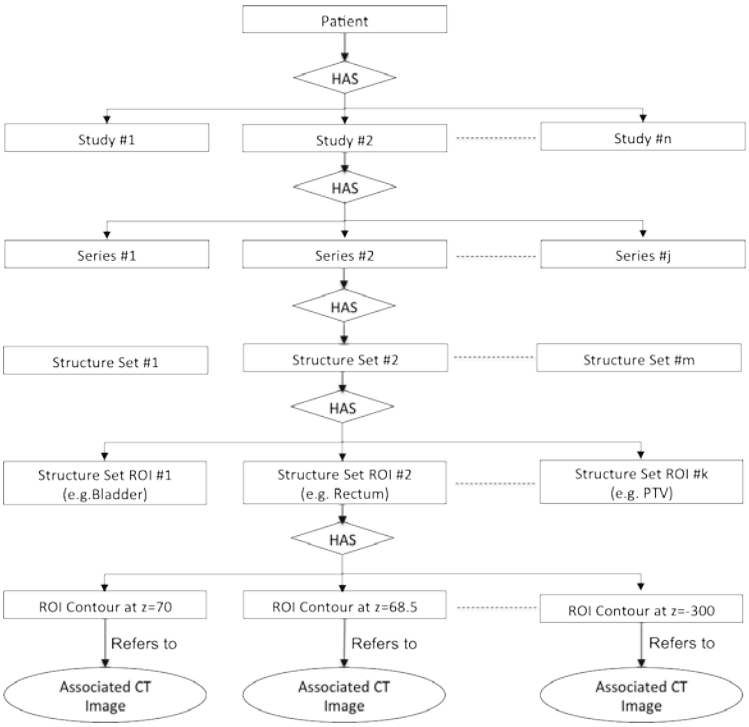

Figure 4. Data Model of the RT Structure Set Object

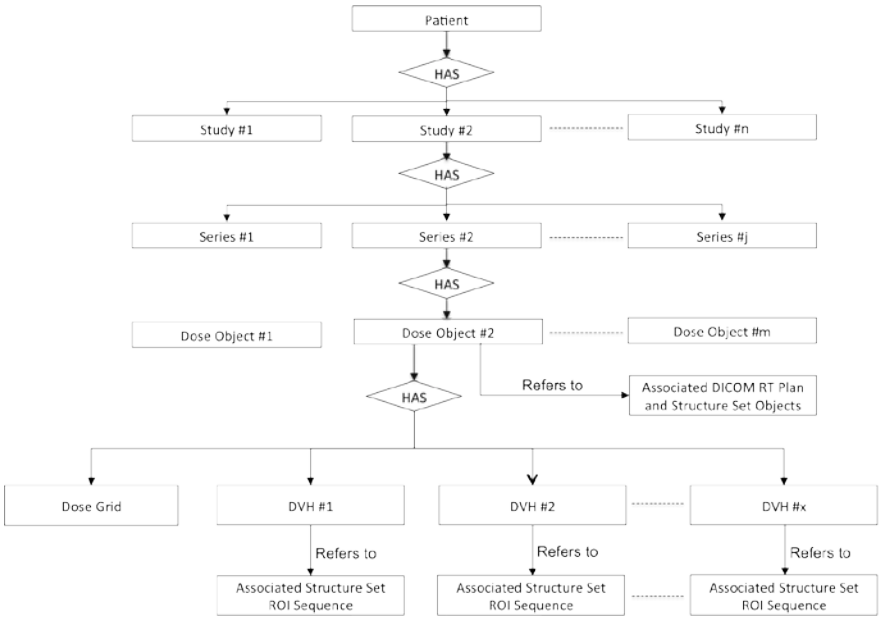

Figure 5. Data Model of the RT Dose Object

The Dose object contains the actual dose points generated by the treatment planning system. The dose grid is stored in the form of a 3D image, wherein each pixel value corresponds to dose magnitude scaled by the 'DoseScaling' attribute. The dose slice locations do not necessarily correspond directly with CT slice locations, and may need to be registered. All our data sets had to be registered separately via interpolation. Some treatment planning systems offer the option of exporting the Dose Volume Histograms as part of the DICOM RT Dose object as well. Figure 5 shows the relationship between the different elements of the Dose object.

2.3 Knowledge Discovery

Once the basic DICOM objects have been uploaded to the system, data mining can be employed to extract useful features regarding the patient's anatomy as well as dose delivery. Since a patient's anatomy is believed to play a role in limiting the sparing of critical organs, the following features related to patient anatomy were extracted:

1) ROI Volume: Treatment planning systems may or may not include information related to volumes of organs in the exported DICOM files. Additionally, the algorithms used by different vendors lead to variability in these computations. We have chosen to re-calculate ROI volumes in order to deal with this uncertainty, and maintain consistency among data sets obtained from different treatment planning systems. In order to achieve this, the ROI contours obtained from the Structure Sets were overlaid on the associated CT slices in order to create solid ROI masks in the form of binary 3D images. A count of all the 'on' pixels multiplied by pixel spacing and slice thickness provides the ROI volume.
2) Volumetric Overlap between critical structures and the PTV: An intersection of the solid masks created for the critical structures and the PTV was carried out. The volumes of these intersecting regions were then calculated. That fraction of the total volume of an organ, which intersects with the PTV, was used as the final feature by dividing the intersecting volume by the total volume of the organ.
3) Distances between ROIs: The centroid of each ROI was calculated and then the Euclidean distance between the centroid of each critical organ and the PTV was determined.
4) Maximum distance of 50%, 75% and 90% of the volume of an ROI from the PTV: An overlap volume histogram was computed for each ROI-PTV pair. From this OVH, we extracted the maximum distance of 50% of the volume of an ROI from the nearest surface of the PTV. We then repeated the procedure for 75% and 90% of the volume of each ROI.

Further, in order to relate these geometrical features to the dose distribution, we calculated the following dose parameters:

1) D50: Dose delivered to 50% of the volume of an ROI
2) D75: Dose delivered to 75% of the volume of an ROI
3) D90: Dose delivered to 90% of the volume of an ROI

These values are interpolated from the Dose Volume Histogram.

3. RESULTS

Out of the collected data set of 42 patients, 14 were used to examine the relationship of dose delivered to an organ and the volumetric overlap of that organ with the PTV. Theoretically, as overlap increases, it becomes increasingly more difficult to spare the organ while still maintaining sufficient dose to the PTV. However, certain cases do exist wherein a patient with a lower overlap receives the same dose to the bladder as another patient with a much higher degree of overlap. A lot of these cases may be explained by other factors such as the distance between the bladder and the PTV. Our next step is to examine these additional relationships in combination with the overlap-dose relationship to create a model to relate patient anatomy to dose delivery. So far, our results verify the general trend of increase in dose to the ROI with an increase in overlap between that ROI and the PTV.

We plotted the dose delivered to 50% of ROI volumes versus the percentage volumetric overlap of the ROIs with the PTV. Figure 6 shows this scatter plot for the bladder, with 14 patients. Figure 7 shows the same plot for the rectum. We can see that that as the percentage overlap increases, the dose delivered to 50% of the bladder and the rectum also increases.

Table 1 shows the actual measurements for patients with IDs of 8 and 13. We can see that the bladder percentage-overlap for Patient #13 is 4.7% higher than for Patient #8. So we would expect that Patient #8 be more easily spared and receive a lower dose than Patient #13. However, that is not the case, as both bladders receive similar amounts of dose. The same pattern repeats for the rectum, where similar doses are given to patients who differ in their rectal percentage-overlap by 5%. This may be due to the fact that the PTV volume for Patient #8 is a lot larger than for the other patients. This may or may not indicate a larger tumor (the PTV includes regions immediately surrounding the tumor, as dictated by the nature of the tumor and the patient's anatomy). Adding more features and running this analysis on a larger data set will yield more conclusive results.

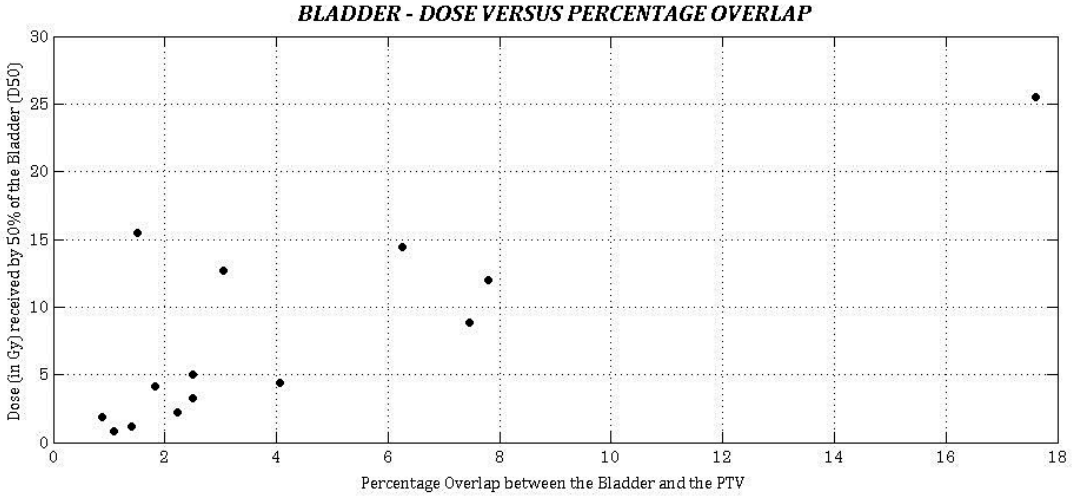

Figure 6. Bladder Dose versus Percentage Overlap for 14 patients

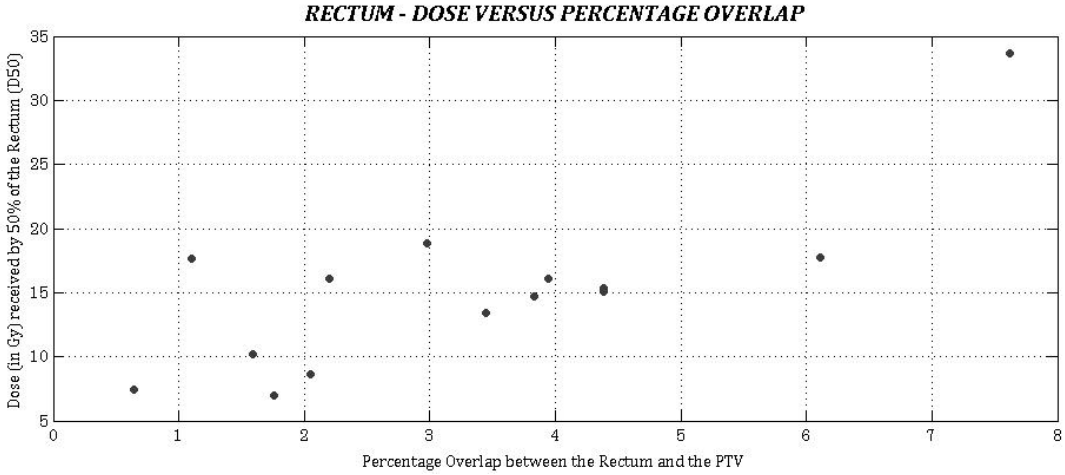

Figure 7. Rectum Dose versus Percentage Overlap for 14 patients

Table 1. Percentage volumetric overlap and dose to 50% of the bladder and rectum for patients #8 and #13.

	PATIENT #8		PATIENT #13	
	Percentage Overlap	**D50**	**Percentage Overlap**	**D50**
Bladder	1.5182	15.5141	6.252	14.4173
Rectum	1.1017	17.6167	6.1116	17.7066

4. DISCUSSION

The benefits of such a decision support system for research purposes are numerous. Most imaging informatics research tools cannot be properly evaluated and validated for lack of efficient integration into the clinical environment for validation and testing. This system can easily be incorporated into the clinical workflow in the following manner:

1) The system is web based. As a result, the dosimetrists or oncologists involved in testing can easily access the system either on their workstations, work computers, laptops or tablets. This allows for easy integration.

2) Since the system is DICOM compliant, users can export data from multiple treatment planning systems, allowing for a certain degree of vendor-independence (i.e., as long as the vendor supports DICOM export).

3) End-users do not have to deal with technical scripts, tedious input parameter specifications, etc. This makes the tool easy to use for clinical personnel.

The biggest impact of this system is on personalizing treatments to individuals. Our ultimate objective is to take this even further by incorporating outcomes data, and linking the patient's anatomy and actual dose delivered to the overall effectiveness of the treatment and the impact of the treatment on the patient's quality of life, measured by treatment toxicity. A system that incorporates all three major facets of the patient's treatment process could prove to be very powerful in providing decision support in radiation therapy treatment planning.

This system can be expanded to include other applications in the future, such as comparison studies of the effectiveness of different treatment modalities; recommendations of plan parameters other than dose constraints for critical organs; etc.

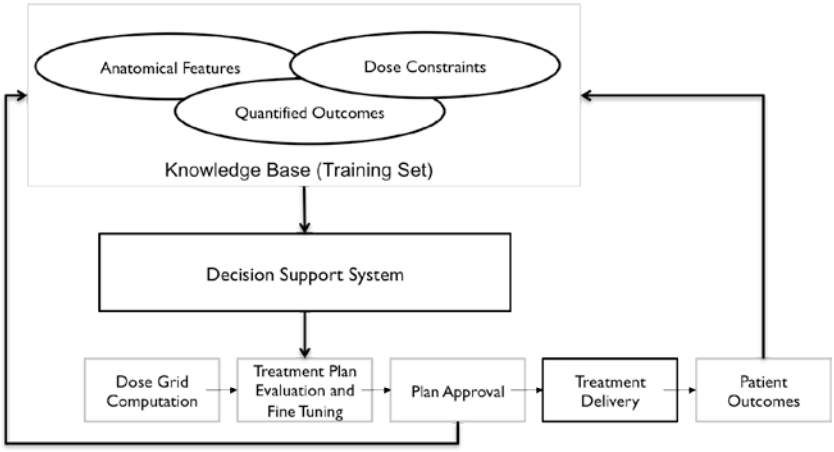

Figure 8. Incorporating the system with outcomes information into the clinical workflow. The patient's outcomes information and the new treatment plan DICOM objects are entered into the Knowledge Base to update the classifier.

5. CONCLUSION

We have presented the concept of an imaging informatics based decision support system for radiation therapy treatment planning, with a focus on dose constraint predictions and recommendations for prostate cancer radiotherapy. This system was tested with 42 patients, and found to show considerable promise in improving the efficiency of treatment plan evaluation.

REFERENCES

[1] Digital Imaging and Communications in Medicine (DICOM) Part 3. Information object definitions. PS3.3-2009
[2] Law M. Y. Y., Liu B. J., "Informatics in Radiology – DICOM RT and Its Utilization in Radiation Therapy", RadioGraphics 2009; 29:655-667

[3] Kazhdan M., Simari P., McNutt T., Wu B., et al., "A Shape Relationship Descriptor for Radiation Therapy Planning", MICCAI 2009; 5762:100-108
[4] Wu B., Ricchetti F., Sanguineti G., Kazhdan M., et al., "Patient geometry-driven information retrieval for IMRT treatment plan quality control", Med Phys. 2009;36(12):5497-505

Integration of Imaging Informatics-based Multiple Sclerosis eFolder System for multi-site clinical trials utilizing IHE Workflow Profiles

Kevin Ma[a], Nakul Reddy[a], Ruchi Deshpande[a], Lilyana Amezcua[b], Brent Liu[a]
[a]Image Processing and Informatics Laboratory, Dept of Biomedical Engineering, Univ. of Southern California, 734 West Adams Blvd.. Los Angeles, CA 90089
[b]Dept. of Neurology, Univ. of Southern California, 1520 San Pablo St. Los Angeles, CA 90033

ABSTRACT

At last year's SPIE, we presented a multiple sclerosis (MS) eFolder as an integrated imaging-informatics based system to provide several functionalities to both clinical and research environments. The eFolder system combines patients' clinical data, radiological images and computer-aided lesion detection and quantification results to aid in longitudinal tracking, data mining, decision support, and other clinical and research needs.

To demonstrate how this system can be integrated in an existing imaging environment such as a large-scale multi-site MS clinical trial, we present a system infrastructure to streamline imaging and clinical data flow with postprocessing (CAD) steps. The system stores clinical and imaging data, provides CAD postprocessing algorithm and data storage, and a web-based graphical user interface (GUI) to view clinical trial data and monitor workflow. To evaluate the system infrastructure, the MS eFolder is set up in a simulated environment with workflow scenarios, including DICOM store, query, and retrieve, automatic CAD steps, and data mining based on CAD results. This project aims to discuss the methodology of setting up eFolder system simulation with a connection to a CAD server component, simulation performance and test results, and discussion of eFolder system deployment results.

Keywords: multiple sclerosis, system integration, MRI, DICOM, IHE

1. INTRODUCTION

This paper aims to present the methodology of integrating a disease-centric imaging informatics system (our multiple sclerosis eFolder) in an existing informatics environment, such as a PACS or an enterprise-scale imaging clinical trial. The methodology includes how to integrate a post-processing component of the eFolder in the existing imaging workflow. The results of the integration will show how to apply a system like eFolder as an informatics solution for real-world clinical environments and large-scale clinical trials.

1.1. Multiple Sclerosis

Multiple Sclerosis (MS) is an autoimmune neurological disease that affects approximately 2.5 million people worldwide, and proximately 200 new patients are diagnosed with MS each week in the United States. The body's own immune system attacked the central nervous system, causing damages and scar tissues (called lesions) in brain parenchyma, spinal cord, and optic nerves[1]. Its symptoms vary greatly and in the most severe cases can be disabling and life-threatening. Currently there is no cure for MS, and treatments for MS include disease management, reducing number and severity of attacks, and improve patients' ability to function in daily lives[2, 3]. Therefore, longitudinal disease tracking of patients become key in MS treatment.

Magnetic Resonance Imaging (MRI) is a commonly-used tool in diagnosing and monitoring MS by visually displaying lesions[4]. Lesions in white matter appears hyperintense in MR sequences T2 and FLAIR, while lesions may appear hypointense in T1 sequences. Figure 1 shows a MS patient's MRI in the three sequences.

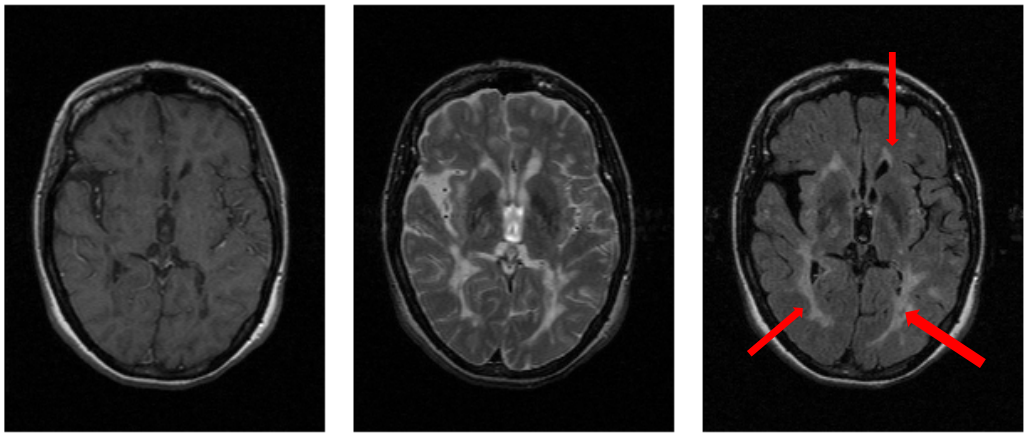

Figure 1. Three axial brain images of an MS patient. The left-most image is T1-weighted, the middle image is T2-weighted, and the right-most image is FLAIR. White regions in FLAIR image (as pointed by arrows) indicates MS lesions in white matter

In longitudinal tracking, existing individual MS lesions need to be identified and quantified for monitoring patients' responses to treatments as well as disease progress. To solve these challenges, an imaging-informatics based eFolder has been designed to store and display MS patient data with MR images and MS lesion quantification results. The benefits of the eFolder include integrated patient data repository, an automatic lesion detection and quantification system to allow disease tracking on MR, and a data mining tool for both clinical and research purposes.

1.2. Design of MS eFolder

Figure 2 shows design components of the MS eFolder system.

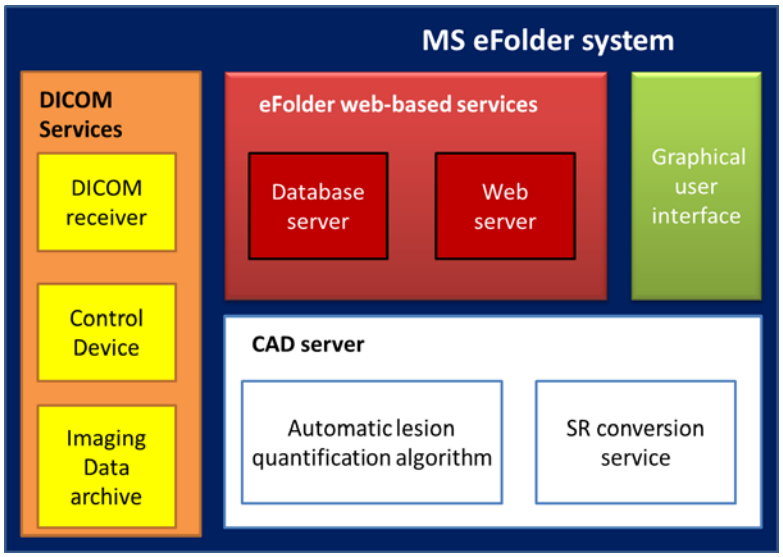

Figure 2. MS eFolder system diagram. The system itself contains three components: eFolder web-based services (red), graphical user interface (green), and CAD component (white). DICOM services (in orange) provide DICOM-based operations needed for eFolder system integration in clinical environments

The MS eFolder system has three main design components: database, graphical user interface, and a computer-aided detection (CAD) system that can quantify lesion volume and number of lesions.

1.2.1. Database design

The eFolder database stores text data such as patient history, MR image locations, and lesion quantification results. Database schema has been developed in MySQL The database structure is built such that one single patient has a unique data entry regarding demographics and social data, has a list of all MR studies regarding to MS, and a list of all CAD results (in Structured Reporting, or SR, format) available for that patient. The data therefore is patient-centric and allows quick access to a patient's historical data. Patient demographic data is collected and designed via physicians' survey forms. The imaging database follows the DICOM structure to store metadata from headers. The CAD results database stores quantified lesion statistics on both study and image level.

1.2.2. Graphical User Interface design

A graphical user interface (GUI) is needed to display all the information available in the eFolder, as it ties everything together in a presentable and user-friendly way for navigation of data. The web-based GUIs have the following characteristics:

- The GUI need to be web-based to allow remote access using thin-client architecture. Computations and visualizations are completed on the server side for a light-weight and fast GUI.
- The GUI needs to be comprehensive. It needs to display patient clinical data, imaging data, and CAD results on the same interface. It allows physicians and radiologists to access all of the information related to the data query.
- The system needs to be dynamic and allow display of 3D images and manipulations of images presented. An attractive viewing interface allows for a more clarified presentation
- The GUI needs to allow flexible and intelligent data mining. With a large number of patients' information stored in the eFolder system, any clinician and researcher should be able to look up MS patients on a variety of different search criteria, ranging from patient demographic data to lesion analytical results.

Figure 3 displays the eFolder's GUI.

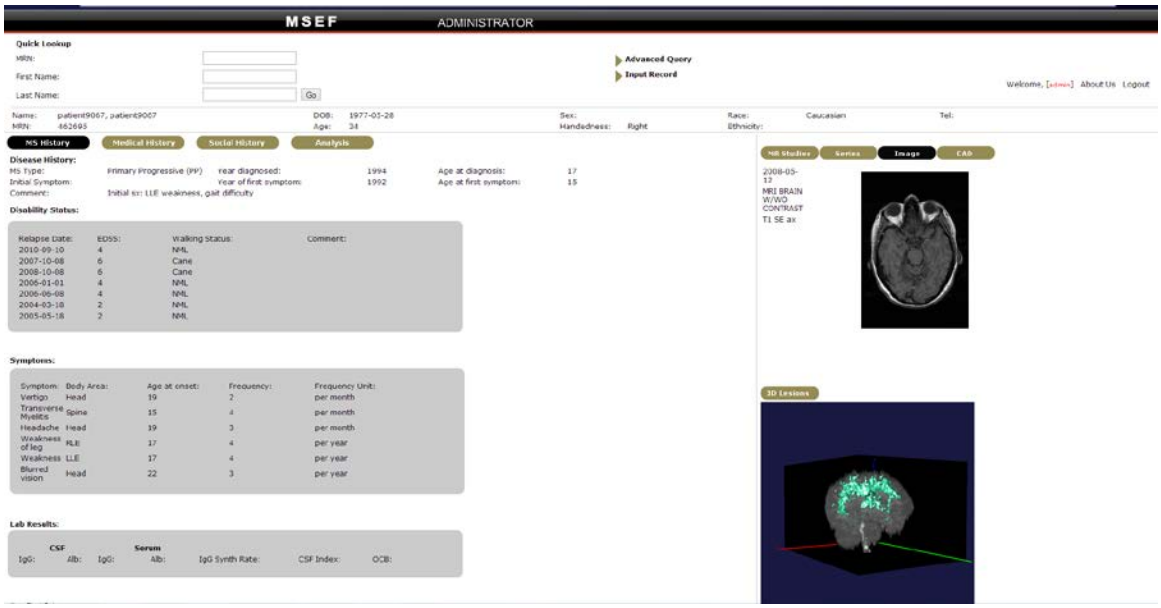

Figure 2. MS eFolder graphical user interface. Left panel displays patient information, right top panel displays MR images, and right bottom panel displays lesion information

1.2.3. Computer-aided Lesion Detection (CAD) and quantification system

The MS CAD algorithm is designed to output lesion volumes, lesion locations, and total lesion load. The detailed algorithm design splits up into three parts: preprocessing, lesion voxel identification by probability thresholding, and lesion quantification. The algorithm has been prototyped in MATLAB and has been refined to increase post-processing efficiency by reducing processing time.

The algorithm is designed on 3-D MRI brain images. It uses T1 and FLAIR (Fluid attenuated inversion recovery) axial sequences. The algorithm converts the series of MR images into a three-dimensional matrix for 3-D lesion analysis. Lesion voxel classification is based on Statistical Parametric Mapping (SPM) brain image analysis toolkit for MATLAB[4]. Grey matter and white matter are first segmented, and an expectation minimization algorithm for k multidimensional Gaussian mixture[5] is applied to the brain images. The estimation results are used to determine the likelihood of a lesion voxel based on whether the voxel intensity is outside the predetermined normal range. The normal range is current set at within 3 standard deviations of normal FLAIR intensities.

The results from the voxel classification algorithm is then clustered and quantified based on DICOM values, and the final output includes individual lesion volumes in 3D, lesion locations in coordinate space, and total lesion load for the study.

1.3. IHE Postprocessing workflow integration profile

The goal of current progress in MS eFolder research is to integrate all of the components of eFolder together and fit into a real-life clinical workflow. IHE (Integrating the Healthcare Enterprise) provides a design of how to include a post-processing step inside a typical clinical workflow[6]. Figure 4 shows the integrated workflow with a post-processing workstation.

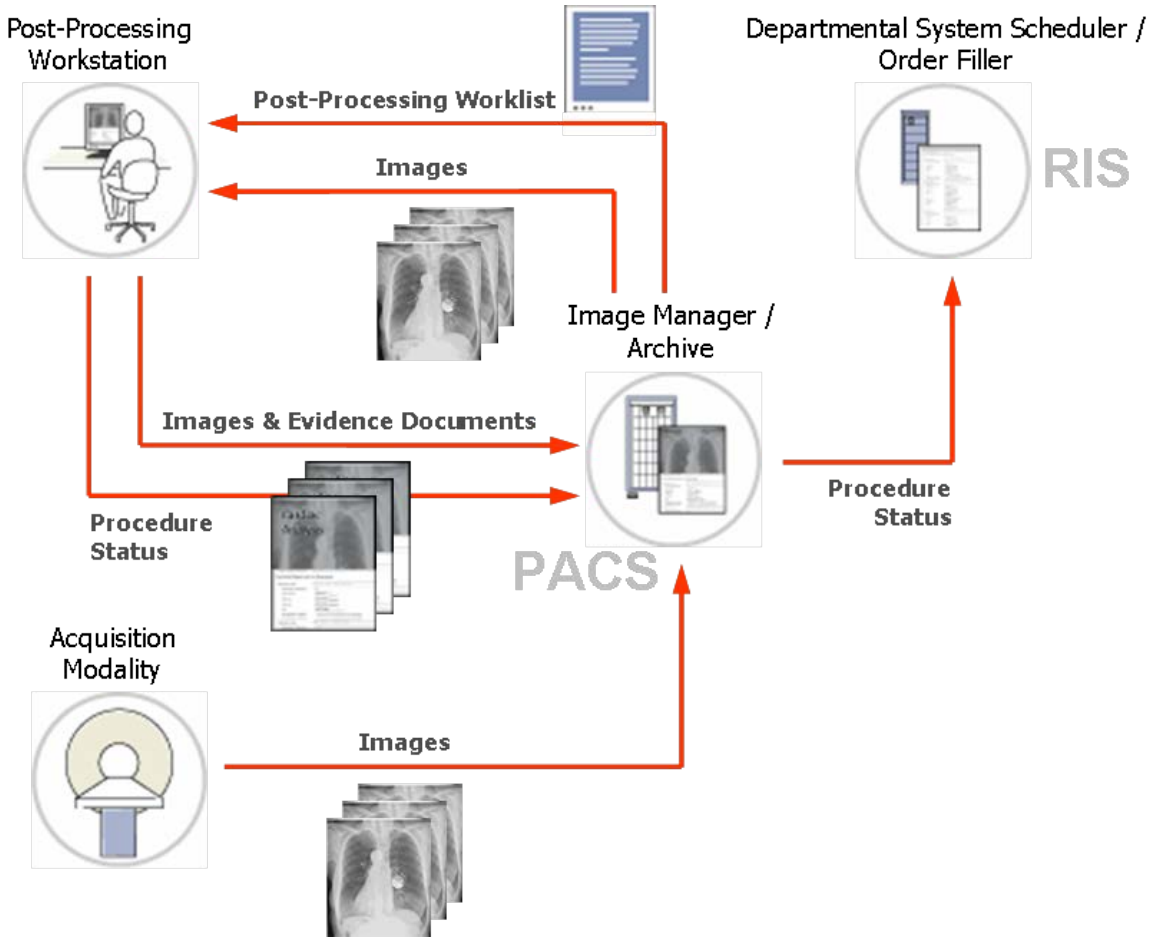

Figure 4. IHE Post-processing workflow diagram. The workflow begins with image acquisition, includes image storage solution (PACS) and an addition post-processing step. The entire process is monitored by RIS (radiology information system)[6]

First, images are acquired from modality and then sent to PACS for storage. RIS is informed of the existence of the study and provides a status tracking service to mark the study as in claimed, in progress, or completed. The post-processing workstation queries PACS for a worklist to retrieve the studies. The studies are processed, and the resulting images and documents are sent back to PACS for storage.

2. METHODS

The MS eFolder design is modeled after the IHE workflow profile to show its use in a clinical environment. To accomplish the tasks, a simulated clinical environment with MS eFolder is set up in the Image Processing and Informatics laboratory. Figure 5 shows the conceptual diagram of MS eFolder's setup, modified from Figure 4.

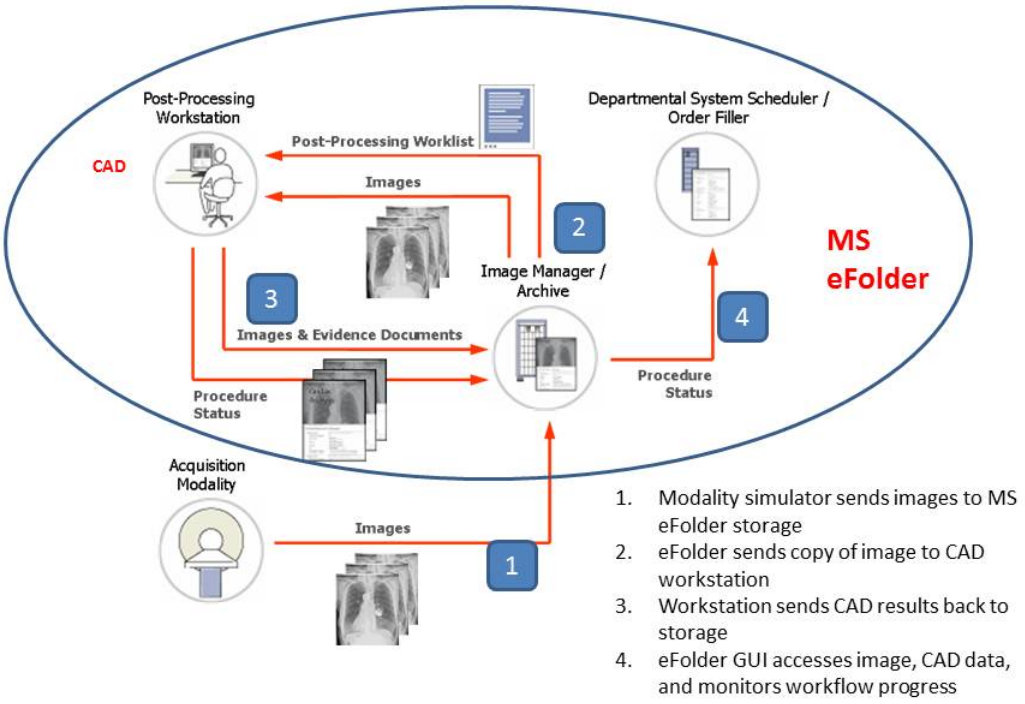

Figure 5. MS eFolder workflow diagram with IHE postprocessing profile. The blue circle indicates all of the components included in the eFolder. The steps 1 through 4 indicates the order of workflow of the demonstration.

The workflow for MS eFolder integration is defined in four steps:

1. MR images are sent from modality simulator to the eFolder server for archiving
2. The eFolder server sends a copy of the images to the CAD Workstation for postprocessing analysis
3. The CAD Workstation sends the completed CAD report back to eFolder server for archiving
4. At the completion of each of the previous steps, a status tracking tool inside eFolder displays alerts of the study progress to the user

The methodology of each step is described in detail later on in this section.

2.1. Laboratory Environment System Setup

Figure 6 displays the physical components diagram of the MS eFolder system setup in order to simulate the workflow steps outlined in Figure 5.

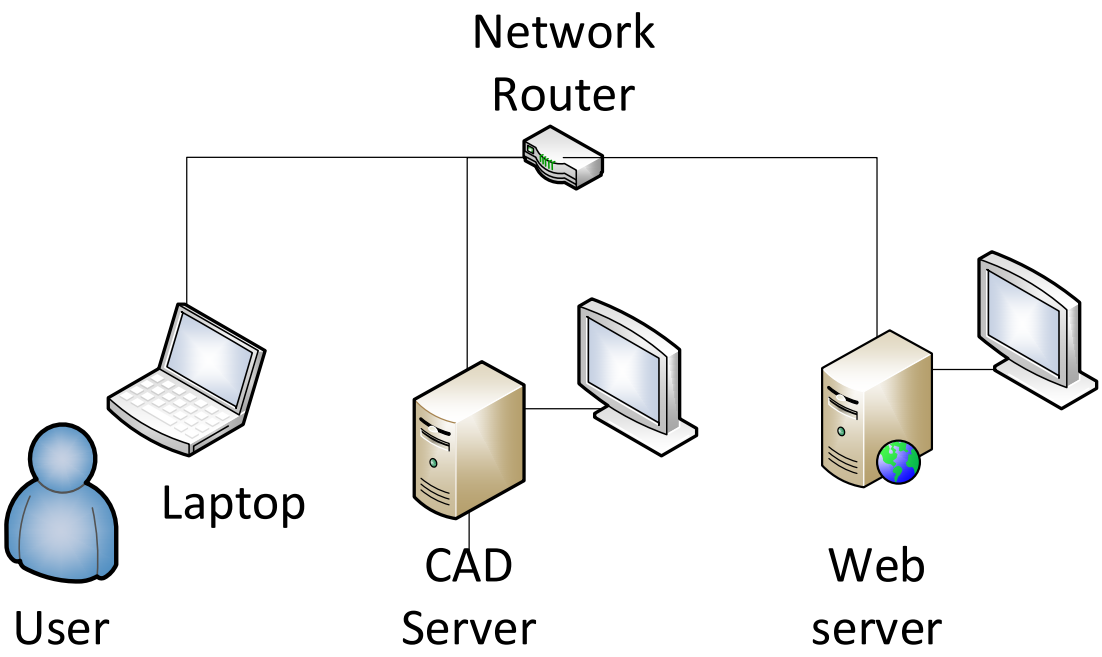

Figure 6. MS eFolder components diagram. The entire system includes 3 hardware components (Windows-based personal computers) and a closed network for demonstration purposes.

The hardware environment is set up in a laboratory environment. There are two Windows-based desktop towers, one performs as the eFolder archiving and web server and the other as the CAD workstation. Another laptop is connected to the network to simulate the user accessing the eFolder system. The eFolder network is LAN-based, connected via Ethernet cables and managed by a router. The router, a D-Link EBR 2310 series wired router, assigns unique IP addresses to the hardware components in the network. The eFolder web/archiving server is a Dell® Dimension 9150 series desktop tower, running Windows XP Professional. A wamp (Windows Apache/MySQL/PHP) server program is installed on the desktop to run the eFolder's web-based interface, PHP scripts such as database connection and DICOM parsing (will be discussed in more detail in Section 2.2), and the MySQL-based eFolder database. The CAD workstation is a Dell® Dimension 9200 series desktop tower, running Windows 7 Professional. MATLAB version 2011b is installed on the CAD workstation to run the MS CAD post-processing program. The laptop is used to access the system, and there are no system requirements as long as the laptop has a web browser to view the eFolder GUI. This allows the eFolder system to be accessed on the network by portable devices such as tablet computers or smart mobile phones.

2.2. Data Collection

Image and patient data used in the MS eFolder setup is the same as existing eFolder data that has been collected over 3 years. A total of 72 patients are collected: 36 Hispanic and 36 Caucasian patients. The patients of two groups are matched by gender, age (within 5 years), disease duration (within 5 years), and disease type (all are relapse-remitting). All brain MR studies are collected at University of Southern California Academic Medical Center and Los Angeles County Hospital. MR images are in DICOM format and anonymized. All studies contain noncontrast T1 and FLAIR axial slices as required by the MS CAD algorithm. Patient information has been collected by the Department of Neurology at University of Southern California via patient surveys. The survey forms have been converted to Microsoft Excel format, and then entered into the MySQL-based MS eFolder database.

2.3. Image Acquisition Workflow Simulation (Step 1 in Figure 5)

The first step is to simulate DICOM images transferring from image modality to the PACS server for storage. In this system simulation, the eFolder web server serves as an image storage server. Images are sent to the eFolder server from the laptop via the open-source DICOM toolkit dcmtk7, installed on both the laptop (image sender) and the eFolder server (image receiver). The laptop acts as Storage SCU and the eFolder web server acts as the Storage SCP. The Storage SCP constantly listens to the dedicated DICOM port for incoming DICOM images. When DICOM images are sent to the server, the storage SCP stores all DICOM images in a temporary folder. A PHP script then is used to parse DICOM data to store metadata inside eFolder database, alert the status tracker the existence of the study, and moves the DICOM data into an archiving folder.

2.4. Worklist and Image data transfer to CAD Workstation (Step 2 in Figure 5)

The second step is for the DICOM studies to be sent to the CAD workstation for post-processing analysis. In this simulation, users can access the status tracking page from the eFolder GUI (as shown in Figure 7) to select a study to send images to CAD workstation.

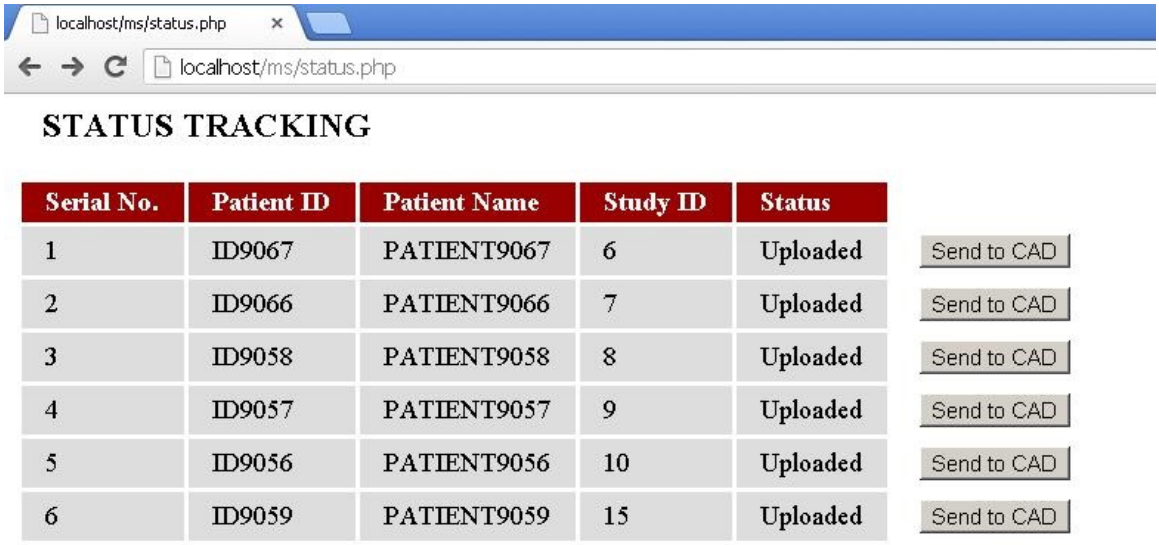

Figure 7. Status tracking page for MS eFolder post-processing workflow. Users can select a study to be sent to the CAD workstation.

The selected DICOM study are then sent to the CAD workstation via FTP (file transfer protocol). On the CAD workstation, the CAD program is running continuously and listens to the destination folder of the FTP transfer to process the new DICOM study. During this time, the status tracker would show that the selected study has been sent for post-processing, as shown in Figure 8.

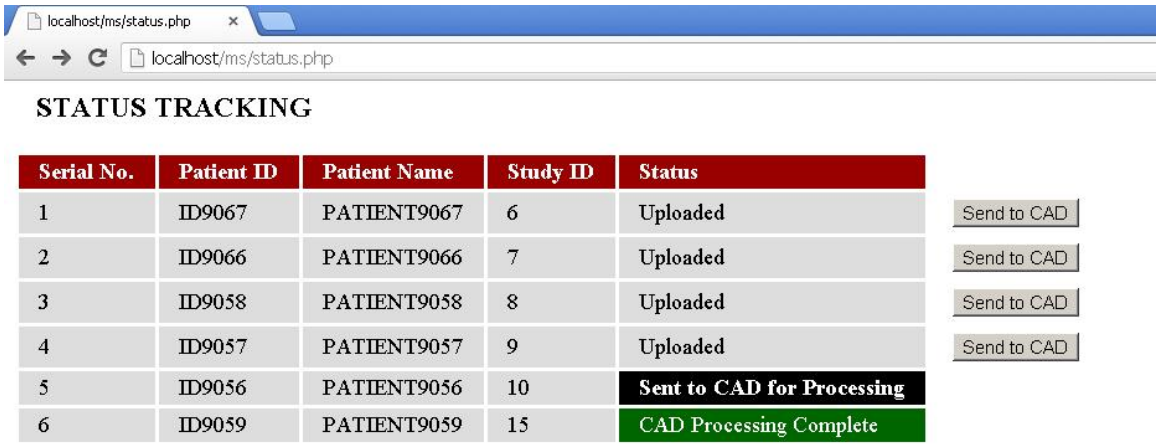

Figure 8. Status tracking page for MS eFolder post-processing workflow after a study (Study ID 10) has been sent to the CAD workstation, and after another study (Study ID 15) has been processed and sent back to the server.

2.5. Sending CAD results to eFolder server for storage (Step 3 in Figure 5)

After the post-processing step is completed, the CAD program sends the results back to the storage server. Because the storage server is DICOM-compliant, the CAD program needs to send a DICOM-SR (DICOM structured report) object for archiving. The MATLAB program first outputs the CAD results, including DICOM header information, reference images, and MS lesion quantification analysis results, into an XML document. The document is then sent to the eFolder server, where it is converted to DICOM-SR object via dcmtk toolkit, and stored in the archive folders. The eFolder GUI provides a web-based DICOM-SR viewer for users to view post-processing results. Figure 9 shows an example of SR shown on the eFolder GUI.

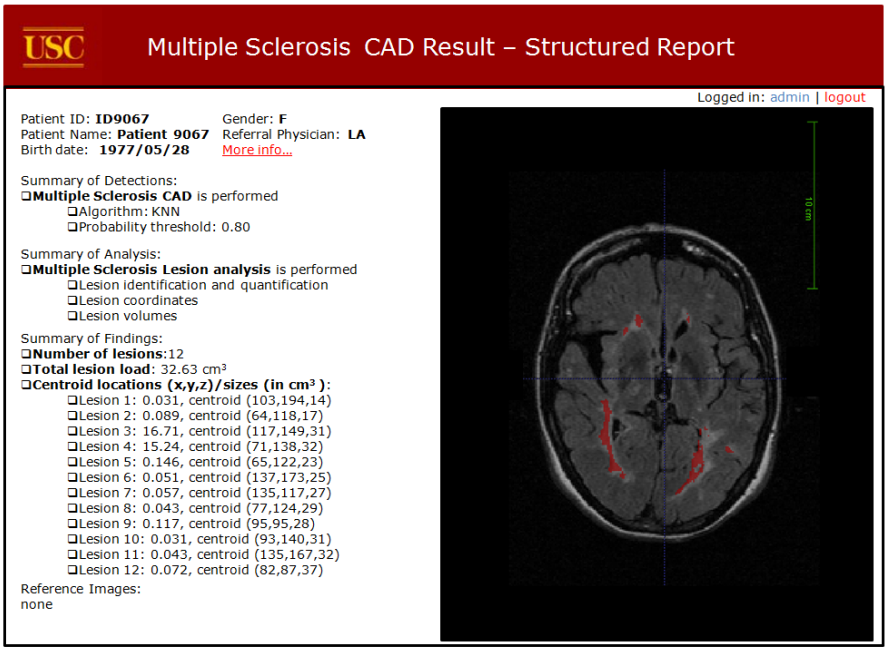

Figure 9. DICOM-SR viewer in MS eFolder GUI

The CAD program also connects to the MySQL-based eFolder database directly via a MATLAB-MySQL connector[8]. The program updates the status tracker database and the CAD results database automatically. Figure 8, as shown previously, shows an example of a study that has been completed on the status tracker.

3. RESULTS AND DISCUSSIONS

3.1. Results and Current Status

Preliminary tests of the MS eFolder system with integrated workflow were successful in the laboratory environment. Five different studies out of the MS eFolder dataset have been used in testing. Each workflow steps described in the methodology section have been successfully tested except the DICOM-SR portion, which is currently under development. The entire system has been demonstrated at the Radiological Society of North American (RSNA) in November, 2012.

3.2. Discussion and Future Work

The system simulation, along with the eFolder system features, are currently still ongoing. The eFolder's CAD algorithm has been redesigned based on a less computationally demanding algorithm, and the preliminary tests in the system simulation shows a marked improvement in processing speed, allowing the live workflow demonstration to be possible. Future work of this workflow integration includes finishing DICOM-SR component and integration with a test PACS server. Other future works involving the eFolder project involving upgrading image viewer to fully WADO-compliant DICOM viewer and a DICOM-SR viewer.

4. CONCLUSION

We have presented a multiple sclerosis eFolder system as an imaging informatics solution for multiple sclerosis patients records system. The eFolder system includes an automatic lesion quantification algorithm for calculating MS lesion volume and lesion location for brain MR studies. The system is being integrated into a simulated clinical environment, following post-processing workflow profile guidelines from IHE. The simulated workflow is designed by sending DICOM images to eFolder server, which acts as PACS storage server. The CAD workstation is set up in the same eFolder network. DICOM data is sent from eFolder server to CAD workstation, then CAD workstation uploads the results back to the eFolder server for display. We have demonstrated the methodology of the eFolder system with the simulated workflow, and that data transmission and workflow steps all work successfully as designed. Future work of this project include creating and sending DICOM-SR objects for storage, and upgrade the image display feature to display DICOM-SR objects as well as a clinical evaluation phase.

REFERENCE

[1] National Multiple Sclerosis Society http://www.nationalmssociety.org/about-multiple-sclerosis/index.aspx
[2] S Ringold, C Lynn, R Glass "Multiple Sclerosis" JAMA. 2005;293(4):514
[3] D Hafler "Multiple Sclerosis" J. Clin. Invest. 2004, 113(6):788-794
[4] Statistical Parametric Mapping http://www.fil.ion.ucl.ac.uk/spm/
[5] P Tsui "Fast EM_GM" http://www.mathworks.us/matlabcentral/fileexchange/9659 downloaded from MATLAB Central
[6] IHE Post-processing Workflow http://wiki.ihe.net/index.php?title=Post-Processing_Workflow
[7] DCMTK-DICOM Toolkit http://dicom.offis.de/dcmtk.php.en
[8] R Almgren, "MySQL Database Connector" http://www.mathworks.com/matlabcentral/fileexchange/8663-mysql-database-connector

A multimedia system for decision support in neurological classification of pain in spinal cord injury patients

Sneha K. Verma[1], Dr. Sophia Chun[2], Brent J. Liu[1]
[1] IPILab, Dept. of Biomedical Engineering, USC, [2] VA Clinics

ABSTRACT

Pain is a common complication after spinal cord injury which highly affects the patient lifestyle and well-being. For better treatment, accurate classification of pain becomes very important, which directly depends on the information provided by patients to the physicians. Currently, with the limited knowledge about the pain related information, patients end up taking medications which are not suitable or required. At Loma Linda Proton Treatment and Research Center, technical advances are being made, to treat functional disorders of spinal portion of the central nervous system using radio surgery. This paper presents overall workflow design for the project. Also in this paper, we are introducing a web based pain classifier tool that allows a patient to select multiple pain locations and group them according to the pain properties, such as severity of pain, location of pain, occurrences of the pain etc. This computer-aided pain classifier tool can be integrated with medical imaging so that if physicians want to compare pain information provided by patients with imaging data, they can do it all at the same time. Pain classifier application described here, is going to be a major component for patient recruitment in phase 0 of the study.

Keywords: pain; spinal cord injury; nociceptive; neuropathic; decision support system.

1. INTRODUCTION

Pain is a common complication after spinal cord injury (SCI), which can significantly impact upon a person's functional ability and independence, psychological well-being, ability to return to work and quality of life. At Loma Linda Proton Treatment and Research Center, technical advances are being made to make it possible to use stereotactic proton radiation therapy to treat function disorders of the spinal portion of the central nervous system. The projects aims toward designing and implementing clinical protocol for treating neuropathic pain related to SCI. However for better treatment design, recruitment of patients with neuropathic pain is required, for which accurate classification of pain becomes very important. Currently, classification directly depends on the quality of the information provided by patients to the physicians. This lack of reliable classification brings up the need to design an efficient computer-aided pain classifier for Phase 0 of this study. In this paper we are presenting the design of the overall work flow for the proton therapy for spinal cord injury system which uses web based pain classifier for the patient recruitment and in order to do so, we will focus on two parts, first an introduction of the proton therapy for spinal cord injury system, and secondly on giving some details for pain classifier which was built for patient recruitment. Key components for the system include:

- Input data sources
- Data gateway
- Graphical user interface – Pain classifier module
- Server that contains database and file storage system which allows storage of DICOM, Non-DICOM data
- Decision support tools

These components will be further discussed in the following sections.

2. METHODS

This section gives a short background on Pain classification history. It than gives a detail overview for the proton therapy for spinal cord injury system workflow and its various components.

2.1 Pain classification background

Pain continues to be a significant management problem in people with SCI. Despite this there is little consensus regarding the nature, terminology and definitions of the various types of pain that occurs following SCI. This has led to large variation in the reported incidence and prevalence of pain following spinal cord injury. Treatment studies have been hampered by inconsistent and inaccurate identification of pain types. But recently group of researchers presented their effort to classify pain in a systematic way which is shown in figure 1. The classification organizes SCI pain hierarchically into three tiers [1] [2]:

- **The first tier** (Tier 1) includes the types of nociceptive pain, neuropathic pain, other and unknown pain.
- **The second tier** (Tier 2) includes for the neuropathic and nociceptive categories various subtypes of pain identifies in previous SCI classification.
- **The third tier** (Tier 3) is used to specify the primary pain source at the organ level as well as the pathology, if either is known. For the other pain category, this tier is used to specify distinct recognized pain entities or syndromes which do not fulfill the criteria for nociceptive or neuropathic pain.

Nociceptive is a pain arising from activation of nociceptors, where a nociceptor is defined as a peripheral nerve ending or a sensory receptor that is capable of transducing and encoding noxious stimuli. Musculoskeletal pain refers to pain occurring in a region where there is at least some preserved sensation and that is believed to be arising from nociceptors within musculoskeletal structure (muscles, tendons, ligaments, joints, bones). Visceral pain refers to pain located (usually) in the thorax, abdomen or pelvis, which is believed to be primarily generated in visceral structures. Other nociceptive pain refers to nociceptive pain that do not fall into musculoskeletal or visceral categories. Neuropathic pain is caused by a lesion or disease of the somatosensory nervous system.

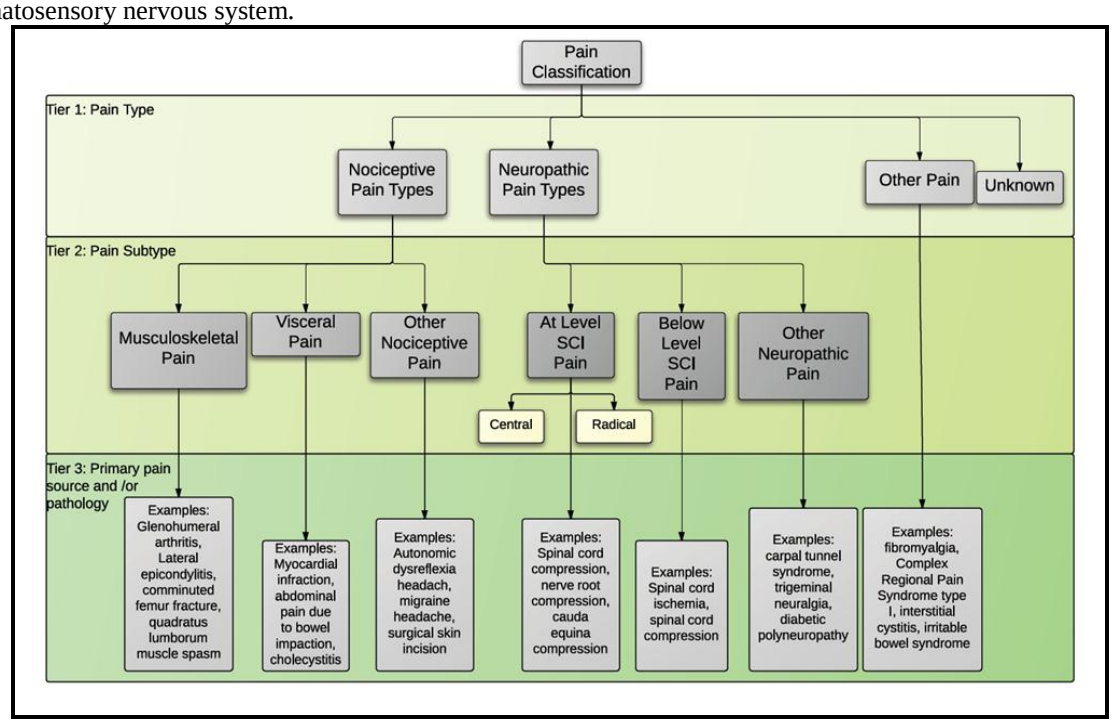

Figure 1 Pain classification

At level SCI pain refers to neuropathic pain that is electric and shooting pain and is hypersensitive in the dermatomes close to the level of injury. Below level SCI pain refers to pain with the same burning, shooting, electric qualities as the previous type of pain but it is located diffusely below the level of injury usually bilaterally in the buttocks and legs. Other neuropathic pain refers to neuropathic pain that is present above, at or below the neurological level of injury but pathologically is not related to the SCI. Other pain types defined as pain that occurs when there is no identifiable noxious stimulus nor any detectable inflammation or damage to the nervous system responsible for the pain. It is also described as dysfunctional pain. Unknown pain refers only to pain of unknown etiology and not to pain of seemingly mixed etiology that is a pain with both nociceptive and neuropathic qualities. [1][2][3]

2.2 Work flow Analysis

The workflow for the current study is based on the general proton therapy workflow. Below we are summarizing various stages of the study, as shown in figure 2 that includes:

- **Patient Recruitment** – In order to test the validity of the hypothesis that proton therapy can be used to treat functional disorder of the spinal region, it is very necessary to recruit patients with specific type of pain. Recruitment data which is text is generated at this stage.

- **Consultation** – At this point the physician will meet with the patients in order to consult about the treatment plan. Form based data is collected at this point.

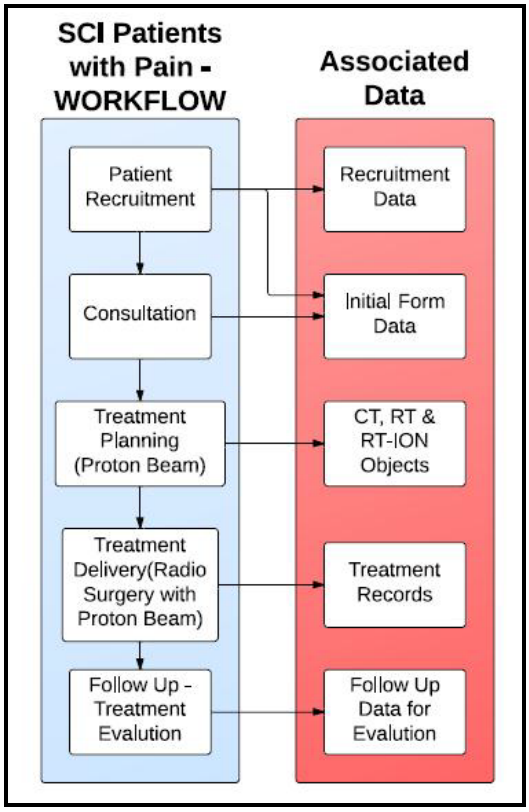

Figure 2 SCI Patients Study Workflow

- **Treatment planning** – According to the patient needs a treatment plan is designed for proton beam therapy. At this stage different DICOM objects will be captured which are described in the next section.

- **Treatment delivery** – Treatment will be delivered at this stage and treatment records will be generated.

- **Follow up / Treatment assessment** - At this stage the improvement in patient condition will be accessed using biomarkers.

2.3 Data Elements and Data Model

For efficient data mining algorithms and a computer based decision support system to work, proper organization and accessibility of data is essential. Data from proton therapy is contained in various DICOM objects as well as other data objects as described below:

- **RT Structure Set**: To carry out radiotherapy treatment planning, the target tissue and organs at risk (OAR) are defined. This process of segmentation of the tomographic images or drawing contours of target tumor and OARs leads to a set of structures, which are defined by DICOM RT structure set object.
- **RT Dose**: Treatment planning systems calculate the radiation dose distribution as a matrix of points with associated doses. These dose grid files are supported in the DICOM RT dose object. Definitions also exist in the DICOM RT dose specifications to store relationship between dose and structures through dose volume histograms and dose region of interest (ROI) statics.
- **RT image**: The RT image object addresses the requirement for image transfer found in general radiotherapy applications performed on conventional simulators, virtual simulations, and portal imaging devises. Such images may either be acquired directly from the device or digitized using a film digitizer.
- **RT ION Plan**: The RT Ion plan addresses the requirement for transfer of treatment plans generated by manual entry, a virtual simulation system, or a treatment planning system before or during a course of proton therapy treatment. Such plans may contain fractionation information, and define proton beams.
- **RT ION Beams treatment record**: The RT ion beams treatment record addresses the requirement for transfer of treatment session reports generated by a treatment verification system during a course of proton beam treatment, with optional cumulative summary information. It may also be used for transfer of treatment information during delivery
- **SCI Pain Related Data**: SCI pain data is a holding place for all information regarding pain type. It contains location of pain, groups details, intensity of pain and all different kind of information that get generated during pain classification for patient recruitment and treatment evaluation phase.

2.4 System Architecture

Based on the workflow of the study, as described in the workflow analysis section, the system architecture has been designed. The overview of the system is show in the figure 3, and each of the key components is described below:

- **Input Data** - It consists of different forms of data which are either generated or collected at various stages in the workflow. It consists of following:
  - **Recruitment Data** – This data comprises of pain classification object. It contains information for pain sites such as dermatome level, anatomical region, joint related information, ASIA level etc. It also consists text data that indicates of anyone pain location is associated with any other pain location. If there is a relation between multiple pain locations than it also gives details about how they are related.
  - **Initial Form Data** – This consists of the text based form data that is collected during patient recruitment, treatment and follow up.
  - **CT, RT & RT-ION Objects** – This consists of CT images and DICOM objects such as RT structure set, RT Dose, RT Image , RT ION Plan , RT ION Beams treatment record. All are described in Data model section above.
  - **Treatment Records** – These are the records collected from the patient charts.

- **Data Gateway**- The data gateway is responsible to get DICOM and non-DICOM data which is collected or generated at various stages of the work flow, and store it properly inside the system database. Data gateway has two small modules as described below:

  - **DICOM Module** – The DICOM module allows the system to receive DICOM RT and DICOM RT ION objects from PACS or any TPS that can export DICOM Objects. This allows the data to be uploaded to the system through an upload web interface. Upon receiving the DICOM object the DICOM receiver transfers it to the server and triggers the DICOM extractor to update the database and obtain the knowledge information. Query/ Retrieve Tool which will be available in future will be able to provide user the ability to query and retrieve DICOM studies from PACS, TPS, or any DICOM storage node to the Server.

  - **Non-DICOM Module** – The non-DICOM module has two components: Text processing module and DICOM RT converter. The former is designed to handle clinical data in a non-DICOM format (text, Excel spreadsheet etc) and the later to convert data which are defined in DICOM standard to DICOM objects.

- **Server** - Server provides computational power to other components of the system such as decision support tool, web interface and data gateway. All data, DICOM and non-DICOM, is stored and accessed using the central database. This database design is according to the DICOM data model which is explained in previous section. The design of the database plays a major role as it affects the response time of the entire system as a whole. Also various data objects that are collected has to be stored in the file system using this data base, therefore it is necessary that all form of data is taken into consideration before designing and implementing it. File storage is a major physical memory holder which contains entire data at one place.

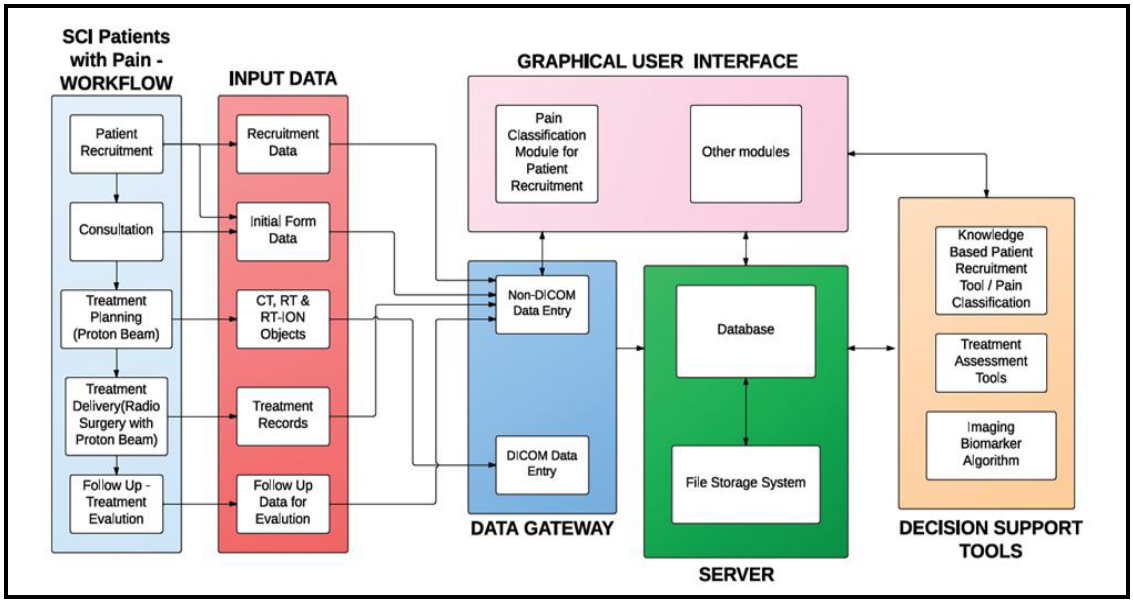

Figure 3 System Architecture

- **Graphical User Interface** - This is the front end of the system, which allows users (patients, physicians and researchers) to interact with the system. Right now the system has pain classifier developed and is under testing process. In future various modules for treatment assessment will also be available.

- **Decision Support Tools** - There are various decision support tools that can be built upon the knowledge that is contained in the server regarding patient history, pain information, treatment planning and outcomes. Our focus here

is to collect all the information, and determine some efficient data mining algorithm to train the system so that it can pull out information which can later help in evaluation of the treatment. Also once its working it can be used to improve the effectiveness of the treatment. Also for this project the decision support tools are very use full in the patient recruitment process. We have developed one such tool, for pain classification which is explained in the next section.

3. RESULTS

The system infrastructure for supporting SCI Patients undergoing the study has been designed including storing all data from screening to treatment to outcomes

Pain classifier for patient recruitment tool has been designed and has been implemented using simple tools such as jQuery and PHP. We have been able to implement a tree based pain classification model, which was described earlier in background section. The pain classifier uses three layers of information templates in order to classify any pain. Three layers of information are:

- **Dermatome (Parameter 1)** – This represents which dermatome each pain location belongs to.
- **Anatomical Region (Parameter 2)** – This indicates which anatomical region each pain location belongs to.
- **Joint or non-Joint Location (Parameter 3)** – This indicates if the pain location is a joint or not.

In order to determine values to the three parameters (1, 2, 3), the three templates are merged into a single image as shown in the figure 4 below. Once the user (patient or physician), selects a location, all three parameters gets corresponding values. After this the pain on multiple locations is grouped according the relative occurrence of the pain, or intensity of the pain. Based on this the pain is classified for each location for every patient. After this follow up questions are asked.

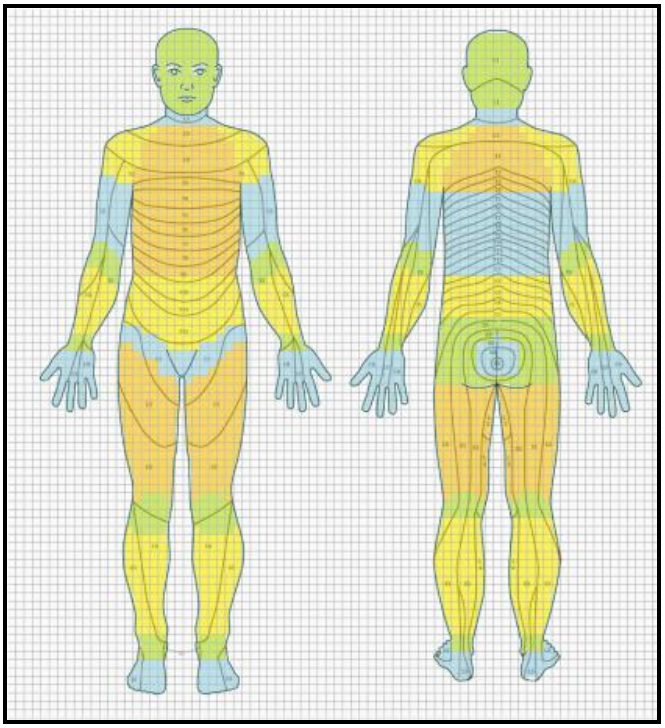

Figure 4 Dermatome information merged with Anatomical and joint information

The key features of this pain classifier are:

- It is a web based system therefore it has as high accessibility.
- It allows filtering the noise in the data. It asks follow up questions based on the classification of pain; therefore extra data is not recorded.
- Pain classification makes sure that the patients with the right kind of pain are getting recruited for the study.

Figure 5 gives the overview of the current pain classification system; it shows how the three layers of information are hidden behind a blank image.

4. CONCLUSION AND FUTURE WORK

In this paper we have presented an efficient workflow design for utilizing proton therapy for treating neuropathic pain after SCI. We also described different key components of the system architecture and gave a background on the importance of pain classification for a better treatment. Pain classification tool which was presented is a major component of patient recruitment which also affects the success of this project.

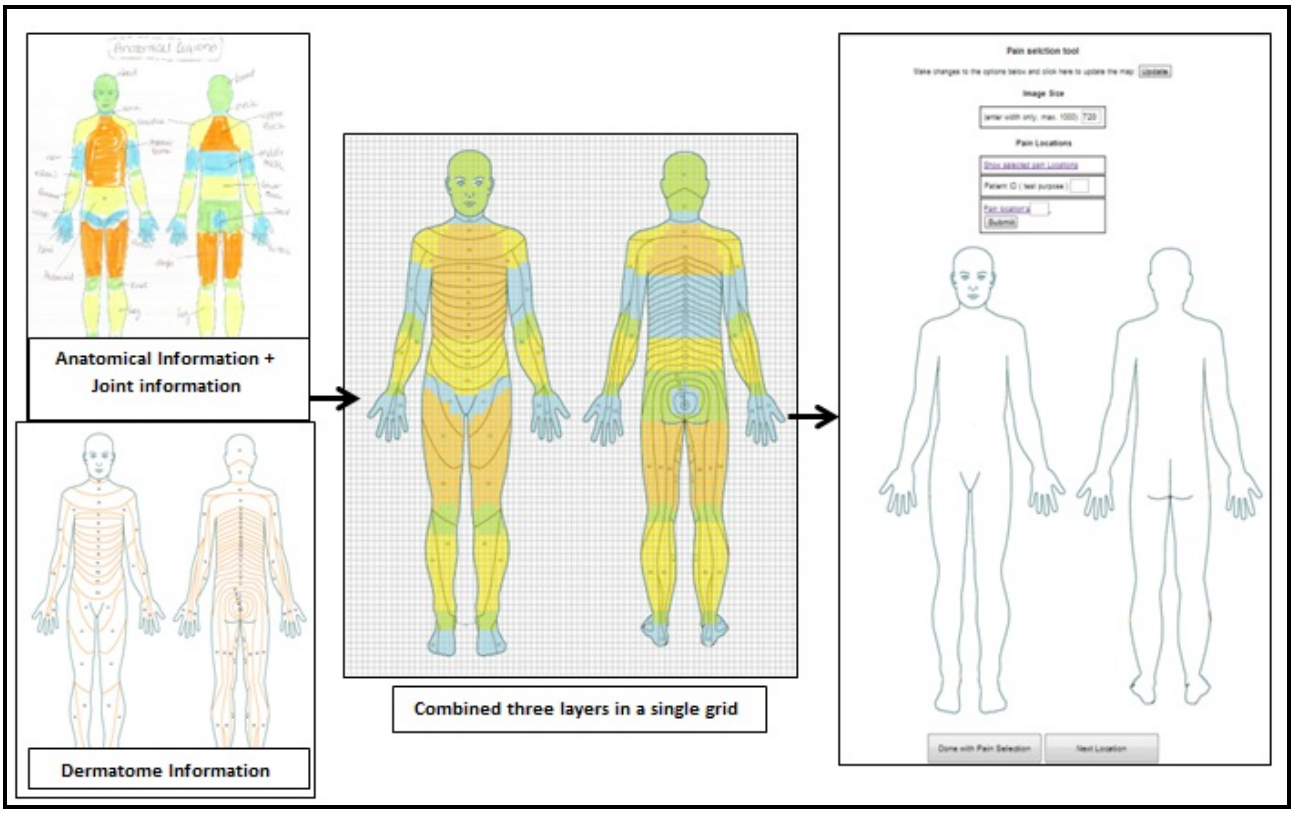

Figure 5 Graphical user interfaces

A system has been designed and developed in order to support study objects and infrastructure for future data mining and knowledge discovery. The system is designed and the system architecture similar to an electronic patient record (ePR). The concept of the ePR is a patient/subject/animal –based digital folder of clinical information obtained from various information sources. The components of an ePR include an information model, a clinical data repository, a web-based application for users, a security model, and built-in decision support.

The current version of the design has following features that support further research in the following phases of the project including:

- **Patient/Subject recruitment for clinical studies:** The system supports the pain classifier for recruitment of patients into the clinical study. This includes various forms and web based pain selection tools together with rules-based decision tree providing decision support for determining subject recruitment for the clinical study.

- **Management of data acquired from patient/subjects enrolled in the clinical study:** The system supports integration and standardization of imaging informatics data acquired from the clinical study including imaging studies, quantitative biomarkers, clinical evaluation forms, outcomes data, and treatment planning data from the treatment planning system utilized to administer the radiation dose.

The finished product is expected to be a CDSS based on a multi-media ePR system with all data acquired during the research and clinical studies integrated into a web-based system which will provide data anywhere, anytime and on any device.

REFERENCES

[1] Siddall PJ, Taylor DA, Cousins MJ, Classification of pain following spinal cord injury. Spinal Cord (1997) 35, 69-75

[2] Bryce TN, Biering-Soreson F, Finnerup NB, et al International Spinal Cord Injury Pain Classification: Part I. Background and Description. Spinal Cord(2012) 50, 413-417

[3] Middleton J, Siddall P, Managing Pain for adults with spinal cord injury. Rural Spinal Cord Injury Project,June 2002 Revised 2004

[4] Zhang A, Gertych A, Liu BJ, Automatic Bone Age Assessment for Young Children from Newborn to 7-Year-Old Using Carpal Bones, Computerized Medical Imaging and Graphics, 31:4-5, pp. 311-321, 299-310, 2007.

[5] Zhang A, Sayre J, Vachon L, Liu BJ, Huang HK, Cross-racial Discrepancies of Growth Patterns in Bone Age Assessment using the Greulich and Pyle Atlas, Radiology, V. 290, No. 1, pp. 228-235, 2009.

[6] Fernandez, J., Deshpande, R., Wang, X., Liu, B., Brazaitis, M., Munter, F., Liu, M., "Evaluation of a stand-alone computer-aided detection system for acute intra-cranial hemorrhage in emergency environments" in Medical Imaging 2011: Advanced PACS-based Imaging Informatics and Therapeutic Applications, edited by William W. Boonn, Brent J. Liu, Proceedings of SPIE Vol. 7967 (SPIE, Bellingham, WA 2011) 79670H.

Imaging Informatics-based Multimedia ePR System for Data Management and Decision Support in Rehabilitation Research

Ximing Wang[a], Sneha Verma[a], Yi Qin[a], Josh Sterling[a], Alyssa Zhou[a], Jeffrey Zhang[a], Clarisa Martinez[b], Narissa Casebeer[b], Hyunwook Koh[b], Carolee Winstein[b], Brent Liu[a]

[a]Image Processing and Informatics Lab, University of Southern California, 734 W Adams Blvd, Los Angeles, CA 90089;
[b]Motor Behavior and Neurorehabilitation Lab, Div. of Biokinesiology and Physical Therapy, USC;

ABSTRACT

With the rapid development of science and technology, large-scale rehabilitation centers and clinical rehabilitation trials usually involve significant volumes of multimedia data. Due to the global aging crisis, millions of new patients with age-related chronic diseases will produce huge amounts of data and contribute to soaring costs of medical care. Hence, a solution for effective data management and decision support will significantly reduce the expenditure and finally improve the patient life quality. Inspired from the concept of the electronic patient record (ePR), we developed a prototype system for the field of rehabilitation engineering. The system is subject or patient-oriented and customized for specific projects. The system components include data entry modules, multimedia data presentation and data retrieval. To process the multimedia data, the system includes a DICOM viewer with annotation tools and video/audio player. The system also serves as a platform for integrating decision-support tools and data mining tools. Based on the prototype system design, we developed two specific applications: 1) DOSE (a phase 1 randomized clinical trial to determine the optimal dose of therapy for rehabilitation of the arm and hand after stroke.); and 2) NEXUS project from the Rehabilitation Engineering Research Center(RERC, a NIDRR funded Rehabilitation Engineering Research Center). Currently, the system is being evaluated in the context of the DOSE trial with a projected enrollment of 60 participants over 5 years, and will be evaluated by the NEXUS project with 30 subjects. By applying the ePR concept, we developed a system in order to improve the current research workflow, reduce the cost of managing data, and provide a platform for the rapid development of future decision-support tools.

Keywords: Rehabilitation engineering, electronic Medical Record, ePR, System integration

1. INTRODUCTION

With the rapid development of science and technology, the present-day rehabilitation research and training approaches are equipped with modern technology, such as computer-aided data-processing, statistical methods, database systems, nanotechnology and medical imaging.

Enhanced with the new technology, large-scale rehabilitation centers and clinical rehabilitation trials usually involve a large volume of treatment recording data, questionnaires and multimedia data. The multimedia data are in a variety of forms, including biometric waveform data (EMG kinetic, etc.), video clips, force vectors data and medical imaging data, such as MRI and TMS(Transcranial magnetic stimulation).Moreover, due to the global aging crisis faced by today's world health care system (for example, U.S.'s 76 million baby boomers begin to retire), millions of new patients with age-related chronic diseases (such as Chronic Spinal Cord Injury, hip fracture etc.) will produce huge amounts of data and contribute to soaring costs of medical care. In addition, data processing and analysis is hampered due to the lack of a platform infrastructure for analyzing data. Collaboration between different sites is also difficult to conduct because of the lack of tools for data sharing.

In rehabilitation engineering research centers, as well as clinical rehabilitation trials, effective data management must address several challenges: tracking each participant through the workflow, collecting related data, efficiently sharing data to facilitate collaboration in different sites and providing a platform to develop a tailored computational and predictive statistical model for decision support for an individual subject.
Therefore, we aim to extend the concept of electronic patient record (ePR) system to the field of rehabilitation. The system also provides a platform for the development of data processing tools, such as statistical modeling and computer

aided detection/diagnosis. As an initial first start, we developed two specific systems based on imaging informatics concepts for the NEXUS project and the DOSE trial as examples.

2. METHODOLOGY

To realize the system, we analyzed the workflow of specific studies using database and data model standards (DICOM, HL7 and IHE) and developed a subject or patient-oriented system with basic features and components. Furthermore, the system is customized based on the specific requirements of the project.

2.1. Infrastructure development

To implement the system , we developed a prototype system and customized them based on the requirements of specific projects. As shown in the figure 1, the basic system has a centralized database and a file storage system, a web-based graphical user interface and platforms for integrating decision-support tools and data mining tools. The exchanging multimedia data include subject text demographics data, treatment records, screening and evaluation data, imaging data, video, audio, EMG, waveforms and other formats of the multimedia data.

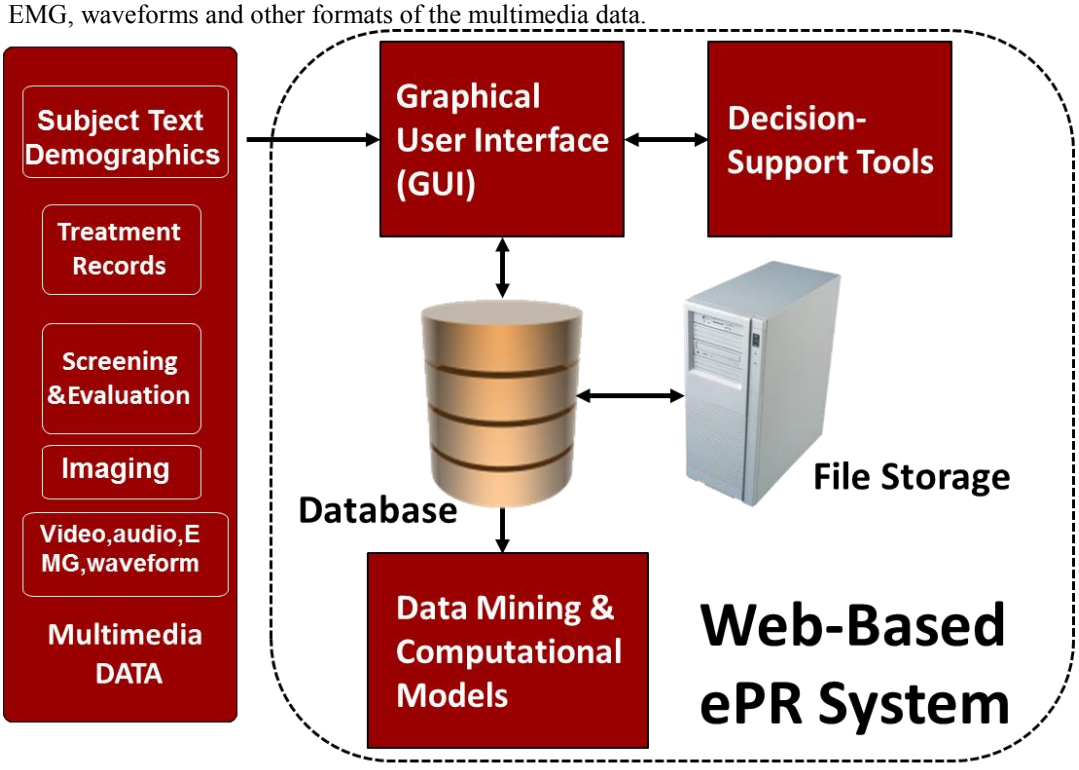

Figure 1 logic model of the prototype multimedia ePR system for rehabilitation

To realize the system, there are several features need to be considered based on the general rehabilitation trial workflow.

2.1.1 Data entry

- E-forms for collecting demographics/questionnaire data.
- Uploading and displaying multimedia data(videos, audio, kinetic, force vector etc).
- Imaging study anonymization and uploading. The images uploaded will be automatically anonymized and linked by subject ID.

2.1.2 Data presentation

- Traditionally database-based retrieval.

- A web-based zero-footprint DICOM(Digital Imaging and Communications in Medicine) viewer with annotation, ROI(Region of interest) and measuring tools.
- Provide a platform for integrating image-processing modules and data mining/computational models. We aim to develop an online tool for applying processing methods and displaying the processing result in the system, which will support the decision-making.

2.1.3 Data sharing.

The system also includes a secured sub-system for sharing data between users in different physical sites.

- Security. Compared to public data sharing systems (e.g. Dropbox, MS Sharepoint or Google Drive) which do not meet standards for protecting participant confidentiality, this data sharing sub-system allow user to store the data in trusted private data center (which has more privacy),
- Simplicity. Although public data sharing systems have lots of advanced features, sometimes they are too complex to learn and the customization is difficult. This light-weight sub-system is straightforward and easy to customize based on specific needs.

2.1.4 User control.

- User groups. The system has the feature for granting different user rights to different user groups.
- User activity tracking and logging. All users' activities will be logged, which is essential for conducting research.

2.1.5 Client side access.

- The system supports access from desktops, laptops, and mobility solutions (eg, iPAD, iPhone).

2.2 Customized system based on DOSE workflow

Based on the model described in the section 2.1, the system was designed for a clinical trial called DOSE and the system was implemented a as an example. DOSE trial aims to determine the optimal dose of stroke rehabilitation for the arm and hand, with a target subject recruitment of 60 stroke subjects with imaging and data collection. As shown in the figure 2,each subject will go through three stages: enrollment, participation, follow-up. In the enrollment stage, each subject will be screened using a series of behavioral assessments. The referred subject will be screened in person and randomized in to different groups. If the subject is enrolled, in the participation stage, the subject will go through three week-bout therapies and the multimedia treatment data, evaluation data, and medical imaging data will be collected. In each therapy cycle, a subject needs to take a pre-test bout, therapy session and a post-test bout. At the follow-up stage, each subject needs 6 monthly follow up. In each follow up session, evaluation data is collected. Upon study completion, the data will be analyzed.

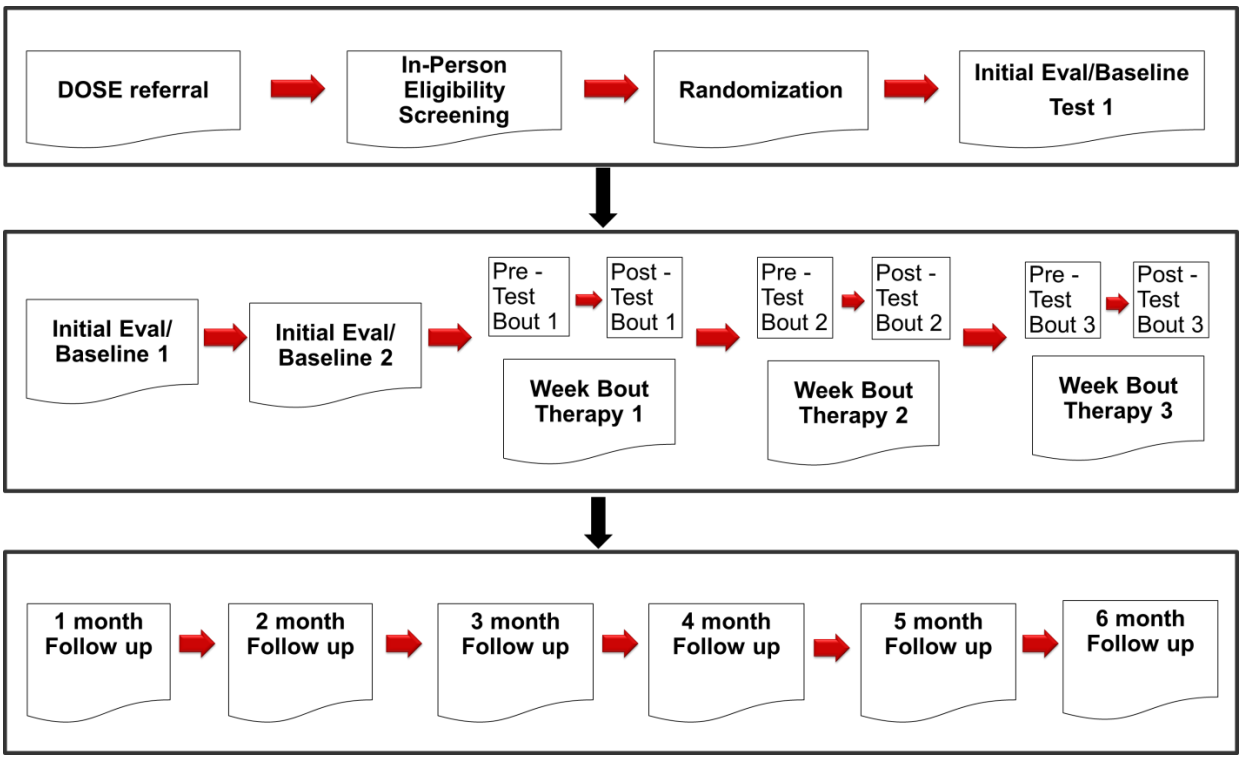

Figure 2 Workflow for each subject in the dose optimization rehabilitation trial

Based on the flow, the system is customized to three sections, screening/enrollment, treatment and evaluation, and report data analysis. The screening component not only collects testing data, but also automatically generates suggestions for making decisions on enrolment based on specified rules. In the treatment and evaluation part, the system provides a data entry solution for different types of data, and also displays the status of the trial's progress for each study participant. The report data analysis part aims to provide not only data retrieval, but also general statistical tools. These tools will show the analysis results online once the data is collected. Therefore, users can avoid a tedious work of downloading data and analyzing them.

There are five user groups in the system.

- Administrator user group. The administrators are responsible for the managing the system and regular users and backing up database regularly. The administrator is assigned to a third party who will not participate in the study.
- Evaluator user group. The study requires the evaluators to be blinded to the treatment data and any data analysis to avoid any bias over the evaluation.
- Physical therapist user group. Physical therapists are required to be blinded to any evaluation data. They only have access to the treatment recording module.
- PI/inspector user group. PI or inspector have the ability to see the whole trial data and status, but not allowed to modify any data.
- Researcher user group. Researchers are able to download the data and do the data analysis, but not allowed to modify or enter any data.

The user control mechanism provides a full logging of all users' action for security reasons and gives each user specific rights based on their responsibility.

The system is set up at a web server, with a database and a file storage system. A web based graphical user interface is developed for users to manage the system. Based on the database and file storage system, we aim to develop computational models and decision-support tools. Currently the computational models and decision-support tools are still in progress. The multimedia data used in the system includes the patient/subject text demographics, treatment records, screening and evaluation, MRI studies and TMS studies data. Client access methods include PC, MAC and

mobile devices such as iPAD, smart phones.

2.3 Customized system based on NEXUS workflow

In addition to the DOSE trial, the system was also designed based on a second project called NEXUS. NEXUS is a project at Rehabilitation Engineering Research Center (RERC), USC, which aims to assess the usability of standing balance virtual reality games specifically designed for rehabilitation. These games are designed to engage the user in therapy exercises in a controlled and customized manner. Figure 3 shows the flow of the NEXUS study. Once each subject is enrolled, the subject will take a pre-interview session, setup session and participate in games and the data is acquired after the game. A post-interview session will be done to conclude the cycle. For the data collection, a participant in a single-session counterbalanced two different dynamic balance tasks in which the participant reached for a virtual target (virtually projected jewel) or a real target(tennis ball), matched for the number and position of target and movements under an ordered set of initial conditions(static standing; dynamic stepping). The overall session includes a set of questionnaires about health of the participant, prior experience with technology and video games, and history of falls. Table 1 shows all the data related with each stages.

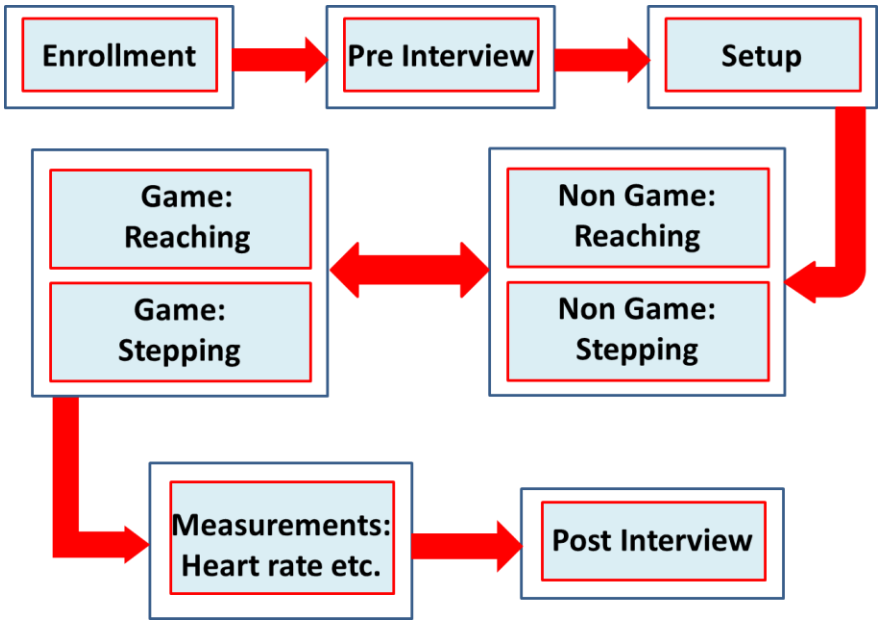

Figure 3 Workflow of the NEXUS trial

Workflow Stage	Clinical Forms	Acquired Data
Pre-Interview	• Informed consent • Demographic Information • Activities Specific Balance Confidence Scale • Immersive Tendencies Questionnaire • Tellegen Absorption Scale • Digit Symbol Coding • Ruff 2 & 7 Test • Four Square Step Test • Berg Balance Scale	• Immersive Tendency to Virtual Reality • Dynamic Balance • Demographic Information • Cognitive Processing and Memory • Attention
Setup	• EMG Electrode Placement • Force Plate Placement • EMG Max Muscle Force Test	None

	• Depth Set-up • Accelerometer & Heart Rate Meter	
Data Collection	• GAME: Reaching • GAME: Stepping	• Probe Reaction Notes • Kinect Data • Video Data • Accelerometer Data • Probe Data
	• NON-GAME: Reaching • NON-GAME: Stepping	• Probe Reaction Notes • Kinect Data • Video Data • Accelerometer Data • Probe Data
	• Accelerometer & Heart Rate Meter	• Heart Rate • Notes
Post Interview Data	• Game Engagement Form • Slater-Usoh-Steed Form • Participant Likert Form • Interview Protocol • Final Question	• Post Exposure Questionnaire • Post Exposure Interview

Table 1 Data to be collected in each stage of the Nexus workflow

The NEXUS project includes data collection stage and data processing stage. For the assessment of multimedia of data which is collected during the data collection process, efficient integration of various data objects would be beneficial to assist in data mining and knowledge discovery, which can give access to various clinicians towards the data in efficient and robust way. We developed one such system, which stores video files of participants doing all tasks, audio of participants giving post interview, text based forms as well as raw data from sources such as Kinect, accelerometer together with the basic data such as heart rate.

To facilitate the data sharing and post-processing, the system focus on providing a solution for distribution of raw data, capture post-processed information, and query retrieval. The raw multi-media data include DICOM medical images, video files and audio files. The DICOM viewer of the system will enable user to look through the images and mark ROI on the images. Moreover, post processing results, such as CAD in medical imaging will be also stored in the database. A data retrieval based on CAD will also be used to facilitate the research. Currently, the data that is being post-processed by different assigned teams working on each of the component of the data, who find the relevance based on many factors. This system will be used as a platform for their collaboration and knowledge discovery.

3. RESULT

3.1. DOSE system

We have implemented the platform for the DOSE system. The computational models and decision support tools are still in the design.

Figure 4 is the personal page for each subject. Once a subject is enrolled, this system will show a summary page to manage all the subject-related data. A timeline overview of participant's trial shows the status of the subject's treatment progress. This overview shows the subjects progress in each stage to facilitate researchers study. Below the timeline overview, users can access the data entry part in each stage of the study for this subject.

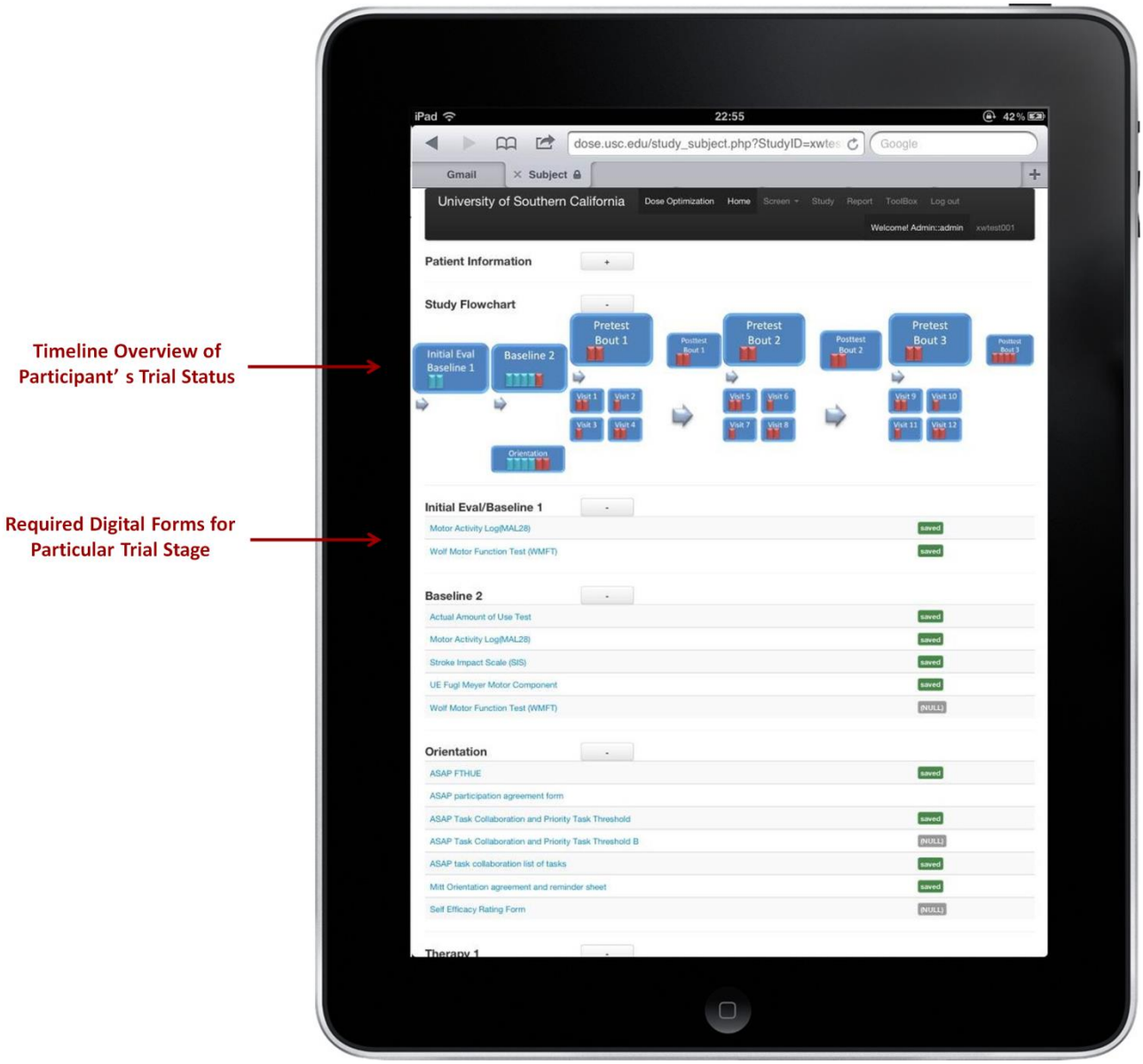

Figure 4 Screen shot of the subject personal page for DOSE system

Figure 5 is an integrated DICOM viewer with measurement tools, ROI tools and annotation tools. The screen shot shows a measurement. The zero-footprint DICOM viewer is an integrated component for data presentation.

Figure 5 Screenshot of the DICOM viewer with a measurement

The system is currently used by the DOSE trial team including three user groups. 10 subjects have been enrolled in the trial, and 60 subjects enrollment are expected in the future 3 years. The screening and part of evaluation data of the enrolled subjects have been entered into the system. Therapy data is still in the progress of collecting.

To evaluate the system, we are collecting user's feedback through questionnaires and surveys. Table 2 shows areas of issues we will be focusing. Time improvements will be compared w/ current paper-based workflow. First we will evaluate the time improvement between using the system and using traditional paper-based research. The time evaluation session include screening of a subject, enrollment decision, evaluation of a trial subject, weekly bout therapy, follow-up evaluation, report generation, and retrieving data.

Additionally, we are going to evaluate the cost of data storage, reliability of the system, user's suggestion and feedback by questionnaire, system performance, data recovery, user's satisfaction and data security.

The time improvement of	Other issues
Screening of a subject	The cost of data storage
Enrollment decision	Reliability of the system
Evaluation of a trial subject	User's suggestion and feedback
Weekly Bout Therapy	System performance
Follow-Up Evaluation	Data recovery
Report Generation	Questionnaire for User satisfaction
Retrieving and query the data	Data security

Table 2 Issues for evaluating the DOSE system

3.2 NEXUS system

The nexus system has been implemented and the data of 60 subjects are collected in the system. The data include demographics data, EMG probe data, kinect data, video data, acceleration data and audio interview data. Figure 6 shows a screen shot of the data search. The search criteria include age, gender, ID, marital status, Hispanic/Latino etc. Before the system is developed, the NEXUS trial encountered difficulties in searching for data based on different specifications. The search function provides a method to query data based multiple specifications of patient. For example, the system allows user to query all the subjects between a specific age range. Users are also able to search new conditions among the results from the previous search.

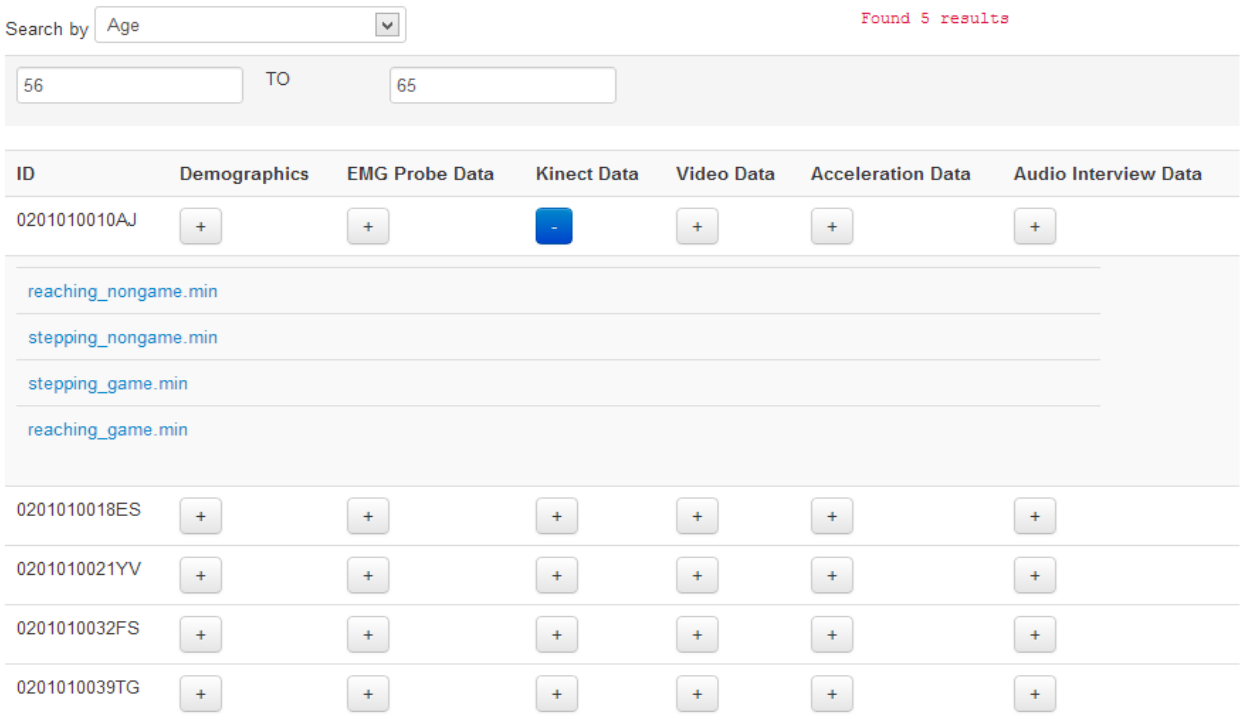

Figure 6 Screenshot of data query in the NEXUS system

The figure 7 shows a web-based video viewer for viewing video files. If a video or audio file is found, then the

viewer allows users to view it online to decide if he wants to download it.

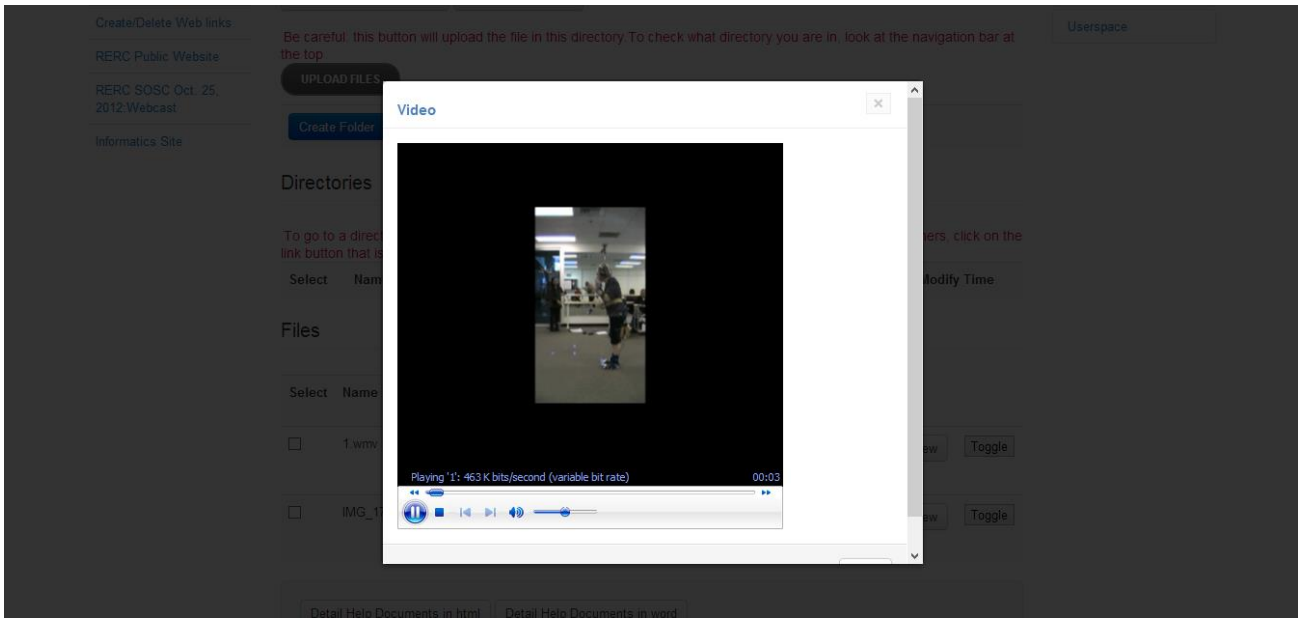

Figure 7 A web-based video viewer in the system

4. FUTURE WORK and CONCLUSION

To facilitate research and clinical trials in Rehabilitation Engineering, we developed a multimedia ePR system model for the rehabilitation. The system model aims to support the integration and data collection of both clinical information and imaging studies. In this paper, we have customized and implemented two systems based on DOSE and NEXUS clinical trial.

The functionality of the system improves the current workflow and provides a platform for the rapid development of future decision-support tools. The final goal is to use this platform to support the development of a predictive computational model to evaluate and predict the effects of therapy dose on recovery outcomes. As Brent Liu et al presented [5], figure 8 shows the final concept of the future rehabilitation ePR system. Once a new patient is enrolled, the decision support tools and predictive computational models are able to provide an individualized treatment plan for optimized outcome.

Future work for DOSE includes developing computational models and decision support tools to provide new patients with a powerful system that can provide the best predicted treatment outcome and plan individually tailored to the specific stroke patient characteristics. Future work for RERC NEXUS includes working with researchers to develop quantitative and visualization tools derived from the stored multimedia data in an integrated GUI.

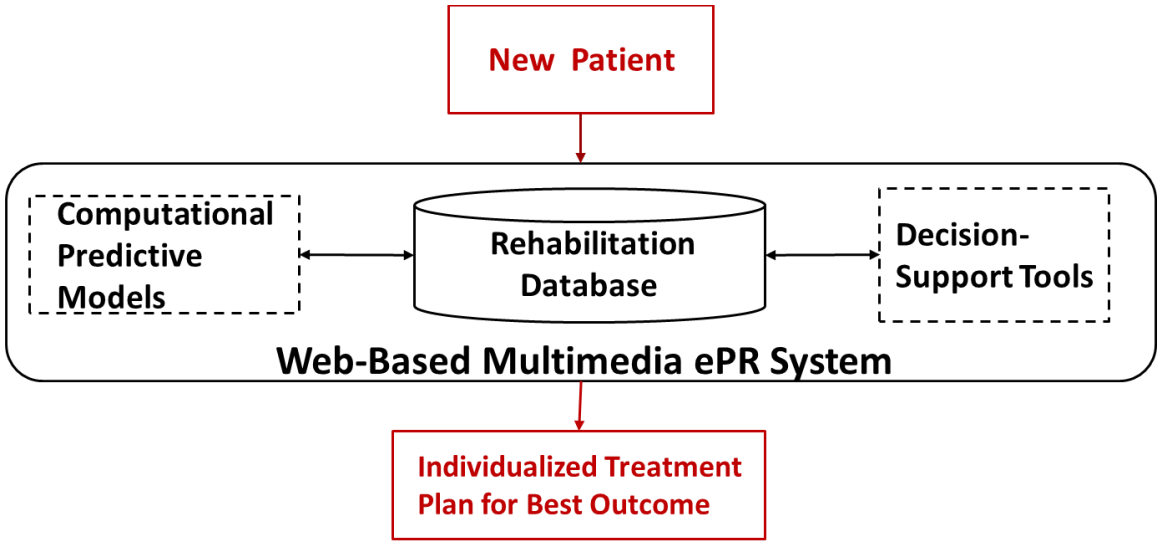

Figure 8 A future model of rehabilitation ePR system to provide new stroke patients with a best predicted treatment plan and outcome. Cited from Brent Liu et al [5]

Acknowledgments This work is supported by NIH/NICHD R01HD065438.

5. REFERENCE

[1] Huang HK. PACS and Imaging Informatics: Principles and Applications. John Wiley & Sons, Hoboken, New Jersey (2010)

[2] Digital Imaging and Communications in Medicine (DICOM) Standard 2009. ftp://medical.nema.org/medical /dicom/2009/ (2009)

[3] Winstein CJ, Requejo PS, Zelinski EM, Mulroy SJ, Crimmins EM, A Transformative Subfield in Rehabilitation Science at the Nexus of New Technologies, Aging, and Disability, Front Psychol. 2012;3:340. doi: 10.3389/fpsyg.2012.00340. Epub 2012 Sep 21.

[4]Ximing Wang, Kathleen A. Garrison, Carolee J. Winstein, Jorge R. Documet, Brent J. Liu, A multimedia comprehensive imaging informatics system with decision support tools for a multisite collaboration research of stroke rehabilitation, Proceedings of SPIE Medical Imaging,2012

[5] Brent J. Liu, Carolee J. Winstein, Ximing Wang, Matt Konersman, Clarisa Martinez, Nicolas Schweighofer, An imaging informatics-based ePR (electronic patient record) system for providing decision support in evaluating dose optimization in stroke rehabilitation, Proceedings of SPIE Medical Imaging, 2012

[6] Dobkin BH Strategies for stroke rehabilitation. Lancet Neurol 3:528-536. (2004)

[7] Winstein CJ, Wing AM, Whitall J Motor control and learning principles for rehabilitation of upper limb movements after brain injury. In: Handbook of Neuropsychology: Plasticity and Rehabilitation (Grafman J, Robertson I, eds), pp 77-137. Amsterdam: Elsevier Science. (2003)

In Memory of Three Pioneers – Ledley (Biomedical Imaging), Greenfield (Medical Physics) and Kangarloo (PACS and Informatics)

H.K. (Bernie) Huang, D.Sc., FRCR (Hon.), FAIMBE
Emeritus Professor of Radiology & Biomedical Engineering
Image Processing and Informatics Laboratory, USC
734 W. Adams Blvd, Los Angeles, CA 90089
berniehkhuang@gmail.com

ABSTRACT

In 2012, we lost three pioneers: Robert S. Ledley in Biomedical Imaging, Moses Greenfield in Medical Physics, and Hooshang Kangarloo in PACS and Informatics. They had their own respective background, interest, and contribution to science and technology that cemented certain cornerstones of today's Biomedical Imaging Informatics. Among other accomplishments, this memory focuses on their contributions related to medical imaging, medical physics, PACS and informatics. The evolution of medical imaging informatics can be traced from the footprints of these three pioneers through the time line shown in the last figure in the paper. Their dedication in contributing to this field would be remembered by their students, fellows and colleagues who are now continuously leading the growth in this field of science and technology.

Keywords: Ledley, Greenfield, Kangarloo, Medical Physics, Biomedical Imagine, PACS, Imaging Informatics

1. INTRODUCTION

In 2012, we lost three pioneers: Robert S. Ledley in Biomedical Imaging, Moses Greenfield in Medical Physics, and Hooshang Kangarloo in PACS and Informatics. They had their own respective background, interest, and contribution to science and technology that cemented certain cornerstones of today's Biomedical Imaging Informatics. Among other accomplishments, this memory focuses on their contributions related to medical imaging, medical physics, PACS and informatics. This author was fortunate to have had the opportunity to be mentored and to worked with them during their progressive career paths.

2. MATERIALS

2.1 Professor Robert Steven Ledley

Figure 1. Robert Steven Ledley (June 28, 1926 – July 24, 2012, aged 86)

Prof. R.S. Ledley, Professor Emeritus of Physiology and Biophysics and Professor of Radiology at Georgetown University Medical School pioneered the use of electronic digital computers in biology and medicine. He contributed two influential articles in *Science*: "Reasoning Foundations of Medical Diagnosis" in 1959 [1] and "Digital Electronic Computers in Biomedical Science" in 1964 [2]. In 1965, he published the fundamental "Use of Computers in Biology and Medicine" book that became the classic of this field [3]. In 1960 he founded the National Biomedical Research Foundation (NBRF) to promote the use of computers and electronic equipment in biomedical research. At NBRF, Ledley pursued several major innovative projects to convert analog to digital images. In films, it was the FIDAC (Film Input to Digital Automatic Computer) in 60s for 35 mm (Fig. 3, upper middle) and DRIDAC (Drum Input to Digital Automatic Computer) in 70s for 8''x10'' (Fig. 3, upper right). In microscopic slides it was the SPIDAC (Specimen Input to Digital Automatics Computer), which automated the analysis of chromosomes in late 70s (Fig. 3, middle and bottom). He also invented the ACTA (Automatic Computerized Transverse Axial), the first whole-body CT scanner in the middle of 70s (Fig. 4). NBRF was affiliated with the Georgetown University Medical School in late 60s as a research laboratory until Ledley's emeritus in 2010. Through the years, he has provided opportunities to many young multidisciplinary open minds to explore the use of computers and electronics in medicine by luring them to participate in his Pattern Recognition Laboratory as interns and research scientists (Fig. 2).

Ledley initiated and remained as the Editor-in-chief of four scientific journals starting from the 1970s: "Pattern Recognition", "Computers in Biology and Medicine", "Computer Languages, Systems and Structures", and "Computerized Medical Imaging and Graphics". These journals are still in publication as of today.

Among many other accomplishments and awards, the ACTA prototype was displayed at the Smithsonian's National Museum of American History, Washington, DC. The museum also established an archive for materials to the development of ACTA. Ledley was inducted into the National Inventors Hall of Fame sponsored by the U.S. Patent and Trademark Office in 1990. And "for pioneering his contributions to biomedical computing and engineering, including inventing the whole-body CT scanner which revolutionized the practice of radiology, and for his role in developing automated chromosome analysis for prenatal diagnosis of birth defects", he was awarded the National Medal of Technology and Innovation by President Bill Clinton in 1997. The National Institutes of Health honored him in a public lecture in 2008: "A Lifetime of Biomedical Computing: A Conversation with Robert Ledley".

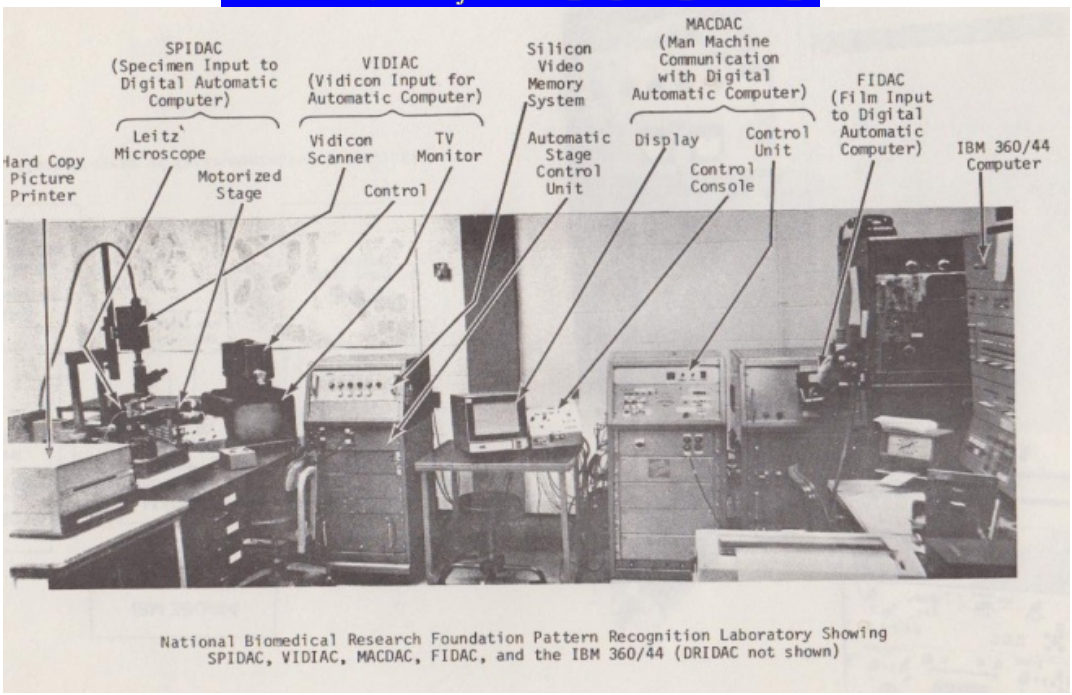

Figure 2. Pattern Recognition Lab, National Biomedical Research Foundation

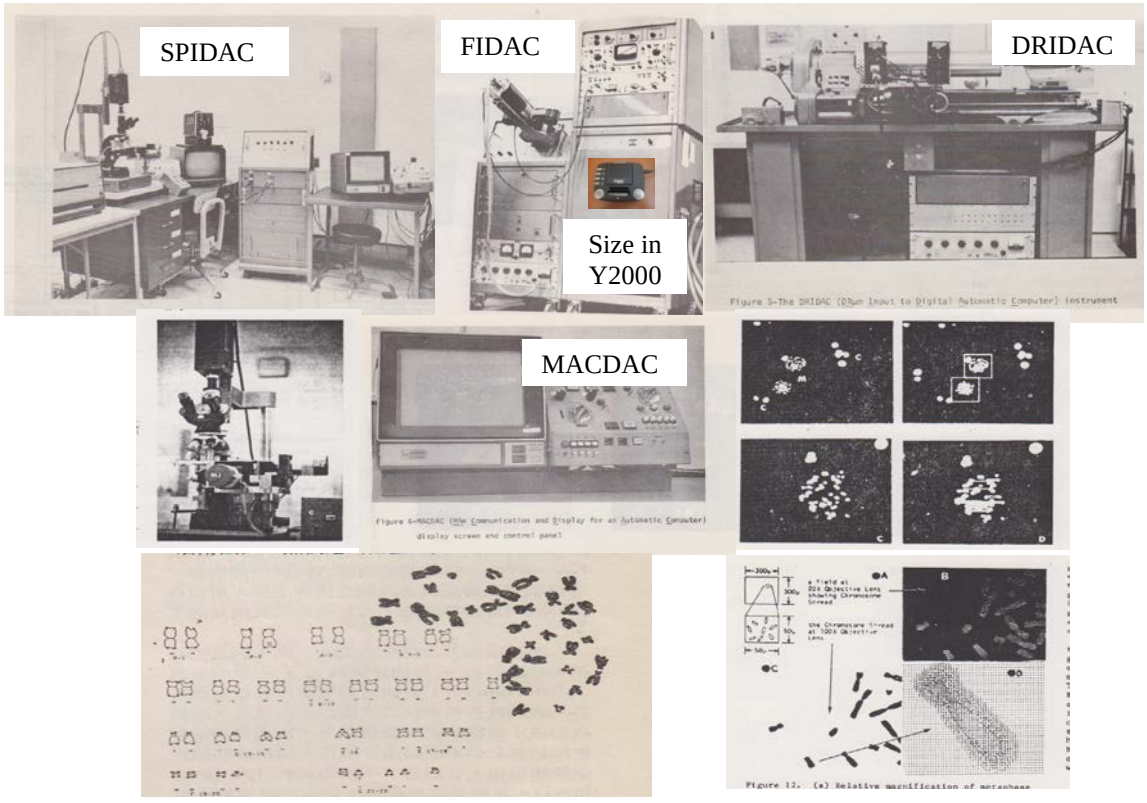

Figure 3. Innovative medical imaging components in the Pattern Recognition Lab in mid 70s: SPIDAC (Specimen Input to Digital Automatic Computer), FIDAC (Film Input to Digital Automatic Computer), DRIDAC (Drum Input to Digital Automatic Computer), MACDAC (Man Machine Interface to Digital Automatic Computer (MACDAC). SPIDAC + VIDAC (video memory) + MACDAC (interface) + IBM360/44 was the equivalent of today's Pathology PACS, showing an example of automatic chromosome analysis – microscopic scanning, detecting two metaphase cells (Low resolution) and chromosomes (High), analyzing each chromosome, and Karyotyping.

Figure 4. LT: ACTA, the first whole body CT scanner, with 2 slices per scan in 4 ½ minutes. The background is the inventor, Professor R. Ledley. RT: The first cross-sectional anatomy book, images in the book were obtained from the ACTA scanner. Williams & Wilkins, 1977.

2.2 Professor Moses Greenfield

Figure 5. Moses Greenfield, March 8, 1916 – July 26, 2012 (97Y)

Professor M. Greenfield, Professor Emeritus of Radiological Sciences, Founder of the Medical Physics PhD Program in UCLA. In 1948, when UCLA established the Department of Radiological Science, Greenfield was recruited to establish the Clinical Physics Lab inside a clinical department. He later formed and was appointed as the Director of the well-known Medical Physics PhD Program at UCLA from 1960 – 1982. After he retired, Greenfield was instrumental in expanding the Graduate Program and adopted the new name of 'Biomedical Physics' Graduate Program to signify a broadened scope by the offering of four subspecialties in: Biophysics/Nuclear Medicine, Medical Imaging, Radiobiology and Experimental Radiation Oncology and Therapeutic Medical Physics. Greenfield was asked to assume the position of Acting Director of the Graduate Program from 1992 - 1996. During his tenure at UCLA, Greenfield co-founded the American Association of Physicists in Medicine (AAPM) and the American College of Medical Physics. He received the William D. Coolidge Award, AAPM, 1991. The 2005 Issue of the Journal of Applied Clinical Medical Physics (JACMP) was dedicated to his accomplishments in this field.

Greenfield received an NIH Training Grant in "Medical Physics" in the late 1970s. With the Graduate Program broadened to "Biomedical Physics" in the 80s, the Training Grant was renewed. The Training Grant has been running continuously until today by the succeeding Directors of the Graduate Program as the Principal Investigator, one of the longest NIH Training Grants in this field. The UCLA Biomedical Physics Program graduated more than 266 MS and PhD degrees (as of 2010), a major contribution to the Medical Physics Profession. Many of the graduates have dedicated to the fields of medical imaging, PACS and Imaging Informatics continuing the research and development efforts.

Figure 6. LT: Professor Greenfield and Mrs. Greenfield. RT: One of the Annual Greenfield Award ceremonies at the Biomedical Physics Graduate Program, UCLA. Dr Greenfield with his long-term colleagues Professors Norman and Hoffman and the awardee Mr. Holdsworth.

2.3 Professor Hooshang Kangarloo

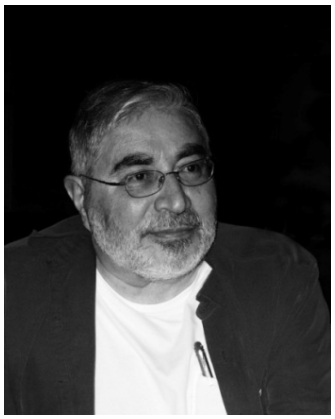

Figure 7. Hooshang Kangarloo Dec 24, 1944 - May 15, 2012 (aged 67)

Professor H. Kangarloo, Professor of Pediatrics, Radiology, and Bioengineering at UCLA was Section Head of Pediatric Imaging from 1978-1987, director of residency training from 1984-1986, and became the first Leo G. Rigler Chairman of the Department of Radiological Sciences from 1986 to 1995. Under his chairmanship, UCLA became renowned as a major innovator in PACS. Using the integrated computed radiography, CT, MR and US images displayed on multiple 1K monitors, the pediatric PACS was on-line for daily clinical use in late 80s. From 1984 to 2005, Kangarloo was the principal investigator of five NIH-funded R01 grants, a training grant from the National Library of Medicine (NLM) in medical imaging informatics and a continuously funded Program Project Grant in digital imaging, PACS and informatics that spanned 20 years. He became Emeritus Professor and Chairman of the Department of Radiological Sciences in 2005 and continued leading the research program in PACS and medical imaging informatics until 2012.

Kangarloo has been recognized as one of the best teachers in his field of research and clinical practice. He was personally responsible for mentoring over a dozen fellows in pediatric radiology and graduated some PhD students in Biomedical Physics and Biomedical Engineering, with the majority now in academic positions. He had been awarded three times each by the Departments of Pediatrics and by the Radiology for outstanding teaching, and was a recipient of UCLA's Gold Medal for teaching excellence and a number of national and international awards in teaching as well.

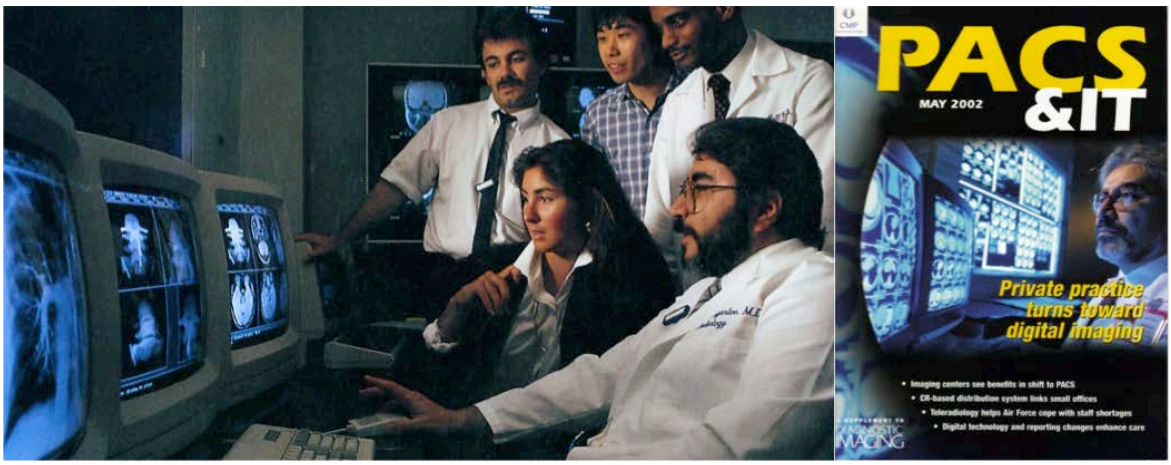

Figure 8. LT: Professor Kangarloo in the Pediatric Radiology reading room used his in-house developed UCLA PACS in late 80s to review cases with his colleague (Professor Hall, upper right) and to teach the residents.

Professor Cho (checker shirt), now Professor at U of Washington, was the PACS manager. RT. Kangarloo interviewed by the Journal of Diagnosis Imaging.

3. RESULTS AND CONCLUSION

The evolution of medical imaging informatics can be traced from the footprints of these three pioneers through the time line shown in Figure 9. Their dedication in contributing to this field would be remembered by their students, fellows and colleagues who are now continuously leading the growth in this field of science and technology.

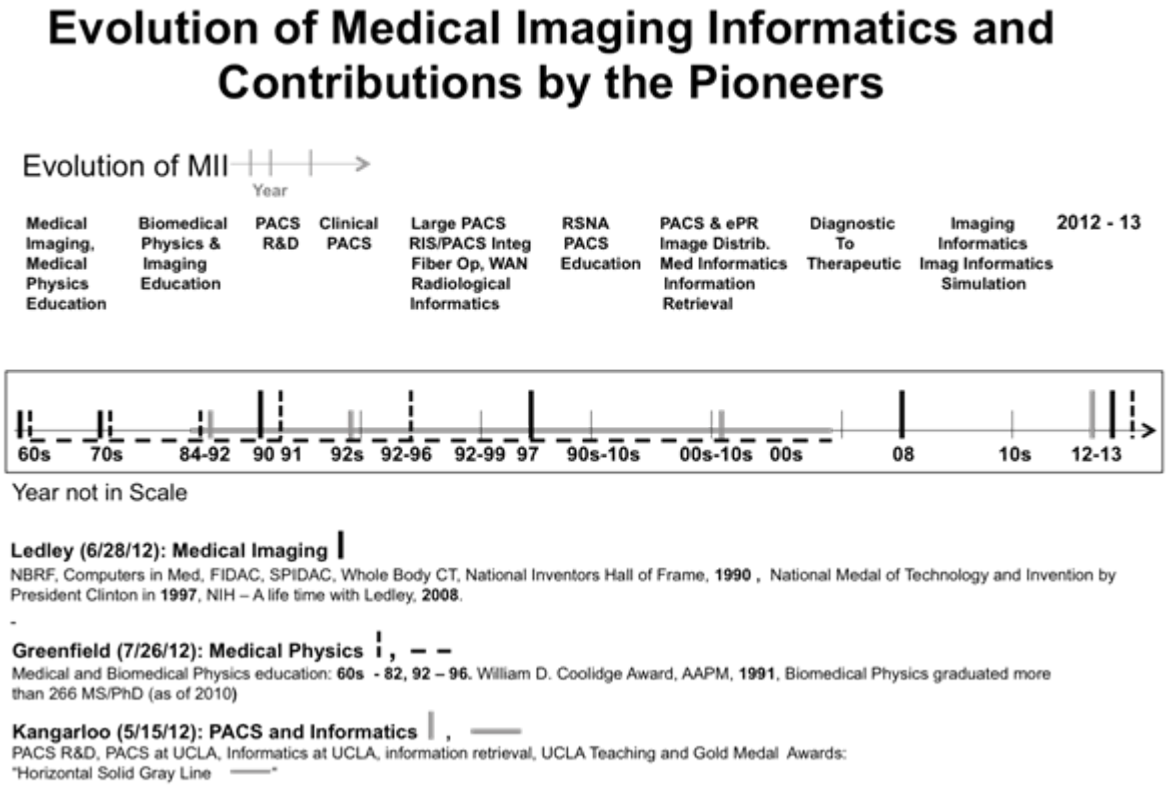

Figure 9. Evolution of Medical Imaging Informatics and the three Pioneers' Contributions

REFERENCES

[1] R.S. Ledley, L.B. Lusted, "Reasoning Foundations of Medical Diagnosis", *Science*, 130:9-21 July 1959.

[2] R.S. Ledley, "High-speed automatic analysis of biomedical pictures", *Science*, 146(3641): 216-223, Oct, 1964.

[3] R.S. Ledley, "Use of Computers in Biology and Medicine", McGraw Hill, NY, 1965.

ACKNOWLEDGEMENTS

Some contents were contributed by Professors Ricky Taira and Mike McNitt Gray. Ms. Ruchi Deshpande assisted in the editing.

SELECTED PEER REVIEW REPRINTS

A novel conformity index for intensity modulated radiation therapy plan evaluation

Fion W. K. Cheung[a)]
Department of Clinical Oncology, Queen Elizabeth Hospital, 999077 Hong Kong Special Administrative Region and Department of Health Technology and Informatics, Hong Kong Polytechnic University, 999077 Hong Kong Special Administrative Region

Maria Y. Y. Law
Medical Physics and Research Department, Hong Kong Sanatorium and Hospital, 999077 Hong Kong Special Administrative Region and Department of Health Technology and Informatics, Hong Kong Polytechnic University, 999077 Hong Kong Special Administrative Region

(Received 3 March 2012; revised 13 June 2012; accepted for publication 19 July 2012; published 4 September 2012)

Purpose: Intensity modulated radiation therapy (IMRT) has gained popularity in the treatment of cancers. Manual evaluation of IMRT plans for head-and-neck cancers has been especially challenging necessitating efficient and objective assessment tools. In this work, the authors address this issue by developing a personalized conformity index (CI) for comparison of IMRT plans for head-and-neck cancers and evaluating its plan quality discerning power in comparison with other widely used CIs.
Methods: A two-dimensional CI with dose and distance incorporated (CI_{DD}) was developed using the MATLAB program language, to quantify the planning target volume (PTV) coverage. Valuable information contained in the digital imaging and communication in medicine (DICOM) RT objects were harvested for computation of each of the CI_{DD} components. Apart from the dose penalty factor, a distance-based exponential function was employed by varying the penalty weight associated with the location of cold spots within the PTV. With the goal of deriving a customized penalty factor, the distances between individual pixel and its nearest PTV boundary was found. Using the exponential function, the impact of distance penalty was substantially larger for cold spots closer to the PTV centroid but petered out quickly wherever they were situated in the vicinity of PTV border. In order to evaluate the CI_{DD} scoring system, three CT image data sets of nasopharyngeal carcinoma (NPC) patients were collected. Ten IMRT plans with degrading qualities were generated from each dataset and were ranked based on CI_{DD} and other existing indices. The coefficient of variance was calculated for each dataset to compare the degree of variation.
Results: The CI_{DD} scoring system that considered spatial importance of each voxel within the PTV was successfully developed. The results demonstrated that the CI_{DD} including four discrete factors could provide accurate rankings of plan quality by examining the relative importance of each cold spot within the PTVs. Apart from the dose penalty factor, a distance-based exponential function was employed taking the specific tumor geometry into account. Compared with other commonly used CIs, the CI_{DD} resulted in the largest coefficient of variance among the ten IMRT plans for each dataset, indicating that its discerning power was the best among the CIs being compared.
Conclusions: The CI_{DD} scoring system was successfully developed to incorporate patient-specific spatial dose information and provide a geometry-based physical index for comparison of IMRT plans for head-and-neck cancers. By taking individual tumor geometry into account, the superiority of CI_{DD} in plan discerning power was demonstrated. The use of CI_{DD} could provide an effective means of benchmarking performance, reducing treatment plan variability, and advancing the quality of current IMRT planning. © *2012 American Association of Physicists in Medicine*. [http://dx.doi.org/10.1118/1.4742848]

Key words: intensity modulated radiation therapy, conformity index, plan evaluation, head-and-neck cancer, digital imaging and communication in medicine

I. INTRODUCTION

Renowned for its dose-sculpting ability, intensity modulated radiation therapy (IMRT) has gained popularity in the treatment of cancers. Evaluation and comparison of IMRT plans for head-and-neck cancers have long been the thorny issues because resultant dose distribution is closely constrained by the subjective experiences of the planners, the patient anatomical geometry, and the complexity of clinical goals.[1,2] To assure the IMRT plan quality, some quantitative quality control measures are absolutely necessary. The International Organization for Standardization (ISO) has suggested standards for use in radiation oncology to achieve consistency of practice and optimal quality.[3] As an extension of slice-by-slice isodose evaluation and dose volume histogram (DVH) analysis, the International Commission on Radiation Units and

Measurements (ICRU) Report 83 recommended the use of conformity indices (CIs) in the routine IMRT reporting.[4] Conformity indice was first proposed in the Radiation Therapy Oncology Group (RTOG) radiosurgery guidelines in 1993 and also described in Report 62 of the ICRU.[5,6] Their definition was the ratio of reference isodose volume to target volume. Depending on the choice of reference isodose volume, the results vary considerably leading to erroneous conclusions. Despite being easy to interpret, it could yield false perfect score in the extreme cases of nonconcordance of target and isodoses. To get around the problem, the Saint-Anne, Lariboisière, Tenon suggested a coverage volume factor which was defined as the fraction of target volume that received a minimum specified therapeutic dose.[7] The index, nevertheless, does not quantify the irradiated critical structure volumes surrounding the target.

Leung *et al.* introduced a credit-based merit function M taking into account all planning target volume (PTV) check point doses which were used as a guideline to approve a treatment plan.[8] M, also known as target coverage factor, was defined as

$$M = \frac{1}{r}\sum_{j=1}^{r}\left\{\frac{\sum_{i=1}^{p}\left(\frac{V_{T_j,D_i}}{V_{T_j,RD_i}}\right)+\sum_{i=1}^{q}\left(1-\frac{V_{T_j,D_i}}{V_{T_j,AD_i}}\right)}{\sum_{i=1}^{p}\left(\frac{100}{V_{T_j,RD_i}}\right)+q}\right\},$$

where p was the number of cold spot checks, q was the number of hot spot checks, r was the number of targets of different prescription doses, V_{T_j,D_i} represented the volume of the jth target (in %) receiving dose of at least the ith dose level, V_{T_j,RD_i} represented the minimum volume of the jth target (in %) receiving at least the ith dose level, and V_{T_j,AD_i} represented the allowable volume of the jth target (in %) receiving at least the ith dose level. Penalty is incurred based on target dose-volume violations. Meanwhile, credit is awarded when the volume exceeds the minimum PTV dose requirement for plan acceptance. The primary strength of this function is its ability to monitor the presence and magnitude of hot and cold spots. Yet, no differential penalty is enforced based on the type of violation.

On the other hand, Miften *et al.* intended to develop the target conformity index (TCI) employing a flexible penalty function.[9] The TCI was defined as

$$\mathrm{TCI} = P_{\mathrm{PTV}} \times \left(\frac{\mathrm{PTV_{TD}}}{\mathrm{PTV}}\right),$$

where $\mathrm{PTV_{TD}}$ was the part of PTV enclosed by the therapeutic dose. An exponential function was adopted to model the target penalty function (P_{PTV}), resulting in different penalty values based on the magnitude of dose-volume violation and the type of violation. The penalty values range between 0 and 1. A more drastic Gaussian function is adopted to penalize cold spot since this is somewhat more of a clinical problem than hot spot. However, insufficient spatial information is available to exactly locate the overdose and underdose regions.

Lomax and Scheib presented healthy tissues conformity index (HTCI) taking into account exclusively the irradiation of healthy tissues.[10] It was determined as the ratio of the target volume covered by the reference isodose to the reference isodose volume. There are several practical limitations that should be kept in mind when using this index. As Leung *et al.* pointed out, HTCI could lead to a potential false perfect score when just a tiny reference dose volume is located inside the target resulting in obviously suboptimal target coverage.[8] More importantly, this evaluation model could break down whenever simultaneous integrated boost approach is applied with several targets receiving different prescribed doses. Though the conformity of high-dose targets is truly reflected, HTCI could give erroneous results for coverage of intermediate- and low-risk targets. A modified HTCI was hence introduced by Leung *et al.* to compensate for these defects.[8] The irradiated target volume as defined represents the target volume whose prescription dose is higher than or equal to the reference dose level. The effect of different doses to targets could hence be demonstrated. To generalize the formula to cater for numerous prescribed doses to various targets, HTCI was redefined as

$$\mathrm{HTCI} = \frac{1}{r}\sum_{i=1}^{r}\left(\frac{TV_{RI,i}}{V_{RI,i}}\right),$$

where r was the number of targets of different prescription doses. $TV_{RI,i}$ represented the target volume covered by the ith reference dose, and $V_{RI,i}$ represented the total isodose volume of the ith reference dose.

Van't Riet *et al.* and Paddick postulated an alternative conformity index (called conformation number) comprising two terms: The first was a measure of dosimetric target coverage, and the second was a measure of normal tissue overdose.[11,12] The conformation number (CN) was defined as

$$\mathrm{CN} = \frac{TV_{RI}}{TV} \times \frac{TV_{RI}}{V_{RI}},$$

where TV_{RI} represented the target volume covered by the reference isodose, TV represented the target volume and V_{RI} represented the volume of the reference isodose.

Using this definition it is clear that CN = 1 when there is a complete target coverage, as well as complete organ sparing. Any deviation in either one of these parameters results in a lower value of CN. CN raises two particular comments. First, it suffers from an inherent loss of information that accounts for more than one factor. Different plans with vastly differing potential outcomes could have the same value of CN. Second, it only addresses a global healthy tissue dose, lumping all nontumor tissue together as normal tissue. A summary table (Table I) compares RTOG, HTCI, and CN in various clinical settings.

Initially proposed for brachtherapy, the conformity index of Baltas *et al.* abbreviated as COIN was the production of CN and a term accounting of critical organ doses.[13] COIN was defined as

$$\mathrm{COIN} = \mathrm{CN} \times \prod_{i=1}^{N_{co}}\left(1-\frac{V_{\mathrm{coref},i}}{V_{\mathrm{co},i}}\right),$$

where N_{co} represented the number of critical organs, $V_{\mathrm{coref},i}$ represented the critical organ volume receiving at least the

TABLE I. Comparison of various indices in relation to various treatment plans.

Treatment plan	Parameters	RTOG	HTCI	CN
	$TV = 6\ \text{cm}^3$ $V_{RI} = 8\ \text{cm}^3$ $TV_{RI} = 6\ \text{cm}^3$	1.33	0.75	0.75
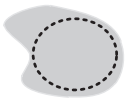	$TV = 6\ \text{cm}^3$ $V_{RI} = 4.8\ \text{cm}^3$ $TV_{RI} = 4.8\ \text{cm}^3$	0.80	1.00	0.80
	$TV = 6\ \text{cm}^3$ $V_{RI} = 6\ \text{cm}^3$ $TV_{RI} = 0\ \text{cm}^3$	1.00	0.00	0.00
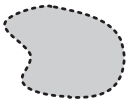	$TV = 6\ \text{cm}^3$ $V_{RI} = 6\ \text{cm}^3$ $TV_{RI} = 6\ \text{cm}^3$	1.00	1.00	1.00

Note. TV = target volume (gray); V_{RI} = volume of the reference isodose (dotted line); TV_{RI} = target volume covered by the reference isodose = intersection of TV and V_{RI}.

reference dose, $V_{\text{co},i}$ represented the critical organ volume, and CN represented the Van't Riet's conformation number. Penalty is given whenever organ at risk (OAR) volumes receive at least the prescription doses. Nevertheless, in many cases, OAR tolerances are much lower than tumor prescription doses. COIN presents two significant drawbacks. First, it provides indissociable information, making it impossible to discern the contribution of each term to the resultant COIN value. The second issue is that COIN is not calculated for each organ at its specific tolerance level. As opposed to the COIN index, critical organ scoring index (COSI) was developed specifically to compare individual critical organ's involvement at different dose levels.[14] The COSI was defined as

$$\text{COSI} = 1 - \frac{V(\text{OAR})_{>\text{tol}}}{\text{TC}_V},$$

where $V(\text{OAR})_{>\text{tol}}$ was the fraction of volume of OAR receiving more than a predefined tolerance dose, and TC_V was the volumetric target coverage, defined as the fractional volume of PTV covered by the prescription isodose.

Any deviation from the perfect score of unity could be either due to insufficient target coverage or critical organ overdose. Its main gain is the ability to distinguish different tolerance doses for different organs, whereas CN only addresses a global healthy tissue dose. Knowing which OAR is being assessed, the physicians could make a more informed choice of the optimal plan. In extreme cases, COSI could be equal to unity when a plan provides a complete organ sparing, regardless of tumor coverage. Though COSI could score target underdose and OAR overdose, it contains no information about the overall plan conformity. Owing to a certain loss of information, different quality plans could have identical COSI values requiring further investigation of DVHs and isodose lines to determine their relative merits.

In the era of personalized cancer medicine, much emphasis has been put on the inherent variability in tumors and the need for a tailor-made treatment regimen.[15] Though a variety of CIs have been proposed to describe the overall plan conformity, few existing indices take individual tumor geometry into account.[16] To bridge the gap, the aim of this study was to develop a patient-specific CI for comparison of IMRT plans for head-and-neck cancers and to evaluate its plan quality discerning power in comparison with other widely used indices.

II. METHODS

In order to quantify the PTV coverage, a two-dimensional conformity index with dose and distance incorporated (CI_{DD}) was developed using the MATLAB version 7.12 (R2011a) (The MathWorks, Inc., Natick, MA). The proposed algorithm for calculation of CI_{DD} was based on two central assumptions. First, adequate gross tumor volume (GTV) coverage is mandatory to reduce the likelihood of local recurrence and improve survival rate. Second, cold spots are generally more acceptable if they are more distant from GTV. The CI_{DD} scoring system contains four major components, namely, GTV coverage factor, GTV underdose factor, (PTV minus GTV) coverage factor, and (PTV minus GTV) underdose and distance factor. Using IMRT with simultaneous modulated accelerated radiation therapy (SMART) boost, the GTV is given a higher total radiation dose within the same treatment period than the surrounding subclinical regions enabling differential dose delivery to different parts of the targets. In our standard treatment guidelines for nasopharyngeal carcinoma (NPC), subscripts with the GTV nomenclature are applied to distinguish between the primary nasopharyngeal tumor (*np* as in GTV_{np}) and nodal gross tumor volume (*n* as in GTV_n). Note that for a typical head-and-neck case, the prescribed dose to

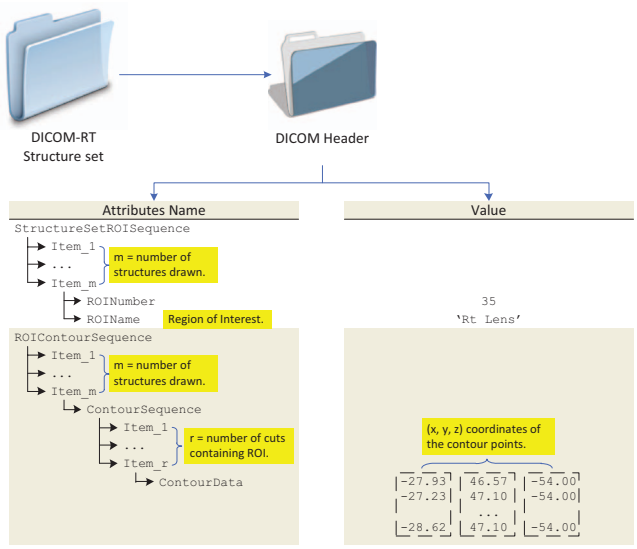

FIG. 1. Attributes of RT Structure Set module required for computation of CI_{DD}.

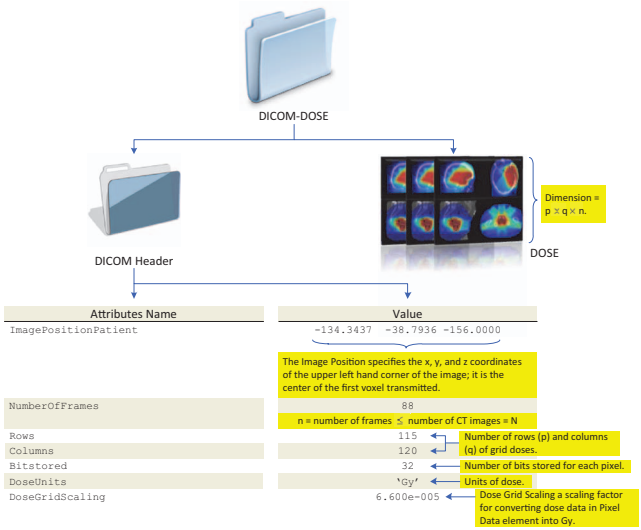

FIG. 2. Attributes of RT Dose module required for computation of CI_{DD}.

the GTV at the primary and nodal sites plus 3 mm margin is 70 Gy, while the PTVs for microscopic disease representing high and low risk disease regions receive 66 Gy and 60 Gy, respectively.

II.A. Data extraction

All digital imaging and communication in medicine (DICOM) RT objects were exported from the ECLIPSE version 8.6 treatment planning system (Varian Medical Systems, Palo Alto, CA). Valuable information contained in the DICOM RT objects was harvested for computation of each CI_{DD} component. Edge-based approach was adopted for extraction of underdose regions within tumor. PTV coverage at each prescribed dose level was evaluated individually. In the DICOM RT Structure Set module, the `StructureSetROISequence` attribute assigns a unique region of interest (ROI) number to each ROI (Fig. 1). The contours of GTV and PTVs defined within the `ROIContourSequence` attribute in the RT Structure Set object were reconstructed.

Following contour reconstruction, the grid doses could be constructed by multiplying each pixel value stored in the image pixel module with the `DoseGridScaling` attribute in the RT dose module (Fig. 2). Next, the three-dimensional (3D) RT Dose matrix and the ROI contours could be mapped onto the CT dataset according to the coordinates of the `ImagePositionPatient` attribute of the RT Dose module and the CT image.

II.B. Calculation of GTV coverage factor

GTV was the most predictive independent survival variable in the multivariate analysis.[17] The concept of selective dose escalation to GTV has recently been advocated as a means of improving local tumor control.[18,19] For each underdose region inside GTV, i.e., GTV receiving less than 70 Gy, the GTV coverage factor G is defined as

$$G = \frac{\sum_{\text{all}I_z} 70\ \text{Gy} \cap (\text{GTV}_n \cup \text{GTV}_{np})}{\sum_{\text{all}I_z} (\text{GTV}_n \cup \text{GTV}_{np})},$$

where I_z is the image of zth cut, $\Sigma_{\text{all}I_z}$ is the volumetric sum of all cuts, $\cap$ is the intersection of two regions, $\cup$ is the union of two regions, GTV_n is the nodal gross tumor volume and GTV_{np} is the nasopharyngeal gross tumor volume.

G equals to 1 if whole GTV is covered by a prescribed dose of 70 Gy and G approaches zero with continuously decreasing volumes of GTV receiving dose of at least 70 Gy. Using similar concepts described by Leong *et al.* and Zheng *et al.*, the geographic miss of tumor was classified as grade 1 or grade 2 according to the locations of cold spots within PTV.[20,21] A grade 1 geographic miss was defined as inadequate GTV coverage while a grade 2 geographic miss was defined as inadequate coverage of PTV excluding GTV. It is widely accepted that GTV coverage should take precedence over PTV coverage and every effort should be made to avoid grade 1 geographic miss.

II.C. Calculation of GTV underdose factor

Tomé and Fowler and Zhao *et al.* demonstrated that there was a precipitous tumor control probability drop with the presence of deep cold spots in the GTV which always had higher malignant cell density than peripheral PTV region.[22,23] Compared to the volume of tumor underdosed, the magnitude of the underdosage may be a more important determinant of tumor control probability.[24] Thus the GTV underdose factor was designed giving penalty based on the extent of underdosage for each GTV pixel.

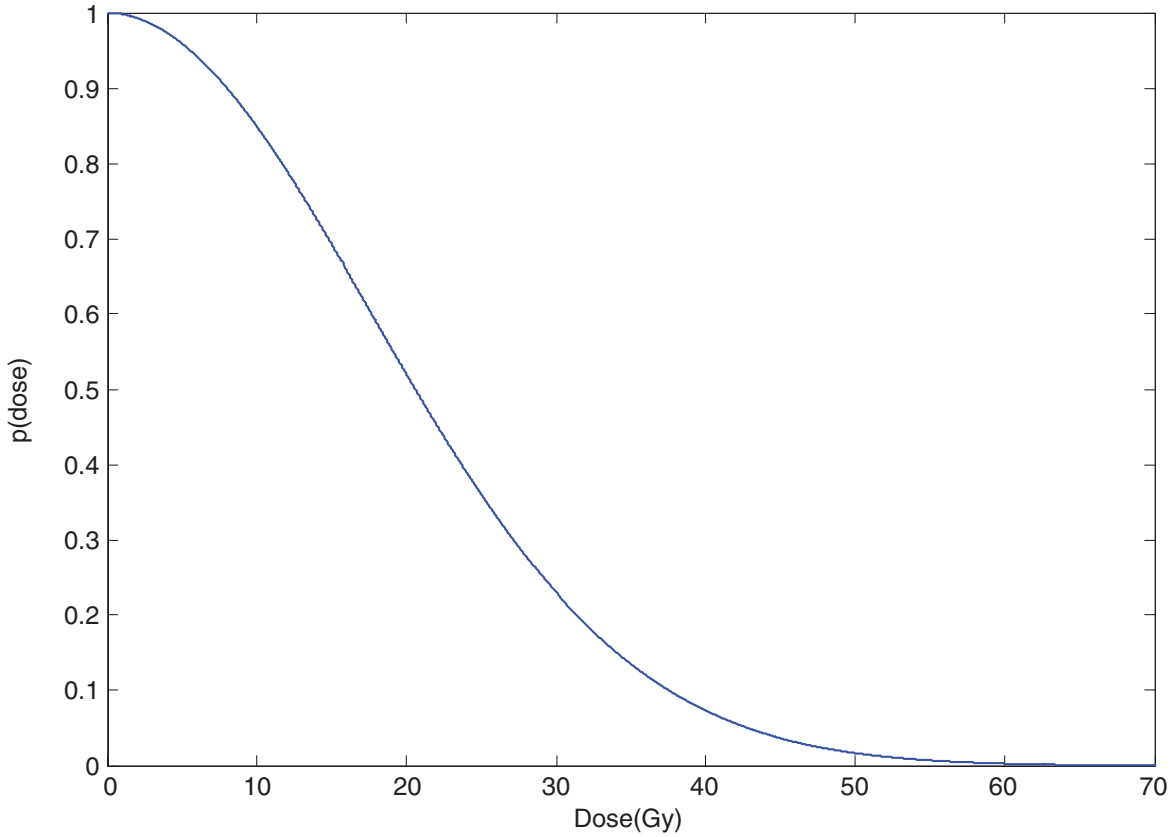

FIG. 3. The penalty function p.

For each underdose pixel inside GTV, the GTV underdose factor P is defined as

$$P(\text{dose}) = 1 - \sum_{\text{all}I_z} p(\text{dose})$$

$$= 1 - \sum_{\text{all}I_z} \exp\left(-\frac{2 \times \text{dose}^2}{35^2}\right), \quad 0 \le \text{dose} \le 70.$$

Similar to the previous study by Miften *et al.*, Gaussian function was applied to penalize the cold spots.[9] This bell-shaped function was chosen because of its exponentially decreasing character. With a central peak, its tails drop towards zero rapidly as x approaches infinity. The use of GTV underdose factor, P(dose), to quantify the dose-volume violations should satisfy the following criterions (as demonstrated in Fig. 3). First, the admissible values of penalty function are non-negative values. Second, no penalty is given when the GTV pixel receiving not less than 70 Gy. Third, maximum penalty is enforced whenever the GTV pixel receives 0 Gy.

II.D. Calculation of (PTV minus GTV) coverage factor

For grade 2 geographic miss, the (PTV minus GTV) coverage factor was introduced as the total probability measures of the underdose region. To meet the needs for comprehensive evaluation of IMRT plan with SMART boost, PTV coverage at each prescribed dose level was considered individually.

For each underdose region inside PTV excluding GTV, the (PTV minus GTV) coverage for PG is defined as

$$PG = \frac{1}{6}\left\{\frac{\sum_{\text{all}I_z} 70\text{ Gy} \cap (\text{PTV}_{n70} - \text{GTV}_n)}{\sum_{\text{all}I_z} (\text{PTV}_{n70} - \text{GTV}_n)} + \frac{\sum_{\text{all}I_z} 70\text{ Gy} \cap (\text{PTV}_{np70} - \text{GTV}_{np})}{\sum_{\text{all}I_z} (\text{PTV}_{np(70)} - \text{GTV}_{np})}\right.$$
$$+ \frac{\sum_{\text{all}I_z} 66\text{ Gy} \cap (\text{PTV}_{n66} - \text{PTV}_{n70})}{\sum_{\text{all}I_z} (\text{PTV}_{n66} - \text{PTV}_{n70})} + \frac{\sum_{\text{all}I_z} 66\text{ Gy} \cap (\text{PTV}_{np66} - \text{PTV}_{np70})}{\sum_{\text{all}I_z} (\text{PTV}_{np66} - \text{PTV}_{np70})}$$
$$\left. + \frac{\sum_{\text{all}I_z} 60\text{ Gy} \cap (\text{PTV}_{n60} - \text{PTV}_{n66})}{\sum_{\text{all}I_z} (\text{PTV}_{n60} - \text{PTV}_{n66})} + \frac{\sum_{\text{all}I_z} 60\text{ Gy} \cap (\text{PTV}_{np60} - \text{PTV}_{np66})}{\sum_{\text{all}I_z} (\text{PTV}_{np60} - \text{PTV}_{np66})}\right\},$$

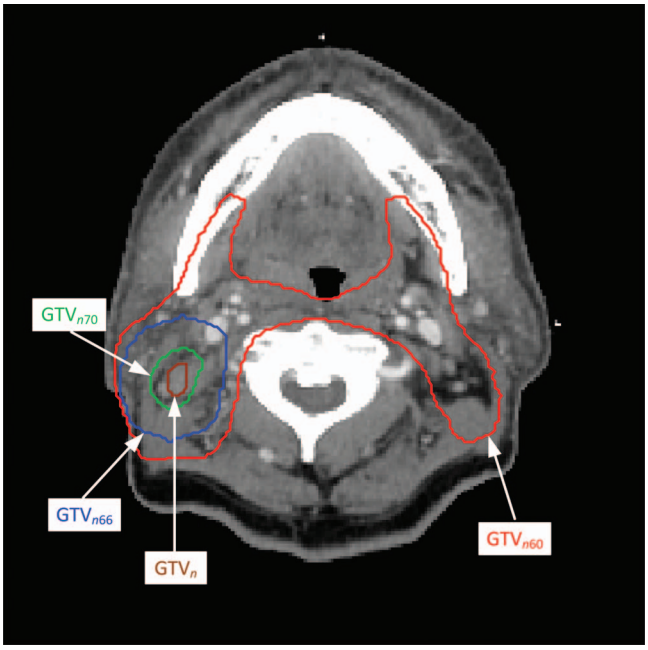

FIG. 4. Diagram showing various target contours required for calculation of the (PTV minus GTV) coverage factor.

where $\text{GTV}_n \supset \text{PTV}_{n70} \supseteq \text{PTV}_{n66} \supseteq \text{PTV}_{n60}$ and $\text{GTV}_{np} \supset \text{PTV}_{np70} \supseteq \text{PTV}_{np66} \supseteq \text{PTV}_{np60}$.

Figure 4 demonstrates the target contours required to calculate the (PTV minus GTV) coverage factor. Three prescription doses are delivered to various PTVs, designated as PTV_{n60}, PTV_{n66}, PTV_{n70}, PTV_{np60}, PTV_{np66}, and PTV_{np70} with the subscripts representing different dose levels prescribed to either primary nasopharyngeal tumor or nodal region. Using the inside-out approach, the nonoverlapping regions (NORs) between (1) GTV_{np} and PTV_{np70}; (2) GTV_n and PTV_{n70}; (3) PTV_{np70} and PTV_{np66}; (4) PTV_{n70} and PTV_{n66}; (5) PTV_{np66} and PTV_{np60}; (6) PTV_{n66} and PTV_{n60} were drawn. The next step in calculating *PG* was to find out the overlapping regions between NORs and their corresponding prescribed dose levels on every single CT slice. For simplicity, Fig. 5 demonstrates how to compute the first term of *PG*. The dark green- and light blue-shaded areas represent the numerator and denominator, respectively.

II.E. Calculation of (PTV minus GTV) underdose and distance factor

The (PTV minus GTV) underdose and distance factor was based on two major hypotheses. First, underdose had the potential to decrease tumor control. Second, there was differing importance of cold spots to the tumor control for grade 2 geographic miss depending on their locations. Therefore, the (PTV minus GTV) underdose and distance factor employed both dose penalty factor and distance based exponential penalty function. By varying the penalty weight associated with the location of cold spots within PTV, the (PTV minus GTV) underdose and distance factor took the specific tumor geometry into account. In the following theorem, two versions of (PTV minus GTV) underdose and distance factor are presented, in the presence and absence of GTV. For each underdose pixel inside (PTV minus GTV) in the presence of GTV, the (PTV minus GTV) underdose and distance factor is defined as

$$P(\text{dose, distance}) = 1 - \sum_{\text{all}I_z} p(\text{dose, distance}) = 1 - \sum_{\text{all}I_z} \exp\left(-\left(\frac{8 \times \text{dose}^2}{d^2} + \frac{8 \times \text{distance}^2}{m^2}\right)\right),$$

where $0 \le \text{dose} \le d$, $d = 60, 66, 70$, $0 \le \text{distance} \le m$ and $m = \max\{\partial\text{PTV} - \partial\text{GTV}\}$ = furthest distance between the boundary of PTV and GTV for each I_z.

For each underdose pixel inside (PTV minus GTV) in the absence of GTV, the (PTV minus GTV) underdose and

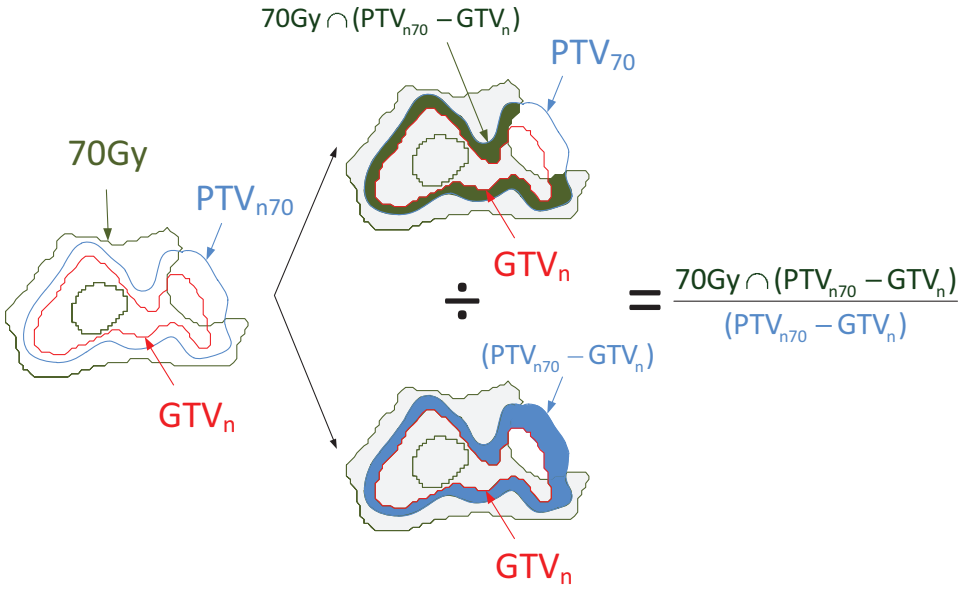

FIG. 5. Diagrammatic calculation of first term of (PTV minus GTV) coverage factor.

distance factor is defined as

$$P(\text{dose, distance}) = 1 - \sum_{\text{all } I_z} p(\text{dose, distance}) = 1 - \sum_{\text{all } I_z} \exp\left(-\left(\frac{8 \times \text{dose}^2}{d^2} + \frac{8 \times \text{distance}^2}{m^2}\right)\right),$$

where $0 \le \text{dose} \le d$, $d = 60, 66, 70$, $0 \le \text{distance} \le m$ and $m = \max\{\partial\text{PTV} - \text{PTV}_c\}$ = furthest distance between the boundary of PTV and the centroid of PTV, i.e., PTV_c for each I_z.

The (PTV minus GTV) underdose and distance factor should satisfy the following conditions. In an extreme scenario where zero dose is delivered to a pixel situated at the boundary of GTV or centroid of PTV, the P(dose, distance) is set to zero imposing the maximum penalty. On the other hand, the P(dose, distance) equals to 1 whichever pixel farthest away from the GTV border receiving not less than its prescribed dose. When pixel within PTV excluding GTV gets zero dose, only the distance factor is considered. In contrast, P(dose, distance) depends only on dose for all pixels located at the boundary of GTV or centroid of PTV.

We start with a more general two-dimensional elliptical Gaussian function, which takes the form

$$f(x, y) = A\exp\left(-\left(\frac{(x - x_0)^2}{2\sigma_x^2} + \frac{(y - y_0)^2}{2\sigma_y^2}\right)\right), \quad -\infty < x, y < \infty,$$

where A = amplitude, x_0, y_0, σ_x and σ_y are real constants. (x_0, y_0) = center of the Gaussian function and σ_x, σ_y controls the x, y spread from the center. The amplitude of $f(x, y)$ occurs when $x = x_0$, $y = y_0$, i.e., $f(x = x_0, y = y_0) = A$.

Noting that

$$\lim_{\substack{x \to x_0 \pm 4\sigma_x, \\ y \to y_0 \pm 4\sigma_y}} f(x, y) = \lim_{\substack{x \to x_0 \pm 4\sigma_x, \\ y \to y_0 \pm 4\sigma_y}} A\exp\left(-\left(\frac{(x - x_0)^2}{2\sigma_x^2} + \frac{(y - y_0)^2}{2\sigma_y^2}\right)\right) = \lim_{\substack{x \to x_0 \pm 4\sigma_x, \\ y \to y_0 \pm 4\sigma_y}} A\exp\left(-\left(\frac{16\sigma_x^2}{2\sigma_x^2} + \frac{16\sigma_y^2}{2\sigma_y^2}\right)\right) = A\exp(-16) \approx 0.$$

By integrating both spatial and dosimetric importance for each pixel (PTV minus GTV) underdose and distance factor was fitted with a two-dimensional elliptical Gaussian function. As illustrated in Fig. 6, the value becomes maximal at the origin of a Cartesian coordinate system and falls off precipitously to zero as x- and y-values approaches infinity. In two dimensions, P(dose, distance) depends on two individual factors, namely, distance and dose penalties (Fig. 6). Both σ_x and σ_y can control the x and y spread from the center. The σ_x and σ_y parameters should be set accordingly to satisfy the following clinical conditions. In an extreme scenario where zero dose is delivered to GTV boundary or centroid of PTV, value becomes zero imposing the maximum penalty. On the other hand, value is maximum whichever pixel farthest away from GTV border (i.e., distance between pixel and GTV border equals to m) receiving not less than prescribed dose (d). Using the two-dimensional elliptical Gaussian function, P(dose, distance) should be substantially smaller for cold spots closer to PTV centroid (i.e., pixel with distance $< m$ receiving dose $< d$). For the Gaussian distribution, a range within 4σ could include 99.9% of data values. Therefore, σ_x and σ_y are set to become $d/4$ and $m/4$, respectively in order to control the spread of such distribution. Like the P(dose), the admissible values of penalty function are non-negative values. No penalty is enforced whenever pixel receives not less than its prescribed dose regardless of its location. Therefore, the penalty function p is given by first normalizing the function $f(x, y)$ (by dividing its amplitude A), choosing $x_0 = y_0 = 0$, $x_0 + 4\sigma_x = d$, i.e., $\sigma_x = d/4$ and letting x = dose, $y_0 + 4\sigma_y = m$, i.e., $\sigma_y = m/4$ and letting y = distance. We then have

$$p(\text{dose, distance}) = \frac{f(\text{dose, distance})}{A} = \exp\left(-\left(\frac{\text{dose}^2}{2(d/4)^2} + \frac{\text{distance}^2}{2(m/4)^2}\right)\right), = \exp\left(-\left(\frac{8\times\text{dose}^2}{d^2} + \frac{8\times\text{distance}^2}{m^2}\right)\right),$$

where $0 \le \text{dose} \le d$, $0 \le \text{distance} \le m$.

As a result, (PTV minus GTV) underdose and distance factor P is defined as

$$P(\text{dose, distance}) = 1 - \sum_{\text{all } I_z} p(\text{dose, distance}).$$

II.F. Calculation of CI_{DD}

To consolidate all four distinct factors into one CI_{DD} score, Euclidean two-norm was applied to represent the quality of a treatment plan. This is similar to the method described by Leung *et al.*[8] Equal weights were assigned to four factors as a good starting point for illustrating the feasibility of the CI_{DD} design concept. For a hypothetical case when 100% of the prescribed dose was homogenously delivered to the multiple PTVs, all four factors should be unity. The CI_{DD} score was defined as the Euclidean two-norm between these four factors and (1, 1, 1, 1) to describe the overall plan quality. The Euclidean two-norm is defined as

$$\text{CI}_{\text{DD}} = \sqrt{(1 - G)^2 + (1 - P(\text{dose}))^2 + (1 - PG)^2 + (1 - P(\text{dose, distance}))^2}.$$

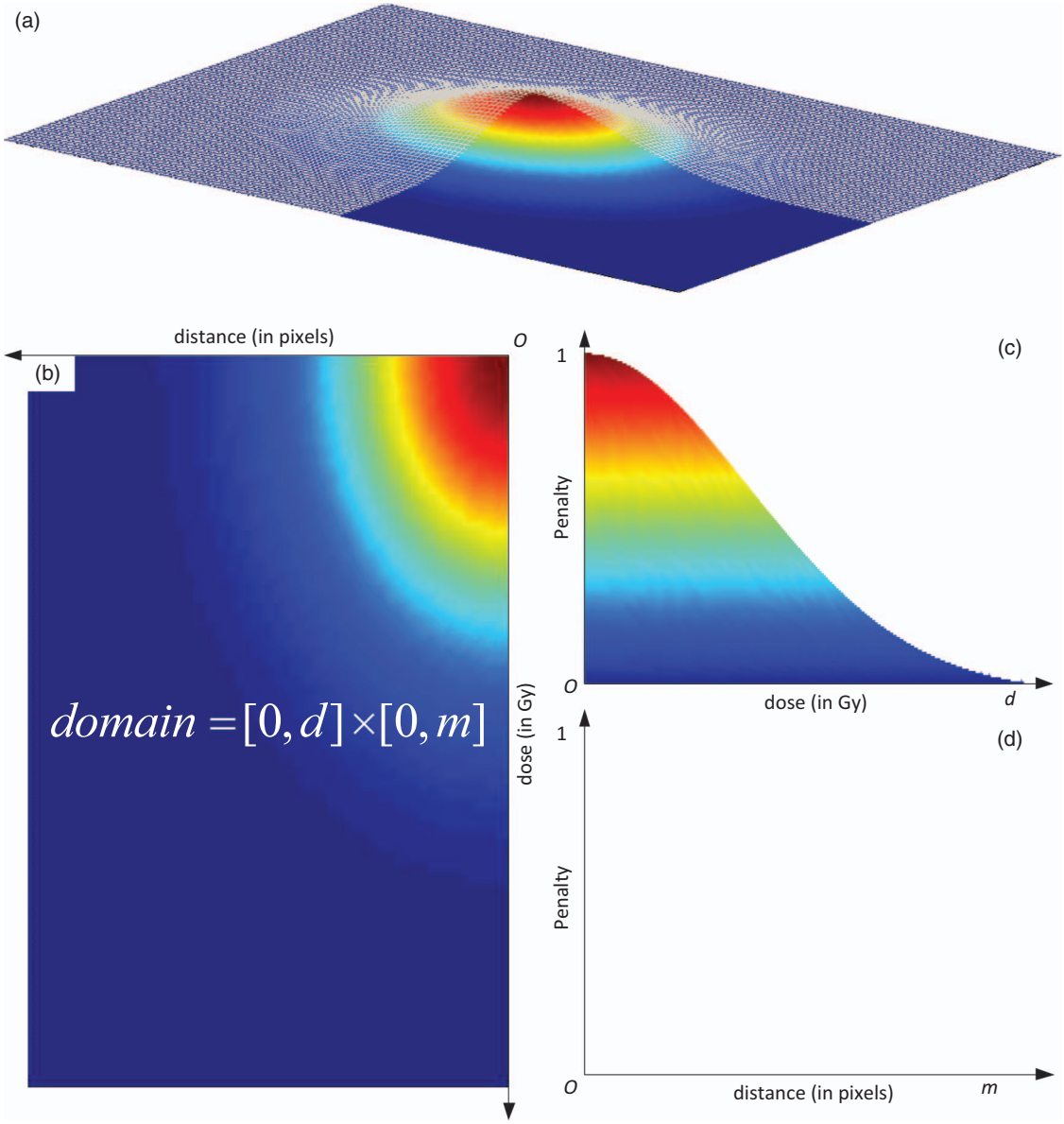

FIG. 6. (a) Two-dimensional (PTV minus GTV) underdose and distance factor; (b) domain of the (PTV minus GTV) underdose and distance factor; (c) penalty with dose; and (d) penalty with distance.

The worst scenario is $\sqrt{4} = 2$ when $G = P(\text{dose}) = PG = P(\text{dose, distance}) = 0$. In clinical situation, it occurs when all GTV and (PTV minus GTV) pixels received 0 Gy. In contrast, CI_{DD} score is zero for a perfect case, i.e., $G = P(\text{dose}) = PG = P(\text{dose, distance}) = 1$. This scenario occurs whenever all GTV and (PTV minus GTV) pixels received not less than the prescribed dose. Unlike other indices, a lower CI_{DD} score indicates better target coverage in this study.

II.G. Evaluation of CI_{DD} scoring system

In order to evaluate the CI_{DD} scoring system, three CT image datasets of NPC cases involving multiple PTVs with different prescription levels were collected. Ten IMRT plans were generated from each dataset using the ECLIPSE treatment planning system (version 8.6) (Varian Medical Systems, Palo Alto, CA). Table II shows the typical optimization parameters for an IMRT NPC plan in clinical practice. For each plan, inverse IMRT plans were optimized using the same sets of constraints as shown in Table II except for the changing priority factors of PTVs. For plan 1 of each dataset, target coverage was assigned the highest priority value of 350 for upper and lower limits. With stepwise relaxation, the priority factors for PTVs were decreased by 20 for each successive IMRT plan. As a result, the plan qualities deteriorated sequentially in terms of target dose conformity from plan 1 to plan 10 for each dataset.

Apart from the CI_{DD} score, the RTOG conformity index, HTCI, CN, target coverage factor were computed. The plan quality discerning power of CI_{DD} was assessed by ranking the ten IMRT plans of each CT dataset based on the CI_{DD} scores and by comparing the results with other indices. The coefficient of variation, also known as "relative variability," represents the ratio of the standard deviation to the mean. As

TABLE II. Optimization parameters for a typical IMRT NPC plan.

Regions of interest (ROIs)	Limits	Dose (Gy)	Volume (%)	Priority
Brainstem	Upper	54	0	300
Brainstem + 3 mm shell	Upper	60	1	300
Spinal cord	Upper	45	0	300
Spinal cord + 3 mm shell	Upper	50	0	300
Temporal lobes	Upper	70	0	250
Optic chiasm	Upper	54	0	250
Optical nerves	Upper	54	0	250
Parotid gland	Upper	26	50	200
PTV_{np70} and PTV_{n70}	Upper	75	0	350
PTV_{np70} and PTV_{n70}	Lower	74	100	350
PTV_{np66} and PTV_{n66}	Upper	72	0	350
PTV_{np66} and PTV_{n66}	Lower	70	100	350
PTV_{np60} and PTV_{n60}	Upper	64	0	350
PTV_{np60} and PTV_{n60}	Lower	63	100	350

Note. PTV_{np} = nasopharyngeal planning target volume; PTV_n = nodal planning target volume; PTV_{np70} = 70 Gy to PTV_{np}; PTV_{n70} = 70 Gy to PTV_n; PTV_{np66} = 66 Gy to PTV_{np}; PTV_{n66} = 66 Gy to PTV_n; PTV_{np60} = 60 Gy to PTV_{np}; PTV_{n60} = 60 Gy to PTV_n.

a dispersion measurement, coefficient of variation is a useful statistic for comparing diversity across datasets. A greater dispersion corresponds to a higher coefficient of variation. To quantify the variation of diversity, the coefficient of variation was calculated for each dataset and compared among different indices. Biological indices like equivalent uniform dose (EUD) based tumor control probability (TCP) and normal tissue complication probability (NTCP) formula derived by Gay and Niemierko were also computed as a vehicle to explain the outcome from different indices.[25]

III. RESULTS

III.A. Evaluation of CI_{DD}

The use of CI_{DD} consisting of four discrete factors allowed planners to assess the dose distribution in greater depth. Coverage of multiple PTVs by various levels of prescribed dose was analyzed separately. Each factor was bounded by 0 and 1, greater value indicated superior plan. Figure 7 summarizes the results of different factors among the ten plans of the first NPC patient. All factors suggested that plan 1 was the most superior in terms of target coverage. The first eight plans provided nearly perfect GTV coverage without GTV underdosage. For plans 9 and 10, there was a drop in both GTV coverage and GTV underdosage factors, but the decrease was more pronounced in GTV coverage factor. Among the ten IMRT plans, the (PTV minus GTV) coverage factor never reached unity suggesting that part of the target outside GTV always received less than the prescribed dose. The values of (PTV minus GTV) coverage factor declined gradually from 0.9 to 0.85 for the first five plans and then fell rapidly down to 0.4 for plan 10. On the other hand, the change in (PTV minus GTV) underdose and distance factor was gradual and subtle initially, but became obvious for the last five plans.

Figures 8 and 9 show the variation of different factors among the ten plans for the second and third NPC patients. In line with expectations, the results for all three patients showed

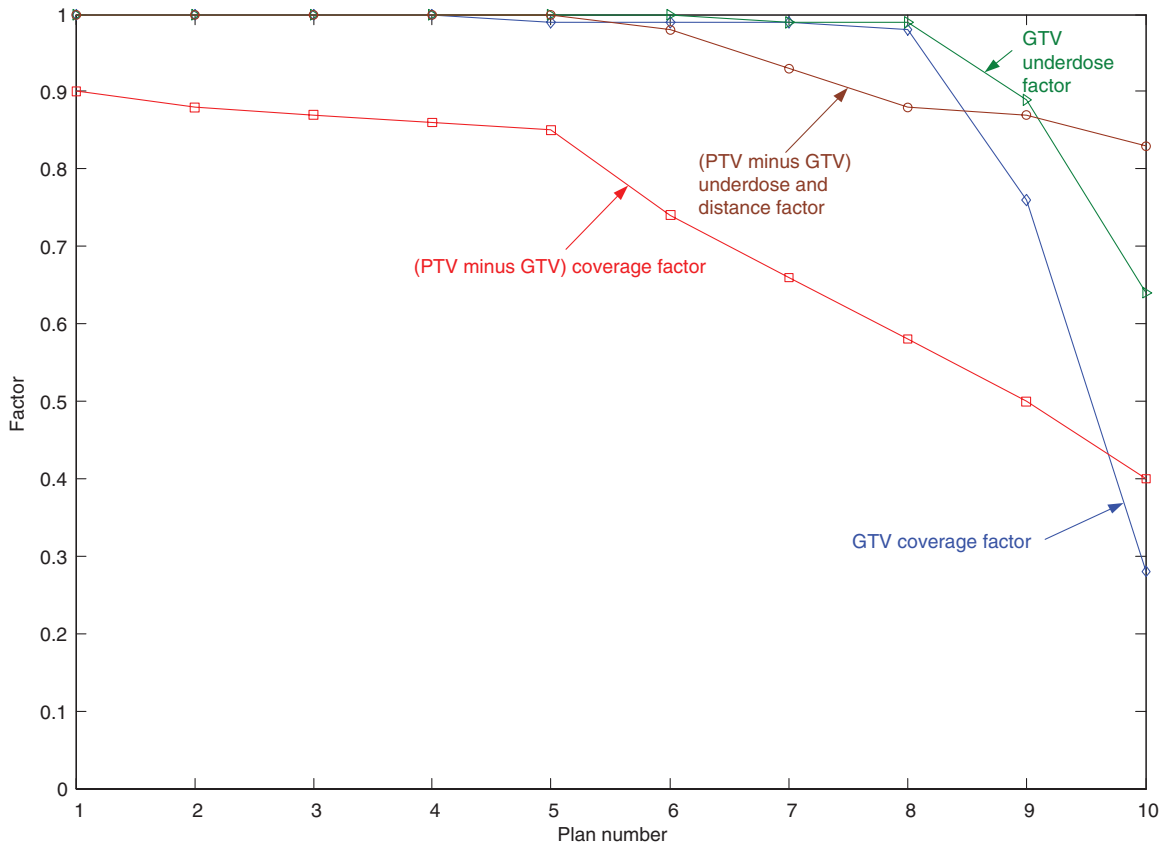

FIG. 7. Graph showing the variation of different factors among ten IMRT plans for the first NPC patient.

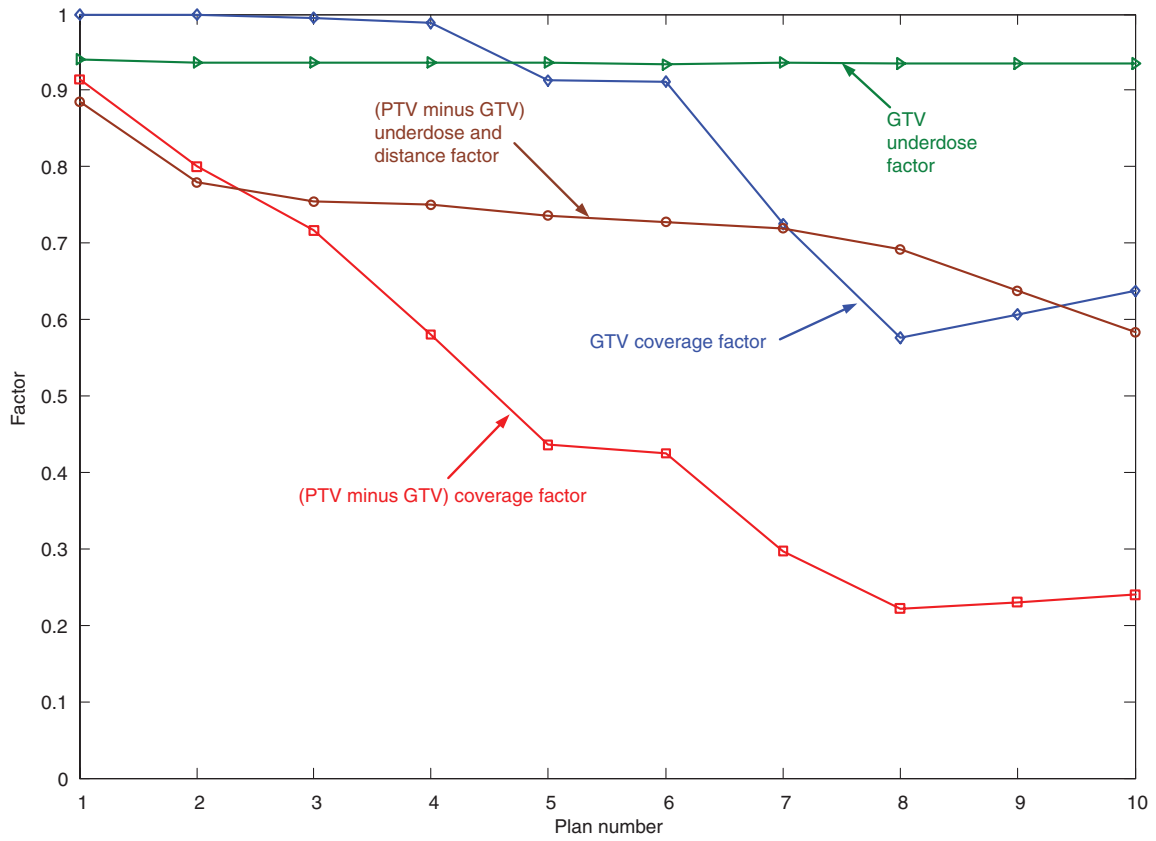

FIG. 8. Graph showing the variation of different factors among ten IMRT plans for the second NPC patient.

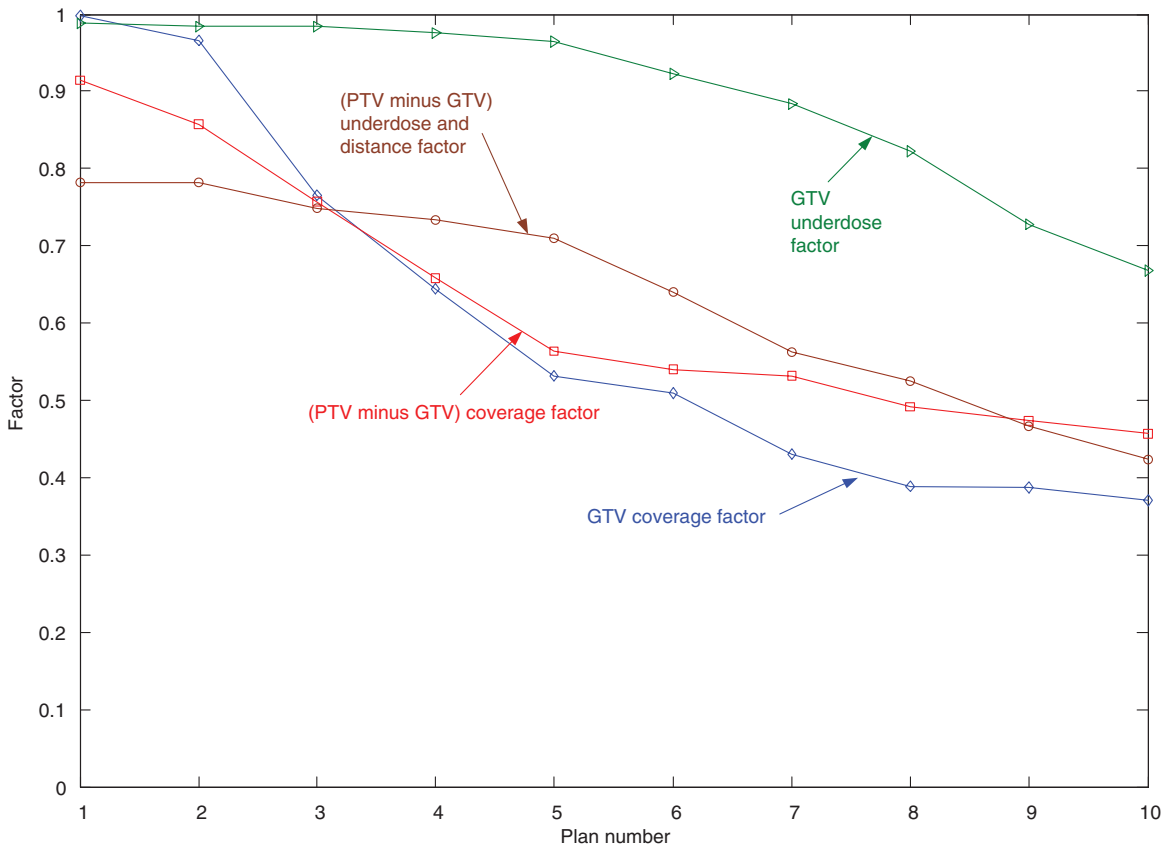

FIG. 9. Graph showing the variation of different factors among ten IMRT plans for the third NPC patient.

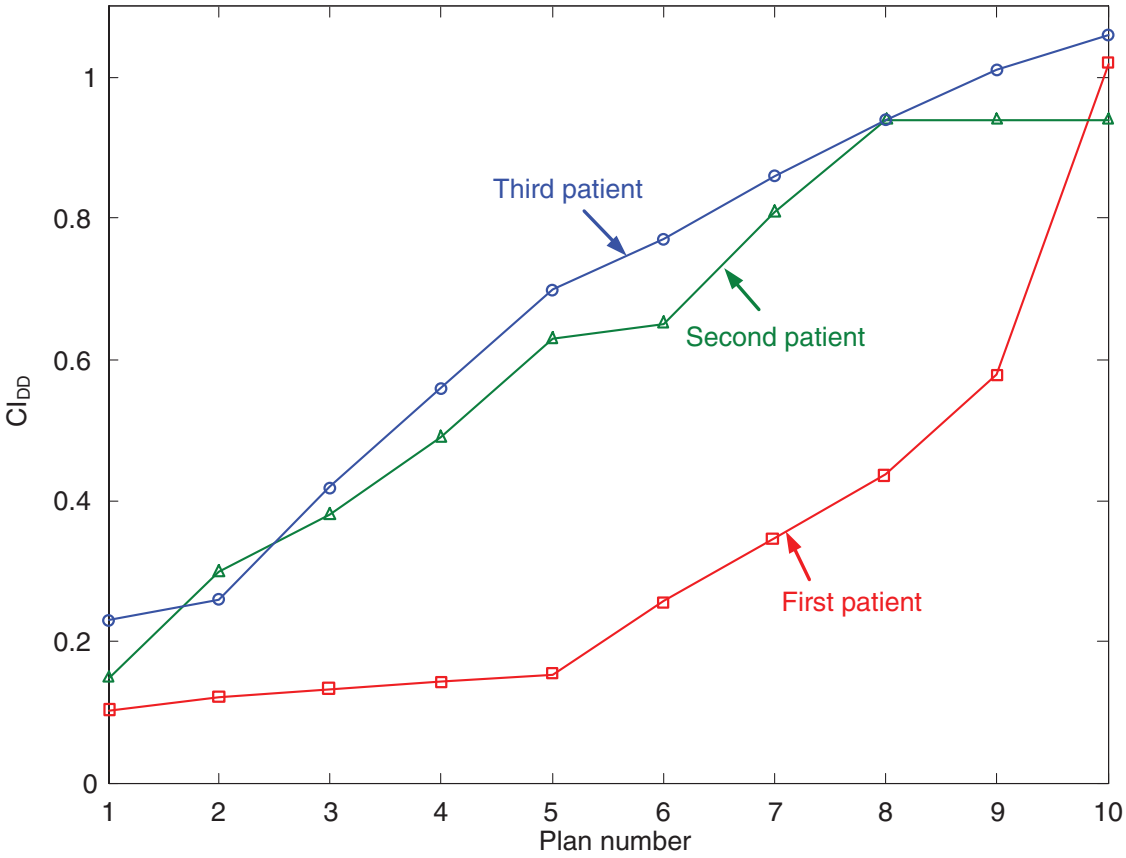

FIG. 10. Graph showing the trend of CI_{DD} scores among ten IMRT plans for three NPC patients.

a general decreasing trend from plan 1 to plan 10. By taking the spatial dose information into account, the target coverage for each subregion of PTV could be assessed separately. The results demonstrated that these four discrete factors could provide accurate rankings of plan quality by examining the relative importance of each cold spot within the PTVs.

III.B. Comparison among CI_{DD} scores

To consolidate all four distinct factors into one CI_{DD} score, Euclidean two-norm was applied to describe the overall plan quality. In contrast to other conventional indices, a lower CI_{DD} score indicated better target coverage. The CI_{DD} score trends for three NPC patients were illustrated in Fig. 10. On the whole, the CI_{DD} scores increased accordingly with increasing plan number for all three NPC patients. Coherent with expectations, plan 1 was the most superior in terms of target coverage as evidenced by the lowest CI_{DD} score among ten IMRT plans for each NPC patient.

III.C. Comparison with various conformity indices

Several conformity indices, namely, RTOG conformity index, HTCI, CN, target coverage factor and CI_{DD} were calculated for each plan. The coefficient of variance was computed for each index to compare their plan quality discerning power. Table III summarizes the scores of all indices and their coefficients of variance for the first NPC patient. For CI_{DD}, lower values indicate better plans, while for the rest, higher values indicate better plans. The best plan suggested by RTOG conformity index, target coverage factor and CI_{DD} was plan 1. Still, plans 3 and 4 had the highest scores of CN. Plan 10 was the most superior when ranking based on HTCI alone but the worst according to CI_{DD} index as well as others. For the first NPC patient, the coefficients of variance of RTOG conformity index, HTCI, CN, target coverage factor and CI_{DD} were 31.73%, 7.65%, 15.23%, 10.88%, and 87.57%, respectively,

TABLE III. Summary of various indices and coefficients of variance for the first NPC patient.

Plan no.	CT_{RTOG}	HTCI	CN	Target coverage factor	CI_{DD}
1	1.37	0.77	0.71	1.00	0.10
2	1.32	0.78	0.71	0.99	0.13
3	1.27	0.80	0.72	0.99	0.13
4	1.25	0.80	0.72	0.99	0.14
5	1.23	0.80	0.71	0.98	0.15
6	1.07	0.86	0.69	0.94	0.26
7	0.99	0.88	0.65	0.89	0.35
8	0.91	0.90	0.60	0.84	0.44
9	0.64	0.93	0.54	0.79	0.48
10	0.35	0.94	0.42	0.72	1.02
μ	1.04	0.85	0.65	0.91	0.33
σ	0.33	0.07	0.10	0.10	0.29
CV	31.73%	7.65%	15.23%	10.88%	87.57%

Note. μ = mean, σ = standard deviation, CV = coefficient of variance.

TABLE IV. Summary of various indices and coefficients of variance for the second NPC patient.

Plan no.	CT_{RTOG}	HTCI	CN	Target coverage factor	CI_{DD}
1	1.33	0.74	0.65	1.00	0.15
2	1.30	0.81	0.66	0.96	0.30
3	1.26	0.86	0.69	0.94	0.38
4	1.23	0.90	0.71	0.90	0.49
5	1.12	0.94	0.72	0.83	0.63
6	0.96	0.93	0.69	0.83	0.65
7	0.82	0.86	0.58	0.74	0.81
8	0.73	0.97	0.54	0.70	0.94
9	0.39	0.97	0.52	0.70	0.94
10	0.36	0.97	0.46	0.70	0.94
μ	0.95	0.91	0.62	0.83	0.62
σ	0.36	0.08	0.09	0.12	0.29
CV	38 .40%	8.70%	14.57%	14.00%	46.09%

Note. μ = mean, σ = standard deviation, CV = coefficient of variance.

which indicated that the CI_{DD} index had the greater plan quality discerning power.

Scores of various indices and relevant coefficients of variance for the second and third patients were listed in Tables IV and V. The coefficients of variance of RTOG conformity index, HTCI, CN, target coverage factor and CI_{DD} for the second NPC patient were 38.4%, 8.7%, 14.57%, 14%, and 46.09%, respectively (Table IV). While for the third NPC patient, the coefficients of variance of RTOG conformity index, HTCI, CN, target coverage factor and CI_{DD} were 34.48%, 5.15%, 17.28%, 8.87%, and 44.39%, respectively (Table V). Three sets of data showed that analysis of different indices could lead to different conclusions, indicating that special caution was required when evaluating treatment plans based on one specific index. Compared with other commonly used indices, the CI_{DD} always resulted in the largest coefficient of variance for all three NPC patients. It implied that CI_{DD} scoring system had the greatest power to rank rival IMRT plans.

TABLE V. Summary of various indices and coefficients of variance for the third NPC patient.

Plan no.	CT_{RTOG}	HTCI	CN	Target coverage factor	CI_{DD}
1	1.31	0.71	0.65	0.99	0.23
2	1. 30	0.79	0.68	0.98	0.26
3	1.24	0.85	0.71	0.94	0.42
4	1.19	0.82	0.72	0.90	0.56
5	1.15	0.81	0.72	0.84	0.70
6	0.93	0.81	0.68	0.83	0.77
7	0.82	0.80	0.54	0.82	0.86
8	0.54	0.83	0.52	0.80	0.94
9	0.42	0.85	0.49	0.80	1.01
10	0.36	0.85	0.44	0.79	1.06
μ	0.95	0.81	0.62	0.87	0.62
σ	0.33	0.04	0.11	0.08	0.30
CV	34 .48%	5.15%	17.28%	8.87%	44.39%

Note. μ = mean, σ = standard deviation, CV = coefficient of variance.

III.D. Comparison with TCP and NTCP

The evaluation results were further validated by the calculation using EUD-based TCP and NTCP. All three NPC patients followed similar patterns from plan 1 to plan 10, as illustrated in Tables VI–XI. Some conclusions could be drawn from the data. First of all, the EUDs of all PTVs suggested that plan 1 was the most superior in terms of target coverage. The TCP values among ten IMRT plans had a slight downward trend from plan 1 to plan 10. In contrast, the minimum EUDs of OARs were mostly found in plan 10, with the lowest NTCP. Nevertheless, the EUDs of all PTVs in plan 10 were much smaller as a result of large cold spots. As a whole, the results were in line with that of the CI_{DD} scores. For CI_{DD}, lower values indicate better plans.

IV. DISCUSSION

It has been widely accepted that GTV is likely to have higher malignant cell density than the remainder of the PTV.[22] Since the locoregional failure rate is significantly related to the minimum dose in the GTV, the assumption of equal merit for different subregions inside PTV is inadequate.[26] Whenever underdosage is present, it is important to know the magnitude, location, and volume of the low dose regions. Cold spots should be at the periphery of PTV, as far from the GTV as possible. Different distribution of underdosed volumes could lead to different tumor control probability outcomes. To incorporate patient-specific spatial dose information, the CI_{DD} scoring system was designed enabling customized plan evaluation. The relative importance of each cold spot within the subregions of the PTVs could be examined using the CI_{DD} scoring system including the four discrete factors. Typically, each factor equals to unity for an ideal plan, whereas the deviation from unity refers to underdose treatments in the corresponding region. In contrast, there is an inverse relationship between CI_{DD} score and plan quality. The smaller the value of CI_{DD}, the better is the overall target coverage. As a result, a plan with cold spots centrally located within the PTV should result in higher CI_{DD} score than the other with more acceptable cold spots on the periphery of the PTV further away from the GTV.

Figure 11 shows the trend of different conformity indices among ten IMRT plans for the first NPC patient. The plan number is represented on the horizontal axis, while the vertical axis shows the index value for each plan. This typical example could clearly demonstrate the weaknesses of each existing index. The RTOG defines three categories of conformity index protocol compliance. RTOG conformity index between 1 and 2 is considered a treatment plan of acceptable dose conformity. Plans with a conformity index value between 2.0 and 2.5 or between 0.9 and 1.0 are classified as having minor deviations. An index less than 0.9 or more than 2.5 is considered a major violation. As shown in Fig. 11, the first seven plans meet the RTOG guidelines with index between 1 and 2, while plans 8–10 are classified as having major violations with RTOG conformity index values less than 0.9. By ignoring the degree of overlap between the prescription

TABLE VI. Summary of EUDs for the PTVs and TCPs of the ten IMRT plans for the first NPC patient using units of gray (Gy).

	EUD (in Gy)							
Plan no.	PTV_{np70}	PTV_{n70}	PTV_{np66}	PTV_{n66}	PTV_{np60}	PTV_{n60}	TCP (PTV_{70})	CI_{DD}
1	71.58	71.97	68.94	68.98	65.95	64.48	88.77%	0.10
2	71.16	71.83	68.64	68.95	65.83	64.27	88.23%	0.13
3	71.25	71.75	68.64	68.88	65.78	64.03	88.25%	0.13
4	71.02	71.57	68.63	68.84	65.76	63.94	87.83%	0.14
5	70.79	71.40	68.63	68.80	65.73	63.85	87.42%	0.15
6	69.44	71.43	68.07	67.96	64.47	60.91	85.82%	0.26
7	69.87	71.33	67.50	66.75	63.50	58.86	86.25%	0.35
8	70.30	71.22	66.94	65.54	62.54	56.80	86.68%	0.44
9	69.41	70.33	66.77	65.28	62.43	56.79	84.58%	0.48
10	68.93	69.82	66.36	64.90	62.24	56.71	83.29%	1.02
μ	70.38	71.26	67.87	67.47	64.39	61.06	86.71%	0.33
σ	0.92	0.68	0.90	1.68	1.56	3.45	0.02%	0.29

Note. μ = mean, σ = standard deviation.

TABLE VII. Summary of EUDs for OARs and NTCPs of the ten IMRT plans for the first NPC patient using units of gray (Gy).

Plan no.	Brainstem	NTCP (%)	Optic Chiasm	NTCP (%)	Left optic nerve	NTCP (%)	Right optic nerve	NTCP (%)	Left temporal lobe	NTCP (%)	Right temporal lobe	NTCP (%)
1	39. 90	0.29	37.78	0.15	48.89	3.17	36.92	1.81	32.67	0.07	38.16	0.44
2	40. 37	0.33	38.34	0.18	49.37	3.56	37.34	2.03	32.65	0.07	38.55	0.49
3	40. 19	0.31	38.16	0.17	49.10	3.33	37.17	1.97	32.56	0.07	38.47	0.48
4	40. 13	0.30	38.12	0.16	48.95	3.11	37.11	1.91	32.44	0.06	38.44	0.47
5	40. 08	0.24	38.07	0.13	48.80	2.66	37.04	1.83	32.33	0.05	38.42	0.36
6	39. 35	0.24	37.32	0.12	48.15	2.25	36.24	1.78	31.61	0.03	37.53	0.26
7	39. 33	0.23	37.23	0.12	47.81	2.21	36.15	1.73	31.13	0.03	37.01	0.25
8	39. 31	0.23	37.15	0.11	47.47	2.15	36.06	1.69	30.64	0.03	36.49	0.25
9	39. 24	0.21	37.06	0.10	47.41	2.12	36.00	1.68	30.61	0.03	36.48	0.25
10	39. 14	0.20	36.95	0.08	47.29	2.05	35.92	1.62	30.55	0.03	36.45	0.25
μ	39. 70	0.26	37.62	0.13	48.32	2.66	36.60	1.81	31.72	0.05	37.60	0.35
σ	0.47	0.00	0.53	0.03	0.79	0.01	0.56	0.13	0.91	0.00	0.91	0.00

Note. μ = mean, σ = standard deviation.

TABLE VIII. Summary of EUDs for the PTVs and TCPs of the ten IMRT plans for the second NPC patient using units of gray (Gy).

	EUD (in Gy)							
Plan no.	PTV_{np70}	PTV_{n70}	PTV_{np66}	PTV_{n66}	PTV_{np60}	PTV_{n60}	TCP (PTV_{70})	CI_{DD}
1	73.98	73.98	69.75	69.39	68.00	67.03	92.25%	0.15
2	72.75	73.24	68.54	67.65	66.08	64.86	90.85%	0.30
3	71.77	72.24	67.70	66.87	65.26	64.05	89.21%	0.38
4	71.07	71.46	66.91	66.12	64.46	63.23	87.78%	0.49
5	70.06	70.53	66.04	65.35	63.77	62.65	85.65%	0.63
6	70.08	70.24	65.95	65.27	63.62	62.42	85.33%	0.65
7	69.48	69.95	64.95	64.04	62.85	61.63	84.22%	0.81
8	69.13	69.57	64.55	63.85	62.43	61.21	83.26%	0.94
9	69.21	69.56	64.41	63.54	62.32	61.05	83.34%	0.94
10	69.28	69.55	64.26	63.14	62.21	60.90	83.43%	0.94
μ	70.68	71.03	66.31	65.60	64.10	62.90	86.53%	0.62
σ	1.67	1.62	1.89	1.92	1.89	1.96	3.30%	0.29

Note. μ = mean, σ = standard deviation.

TABLE IX. Summary of EUDs for OARs and NTCPs of the ten IMRT plans for the second NPC patient using units of gray (Gy).

Plan no.	Brainstem	NTCP (%)	Optic Chiasm	NTCP (%)	Left optic nerve	NTCP (%)	Right optic nerve	NTCP (%)	Left temporal lobe	NTCP (%)	Right temporal lobe	NTCP (%)
1	42.42	0.59	42.96	0.69	48.03	2.58	51.19	5.39	37.88	0.40	38.30	0.46
2	40.83	0.38	41.07	0.40	46.66	1.84	50.36	4.47	35.60	0.19	36.01	0.22
3	40.78	0.37	40.97	0.39	46.55	1.79	49.94	4.06	35.26	0.17	35.80	0.20
4	40.88	0.38	40.74	0.37	46.57	1.80	49.86	3.98	34.94	0.15	35.57	0.19
5	40.93	0.39	40.39	0.33	46.54	1.78	50.02	4.13	34.78	0.14	35.46	0.18
6	40.21	0.31	40.06	0.30	45.59	1.40	49.35	3.54	34.76	0.14	35.28	0.17
7	40.19	0.31	40.01	0.30	46.06	1.58	49.11	3.34	34.09	0.11	35.01	0.16
8	40.11	0.30	39.89	0.28	45.95	1.53	48.94	3.21	33.89	0.11	34.89	0.15
9	40.09	0.30	39.75	0.27	45.93	1.53	48.84	3.14	33.90	0.11	34.79	0.14
10	40.07	0.30	39.61	0.26	45.92	1.52	48.74	3.06	33.91	0.11	34.68	0.14
μ	40.65	0.36	40.54	0.36	46.38	1.73	49.63	3.83	34.90	0.16	35.58	0.20
σ	0.72	0.09	0.99	0.13	0.68	0.33	0.78	0.73	1.21	0.09	1.05	0.09

Note. μ = mean, σ = standard deviation.

TABLE X. Summary of EUDs for the PTVs and TCPs of the ten IMRT plans for the third NPC patient using units of gray (Gy).

	EUD (in Gy)							
Plan no.	PTV_{np70}	PTV_{n70}	PTV_{np66}	PTV_{n66}	PTV_{np60}	PTV_{n60}	TCP (PTV_{70})	CI_{DD}
1	72.14	72.23	68.14	69.02	66.05	66.29	89.53%	0.23
2	71.31	71.62	67.47	68.42	65.14	65.48	88.19%	0.26
3	70.31	71.30	66.72	67.78	64.33	64.71	86.78%	0.42
4	70.06	70.27	66.68	67.72	64.17	64.38	85.35%	0.56
5	69.86	69.03	66.22	67.14	63.86	64.10	83.48%	0.70
6	70.10	68.49	66.00	66.83	63.51	63.63	82.99%	0.77
7	69.97	68.49	65.93	66.69	63.53	63.47	82.83%	0.86
8	69.09	68.83	65.77	66.68	63.23	63.43	82.17%	0.94
9	69.69	68.51	65.61	66.45	63.26	63.15	82.50%	1.01
10	69.80	67.94	65.49	66.39	63.09	62.95	81.74%	1.06
μ	70.27	69.67	66.40	67.31	64.02	64.16	84.56%	0.62
σ	0.87	1.55	0.86	0.89	0.95	1.08	2.75%	0.30

Note. μ = mean, σ = standard deviation.

TABLE XI. Summary of EUDs for OARs and NTCPs of the ten IMRT plans for the third NPC patient using units of gray (Gy).

Plan no.	Brainstem	NTCP (%)	Optic Chiasm	NTCP (%)	Left optic nerve	NTCP (%)	Right optic nerve	NTCP (%)	Left temporal lobe	NTCP (%)	Right temporal lobe	NTCP (%)
1	44.91	1.17	49.67	3.81	50.70	4.83	52.18	6.69	42.98	1.79	39.08	0.58
2	44.41	1.02	49.86	3.99	50.12	4.23	51.31	5.53	42.12	1.41	38.42	0.47
3	44.46	1.04	49.71	3.85	49.95	4.07	51.28	5.49	41.61	1.22	38.63	0.50
4	44 .67	1.10	49.92	4.04	50.33	4.44	51.12	5.30	41.71	1.26	37.95	0.41
5	44.68	1.10	49.84	3.96	50.12	4.23	50.67	4.79	41.55	1.20	37.80	0.39
6	45.01	1.20	49.32	3.51	50.04	4.16	50.26	4.36	41.40	1.15	37.73	0.38
7	45.15	1.25	49.33	3.52	50.12	4.23	50.38	4.49	41.51	1.19	37.76	0.38
8	45.22	1.27	49.19	3.41	49.84	3.97	50.18	4.29	41.27	1.11	37.73	0.38
9	43.81	0.87	49.56	3.72	49.57	3.73	50.25	4.36	40.97	1.02	37.31	0.33
10	44.20	0.97	49.08	3.32	49.59	3.74	50.07	4.18	40.91	1.00	37.31	0.33
μ	44.65	1.10	49.55	3.71	50.04	4.16	50.77	4.95	41.60	1.23	37.97	0.42
σ	0.44	0.13	0.30	0.26	0.34	0.32	0.68	0.80	0.60	0.23	0.57	0.08

Note. μ = mean, σ = standard deviation.

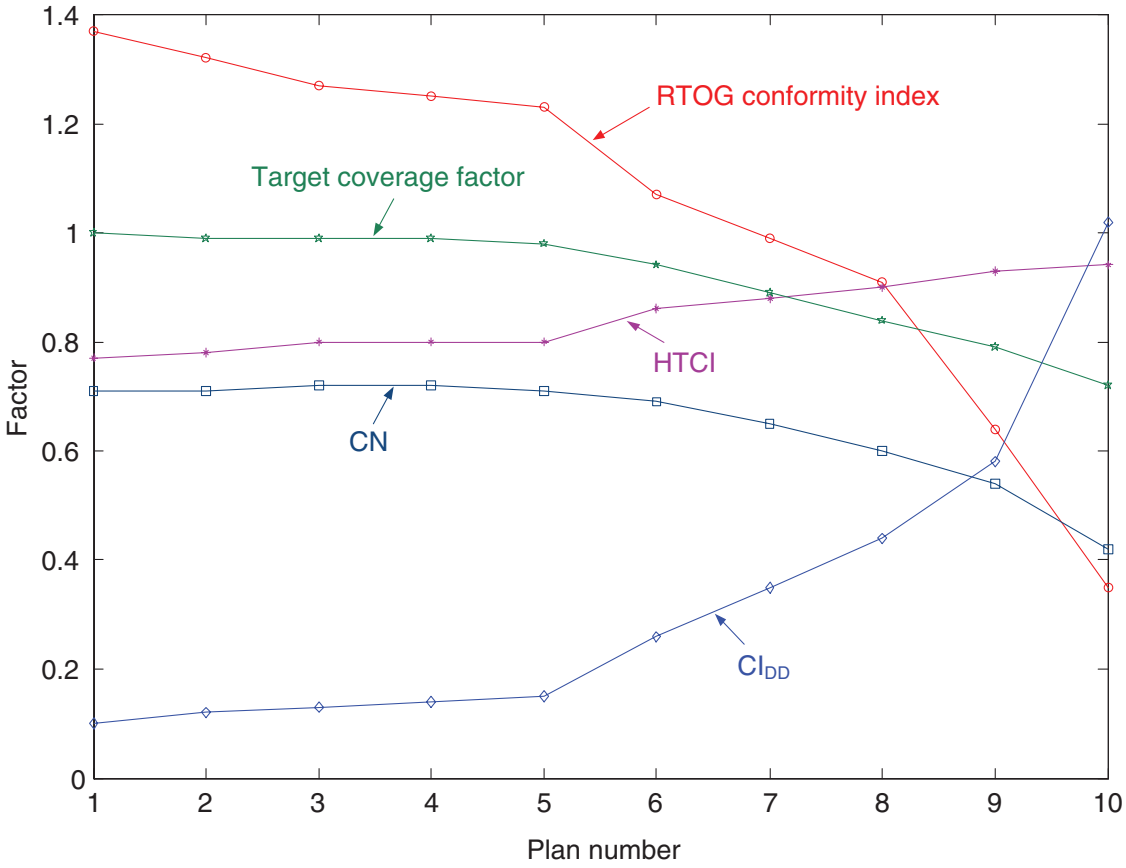

FIG. 11. Graph showing the trend of different physical indices among ten IMRT plans for the first NPC patient.

volume and target volume, planners may unwittingly accept plans with false perfect score of RTOG conformity index.

By definition, HTCI of less than 0.6 is objectively considered as nonconformal.[10] Higher HTCI corresponds to better normal tissue sparing. As illustrated in Fig. 11, the HTCI values of larger than 0.7 are typically attainable for all IMRT plans. Apply the HTCI alone could lead to the conclusion that plan 10 was the most superior. However, both plans 9 and 10 with grade 1 geographic miss are generally undesirable. The major drawbacks of HTCI are that it takes into account exclusively the irradiation of healthy tissues and does not address the issue of target dose conformity. Each IMRT plan should have two primary concerns, namely, target coverage and normal tissue sparing. If treatment toxicity is a serious concern, substantial reduction of dose to OARs may take precedence over target coverage. The final treatment plan decision should always be individualized based not only on comorbidities but also on the use of chemotherapy and other clinical considerations. Obviously, an oversimplification would be made when ranking is solely based on the HTCI.

CN postulated by Van't Riet allowed quantitative evaluation of the tradeoffs between target coverage and critical organ sparing.[11] As either the target underdosage or normal tissue overdosage occurs, the CN value decreases to avoid false positive results. However, no acceptable limit for CN is defined. For the first NPC patient, the CN values are relatively constant for the first five plans (Fig. 11). The shortcoming of this index is that multiple plans with vastly differing clinical outcomes could result in the same CN value. Deviation from unity could be attributed to either insufficient target coverage or inadequate organ sparing.

The target coverage factor by Leung *et al.* evaluated the compliance with treatment protocol by taking all PTV check point doses into account.[8] With a similar pattern to the CN, comparatively subtle variation in target coverage factor is observed among the ten IMRT plans (Fig. 11). It is obvious that the target coverage factor fails to account properly for the relative position of cold spots with respect to the GTV. In other words, large target coverage factor is no guarantee for a good plan. Clearly, vigilance is required when evaluating treatment plans based on one specific index.

Feuvret *et al.* emphasized that a single index may not be a good indicator as it might lead to omission of essential information.[16] Both target coverage factor and EUD of PTVs are criticized for their insensitivity to the spatial location of the cold spots. Their averaging effect could lead to an underestimation of the risk of locoregional tumor relapse due to GTV underdosage. In this study, the CI_{DD} scoring system containing four discrete factors was specially designed to address these issues. By taking the spatial dose distribution into account, the relative importance of each cold spot within the PTVs could be distinguished using four discrete factors. CI_{DD} could provide more comprehensive information on overall target coverage. With the greatest coefficient of variance in

comparison with other existing indices, the CI_{DD} scoring system could improve the plan quality discerning power and help planners select a plan with a preferable spatial dose distribution.

Still, a shortcoming of the CI_{DD} index is that it does not quantify the undesirable dose delivered to the normal tissue. As the target coverage increase, a small amount of surrounding tissue may be inevitably irradiated leading to potential complications. However, a plan could receive the perfect CI_{DD} score of 0 regardless of OARs overdose. Since the CI_{DD} index only focus on target coverage, HTCI takes into account exclusively the irradiation of normal tissue and CN comprises both measures, they cannot be validly compared. To sum up, the CI_{DD} index should not stand alone without being evaluated in conjunction with HTCI which provides a measure of normal tissue overdose. It is expected that the plan quality and consistency could be guaranteed by the use of both CI_{DD} and HTCI for plan evaluation. Nevertheless, clinical judgment and experience remain fundamental in making a final decision for the best interest of the patient.

Some limitations are noted in this study. First, the CI_{DD} index only provided a measure of dosimetric target coverage without assessing normal tissue sparing. In the future, the index could be improved by accounting for the dose-volume effects of OARs. Similar voxel-based spatial analysis could be performed for individual OAR. However, it is not clear how best to penalize the plan if specific OAR dose-volume constraints were violated. Second, the CI_{DD} scoring system was only evaluated based on the dosimetric data but not on the clinical outcomes such as follow-up data. It is worth doing further research by exploring the correlation between the CI_{DD} scoring system and the treatment outcome. Third, Gaussian function was applied to penalize the underdose regions similar to that described in Miften's study.[9] Nevertheless, empirical evidence in this regard was rather scanty. Further radiobiological research is expected to provide a closer look at the effect of cold spots on tumor control. Fourth, it was assumed that equal factor has relatively equal clinical importance and thus equal weights were assigned to the four discrete factors, namely, GTV coverage factor, GTV underdose factor, PTV minus GTV coverage factor, and PTV minus GTV underdose and distance factor. Further refinement of the CI_{DD} model would be necessary. Differential weights could be assigned to each factor according to their clinical importance. For example, higher weighting factor for GTV coverage factor and GTV underdose factor could be applied in the CI_{DD} calculation. Fifth, the distance penalty function was calculated two-dimensionally based on the data from each CT slice. However, the use of 3D distance from GTV surface could provide a better means to characterize the spatial relationship between GTV and PTV. Further study on the 3D calculation should be carried out. Sixth, the CI_{DD} scoring system might not be the best representation of the plan quality since it did not account for the biological impact of the dose deficit. After accumulating sufficient reliable radiobiological data, it might be worth designing a hybrid index that could combine the CI_{DD} scoring system with these biological factors for comprehensive plan evaluation. Lastly, the sample size was relatively small in this study. As a result, the samples might not be a good representation of the larger population making it harder to draw an unbiased conclusion. Future work should increase the sample size and, consequently, increase the statistical power.

V. CONCLUSION

The CI_{DD} for evaluation of IMRT plans for head-and-neck cancers was successfully developed. By taking individual target volume and shape variability into account, the spatial information related to the locations of cold spot within the PTV was incorporated into the CI_{DD} model. The CI_{DD} scoring system is capable of ranking treatment plans with similar DVHs but different distribution of underdosed regions. Compared with other existing quantitative indices, the tailor-made CI_{DD} scoring system results in the largest coefficient of variance, suggesting that its power to differentiate rival plans is the greatest. The use of CI_{DD} could provide an effective means of benchmarking performance, reducing treatment plan variability and advancing the quality of current IMRT planning. As an effective quality control measure, the CI_{DD} could be adopted in the evaluation of plans other than IMRT.

[a]Author to whom correspondence should be addressed. Electronic mail: fioncheung210@yahoo.com.hk

[1]B. Wu, F. Ricchetti, G. Sanguineti, M. Kazhdan, P. Simari, M. Chuang, R. Taylor, R. Jacques, and T. McNutt, "Patient geometry-driven information retrieval for IMRT treatment plan quality control," Med. Phys. **36**, 5497–5505 (2009).

[2]X. Zhu, Y. Ge, T. Li, D. Thongphiew, F. F. Yin, and Q. J. Wu, "A planning quality evaluation tool for prostate adaptive IMRT based on machine learning," Med. Phys. **38**, 719–726 (2011).

[3]T. Pawlicki and A. J. Mundt, "Quality in radiation oncology," Med. Phys. **34**, 1529–1534 (2007).

[4]International Commission on Radiation Units and Measurement (ICRU), "Prescribing, recording and reporting photon beam therapy," ICRU Report No. 83 (ICRU Publications, Washington, DC, 2010).

[5]E. Shaw, R. Kline, M. Gillin, L. Souhami, A. Hirschfeld, R. Dinapoli, and L. Martin, "Radiation therapy oncology group: Radiosurgery quality assurance guidelines," Int. J. Radiat. Oncol., Biol., Phys. **27**, 1231–1239 (1993).

[6]International Commission on Radiation Units and Measurement (ICRU), "Prescribing, recording and reporting photon beam therapy," ICRU Report No. 62 (ICRU Publications, Washington, DC, 1999).

[7]D. Lefkopoulos, P. Grandjean, and K. Platoni, "Progress in optimizing dosimetry plans in stereotactic radiotherapy in the Salt Group," Cancer Radiother **2**, 127–138 (1998).

[8]L. H. Leung, M. W. Kan, A. C. Cheng, W. K. Wong, and C. C. Yau, "A new dose-volume-based plan quality index for IMRT plan comparison," Radiother. Oncol. **85**, 407–417 (2007).

[9]M. M. Miften, S. K. Das, M. Su, and L. B. Marks, "A dose-volume-based tool for evaluating and ranking IMRT treatment plans," J. Appl. Clin. Med. Phys. **5**, 1–14 (2004).

[10]N. J. Lomax and S. G. Scheib, "Quantifying the degree of conformity in radiosurgery treatment planning," Int. J. Radiat. Oncol., Biol., Phys. **55**, 1409–1419 (2003).

[11]A. Van't Riet, A. C. Mak, M. A. Moerland, L. H. Elders, and W. van der Zee, "A conformation number to quantify the degree of conformality in brachytherapy and external beam irradiation: Application to the prostate," Int. J. Radiat. Oncol., Biol., Phys. **37**, 731–736 (1997).

[12]I. Paddick, "A simple scoring ratio to index the conformity of radiosurgical treatment plans: Technical note," J. Neurosurg. **93**, 219–222 (2000).

[13]D. Baltas, C. Kolotas, K. Geramani, R. F. Mould, G. Ioannidis, M. Kekchidi, and N. Zamboglou, "A conformal index (COIN) to evaluate implant quality and dose specification in brachytherapy," Int. J. Radiat. Oncol., Biol., Phys. **40**, 515–524 (1998).

[14]J. Menhel, D. Levin, D. Alezra, Z. Symon, and R. Pfeffer, "Assessing the quality of conformal treatment planning: A new tool for quantitative comparison," Phys. Med. Biol. **51**, 5363–5375 (2006).
[15]A. Chiti, M. Kirienko, and V. Gregoire, "Clinical use of PET-CT data for radiotherapy planning: What are we looking for?," Radiother. Oncol. **96**, 277–279 (2010).
[16]L. Feuvret, G. Noel, J. J. Mazeron, and P. Bey, "Conformity index: A review," Int. J. Radiat. Oncol., Biol., Phys. **64**, 333–342 (2006).
[17]J. D. Bradley, N. Leumwananonthachai, J. A. Purdy, T. H. Wasserman, M. A. Lockett, M. V. Graham, and C. A. Perez, "Gross tumor volume, critical prognostic factor in patients treated with three-dimensional conformal radiation therapy for non-small-cell lung carcinoma," Int. J. Radiat. Oncol., Biol., Phys. **52**, 49–57 (2002).
[18]M. E. Montejo, D. C. Shrieve, B. G. Bentz, J. P. Hunt, L. O. Buchman, N. Agarwal, and Y. J. Hitchcock, "IMRT with simultaneous integrated boost and concurrent chemotherapy for locoregionally advanced squamous cell carcinoma of the head and neck," Int. J. Radiat. Oncol., Biol., Phys. **81**, e845–e852 (2011).
[19]G. Ozyigit, M. Cengiz, G. Yazici, F. Yildiz, M. Gurkaynak, F. Zorlu, D. Yildiz, S. Hosal, I. Gullu, and F. Akyol, "A retrospective comparison of robotic stereotactic body radiotherapy and three-dimensional conformal radiotherapy for the reirradiation of locally recurrent nasopharyngeal carcinoma," Int. J. Radiat. Oncol., Biol., Phys. **81**, e263–e268 (2011).
[20]T. Leong, C. Everitt, K. Yuen, S. Condron, A. Hui, S. Y. Ngan, A. Pitman, E. W. Lau, M. MacManus, D. Binns, T. Ackerly, and R. J. Hicks, "A prospective study to evaluate the impact of FDG-PET on CT-based radiotherapy treatment planning for oesophageal cancer," Radiother. Oncol. **78**, 254–261 (2006).
[21]X. K. Zheng, L. H. Chen, Q. S. Wang, and F. B. Wu, "Influence of [18F] fluorodeoxyglucose positron emission tomography on salvage treatment decision making for locally persistent nasopharyngeal carcinoma," Int. J. Radiat. Oncol., Biol., Phys. **65**, 1020–1025 (2006).
[22]W. A. Tomé and J. F. Fowler, "On cold spots in tumor subvolumes," Med. Phys. **29**, 1590–1598 (2002).
[23]B. Zhao, M. C. Joiner, C. G. Orton, and J. Burmeister, "SABER: A new software tool for radiotherapy treatment plan evaluation," Med. Phys. **37**, 5586–5592 (2010).
[24]H. R. Withers, "Biological aspects of conformal therapy," Acta. Oncol. **39**, 569–577 (2000).
[25]H. A. Gay and A. Niemierko, "A free program for calculating EUD-based NTCP and TCP in external beam radiotherapy," Phys. Med. **23**, 115–125 (2007).
[26]W. T. Ng, M. C. Lee, W. M. Hung, C. W. Choi, K. C. Lee, O. S. Chan, and A. W. Lee, "Clinical outcomes and patterns of failure after intensity-modulated radiotherapy for nasopharyngeal carcinoma," Int. J. Radiat. Oncol., Biol., Phys. **79**, 420–428 (2011).

Zhang et al. Journal of Translational Medicine 2012, 10(Suppl 2):A32
http://www.translational-medicine.com/content/10/S1/A32

JOURNAL OF TRANSLATIONAL MEDICINE

MEETING ABSTRACT Open Access

Building Biomedical Imaging and Informatics e-Science platform for translational medical research

Jianguo Zhang[1*], Kai Zhang[1], Tusheng Wang[1], Yuanyuan Yang[1], Haibo Hu[2], Lisa Xu[2]

From 2012 Sino-American Symposium on Clinical and Translational Medicine (SAS-CTM)
Shanghai, China. 27-29 June 2012

Background

As there are urgent demands to bring medical imaging research and clinical service together more closely to solve the problems related to disease discover, medical research, diagnosis and education, a new imaging and informatics infrastructure and paradigm need to be developed to promote multiple disciplines of medical researchers, clinical physicians and biomedical engineers working together in a secured, efficient, and transparent cooperative environment [1]. In this presentation, we outline our preliminary work of building Biomedical Imaging and Informatics (BMII)"e-Science" platform to support collaborative research among multi-disciplines to enable translational research in multiple affiliated hospitals and academic institutions of Shanghai Jiaotong University (SJTU), and Chinese Academy of Sciences (CAS).

Materials and methods

SJTU has 12 large affiliated hospitals located in multiple districts of Shanghai city with a lot of medical and biomedical imaging modalities (e.g., Clinical CT/MR, Micro-PET/CT) being decentralized used in these hospitals and research centers. Also, there is a powerful Shanghai Synchronic Radiation Facility (SSRF) developed by CAS to support large scale of biomedical imaging researches from molecular level to organ parts [2]. So, we designed and developed the e-Science platform to promote the multi-disciplines working together cross these hospitals and academic institutions, and adopted the Service-Oriented Architecture and grid-based concept to build it. In order to enable efficient collaborating, we designed the work and data flows with Principal Investigator (PI)-oriented information model, and developed a documents/data sharing mechanism based on IHE XDS/XDS-I profiles and the access control standard of XACML in this platform.

Results

We implemented the BMII e-Science platform crossing Shanghai Ruijin Hospital, two campuses of SJTU, SSRS and Shanghai Institute of Technical Physics, CAS. The data communications of the e-Science platform from site to site are fast enough as they are going through the China Education Network in Shanghai with backbone of a few of GB/sec. There were two kinds of collaborations in the e-Science platform, one is to perform real-time interactively or synchronously biomedical imaging experiment among onsite users and remote users, and the other is to share the image data or documents among collaborators.

Conclusions

The developed BMII e-Science platform can promote multiple disciplines of medical researchers, clinical physicians and biomedical engineers working together in a secured, efficient, and transparent cooperative networking environment. Now, the researches, clinical physicians and students can use this e-Science platform to perform biomedical imaging experiments and to do collaborative researching cross multiple hospitals and academic institutions.

Acknowledgements

This research are supported by the grant from the Major State Basic Research Development Program of China (973 Program No.: 2010CB834302) and 985 project of Shanghai Jiaotong University.

* Correspondence: jzhang@mail.sitp.ac.cn
[1]Shanghai Institute of Technical Physics, Chinese Academy of Sciences, Shanghai, China
Full list of author information is available at the end of the article

Author details
[1]Shanghai Institute of Technical Physics, Chinese Academy of Sciences, Shanghai, China. [2]School of Biomedical Engineering and Med-X Research Institute, Shanghai Jiaotong University, Shanghai, China.

Published: 17 October 2012

References

1. Saltz J, Kurc T, Hastings S, *et al*: **e-Science, caGrid, and Translational Biomedical Research.** *IEEE Computer* 2008, **41**:58-66.
2. Xiaoxia Liu, Jun Zhao, Jianqi Sun, Xiang Gu, Tiqiao Xiao, Ping Liu, Lisa X, Xu : **Lung Cancer and Angiogenesis Imaging using Synchrotron Radiation.** *Physics in Medicine and Biology* 2010, **55**:2399-2409.

doi:10.1186/1479-5876-10-S2-A32
Cite this article as: Zhang *et al.*: Building Biomedical Imaging and Informatics e-Science platform for translational medical research. *Journal of Translational Medicine* 2012 **10**(Suppl 2):A32.

JOURNAL OF TRANSLATIONAL MEDICINE

MEETING ABSTRACT Open Access

The role of imaging informatics in clinical translational research: perspectives and challenges from a US academic institution

Brent J Liu

From 2012 Sino-American Symposium on Clinical and Translational Medicine (SAS-CTM) Shanghai, China. 27-29 June 2012

Nearly in all clinical medicine specialties, medical images and other multi-media related data are generated and need to be distributed to points of decision. Recently, the electronic patient record (ePR) with image distribution system is gradually taking over as the method for distribution of multi-media content to the clinical environment. New challenges are accompanying its spread into other clinical fields. Particularly important are the modeling and analysis of workflow of the affected clinical disciplines as well as interface and integration issues with the image-connected electronic patient record. Although the awareness of these issues is increasing rapidly, equally important is the recognition in the professional community that more rigorous scientific methods are needed to handle the clinical system development and deployment. Furthermore, medical imaging informatics is not only based on many existing concepts, theories, terminology, and methodology derived from health informatics, but also deals with different types of data including multi-dimensional medical images, graphics, waveforms, graphics and text which are focused on the cellular, tissue, and organ systems. Accordingly, medical imaging informatics requires new concepts and new tool sets to handle these types of data. This presentation aims to first introduce the basic concepts of Medical Imaging Informatics infrastructure in both research and clinical environments including PACS, RIS, HIS, ePR, standards, databases, and system integration. This will be followed with discussions of new frontier areas of research in medical imaging informatics with some examples of clinical applications in Surgery, Neurology, Oncology, and Neuro-Rehabilitation.

Correspondence: brentliu@usc.edu
Image Processing and Informatics Laboratory (IPILab), Department of Biomedical Engineering, Viterbi School of Engineering, University of Southern California, Los Angeles, California, 90089, USA

Published: 17 October 2012

doi:10.1186/1479-5876-10-S2-A27
Cite this article as: Liu: The role of imaging informatics in clinical translational research: perspectives and challenges from a US academic institution. *Journal of Translational Medicine* 2012 **10**(Suppl 2):A27.

US008313432B2

(12) **United States Patent**
Chiu et al.

(10) **Patent No.: US 8,313,432 B2**
(45) **Date of Patent: Nov. 20, 2012**

(54) **SURGICAL DATA MONITORING AND DISPLAY SYSTEM**

(75) Inventors: **John C. Chiu**, Thousand Oaks, CA (US); **Han K. Huang**, Agoura Hills, CA (US)

(73) Assignee: **SurgMatix, Inc.**, Thousand Oaks, CA (US)

(*) Notice: Subject to any disclaimer, the term of this patent is extended or adjusted under 35 U.S.C. 154(b) by 1101 days.

(21) Appl. No.: **12/143,711**

(22) Filed: **Jun. 20, 2008**

(65) **Prior Publication Data**

US 2008/0319275 A1 Dec. 25, 2008

Related U.S. Application Data

(60) Provisional application No. 60/936,639, filed on Jun. 20, 2007.

(51) **Int. Cl.**
A61B 5/00 (2006.01)

(52) **U.S. Cl.** **600/300**; 600/301; 705/2; 705/3

(58) **Field of Classification Search** ..... None
See application file for complete search history.

(56) **References Cited**

U.S. PATENT DOCUMENTS

4,817,091	A *	3/1989	Katzman et al.	714/6.13
5,262,944	A *	11/1993	Weisner et al.	600/300
5,331,549	A *	7/1994	Crawford, Jr.	600/513
5,788,688	A *	8/1998	Bauer et al.	606/1
5,819,229	A *	10/1998	Boppe	705/2
5,848,173	A *	12/1998	Sato et al.	381/398
6,928,490	B1 *	8/2005	Bucholz et al.	709/249
2002/0177758	A1 *	11/2002	Schoenberg et al.	600/300
2002/0188213	A1	12/2002	Bardy	
2003/0153818	A1	8/2003	Bocionek et al.	
2003/0156745	A1 *	8/2003	Saito et al.	382/128
2004/0059604	A1 *	3/2004	Zaleski	705/2
2005/0038326	A1	2/2005	Mathur	
2005/0101844	A1	5/2005	Duckert et al.	
2005/0149363	A1 *	7/2005	Loiterman et al.	705/3
2006/0085299	A1 *	4/2006	Goll et al.	705/28
2006/0206011	A1 *	9/2006	Higgins et al.	600/300
2006/0226308	A1 *	10/2006	White et al.	248/122.1
2007/0168461	A1 *	7/2007	Moore	709/217
2007/0260126	A1 *	11/2007	Haumann et al.	600/300

* cited by examiner

Primary Examiner — Henry M. Johnson, III
Assistant Examiner — Marie Archer
(74) *Attorney, Agent, or Firm* — James W. Hill; McDermott Will & Emery LLP

(57) **ABSTRACT**

A surgical data monitoring and display system is described. In some embodiments, the system includes a data storage module that stores retrospective data and real-time surgical data concerning a patient, a first processing module that receives and processes the retrospective data into processed retrospective data, and a second processing module that receives and processes the real-time data into processed real-time data. Each of the first processing module and the second processing module transmits their processed data to first and second display modules, respectively, before or during performance by a healthcare provider of a medical or surgical procedure on the patient.

32 Claims, 19 Drawing Sheets

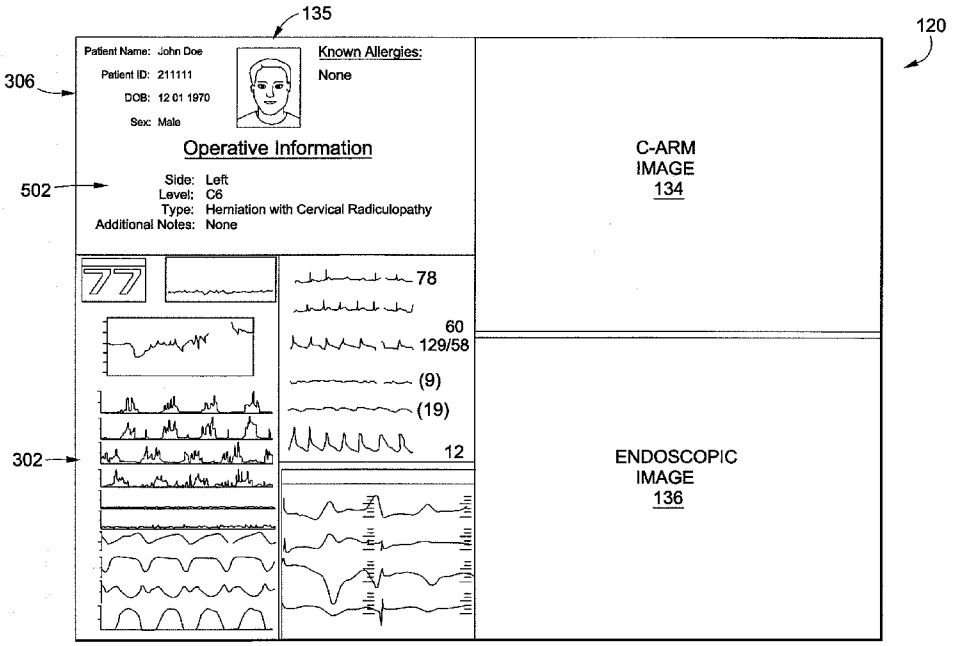

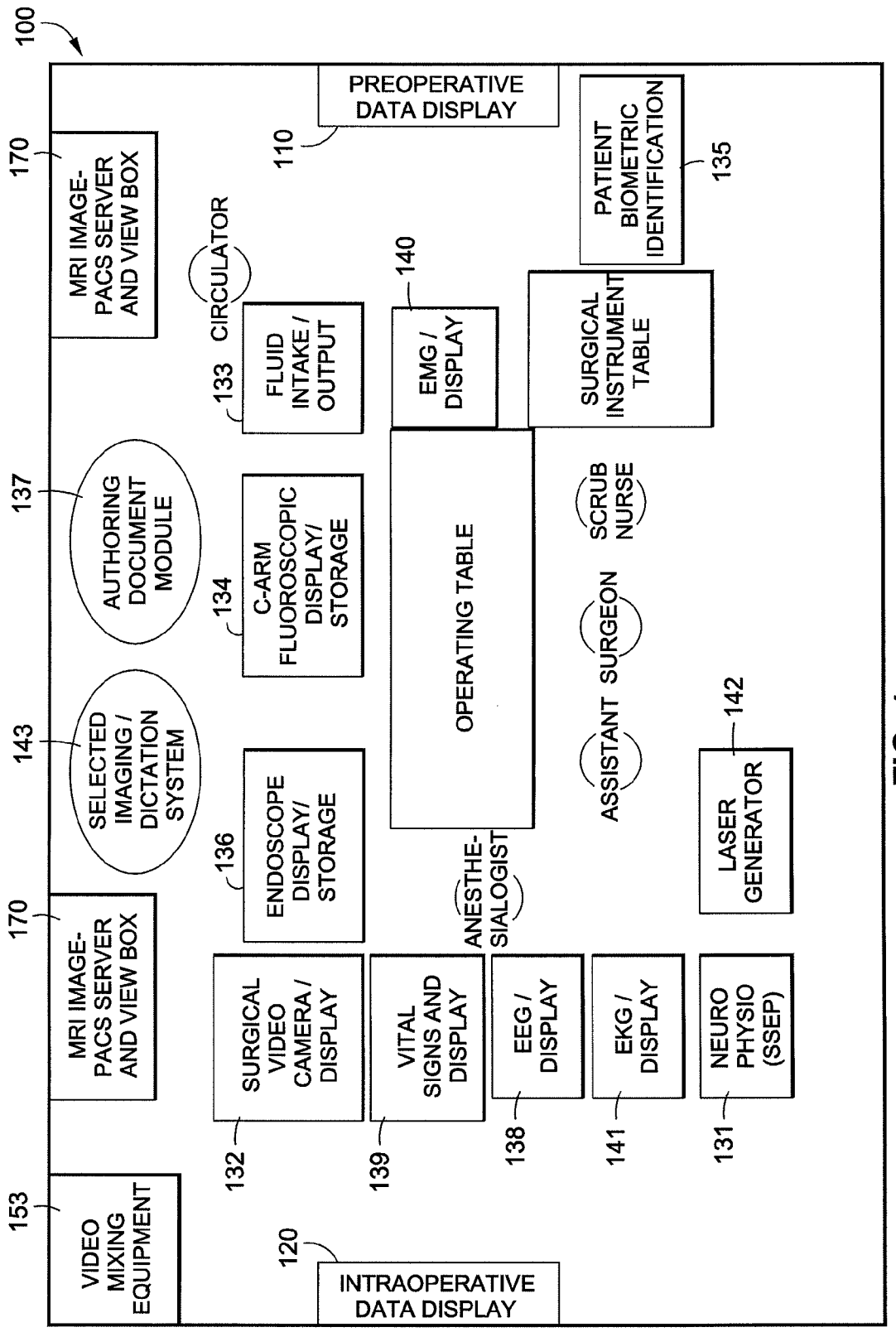
100
PREOPERATIVE DATA DISPLAY
110
MRI IMAGE-PACS SERVER AND VIEW BOX
170
PATIENT BIOMETRIC IDENTIFICATION
135
CIRCULATOR
133
FLUID INTAKE / OUTPUT
EMG / DISPLAY
140
SURGICAL INSTRUMENT TABLE
AUTHORING DOCUMENT MODULE
137
C-ARM FLUOROSCOPIC DISPLAY/ STORAGE
134
OPERATING TABLE
SCRUB NURSE
SURGEON
ASSISTANT
SELECTED IMAGING / DICTATION SYSTEM
143
ENDOSCOPE DISPLAY/ STORAGE
136
ANESTHE-SIALOGIST
LASER GENERATOR
142
MRI IMAGE-PACS SERVER AND VIEW BOX
170
SURGICAL VIDEO CAMERA / DISPLAY
VITAL SIGNS AND DISPLAY
EEG / DISPLAY
EKG / DISPLAY
NEURO PHYSIO (SSEP)
132
139
138
141
131
VIDEO MIXING EQUIPMENT
153
120
INTRAOPERATIVE DATA DISPLAY

FIG. 1

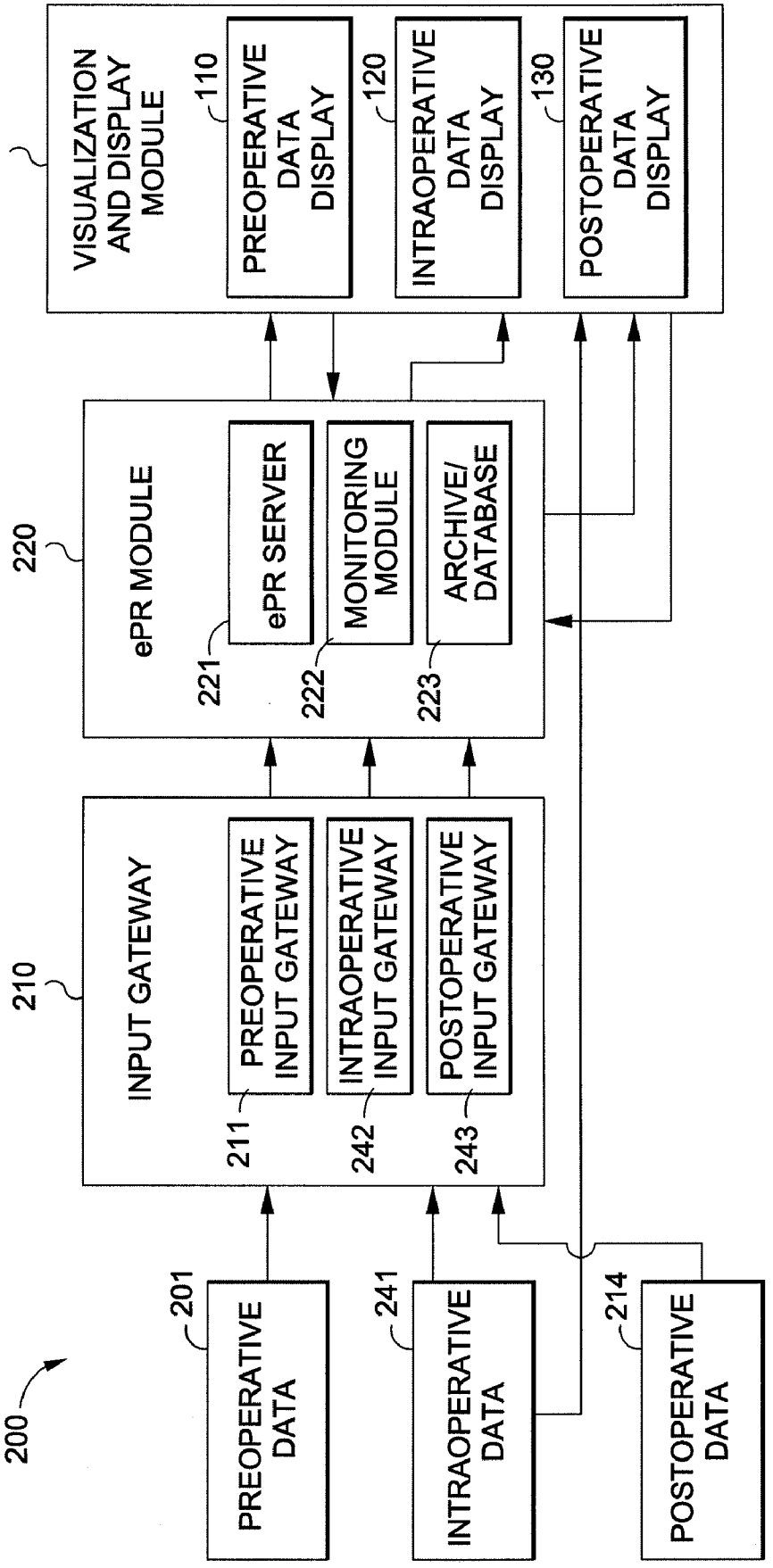
200
PREOPERATIVE DATA
201
INTRAOPERATIVE DATA
241
POSTOPERATIVE DATA
214
INPUT GATEWAY
210
PREOPERATIVE INPUT GATEWAY
211
INTRAOPERATIVE INPUT GATEWAY
242
POSTOPERATIVE INPUT GATEWAY
243
ePR MODULE
220
ePR SERVER
221
MONITORING MODULE
222
ARCHIVE/ DATABASE
223
VISUALIZATION AND DISPLAY MODULE
230
PREOPERATIVE DATA DISPLAY
110
INTRAOPERATIVE DATA DISPLAY
120
POSTOPERATIVE DATA DISPLAY
130

FIG. 2

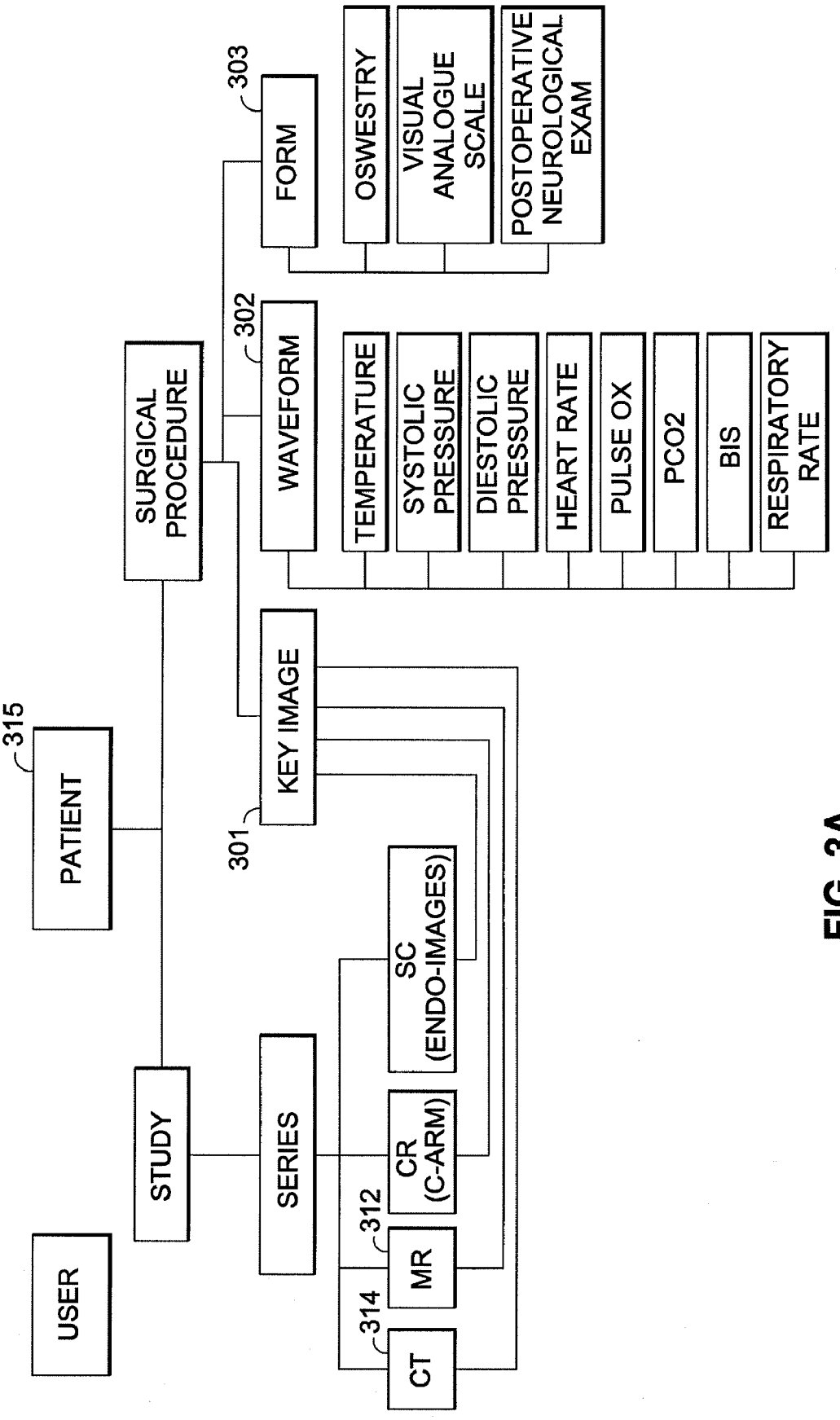
USER
STUDY
SERIES
CT
MR
CR (C-ARM)
SC (ENDO-IMAGES)
312
314
PATIENT
315
KEY IMAGE
301
SURGICAL PROCEDURE
WAVEFORM
302
TEMPERATURE
SYSTOLIC PRESSURE
DIESTOLIC PRESSURE
HEART RATE
PULSE OX
PCO2
BIS
RESPIRATORY RATE
FORM
303
OSWESTRY
VISUAL ANALOGUE SCALE
POSTOPERATIVE NEUROLOGICAL EXAM

FIG. 3A

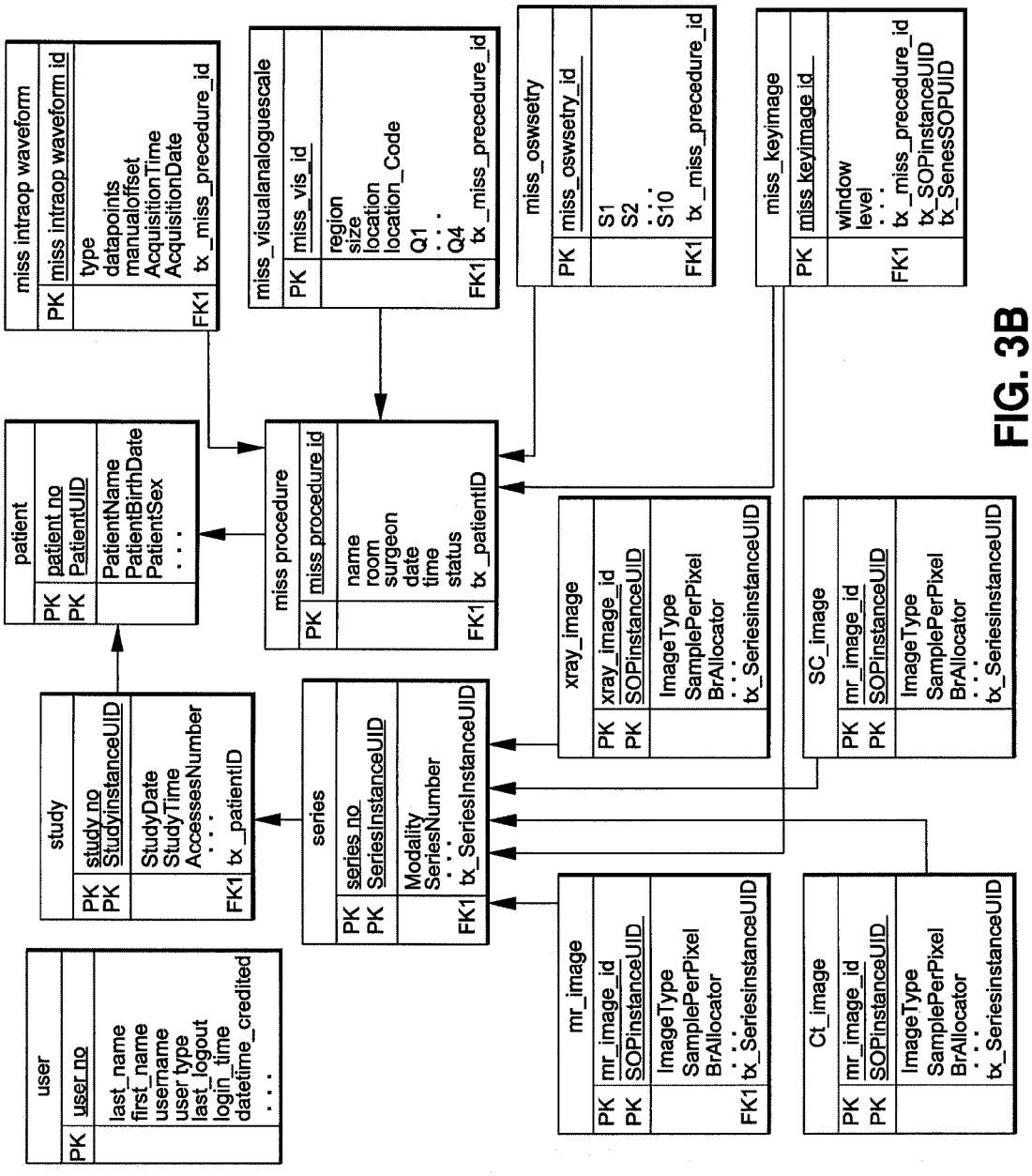
miss intraop waveform
PK miss intraop waveform id
type
datapoints
manualoffset
AcquisitionTime
AcquisitionDate
FK1 tx_miss_precedure_id
miss_visualanaloguescale
PK miss_vis_id
region
size
location
location_Code
Q1
. . .
Q4
FK1 tx_miss_precedure_id
miss_oswsetry
PK miss_oswsetry_id
S1
S2
. . .
S10
FK1 tx_miss_precedure_id
miss_keyimage
PK miss keyimage id
window
level
. . .
FK1 tx_miss_precedure_id
tx_SOPinstanceUID
tx_SenesSOPUID
patient
PK patient no
PK PatientUID
PatientName
PatientBirthDate
PatientSex
. . .
miss procedure
PK miss procedure id
name
room
surgeon
date
time
status
FK1 tx_patientID
study
PK study no
PK StudyinstanceUID
StudyDate
StudyTime
AccessesNumber
. . .
FK1 tx_patientID
series
PK series no
PK SeriesInstanceUID
Modality
SeriesNumber
. . .
FK1 tx_SeriesInstanceUID
xray_image
PK xray_image_id
PK SOPinstanceUID
ImageType
SamplePerPixel
BrAllocator
. . .
tx_SeriesinstanceUID
SC_image
PK mr_image_id
PK SOPinstanceUID
ImageType
SamplePerPixel
BrAllocator
. . .
tx_SeriesinstanceUID
user
PK user no
last_name
first_name
username
user type
last_logout
login_time
datetime_credited
. . .
mr_image
PK mr_image_id
PK SOPinstanceUID
ImageType
SamplePerPixel
BrAllocator
. . .
FK1 tx_SeriesinstanceUID
Ct_image
PK mr_image_id
PK SOPinstanceUID
ImageType
SamplePerPixel
BrAllocator
. . .
tx_SeriesinstanceUID

FIG. 3B

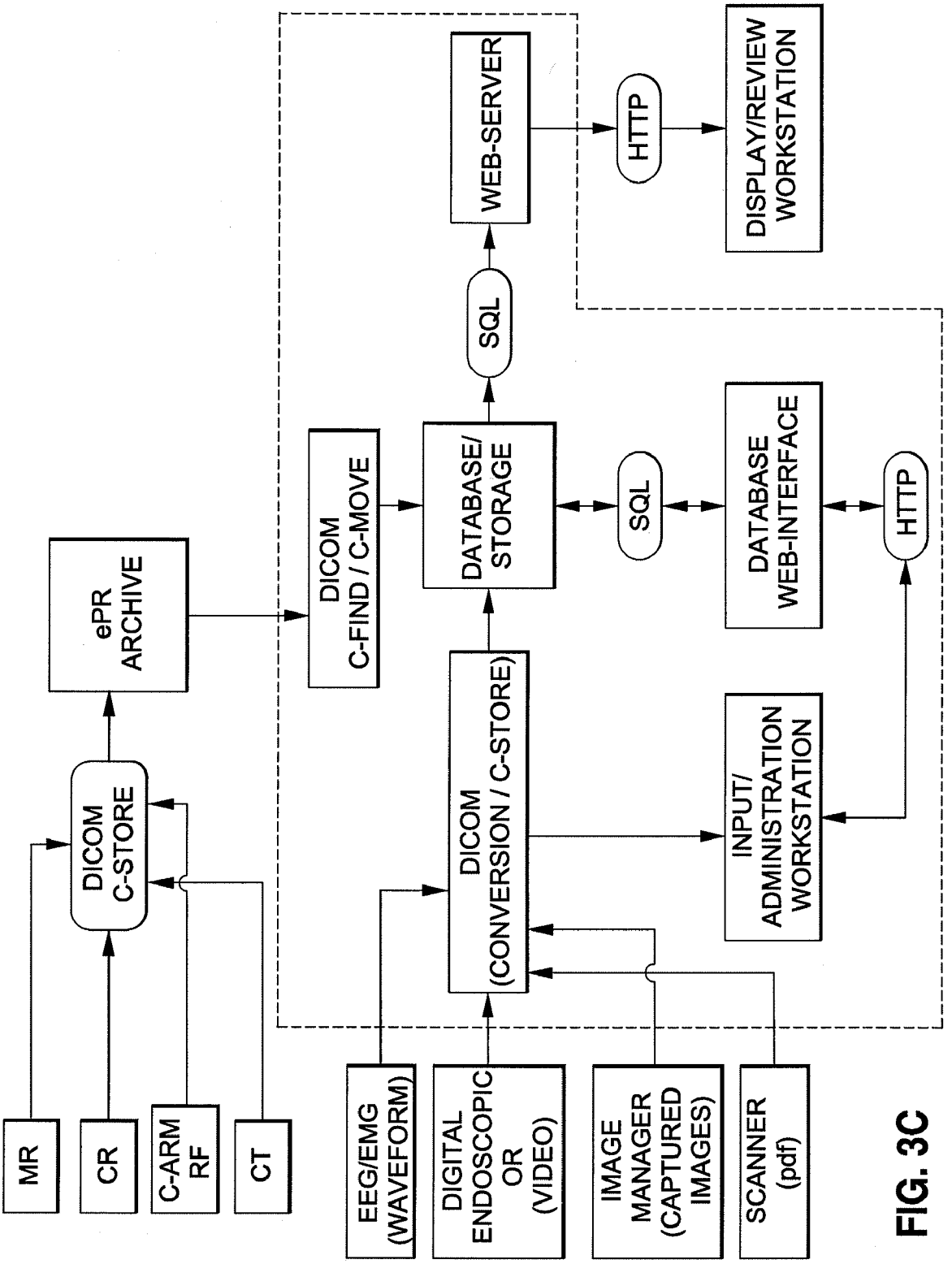
MR
CR
C-ARM RF
CT
DICOM C-STORE
ePR ARCHIVE
EEG/EMG (WAVEFORM)
DIGITAL ENDOSCOPIC OR (VIDEO)
IMAGE MANAGER (CAPTURED IMAGES)
SCANNER (pdf)
DICOM (CONVERSION / C-STORE)
DICOM C-FIND / C-MOVE
DATABASE/ STORAGE
SQL
SQL
WEB-SERVER
HTTP
DISPLAY/REVIEW WORKSTATION
DATABASE WEB-INTERFACE
HTTP
INPUT/ ADMINISTRATION WORKSTATION

FIG. 3C

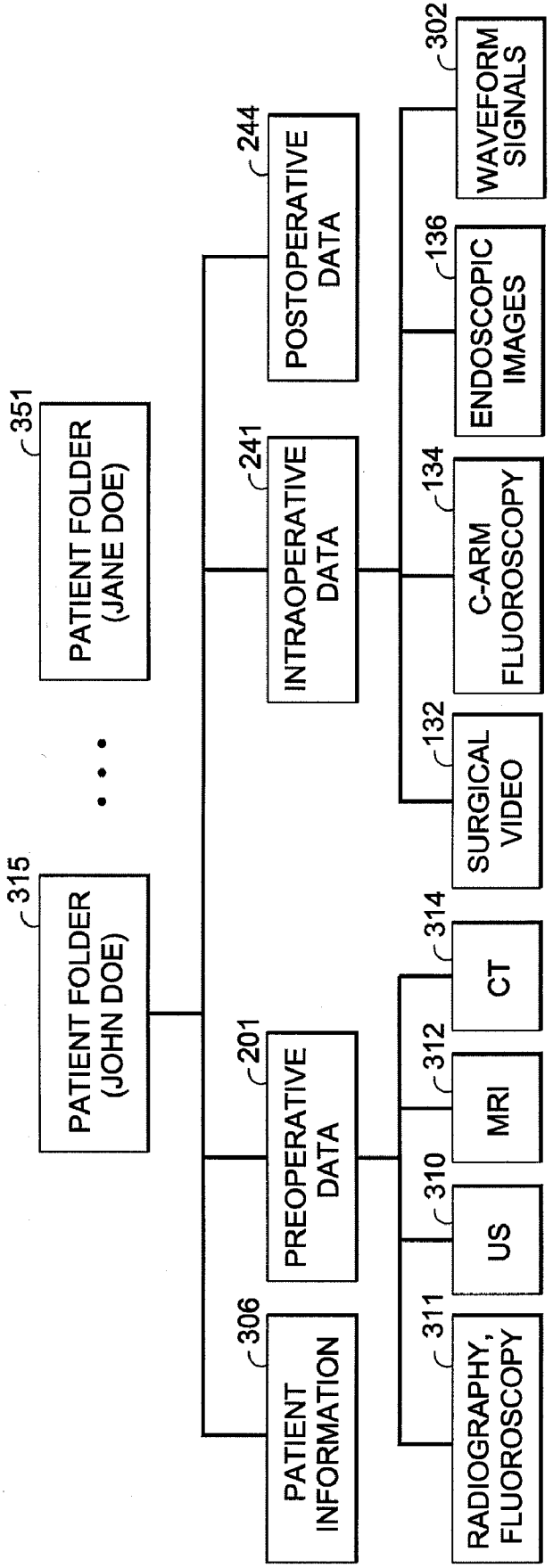
315
PATIENT FOLDER (JOHN DOE)
351
PATIENT FOLDER (JANE DOE)
306
PATIENT INFORMATION
201
PREOPERATIVE DATA
241
INTRAOPERATIVE DATA
244
POSTOPERATIVE DATA
311
RADIOGRAPHY, FLUOROSCOPY
310
US
312
MRI
314
CT
132
SURGICAL VIDEO
134
C-ARM FLUOROSCOPY
136
ENDOSCOPIC IMAGES
302
WAVEFORM SIGNALS

FIG. 3D

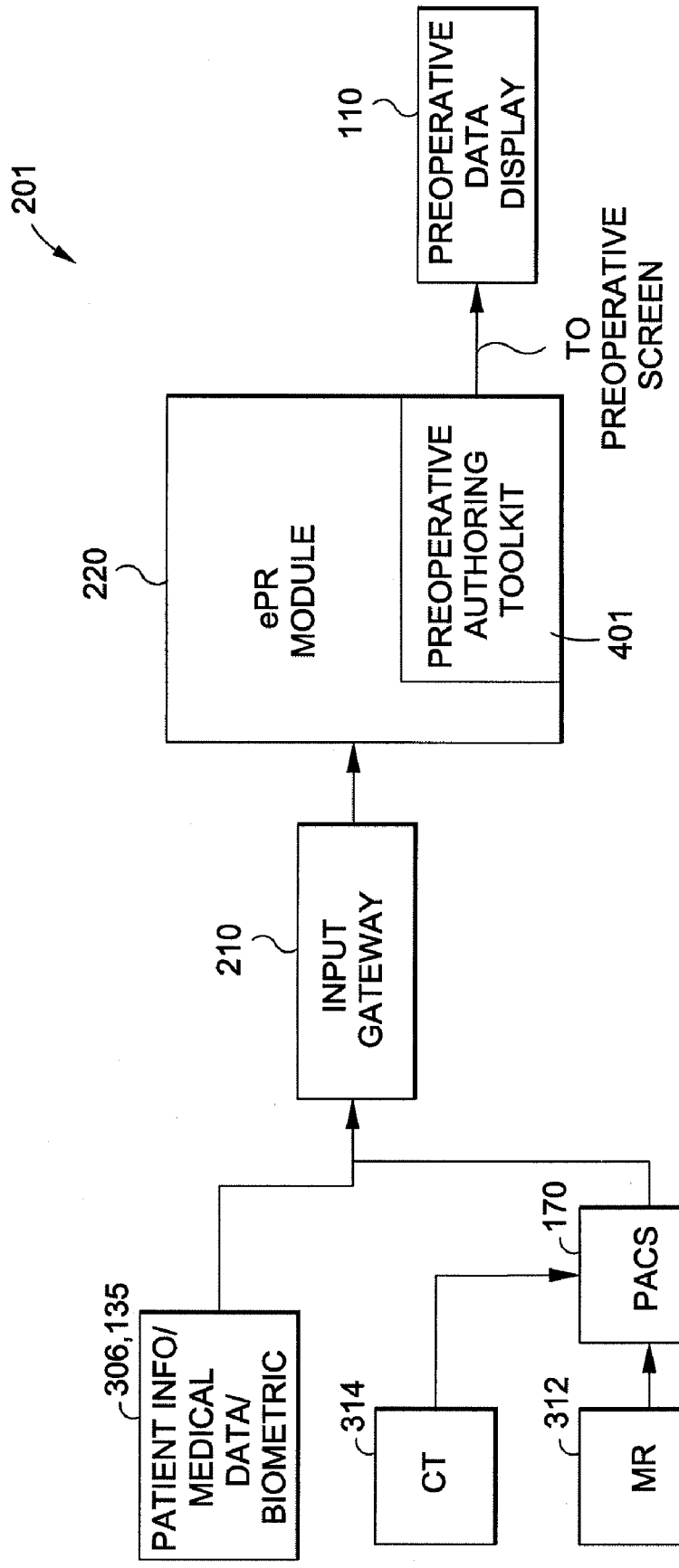
201
110
PREOPERATIVE DATA DISPLAY
TO PREOPERATIVE SCREEN
220
ePR MODULE
PREOPERATIVE AUTHORING TOOLKIT
401
210
INPUT GATEWAY
306,135
PATIENT INFO/ MEDICAL DATA/ BIOMETRIC
314
CT
312
MR
170
PACS

FIG. 4A

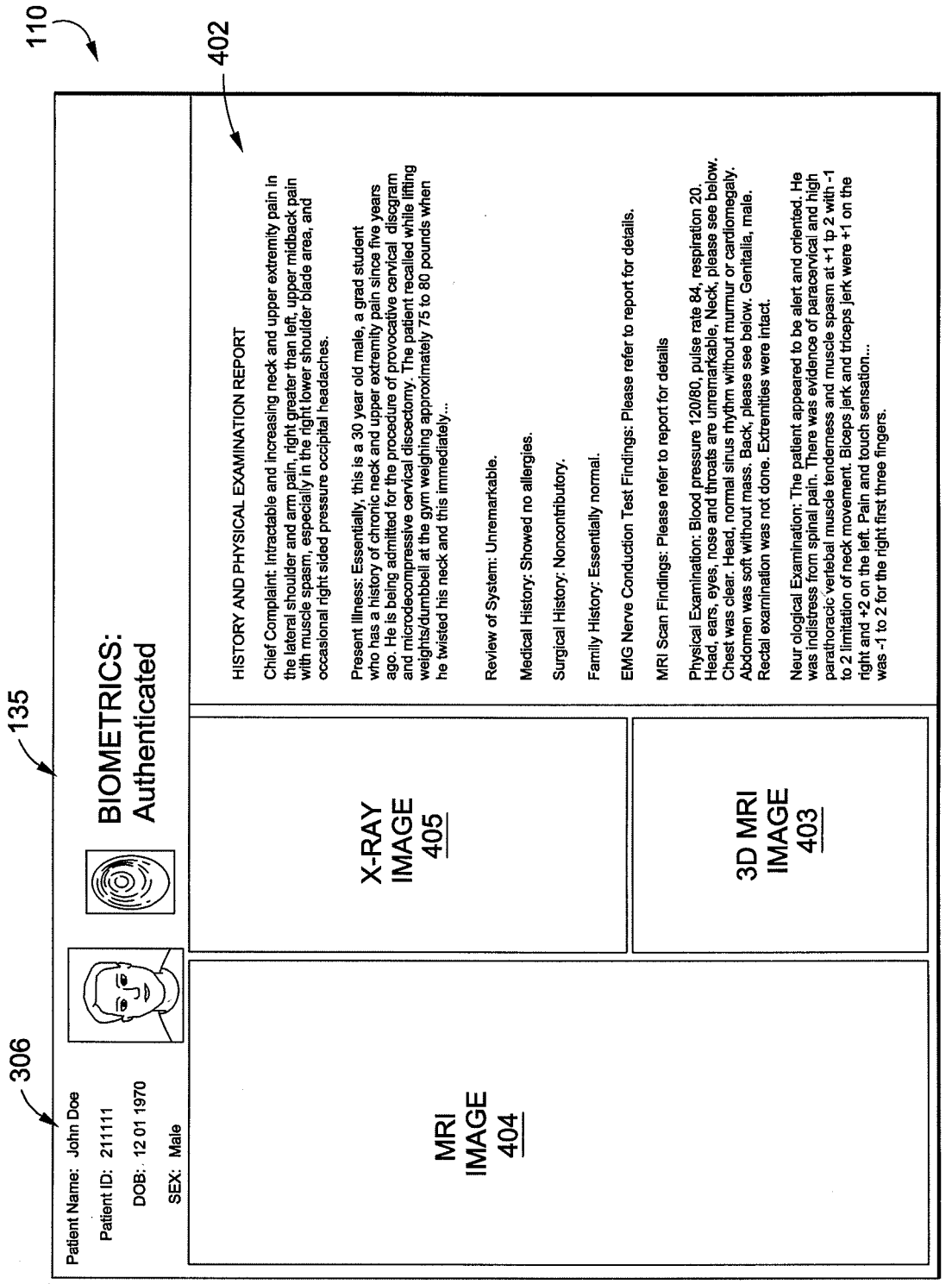
110
135
306
402
Patient Name: John Doe
Patient ID: 211111
DOB: 12 01 1970
SEX: Male
BIOMETRICS:
Authenticated
MRI IMAGE 404
X-RAY IMAGE 405
3D MRI IMAGE 403
HISTORY AND PHYSICAL EXAMINATION REPORT
Chief Complaint: intractable and increasing neck and upper extremity pain in the lateral shoulder and arm pain, right greater than left, upper midback pain with muscle spasm, especially in the right lower shoulder blade area, and occasional right sided pressure occipital headaches.
Present Illness: Essentially, this is a 30 year old male, a grad student who has a history of chronic neck and upper extremity pain since five years ago. He is being admitted for the procedure of provocative cervical discgram and microdecompressive cervical discectomy. The patient recalled while lifting weights/dumbbell at the gym weighing approximately 75 to 80 pounds when he twisted his neck and this immediately...
Review of System: Unremarkable.
Medical History: Showed no allergies.
Surgical History: Noncontributory.
Family History: Essentially normal.
EMG Nerve Conduction Test Findings: Please refer to report for details.
MRI Scan Findings: Please refer to report for details
Physical Examination: Blood pressure 120/80, pulse rate 84, respiration 20. Head, ears, eyes, nose and throats are unremarkable, Neck, please see below. Chest was clear. Head, normal sinus rhythm without murmur or cardiomegaly. Abdomen was soft without mass. Back, please see below. Genitalia, male. Rectal examination was not done. Extremities were intact.
Neur ological Examination: The patient appeared to be alert and oriented. He was indistress from spinal pain. There was evidence of paracervical and high parathoracic vertebal muscle tenderness and muscle spasm at +1 tp 2 with -1 to 2 limitation of neck movement. Bloceps jerk and triceps jerk were +1 on the right and +2 on the left. Pain and touch sensation.... was -1 to 2 for the right first three fingers.

FIG. 4B

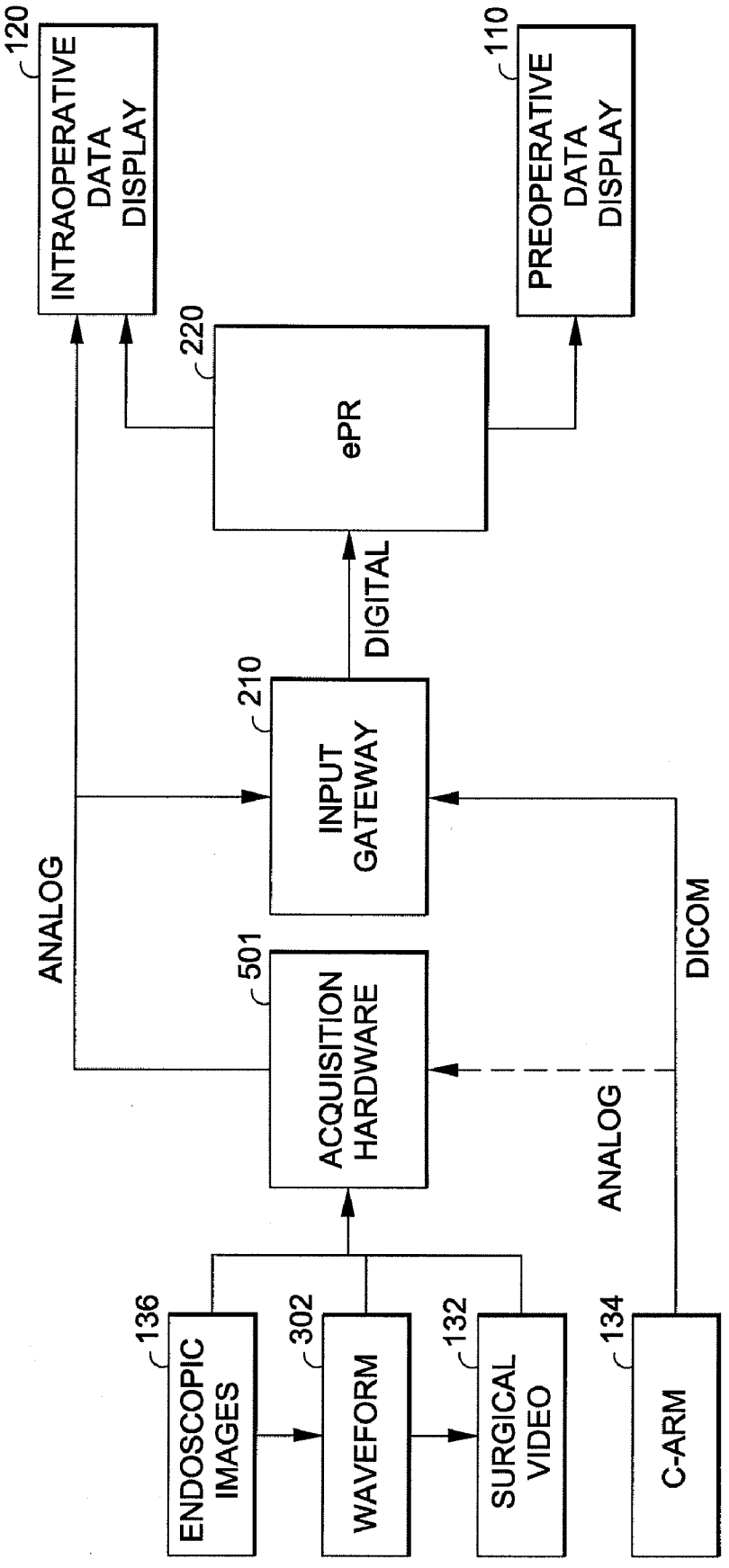
120
INTRAOPERATIVE DATA DISPLAY
110
PREOPERATIVE DATA DISPLAY
220
ePR
DIGITAL
210
INPUT GATEWAY
ANALOG
501
ACQUISITION HARDWARE
DICOM
ANALOG
136
ENDOSCOPIC IMAGES
302
WAVEFORM
132
SURGICAL VIDEO
134
C-ARM

FIG. 5A

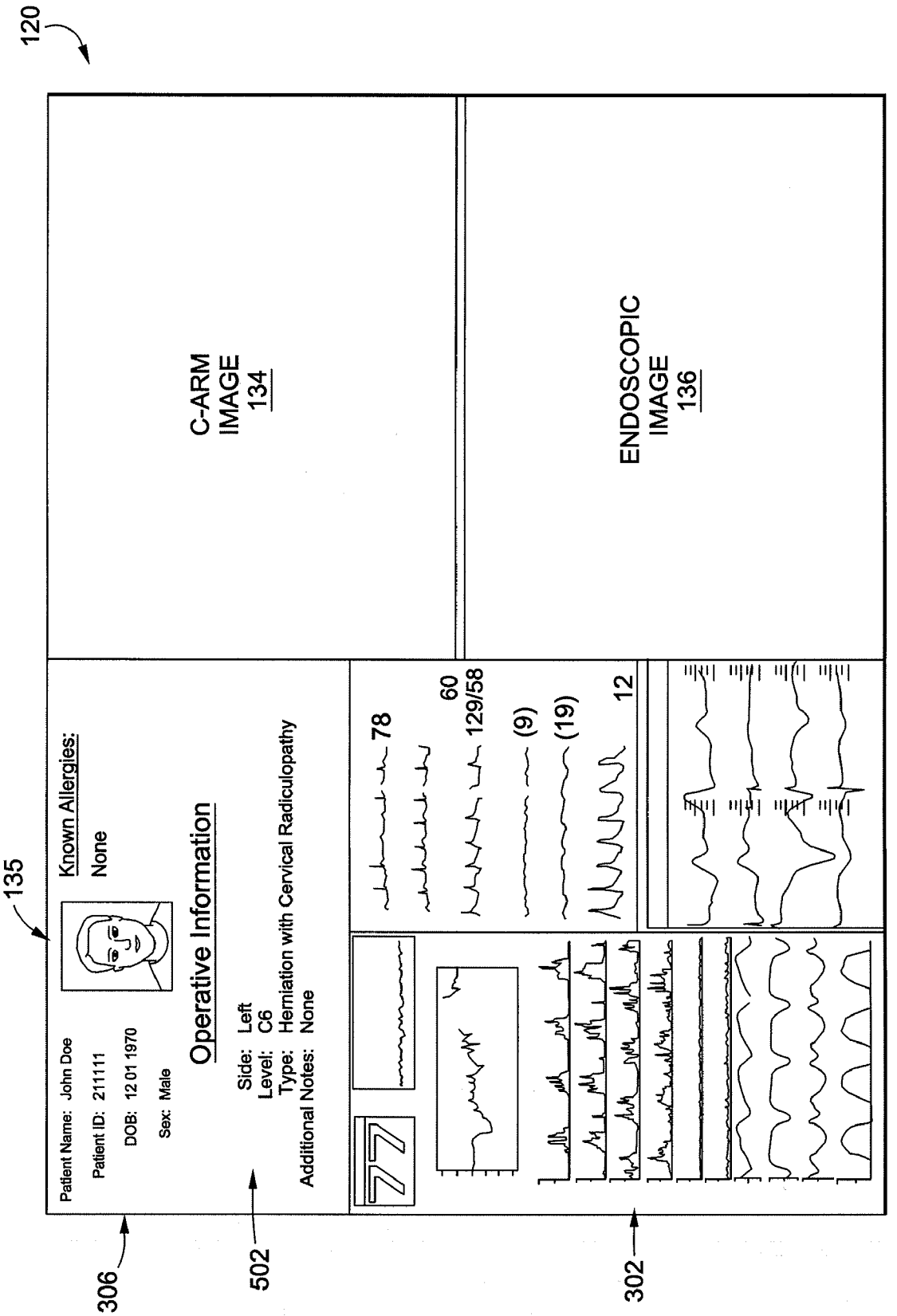
120
135
306
502
302
Patient Name: John Doe
Patient ID: 211111
DOB: 12 01 1970
Sex: Male
Known Allergies:
None
Operative Information
Side: Left
Level: C6
Type: Herniation with Cervical Radiculopathy
Additional Notes: None
C-ARM IMAGE 134
ENDOSCOPIC IMAGE 136
78
60
129/58
(9)
(19)
12

FIG. 5B

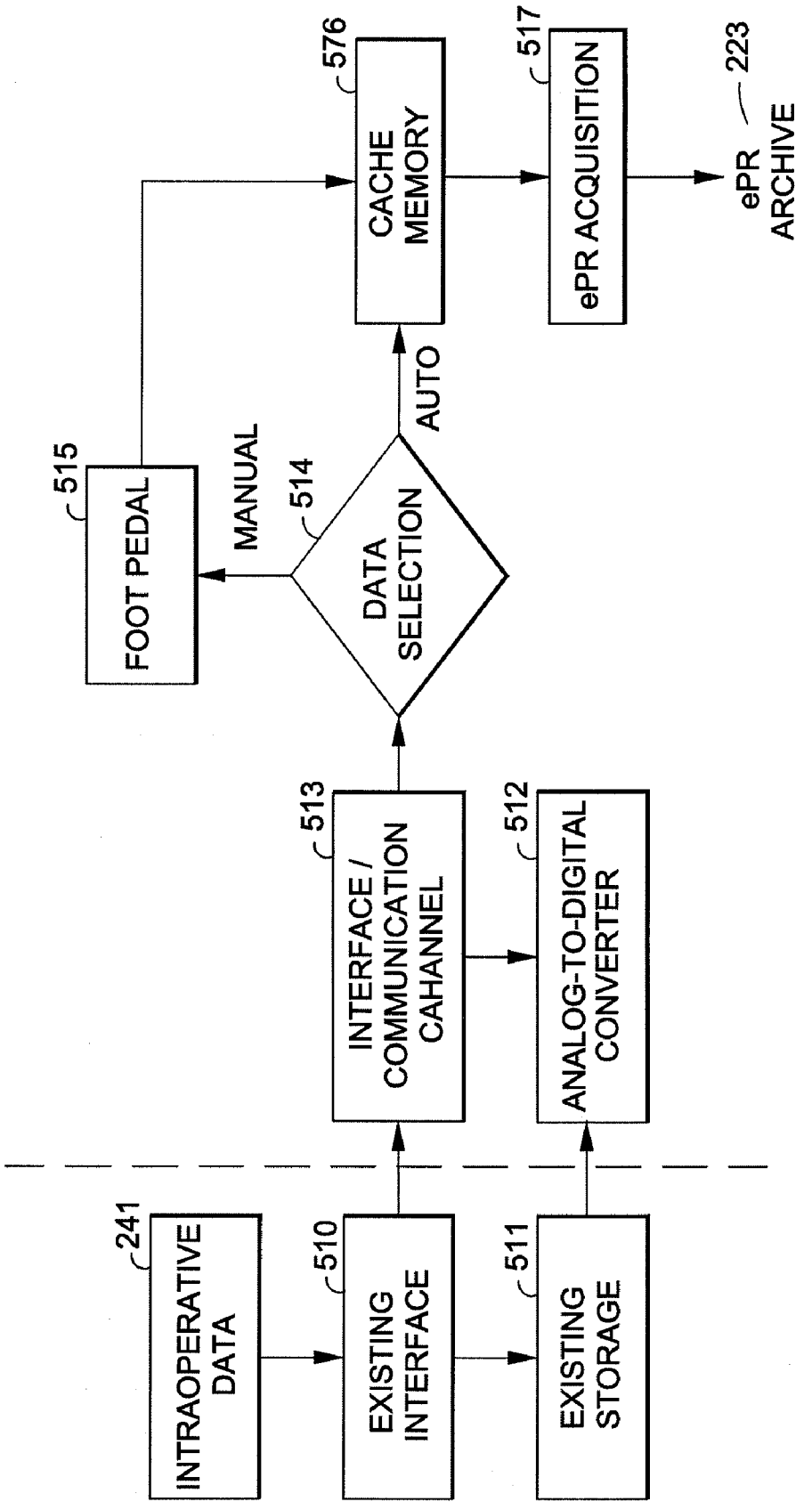
241
INTRAOPERATIVE DATA
510
EXISTING INTERFACE
511
EXISTING STORAGE
513
INTERFACE / COMMUNICATION CAHANNEL
512
ANALOG-TO-DIGITAL CONVERTER
514
DATA SELECTION
MANUAL
AUTO
515
FOOT PEDAL
576
CACHE MEMORY
517
ePR ACQUISITION
223
ePR ARCHIVE

FIG. 5C

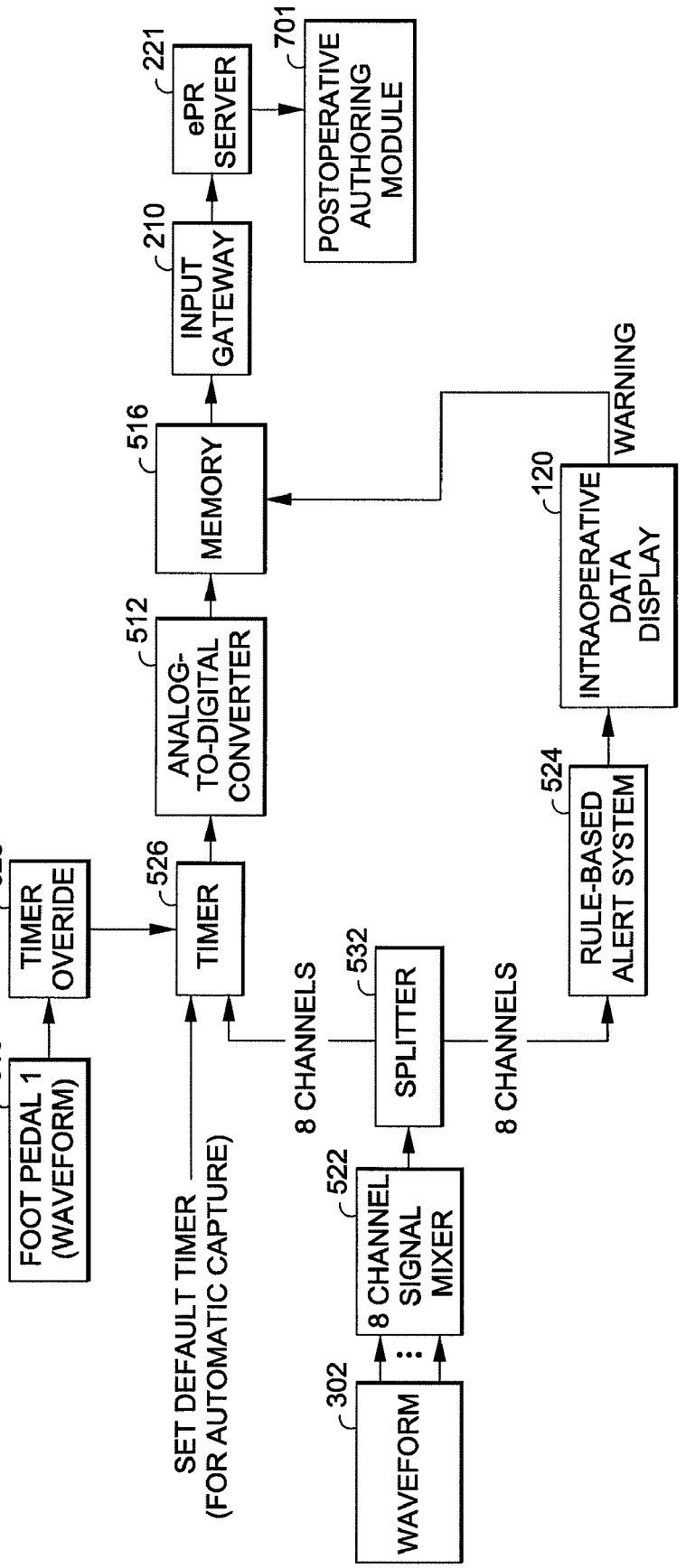
WAVEFORM
302
8 CHANNEL SIGNAL MIXER
522
SPLITTER
532
8 CHANNELS
8 CHANNELS
RULE-BASED ALERT SYSTEM
524
INTRAOPERATIVE DATA DISPLAY
120
WARNING
MEMORY
516
ANALOG-TO-DIGITAL CONVERTER
512
TIMER
526
SET DEFAULT TIMER (FOR AUTOMATIC CAPTURE)
TIMER OVERIDE
525
FOOT PEDAL 1 (WAVEFORM)
515
INPUT GATEWAY
210
ePR SERVER
221
POSTOPERATIVE AUTHORING MODULE
701

FIG. 5D

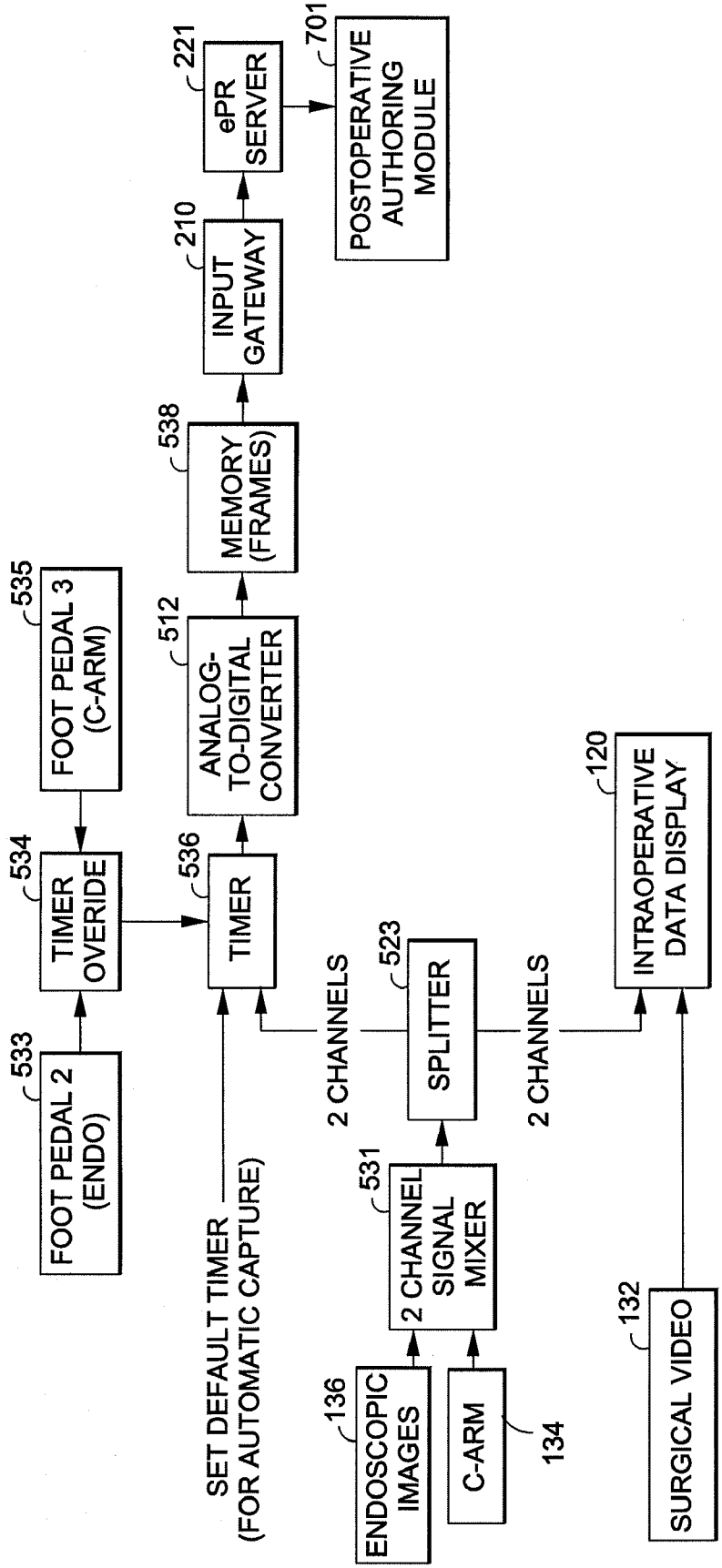
701
POSTOPERATIVE AUTHORING MODULE
221
ePR SERVER
210
INPUT GATEWAY
538
MEMORY (FRAMES)
512
ANALOG-TO-DIGITAL CONVERTER
535
FOOT PEDAL 3 (C-ARM)
534
TIMER OVERIDE
536
TIMER
533
FOOT PEDAL 2 (ENDO)
SET DEFAULT TIMER (FOR AUTOMATIC CAPTURE)
2 CHANNELS
523
SPLITTER
2 CHANNELS
120
INTRAOPERATIVE DATA DISPLAY
531
2 CHANNEL SIGNAL MIXER
136
ENDOSCOPIC IMAGES
C-ARM
134
132
SURGICAL VIDEO

FIG. 5E

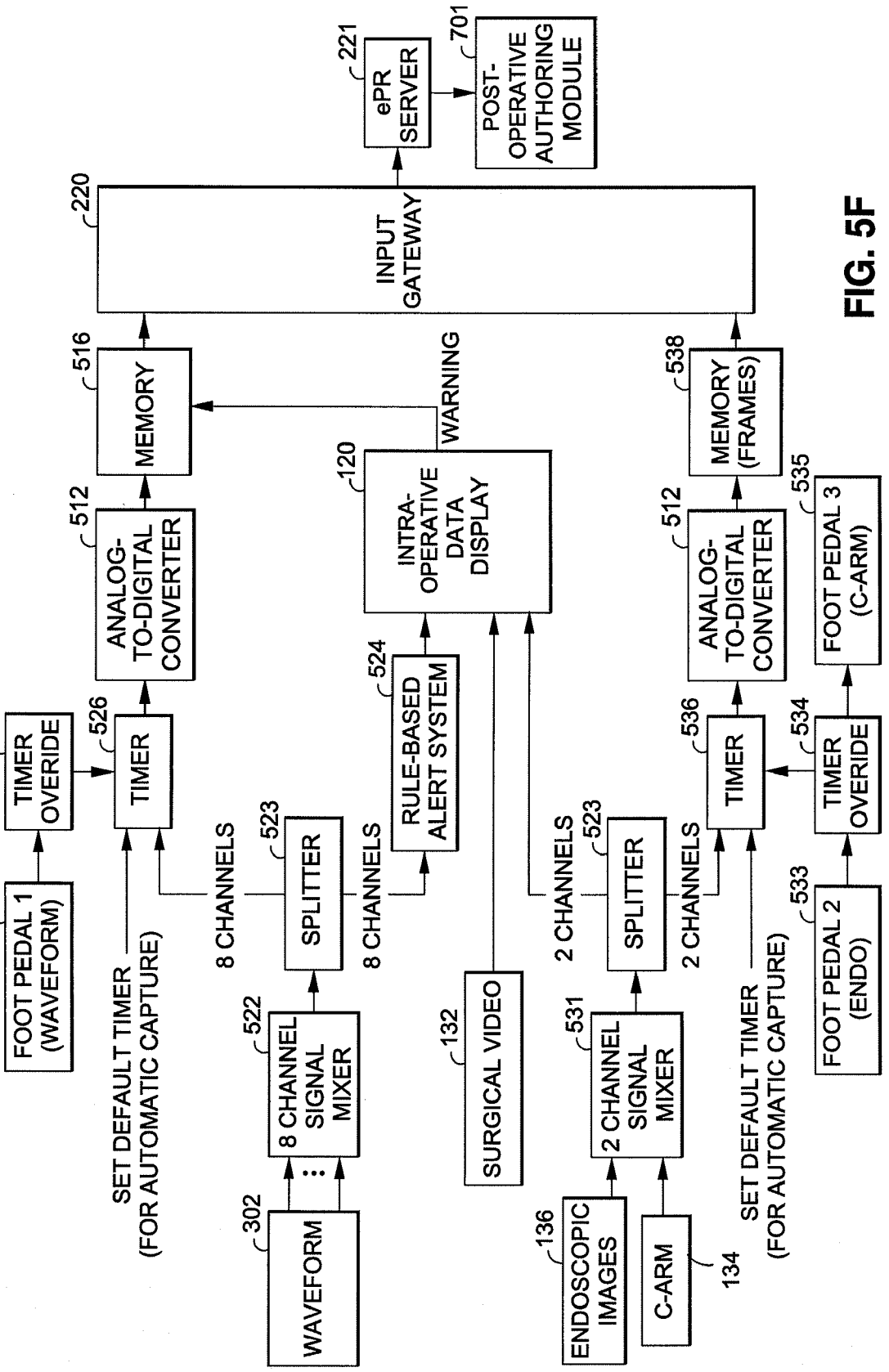
221
ePR SERVER
701
POST-OPERATIVE AUTHORING MODULE
220
INPUT GATEWAY
516
MEMORY
WARNING
120
INTRA-OPERATIVE DATA DISPLAY
538
MEMORY (FRAMES)
512
ANALOG-TO-DIGITAL CONVERTER
512
ANALOG-TO-DIGITAL CONVERTER
535
FOOT PEDAL 3 (C-ARM)
525
TIMER OVERIDE
526
TIMER
524
RULE-BASED ALERT SYSTEM
536
TIMER
534
TIMER OVERIDE
515
FOOT PEDAL 1 (WAVEFORM)
SET DEFAULT TIMER (FOR AUTOMATIC CAPTURE)
8 CHANNELS
523
SPLITTER
8 CHANNELS
2 CHANNELS
523
SPLITTER
2 CHANNELS
SET DEFAULT TIMER (FOR AUTOMATIC CAPTURE)
533
FOOT PEDAL 2 (ENDO)
522
8 CHANNEL SIGNAL MIXER
132
SURGICAL VIDEO
531
2 CHANNEL SIGNAL MIXER
302
WAVEFORM
136
ENDOSCOPIC IMAGES
134
C-ARM

FIG. 5F

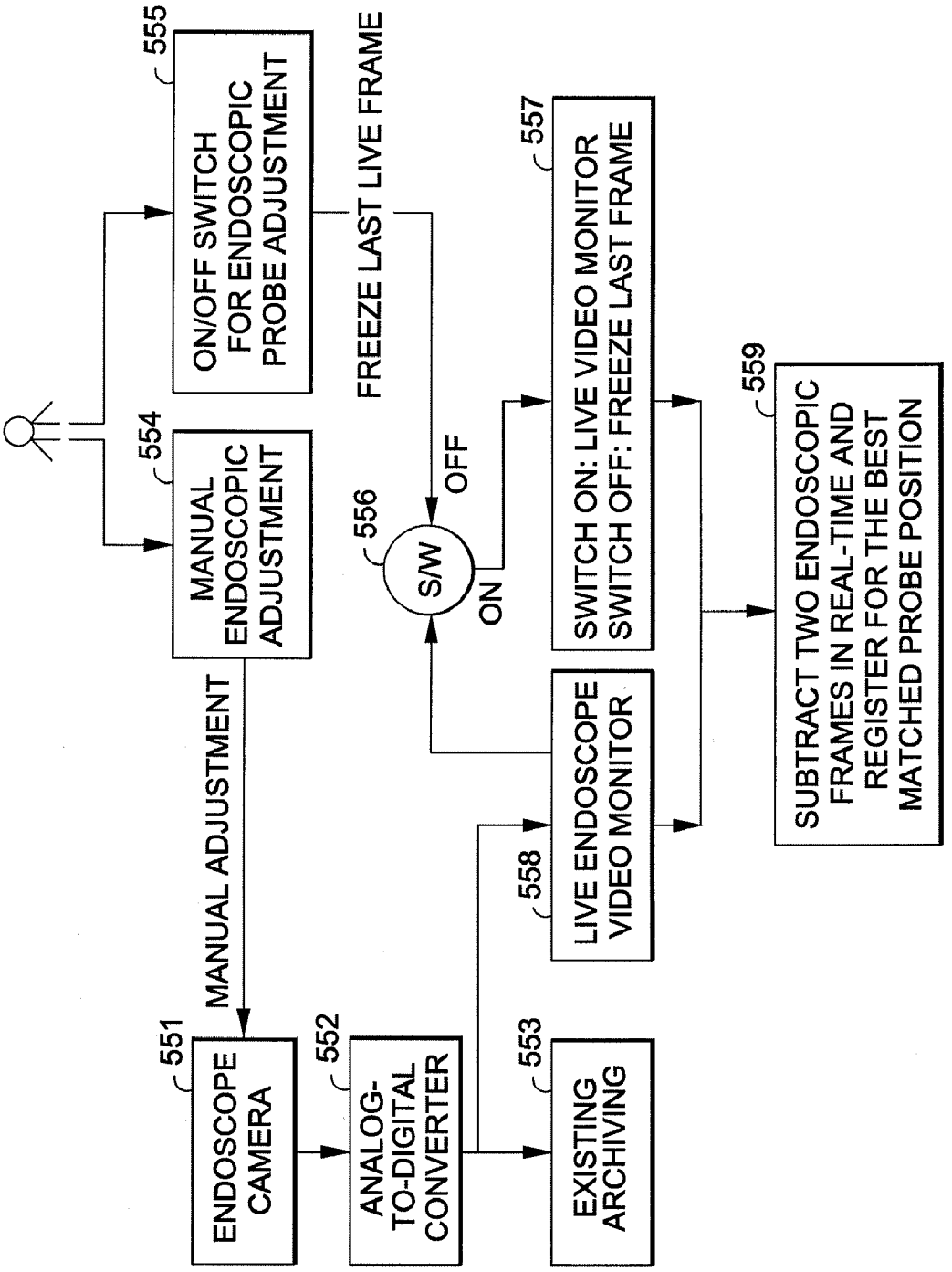
555
ON/OFF SWITCH FOR ENDOSCOPIC PROBE ADJUSTMENT
554
MANUAL ENDOSCOPIC ADJUSTMENT
FREEZE LAST LIVE FRAME
556
S/W
OFF
ON
557
SWITCH ON: LIVE VIDEO MONITOR
SWITCH OFF: FREEZE LAST FRAME
559
SUBTRACT TWO ENDOSCOPIC FRAMES IN REAL-TIME AND REGISTER FOR THE BEST MATCHED PROBE POSITION
MANUAL ADJUSTMENT
551
ENDOSCOPE CAMERA
552
ANALOG-TO-DIGITAL CONVERTER
553
EXISTING ARCHIVING
558
LIVE ENDOSCOPE VIDEO MONITOR

FIG. 5G

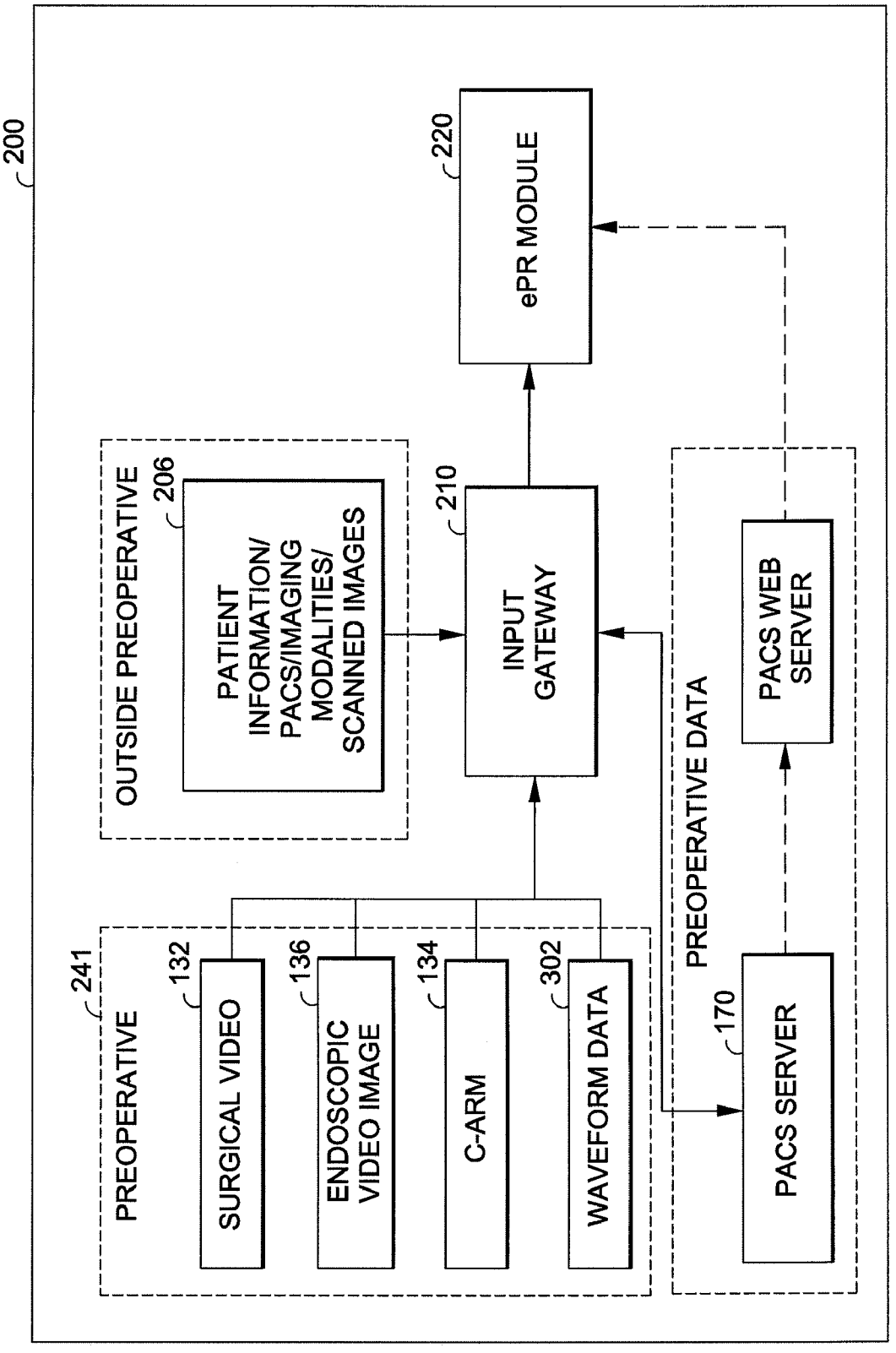
200
220
ePR MODULE
OUTSIDE PREOPERATIVE
206
PATIENT INFORMATION/ PACS/IMAGING MODALITIES/ SCANNED IMAGES
210
INPUT GATEWAY
PREOPERATIVE DATA
PACS WEB SERVER
241
PREOPERATIVE
132
SURGICAL VIDEO
136
ENDOSCOPIC VIDEO IMAGE
134
C-ARM
302
WAVEFORM DATA
170
PACS SERVER

FIG. 6

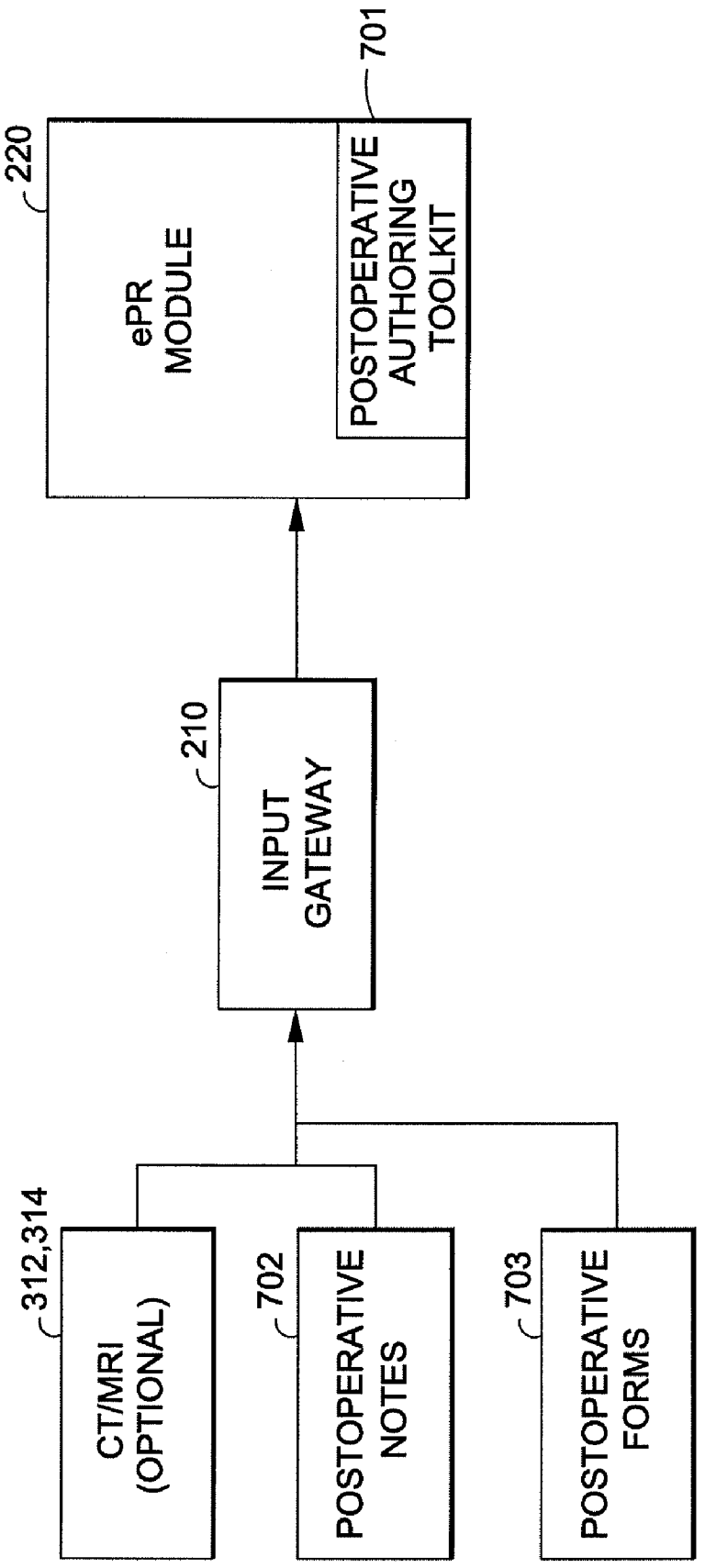
220
ePR MODULE
701
POSTOPERATIVE AUTHORING TOOLKIT
210
INPUT GATEWAY
312,314
CT/MRI (OPTIONAL)
702
POSTOPERATIVE NOTES
703
POSTOPERATIVE FORMS

FIG. 7A

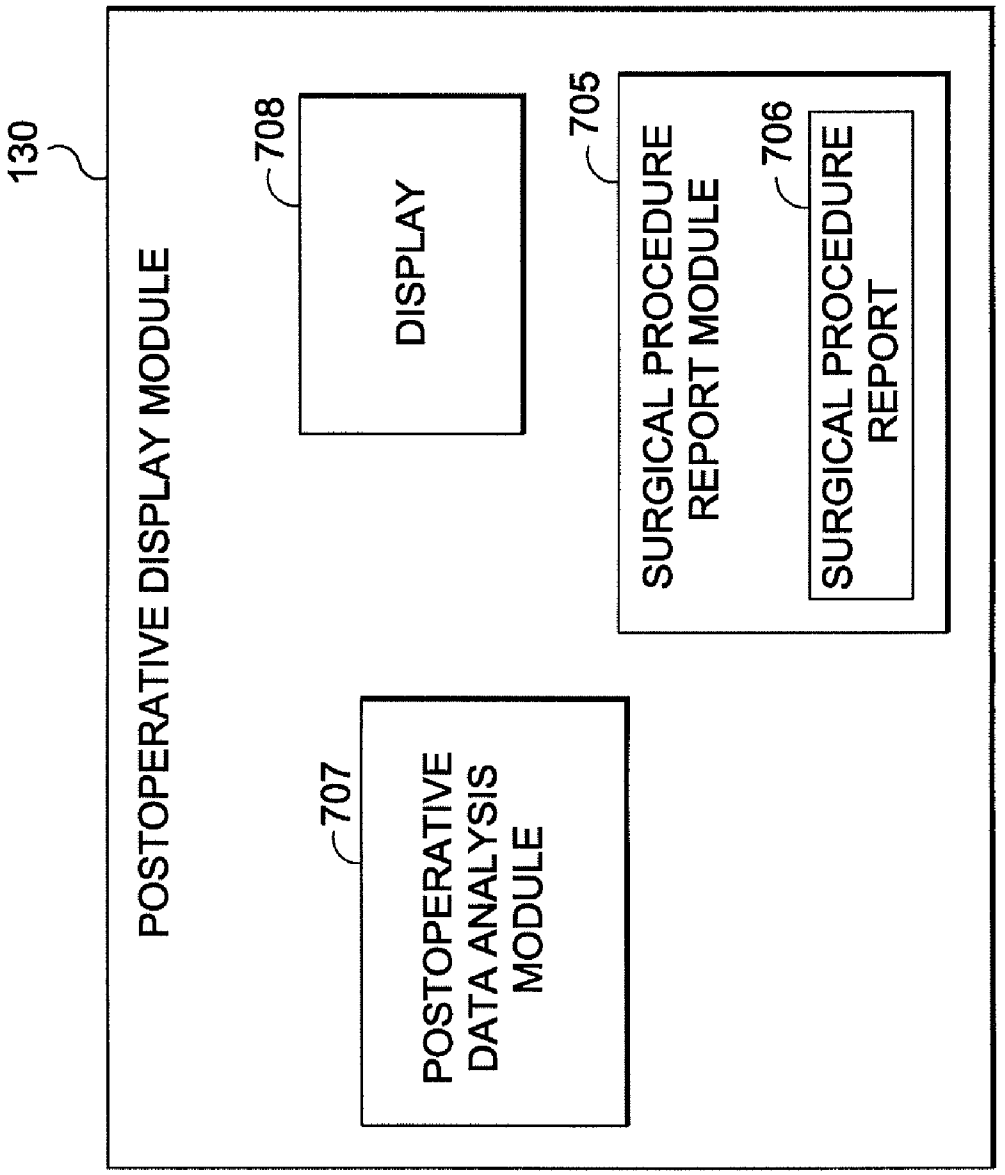
130
POSTOPERATIVE DISPLAY MODULE
708
DISPLAY
705
SURGICAL PROCEDURE REPORT MODULE
706
SURGICAL PROCEDURE REPORT
707
POSTOPERATIVE DATA ANALYSIS MODULE

FIG. 7B

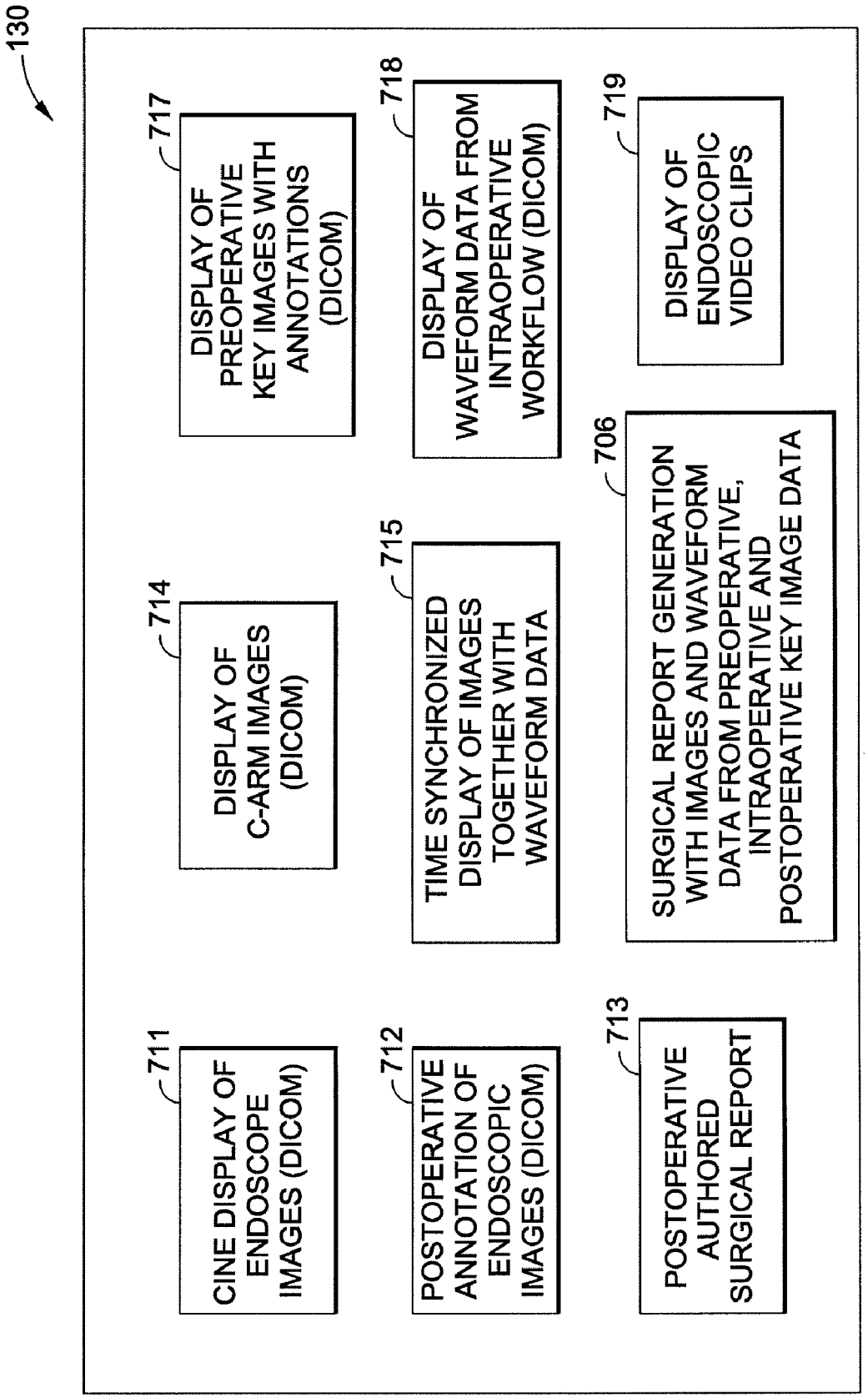
130
711
CINE DISPLAY OF ENDOSCOPE IMAGES (DICOM)
712
POSTOPERATIVE ANNOTATION OF ENDOSCOPIC IMAGES (DICOM)
713
POSTOPERATIVE AUTHORED SURGICAL REPORT
714
DISPLAY OF C-ARM IMAGES (DICOM)
715
TIME SYNCHRONIZED DISPLAY OF IMAGES TOGETHER WITH WAVEFORM DATA
706
SURGICAL REPORT GENERATION WITH IMAGES AND WAVEFORM DATA FROM PREOPERATIVE, INTRAOPERATIVE AND POSTOPERATIVE KEY IMAGE DATA
717
DISPLAY OF PREOPERATIVE KEY IMAGES WITH ANNOTATIONS (DICOM)
718
DISPLAY OF WAVEFORM DATA FROM INTRAOPERATIVE WORKFLOW (DICOM)
719
DISPLAY OF ENDOSCOPIC VIDEO CLIPS

FIG. 7C

SURGICAL DATA MONITORING AND DISPLAY SYSTEM

PRIORITY CLAIM

This application claims the benefit of U.S. Provisional Application Ser. No. 60/936,639, filed on Jun. 20, 2007, and titled "SURGICAL DATA MONITORING AND DISPLAY SYSTEM," the entirety of which is hereby incorporated by reference.

BACKGROUND OF THE INVENTION

1. Field of the Invention

Embodiments of the invention relate to information display systems. More specifically, some embodiments of the invention relate to a multidisplay system for operating rooms or medical procedure rooms.

2. Description of the Related Art

Surgeons need to know various items of information concerning a patient before, during, and after surgery, but this information is often delivered asynchronously, incompletely, or in an otherwise non-centralized, piecemeal, or delayed fashion.

SUMMARY OF THE INVENTION

It is important in an operating room setting for a surgeon to have access to many different types of patient information. For example, a surgeon may need preoperative information (i.e., information available before surgery or "retrospective" information), such as a patient's identification, medical history, prior imaging or laboratory studies, and three dimensional (3-D) magnetic resonance (MR) or computed tomography (CT) rendering, and a surgical plan. A surgeon may also need intraoperative information (i.e., information during a surgery or "real-time" information), such as vital signs, fluid intake and output electrocardiographic data, neurophysiological data (e.g., somatic sensory evoked potentials (SSEP) data), electroencephalographic data, electromyogram data, pulse oximetry data, digital C-arm fluorographic images, endoscopic video images, additional verification medical images, and live surgical video images. In some cases, a surgeon may want to verify information intraoperatively, such as a patient's biometric information for patient verification. In some instances, the surgeon may postoperatively (i.e., after surgery) review both the preoperative and intraoperative information in order to document in the patient's record the surgical procedure performed, the patient's immediate postoperative condition, and the surgical outcome.

In many cases, some or all of the preoperative, intraoperative, or postoperative information may not be easily accessible by the surgeon. In some cases, if some of this information is available in the operating room, it may be presented on multiple displays or through other output devices inaccessible to the surgeon from any one location. In these cases, the surgeon may have to rely on others in order to obtain the information, which could be problematic in a time-critical environment.

Consequently, a system is needed for making intraoperative data (e.g., real-time surgical and/or medical data), preoperative data (i.e., retrospective or historical patient data), and postoperative data immediately accessible to a surgeon or other healthcare practitioner in a patient care area.

In certain embodiments, a surgical data monitoring and display system for use in an operating room or another patient care room is disclosed. The system includes a data storage module that stores retrospective data and real-time surgical data concerning a patient, and a first processing module that receives the retrospective data, processes the retrospective data into processed retrospective data, and transmits the processed retrospective data to a first display module before or during performance of a medical or surgical procedure on the patient by a healthcare provider. The system also includes the first display module, which displays the processed retrospective data, a first gateway that receives the retrospective data from a server and transmits the retrospective data to the data storage module, and a second processing module that receives the real-time data, processes the real-time data into processed real-time data, and transmits the processed real-time data to a second display module before or during performance of the medical or surgical procedure on the patient by the healthcare provider. The system further includes the second display module, which displays the processed real-time data. The real-time data concerning the patient includes at least two of the following: electrocardiographic data, electroencephalographic data, pulse oximetry data, videoscopic data, and vital sign data. The retrospective data includes at least one of imaging data, patient identification information, past medical history information, physical examination information, data concerning a past procedure performed on the patient, and data concerning another patient or a teaching case. The real-time data is acquired during performance of the medical or surgical procedure on the patient. The first display module and the second display module are positionable in the operating room or another patient care room such that they are viewable by the healthcare provider during the performance by the healthcare provider of the medical or surgical procedure on the patient. The system yet further includes a third processing module configured to receive postoperative data, the retrospective data, and the real-time data, and further configured to process at least one of the postoperative data, the retrospective data, and the real-time data into report data, and a third display module, which displays the report data.

In certain embodiments, the system includes an alert module, coupled to the second processing module and configured to provide a visible alert when a predetermined threshold of the real-time data is exceeded. The visible alert includes at least one of moving displayed real-time data from a first location, less prominent on a display of the second display module to the healthcare provider, to a second location, more prominent on the display of the second display module to the healthcare provider, and enlarging a display, of first set of the processed real-time data, displayed at a first, smaller size on a display of the second display module, to a second, larger size on the display of the second display module. The first set of the processed real-time data includes at least one of electrocardiographic data, electroencephalographic data, pulse oximetry data, videoscopic data, and vital sign data. The display of the second display module further displays a second set of the processed real-time data adjacent to the display of the first set of the processed real-time data, the second set of the processed real-time data includes at least one of electrocardiographic data, electroencephalographic data, pulse oximetry data, videoscopic data, and vital sign data. When the display of the first set of the processed real-time data is enlarged to the second, larger size on the display of the second display module, the display of the first set of the processed real-time data (i) overlaps the display of the second set of the processed real-time data, and/or (ii) the display of the second set of the processed real-time data is reduced in size.

In certain embodiments, the visible alert further includes changing a color of displayed real-time data on a display of the second display module. In certain embodiments, the sys-

tem includes alert module, coupled to the second processing module and configured to provide a visible alert when a predetermined threshold of the real-time data is exceeded. The visible alert includes changing a color of displayed real-time data on a display of the second display module. In certain embodiments, the first gateway is configured to receive and transmit the retrospective data according to a predefined priority configuration. In certain embodiments, the first processing module and the second processing module comprise the same hardware or software processor. In certain embodiments, at least two of the first processing module, the second processing module, and third processing module provide fault tolerance for each other. In certain embodiments, the system includes a fourth display module configured to provide fault tolerance for each of the first display module, the second display module, and third display module. In certain embodiments, the report data includes a patient surgery record. In certain embodiments, the vital sign data includes at least one of a heart rate, a respiratory rate, a blood pressure, and a body temperature. In certain embodiments, the system includes a second gateway that receives the real-time data from a server and transmits the real-time data to the data storage module, and a third gateway that receives the postoperative data and transmits the postoperative data to the data storage module. In certain embodiments, each of the first gateway, the second gateway, and the third gateway provide fault tolerance for each other. In certain embodiments, the first gateway, the second gateway, and the third gateway constitute the same node on a computer network. In certain embodiments, the system includes an imaging server, the first processing module receives the retrospective data from the imaging server, and the retrospective data includes imaging data. In certain embodiments, the imaging server includes a picture archiving and communications system (PACS) server. In certain embodiments, the real-time data further includes at least one of electromyogram (EMG) data, imaging data, computed tomography (CT), magnetic resonance image (MRI) data, ultrasound data, C-Arm image data, fluoroscopy data, and X-Ray data.

In certain embodiments, a surgical data monitoring and display system for use in an operating room or another patient care room is disclosed. The system includes a data storage module that stores real-time surgical data concerning a patient, a first processing module that receives the real-time data, processes the real-time data into processed real-time data, and transmits the processed real-time data to a first display module before or during performance of a medical or surgical procedure on the patient by the healthcare provider, and the first display module, which displays the processed real-time data. The real-time data concerning the patient includes at least two of the following: electrocardiographic data, electroencephalographic data, pulse oximetry data, videoscopic data, and vital sign data. The real-time data is acquired during performance of the medical or surgical procedure on the patient. The first display module is positionable in the operating room or another patient care room such that they are viewable by the healthcare provider during the performance by the healthcare provider of the medical or surgical procedure on the patient. The system also includes a second processing module configured to receive postoperative data, retrospective data, and the real-time data, and further configured to process at least one of the postoperative data, the retrospective data, and the real-time data into report data, a second display module, which displays the report data, and an alert module, coupled to the first processing module and configured to provide a visible alert when a predetermined threshold of the real-time data is exceeded. The visible alert includes at least one of moving displayed real-time data from a first location, less prominent on a display of the first display module to the healthcare provider, to a second location, more prominent on the display of the first display module to the healthcare provider, and enlarging a display of first set of the processed real-time data, displayed at a first, smaller size on a display of the first display module, to a second, larger size on the display of the first display module. The first set of the processed real-time data includes at least one of electrocardiographic data, electroencephalographic data, pulse oximetry data, videoscopic data, and vital sign data. The display of the first display module further displays a second set of the processed real-time data adjacent to the display of the first set of the processed real-time data, the second set of the processed real-time data includes at least one of electrocardiographic data, electroencephalographic data, pulse oximetry data, videoscopic data, and vital sign data. When the display of the first set of the processed real-time data is enlarged to the second, larger size on the display of the first display module, the display of the first set of the processed real-time data (i) overlaps the display of the second set of the processed real-time data, and/or (ii) the display of the second set of the processed real-time data is reduced in size.

In certain embodiments, the system includes a third processing module that receives the retrospective data, processes the retrospective data into processed retrospective data, and transmits the processed retrospective data to a third display module before or during performance of the medical or surgical procedure on the patient by the healthcare provider, the third display module, which displays the processed retrospective data, and a third gateway that receives the retrospective data from a server and transmits the retrospective data to the data storage module. In certain embodiments, the third gateway is configured to receive and transmit the retrospective data according to a predefined priority configuration. In certain embodiments, the first processing module, the second processing module, and the third processing module comprise the same hardware or software processor. In certain embodiments, at least two of the first processing module, the second processing module, and third processing module provide fault tolerance for each other. In certain embodiments, the system includes a fourth display module configured to provide fault tolerance for each of the first display module, the second display module, and third display module. In certain embodiments, the report data includes a patient surgery record. In certain embodiments, the vital sign data includes at least one of a heart rate, a respiratory rate, a blood pressure, and a body temperature. In certain embodiments, the system includes a second gateway that receives the postoperative data and transmits the postoperative data to the data storage module, and a third gateway that receives the real-time data from a server and transmits the real-time data to the data storage module. In certain embodiments, each of the first gateway, the second gateway, and the third gateway provide fault tolerance for each other. In certain embodiments, the first gateway, the second gateway, and the third gateway constitute the same node on a computer network. In certain embodiments, the system includes an imaging server, the third processing module receives the retrospective data from the imaging server, and the retrospective data includes imaging data. In certain embodiments, the imaging server includes a picture archiving and communications system (PACS) server. In certain embodiments, the real-time data further includes at least one of electromyogram (EMG) data, imaging data, computed tomography (CT), magnetic resonance image (MRI) data, ultrasound data, C-Arm image data, fluoroscopy data, and X-Ray data.

For purposes of summarizing the invention, certain aspects, advantages, and novel features of the invention have been described herein. It is to be understood that not necessarily all such advantages may be achieved in accordance with any particular embodiment of the invention. Thus, the invention may be embodied or carried out in a manner that achieves or optimizes one advantage or group of advantages as taught herein without necessarily achieving other advantages as may be taught or suggested herein.

BRIEF DESCRIPTION OF THE DRAWINGS

A general architecture that implements the various features of the invention will now be described with reference to the drawings. The drawings and the associated descriptions are provided to illustrate embodiments of the invention and not to limit the scope of the invention. Throughout the drawings, reference numbers are re-used to indicate correspondence between referenced elements.

FIG. **1** illustrates an operating room layout which includes a surgical data monitoring and display system according to one embodiment of the invention.

FIG. **2** illustrates a data workflow of the surgical data monitoring and display system according to one embodiment of the invention.

FIG. **3**A illustrates a high-level database schema of an electronic patient record (ePR) module according to one embodiment of the invention.

FIG. **3**B illustrates a low-level database schema of the ePR module of FIG. **3**A according to one embodiment of the invention.

FIG. **3**C illustrates a data workflow of the surgical data monitoring and display system according to one embodiment of the invention.

FIG. **3**D illustrates another database schema of the ePR module of FIG. **3**A according to one embodiment of the invention.

FIG. **4**A illustrates a preoperative workflow according to one embodiment of the invention.

FIG. **4**B illustrates a sample screenshot from a preoperative data display according to one embodiment of the invention.

FIG. **5**A illustrates an intraoperative workflow featuring intraoperative data acquisition hardware according to one embodiment of the invention.

FIG. **5**B illustrates a sample screenshot from an intraoperative data display according to one embodiment of the invention.

FIG. **5**C illustrates a data workflow for acquiring and storing intraoperative data using the intraoperative data acquisition hardware of FIG. **5**A according to one embodiment of the invention.

FIG. **5**D illustrates a data workflow for acquiring and storing intraoperative waveform data using the intraoperative data acquisition hardware of FIG. **5**A according to one embodiment of the invention.

FIG. **5**E illustrates a data workflow for acquiring and storing intraoperative videos and images using the intraoperative data acquisition hardware of FIG. **5**A according to one embodiment of the invention.

FIG. **5**F illustrates a data workflow for integrating the features of FIGS. **5**D and **5**E according to one embodiment of the invention.

FIG. **5**G illustrates a data workflow for using a single camera endoscopic system and/or other acquisition device with a playback mechanism for interactive endoscopic probe position correction during surgery according to one embodiment of the invention.

FIG. **6** illustrates a data workflow for preoperative and intraoperative data according to one embodiment of the invention.

FIG. **7**A illustrates a postoperative workflow according to one embodiment of the invention.

FIG. **7**B illustrates a block diagram of the postoperative display module, including an authoring tool kit for generating a surgical procedure report, according to one embodiment of the invention.

FIG. **7**C illustrates a sample screenshot from a postoperative data display according to one embodiment of the invention.

DETAILED DESCRIPTION OF EXEMPLARY EMBODIMENTS

FIG. **1** illustrates an operating room layout **100** which includes a surgical data monitoring and display system according to one embodiment of the invention. As used herein, the term "data" includes, without limitation, textual data, waveform data and image data. The surgical data monitoring and display system can obtain and display intraoperative (real-time medical or surgical) data and preoperative data from many different sources. As used herein, the term "preoperative data" and "intraoperative data" includes, without limitation, surgical, medical, physiological, or psychiatric information that is preoperative, intraoperative, postoperative, or surgical in nature. The illustrated operating room layout **100** includes a plurality of data sources and devices, including video mixing equipment **153**, a magnetic resonance image (MRI) Picture Archive and Communication System (PACS) server and view box **170**, an imaging/dictation system **143**, an authoring document module **137**, a surgical video camera/display **132**, an endoscope display/storage **136**, a C-arm fluoroscopic display/storage **134**, a fluid intake/output **133**, a vital sign display **139**, an electromyogram (EMG) display **140**, an electroencephalograms (EEG) display **138**, a patient biometric identifier **135**, a neuro-physiological monitor **131**, an electrocardiogram (EKG) display **141**, a laser generator **142**, an intraoperative data display **120**, and a preoperative data display **110**.

In certain embodiments, the laser generator **142** is modified to record input voltage, ampere, and output laser energy. The recorded output laser energy can dictate the level of laser power delivered to a patient, and that information can allow a surgeon to monitor the amount of cutting and healing of tissues, such as by viewing the energy level on the intraoperative display **120** during surgery.

In certain embodiments, the surgical video camera/display **132** and video-mixing equipment **153** are configured to create another recording for postoperative use by using either the historical data or the real-time data. Sample postoperative uses include documentation or use as an instructive student training video.

The surgical data monitoring and display system comprises the integration of image and data information sources, including preoperative data, intraoperative data, and postoperative data. Preoperative data can include, for example, image information such as images from radiography, including myelograms, fluoroscopy **134**, MRI **170**, X-ray tomograms, computed tomography (CT) **170**, and/or ultrasound (US). Preoperative data can also include, for example, information concerning other patients and/or teaching cases, procedures, surgical protocol, instruction manuals, patient history data, evaluation data, identification data, biometric data, scanned data (which may be stored as PDF files), and previously recorded intraoperative data.

Intraoperative data can include, for example, real-time information from various sources used during surgery, such as surgical video **132**, C-ARM fluoroscopy **134**, endoscopic images **136**, and waveform signals, such as from EEG **138**, EMG **140**, EKG **141**, vital signs **139**, neuro-physiological monitors **131** (e.g., monitoring somatic sensory evoked potentials (SSEP) data), fluid intake and output **133**, and patient biometric identification **135**. Postoperative data can include, for example, authored, dictation, and/or imaging information received from the selected imaging/dictation system **143**, surgical procedure reports, postoperative graphical user interface data, data received in a recovery room, such as from input devices similar to the intraoperative devices discussed above, sensor input from a telemetry device, data entered manually after the completion of the surgical procedure, or any other data received after the completion of the surgical procedure.

In certain embodiments, the intraoperative data and preoperative data are displayed on a plurality of displays. In the illustrated embodiment, two displays, preoperative data display **110** and intraoperative data display **120**, are used. In certain embodiments, one display can be used. Any display technology can be used, including, but not limited to, plasma displays, liquid crystal displays (LCD), nanocrystal displays, three-dimensional (3D) displays, cathode ray tube (CRT) displays, light emitting diode (LED) displays, nano-emissive displays, and projection displays. In certain embodiments, preoperative data and/or intraoperative data is selected for display by interacting with the electronic patient record (ePR) server **221**, described further below with reference to FIG. **2**.

In certain embodiments, the surgical data monitoring and display system is configured to connect to the preoperative, intraoperative, and postoperative data sources discussed above. In certain embodiments, the intraoperative data sources need to be synchronized against a master clock because the real-time information, such as text, waveform data and images, generated from intraoperative data sources can each have its own independent clock cycle synchronized against its own independent internal clock.

With regards to intraoperative data sources that produce waveform data (e.g., EEG **138**, vital signs **139**, EMG **140**, EKG **141**, output from a laser generator **142**, and pressure waves and values from transducers associated with intravascular or intracardiac catheters, such as a Swan-Ganz catheter), the internal clock each data source is converted to a master clock so that each data source is synchronized. The master clock is used to trigger the interaction of each of the devices. The internal clocks may thus be converted to an acceptable rate favorable to a surgical procedure so that data input to an input gateway (e.g., input gateway **210** in FIG. **2**, discussed in further detail below) is acquired according to a preset time unit, and controlled by a single master clock. Similarly, the display of each of the intraoperative data sources that produce waveform data is sampled to display data at the proper coordinates of the intraoperative display **120** at the appropriate time according to the master clock.

In certain embodiments, the surgical data monitoring and display system obtains preoperative data from an information archive, such as a data server. In the illustrated embodiment, preoperative data is retrieved from storage at least in part on a PACS image server **170**. In certain embodiments, the surgical data monitoring and display system obtains intraoperative data from intraoperative surgical sources, as discussed above. Because of the large amount of data that can potentially be received from these sources, and because of the need to archive and display the data, the surgical data monitoring and display system advantageously converts received data to compatible formats using an advantageous combination of industrial standards and innovative high speed communication protocols, such as the Digital Imaging and Communication in Medicine (DICOM) standard.

In certain embodiments, image data produced and received from intraoperative data sources (e.g., C-ARM fluoroscopy **134**, endoscope **136**, and/or others, depending on the necessity of imaging-guided requirements during the surgery) may not conform to the DICOM standard in its original form. Consequently, in certain embodiments, the intraoperative image data is conformed to the DICOM standard during a high rate image data acquisition process. The data acquisition rate may be synchronized against the same master clock used to synchronize the intraoperative waveform data.

In certain embodiments, it may take at least three times longer to acquire intraoperative image data as compared to a sample of intraoperative waveform data, consequently, clinical experience of a physician may be used to determine how to synchronize each of the intraoperative image data and intraoperative waveform data to the master clock so that the intraoperative image data and intraoperative waveform data are displayed according to a surgically acceptable time scale.

Intraoperative image data may be annotated during surgery to pinpoint a location of a lesion, such as for image-guided surgery. In certain embodiments, annotations may be added on image data while the image data is being acquired, and later archived the image data with the annotations. Furthermore, images may selectively be displayed on the intraoperative display **120** with or without annotations. Allocation of proper real estate on the intraoperative display **120** along with sampled waveform data in real-time with continuous data acquisition is advantageously achieved. The feature allowing annotations to be added on image data while the image data is being acquired may advantageously be used with the DICOM Structured Reports standard, which uses pointers to store and retrieve pertinent waveform data and images along with annotation overlay.

FIG. **2**A illustrates a data workflow **200** of the surgical data monitoring and display system according to one embodiment of the invention. The input gateway **210** includes three input gateways: preoperative input gateway **211** (e.g., a first sub-gateway for retrospective data), intraoperative input gateway **242** (e.g., a second sub-gateway for real-time data), and postoperative input gateway **243** (e.g., a third sub-gateway for post-surgical data). In certain embodiments, preoperative input gateway **211** receives and processes preoperative data **201** before a surgical procedure begins that may use the preoperative data. The intraoperative input gateway **242** receives and processes intraoperative data **241**. The postoperative input gateway **243** receives and processes postoperative data **244**. In certain embodiments, each of the preoperative input gateway **211**, intraoperative input gateway **242**, and postoperative gateway **243** has its own designated priority of receiving and processing preoperative, intraoperative, and postoperative data respectively.

The postoperative input gateway **243** is configured to provide selected postoperative data to ePR module **220**, and incorporate preoperative and postoperative data, such as questionnaires. The postoperative input gateway **243** is also configured to conform postoperative data to standards (e.g., image and data standards) used for data processed through the preoperative input gateway **211** and intraoperative input gateway **242**. The postoperative input gateway **243** is yet further configured to organize any combination of a patient's preoperative data, intraoperative data, and postoperative data into the ePR module **220**.

In certain embodiments, input gateway **210** provides fault tolerance. In certain other embodiments, the input gateway **210** does not provide fault tolerance. In certain embodiments, the fault-tolerance of the input gateway **210** has the ability to automatically use either of the preoperative input gateway **211**, intraoperative input gateway **242**, or postoperative input gateway **243** to receive both preoperative, intraoperative, and postoperative data should any of the other input gateways fail.

In addition to retrieving and transmitting data, the input gateway **210** is configured to act as a portal for converting and/or connecting multiple network connections which may use different standards and/or protocols, such as an interface between a World Wide Web or intranet server and an information source. The input gateway **210** can also act as a router configured to receive input from multiple sources, including the Internet. The input gateway **210** advantageously features methods to assure the fault tolerance of each of the two input gateways **211**, **342**, as discussed above. The input gateway **210** also advantageously features software and/or hardware to convert data and communications in non-industry-standard formats to industry-standard formats

In certain embodiments, preoperative data **201** is transmitted from the preoperative input gateway **211** of the input gateway **210** to the ePR module **220**. Similarly, in certain embodiments, after intraoperative data **341** has been transmitted to the intraoperative gateway **342** of the input gateway **210**, the input gateway **210** processes the intraoperative data **341**, and transmits the processed intraoperative data **341** to the ePR module **220**. The ePR module **220** further processes the intraoperative data, and transmits the intraoperative data to the visualization and display module **330** so that the intraoperative data can be displayed **122**.

In certain embodiments, the ePR module **220** comprises an ePR server **321**, a monitoring module **322**, and an archive/database **323** (i.e., a data storage module). In certain embodiments, the ePR module **220** comprises a processing module that processes the historical data. The ePR server **221** supervises data received from the input gateway **210**, and distributes data to the visualization and display module **330**. The monitoring module **222** sorts and directs multiple inputs to the ePR module **220** and distributes multi-faceted output data. The archive/database module **223** stores data.

The ePR module **220** processes the historical data and sends the processed historical data to the visualization and display module **330** so that the processed historical data can be displayed **112**.

In the illustrated embodiment, the ePR module **220** provides fault tolerance. In certain other embodiments, the ePR module **220** does not provide fault tolerance. The ePR module **220** has built-in fault-tolerance for any of its three components: ePR server **321**, monitoring module **322**, and archive/database **323**. Replication, redundancy, and/or diversity of components and data storage can be used to provide fault-tolerance if a component of the ePR module **220** fails during operation.

Fault tolerance provides multiple levels of backup in each component, such as for the interface units for each of preoperative data **201**, intraoperative data **241**, and postoperative data **244**, input gateway **210**, which includes preoperative input gateway **211**, intraoperative input gateway **242**, and postoperative input gateway **243**, ePR module **220** and its components, ePR server **221**, monitoring module **222**, and archive/database **223**; and visualization and display module **230** and its components, preoperative data display **110**, intraoperative data display **120**, and postoperative data display **130**.

In certain embodiments, there are two fault-tolerant resources, software and hardware. The types of software include (1) function software configured to perform special functions specified in the completed system, (2) operation software which directs, monitors and supports the function software, and (3) fault-tolerant software. Function software, such as software for input gateway functions, query/retrieve data functions, archived functions, and display functions is configured for a clinical environment. Operation software may use off-the-shelf computer operating systems and commercially available databases. Fault-tolerant software is also configured for clinical evaluation.

The second fault-tolerant resource is hardware. In certain embodiments, if a hardware failure occurs, the fault-tolerant software will perform three steps to recover the failure (1) the fault-tolerant software detects the hardware failure and automatically shifts the operation to backup hardware, (2) the system operator can manually replace the failed hardware, and (3) the fault-tolerant software can then detect that the failed hardware has been replaced, and shift back to normal operation using the replaced hardware. The hardware fault tolerance used in this system is based at least in part on the concept of Triple Modular Redundancy (TMR). The TMR concept may be applied across the surgical data workflow described in FIG. **2**, beginning with when the input gateway **210** receives any input data from a intraoperative device until that input data is successfully archived in the ePR module **220** and displayed using the visualization and display module **230**.

According to one implementation of fault tolerance for the surgical data monitoring and display system illustrated in FIG. **2**, a signal from an input device is sent substantially simultaneously to three similar universal interface units associated with preoperative data **201**, intraoperative data **241**, and postoperative data **244**, regardless of whether the signal is itself preoperative data **201**, intraoperative data **241**, or postoperative data **244**. The signal may be sent automatically or manually. If the appropriate interface unit receives and verifies the receipt of the signal, the identical signal in other two interface units can be discarded. If, however, that interface unit does not receive and/or verify receipt of the proper signal, that unit will automatically request the signal from one of the other two interface units. The appropriate interface unit may then transmit the signal to the fault-tolerant input gateway **210**, and from there, the signal may be transmitted by the fault-tolerant ePR module **220**. In certain embodiments, the probability of success that at least one of the three interface units will receive the signal is 99.999%. Once the signal leaves an interface unit and is received by the fault-tolerant input gateway **210**, the responsibility of the interface unit is completed. A similar method may be used if the input signal is an image or another form of data.

According to one implementation of fault tolerance for the surgical data monitoring and display system illustrated in FIG. **2**, there are three identical ePR modules **220**. One of the three ePR modules **220** serves as the primary ePR module **220** and the other two ePR modules **220** (not illustrated) serve as backups. Each ePR module **220** has three identical ePR servers **321**, monitoring modules **322**, and archive/databases **323**. A signal from an input gateway **211**, **242**, or **243** is automatically sent to all three ePR modules **220** simultaneously. The signal may then be placed in an ePR procedure queue and archived properly. A failure in any component in the primary ePR module will automatically cause the signal to be sent to the second ePR module, and if that has failed, then the signal is sent to the third ePR module. The visualization and display module **230** is configured to request data from the ePR mod-

ule **220** for any of the preoperative data display **110**, intraoperative data display **120**, and postoperative data display **130**. The probability of success of the ePR module, with three identical modules, to receive and to transmit proper requested data to the visualization and display module **230** is 99.999%.

The software of the visualization and display module **230** is likewise configured for fault tolerance. For hardware fault tolerance, the preoperative data display **110** and intraoperative data display **120** are backed up by a passive third monitor.

The visualization and display module **230** comprises a preoperative data display **110** for preoperative data, an intraoperative data display **120** for intraoperative data, and a postoperative data display **130**. The postoperative data display **130** is used for the display of postoperative documentation of the patient by interactively extracting or otherwise using data from the ePR module **220**. In certain embodiments, the postoperative authoring and display module **130** advantageously uses data mining methods for developing metadata usable for knowledge discovery, and to create teaching files for educational purposes.

In certain embodiments, input gateway **210** includes software configured in accordance with the DICOM standard for use with off-the-shelf computers. In certain embodiments, the software is configured to collect data from acquisition interfaces, such as through the development of a DICOM listener/receiver, a non-DICOM data receiver, and a buffer queue for staging data for transmission and/or conversion. In certain embodiments, the software is configured to conduct DICOM conversion by determining which data arriving in the buffer queue will be converted to DICOM, and advantageously use an automatic DICOM data conversion module to convert the data, wherein the automatic DICOM data conversion module uses a rules-based algorithm developed for automatic data conversion. Input gateway **210** further includes a DICOM-send module configured to send data to ePR module **220** in DICOM format, and a non-DICOM-send module configured to send non-DICOM data to ePR module **220** as necessary. Input gateway **210** also includes a DICOM and a non-DICOM verification procedure to verify that data has been conformed to DICOM standards and, in certain embodiments, stored within ePR module **220**. Input gateway **210** also includes software configured to confirm that data from acquisition interfaces (e.g., preoperative data **201**, intraoperative data **241**, and postoperative data **244**) are successfully received and stored.

Input gateway **210** yet further includes addendum data integration software that is configured to integrate data with existing study data in ePR module **220**. The addendum data integration software is configured to query/retrieve data from ePR module **220** to determine or locate a related study, update ePR module **220** with addendum data, and send to and store the addendum data with the original study in ePR module **220**.

As illustrated, ePR module **220** includes an ePR server **221**, monitoring module **222**, and archive/database **223**. These components can be either software or hardware. In certain embodiments, preoperative data **201** is retrieved before surgery and processed by the preoperative input gateway **211** and stored in ePR module **220**. In certain embodiments, intraoperative data **241** (e.g., data from the surgery) is retrieved by intraoperative input gateway **242** and stored in ePR module **220** for later use. Sampled intraoperative waveform data can be archived in the archive/database **223** of ePR module **220**. In certain embodiments, data stored in the ePR module **220** complies with the DICOM standard.

In certain embodiments, development of the archive/database **223** includes three steps: (1) archive/database **223** schema design, (2) analysis, at a high-level, of the archive/database **223** schema, and (3) validation of the archive/database **223**. The archive/database **223** schema design for preoperative data, intraoperative data, and postoperative data includes determining and/or developing any necessary or key data fields related to preoperative data, intraoperative data, and postoperative data and developing data object relationships within the database schema.

The archive/database **223** schema design for preoperative data, intraoperative data, and postoperative data also includes designing a framework utilizing current DICOM standards and Integrating the Healthcare Enterprise (IHE) workflow profiles, and obtaining off-the-shelf database software that supports the ePR archive database **223** based on performance, flexibility, and modularity. The archive/database **223** schema design further includes development of classes and class structure for database tables based on clinical workflow and DICOM standard and IHE workflow profile, designing tools and method(s) to extract input data, including DICOM header information, from image data, and designing tools and method(s) to query data fields based on surgical clinical workflow. The archive/database **223** schema design yet further includes designing tools and methods to update data fields based on clinical workflow, and designing tools and methods to retrieve data for requesting client.

The second step in the development of the archive/database **223** is analysis of the high-level database schema of the ePR module, the low level database schema based on DICOM standard data model, and the preoperative, intraoperative, and postoperative dataflow model, as illustrated in FIGS. **3**A-**3**D. FIG. **3**A illustrates a high-level database schema of an ePR module **220** according to one embodiment of the invention. Key images **301** are selected by a surgeon and saved during the preoperative and intraoperative surgical procedure. Intraoperative waveform signals **302** are sampled and archived. Preoperative and postoperative forms **303** are sampled and archived. FIG. **3**B illustrates a low-level database schema of the ePR module of FIG. **3**A according to one embodiment of the invention. FIG. **3**C illustrates a data workflow of the surgical data monitoring and display system according to one embodiment of the invention.

FIG. **3**D illustrates a data model of the surgical data monitoring and display system according to one embodiment of the invention. In certain embodiments, the data model is based on the DICOM standard. The data model categorizes and processes patient information **306**, preoperative data **201**, intraoperative data **241**, and postoperative data **244** using a multimedia data model. In the embodiment illustrated, information is organized according to the patient with whom it is associated. Information for patient John Doe **315** is illustrated, although information may be stored for any number of patients **351**.

The information associated with John Doe **301** includes patient information **306**, preoperative data **201**, intraoperative data **241**, and postoperative data **244**. In certain embodiments, the preoperative data **201** includes patient information **306**. In addition to the types of information described above, preoperative data can also include information concerning other patients and/or teaching cases, procedures, surgical protocol, or instruction manuals, and image information. The image information can include data such as images from radiography **311**, including myelograms, fluoroscopy, MRI **312**, X-ray tomograms, computed tomography (CT) **314**, and/or ultrasound (US) **310**. In addition to the types of information described above, in the embodiment illustrated intraoperative data **241** includes information from surgical video **132**, C-ARM fluoroscopy **134**, endoscopic images **136**, and

waveform signals **302**, such as from EEG **138**, EMG **140**, EKG **141**, and patient biometric identification **135**.

In certain embodiments, the ePR data model comprises methods to advantageously arrange and process patient information, preoperative data, intraoperative data, and postoperative data for seamless retrieval and display of the retrieved data on the preoperative data display **110**, intraoperative data display **120**, and postoperative data display **130**, as well as other workstations in the surgical data monitoring and display system **100**. In certain embodiments, special methods are used to categorize and process preoperative data **201** like US data **310**, radiography, fluoroscopy **311**, CT **314**, and MRI **312** and their three dimensional rendering, such as for surgical planning. In certain embodiments, special methods are used to categorize and process intraoperative data **241** including surgical video **132**, C-arm fluoroscopy **134**, endoscopic images **136**, and waveform signals **302**. In certain embodiments, special methods are used to categorize and process postoperative data **244** for patient documentation and training materials.

Returning to FIG. **2**A, the third step in the development of the archive/database **223**, validation of the archive/database **223**, involves three steps. The first sub-step is to use sample preoperative data, intraoperative data, and postoperative data from the preoperative input gateway **211**, intraoperative input gateway **242**, and postoperative input gateway **243** to test the database design, conversion tools, extraction methods, and receiver modules, and validate the extraction and insertion of data into data tables and data field populations. The second sub-step is to refine the archive/database **223** and the database schema based on evaluation of the prior results. The final substep is to test retrieval methods for requesting information from clients, such as a hospital, and to validate data retrieval results from ePR server **221** to confirm the operation integrity of the ePR system.

In certain embodiments, postoperative input gateway **243** is configured to transmit relevant postoperative data to ePR module **220** as well as incorporate preoperative data **201** and intraoperative data **241**. Postoperative input gateway **243** is also configured to conform postoperative data to selected image and data standards in accordance with data that has previously been processed in the preoperative input gateway **211** and intraoperative input gateway **242**. Postoperative input gateway **243** is further configured to organize preoperative data **201**, intraoperative data **241**, and postoperative data **244** of the same patient in the archive/database **223**.

As discussed above, the ePR server **221**, monitoring module **222**, and archive/database **223** components of the ePR module **220** can select information received from the input gateway **210** to display using the visualization and display module **230**. In certain embodiments, any interface or device having the capability to conduct the functions of the fault-tolerant ePR module **220** can be used.

In certain embodiments, each of the ePR module **220**, input gateway **210**, and visualization and display module **230**, as well the components that comprise them, can be networked or otherwise connected according to any method known in the art. For example, each may be a node on a network connected using a wired connection or a wireless connection. In certain embodiments, any of the nodes may be available remotely using an Internet connection. In certain embodiments, any or all of the nodes may be locally available.

FIG. **4**A illustrates a preoperative workflow according to one embodiment of the invention. Input gateway **210** receives patient information **306** and biometric information **135** directly, but receives CT and MR data through PACS server **170**. Input gateway **210** is configured to transmit this information to ePR module **220**, which advantageously features an authoring toolkit **401** with which to evaluate, plan, and approve authored preoperative data that may be displayed on preoperative data display **110**.

FIG. **4**B illustrates a sample screenshot from a preoperative data display **110** according to one embodiment of the invention. The preoperative data display **110** includes patient information **306**, such as the patient's name, identification number, date of birth, and sex, as well as the patient's biometric information **135**, such as a photograph of the patient and the patient's fingerprint. The preoperative data display **110** also includes the patient's history and diagnoses **402**, as well as the patient's consultation sagittal and transversal MRI **404**. The preoperative data display **110** further includes an antero-posterior (AP) X-ray image **405**, and the patient's reconstructed 3-D MRI image **403**. The data displayed on the preoperative data display **110** can be organized according to user preference. The surgical data monitoring and display system is further configured to store the user preference for later use.

FIG. **5**A illustrates a intraoperative workflow featuring intraoperative data acquisition hardware **501** according to one embodiment of the invention. Acquisition hardware **501** receives endoscopic images **136**, waveform data **302**, and surgical video **132** directly, and also receives C-arm data in analog format. Acquisition hardware **501** will be discussed in further detail below with reference to FIGS. **5**C-**5**F. Input gateway **210** receives C-arm data in DICOM format and information from acquisition hardware in analog format. Input gateway **210** converts the analog information into digital format, and transmits the information in digital format to ePR module **220**. Preoperative data display **110** displays information from ePR module **220**, and intraoperative data display **120** displays information from ePR module **220** and acquisition hardware **501**. In certain embodiments, intraoperative data display can advantageously feature interactive probe positioning, such as by using simultaneous freeze frame and live video display, as discussed in further detail with reference to FIG. **5**G.

FIG. **5**B illustrates a sample screenshot from an intraoperative data display **120** according to one embodiment of the invention. The intraoperative data display **120** includes patient information **306** and biometric information **135**, as discussed above with reference to FIG. **4**B. The intraoperative data display **120** also includes information on the surgical procedure to be performed **502**, including, for example, fields for side, level, type, and additional notes. The intraoperative data display **120** further includes intraoperative (e.g., real-time) waveform data **302**, C-arm fluorographic images **134**, and endoscopic images **136**. They are organized by a surgeon's preference. The data displayed on the intraoperative data display **120** can be organized according to user preference. The surgical data monitoring and display system is further configured to store the user preference for later use.

In certain embodiments, in order to display a plurality of waveforms **302** on the intraoperative data display **120**, the individual waveforms **302**, each having its own independent clock, need to be synchronized against the master clock, as discussed above. Additionally, a clinically acceptable display time until should be selected to display all of the waveforms **302** and/or images **134** and **136**. A user can also select locations to display the waveforms **302** on the intraoperative data display **120**.

In certain embodiments, various techniques and methods are used to systematically organize and display data on the intraoperative data display **120**. These techniques and methods may also be applied to the preoperative data display **110**

and postoperative data display **130**. For example, in certain embodiments, the intraoperative data display may be placed toward the left-hand side of the surgeon, as illustrated in FIG. **1**, at a height above surgical equipment and in a position convenient to the surgeon's vision, thereby reducing the time and eye motion required for a surgeon to look up from a surgical procedure to view data that is continuously updated. Likewise, the preoperative data display **110** may be placed toward the right-hand side of the surgeon, also as illustrated in FIG. **1**, at a height above surgical equipment and in a position convenient to the surgeon's vision. In other embodiments, the locations of the intraoperative data display **120** and preoperative data display **110** may be interchanged.

In certain embodiments, a large display may be used for any of the preoperative data display **110**, intraoperative data display **120**, and postoperative data display **130**. In certain embodiments, a small display may be used. In situations where a small display is used and/or where all data sources are not displayed on a display, a subset of the available data sources (e.g., preoperative data **201**, intraoperative data **231**, and postoperative data **244**) may be selectively displayed. For example, if there are twenty available data sources that may be displayed on a display screen, and there is only available space for ten data sources to be displayed, then the system may selectively choose, by a pre-programmed system default, which ten sources may be displayed. Data sources may be selected, changed, enlarged, moved, or otherwise affected by, for example, a control (e.g., a button panel) within reach of the surgical table. In certain embodiments, data may be selected for display using a remote control device, such as a wireless, handheld control panel. For example, a button panel may be used to switch from a single static image to a multiple image panel, or to use zoom and scroll features.

In certain embodiments, waveform data are not displayed continuously, but instead are displayed digitally at a give interval determined by a surgical procedure, built-in algorithm, and/or a given patient condition. In certain embodiments, intraoperative data is configured and/or processed to be displayed at an appropriate or predetermined times on the intraoperative data display **120**. For example, blood pressure may be displayed for an interval of ten seconds followed by the display of the patient's heart rate for an interval of ten seconds. As another example, data sources which constantly change (e.g., heart monitoring data) may be displayed more often and for longer period than data that changes less often (e.g., blood pressure). In certain embodiments, images are displayed in their original image quality, while in other embodiments, they may be displayed using a different quality. In certain embodiments, intraoperative data can be sent directly to and displayed on the intraoperative data display **120** without any delay, while in certain embodiments, intraoperative data may be delayed before being displayed on the intraoperative data display **120**.

In certain embodiments, the surgical data monitoring and display system includes an alert system configured to call attention to data, such as for use with intraoperative data **241** and preoperative data **201**. The alert system may be software configured in the input gateway **210**. The alert system may provide an audible or visible alert, such as, for example, providing an audible alarm when an input signal is outside a preset threshold value for patient protection. This is especially advantageous for intraoperative data, which may undergo a significant change in state during the performance of a medical procedure thereby needing the attention of the physician. For example, a patient's blood pressure may incur a significant drop during surgery, and this intraoperative data would be brought to the attention of the surgeon by the alert system. Visible alerts can include automatically moving the selected intraoperative data on the intraoperative data display **120** to a more prominent location, enlarging the selected intraoperative data, changing the color of the selected intraoperative data, and flashes of light, and audible alerts can include any various type of sound.

FIG. **5**C illustrates a data workflow for acquiring and storing intraoperative data using the intraoperative data acquisition hardware of FIG. **5**A according to one embodiment of the invention. The surgical data monitoring and display system acquires intraoperative data **241** during surgery. For example, intraoperative waveform data such as vital signs are collected continuously and sampled at a predetermined interval depending on the type of waveform, surgical procedure and the patient condition. Once an interval value is determined for each waveform, the interval value is preset as the default for that waveform. In certain embodiments, these values are then archived in real-time. For example, sequential intraoperative fluorographic images can be taken when a surgeon needs to review and confirm a surgical site by a radiological technologist near the surgical table. Several of the intraoperative fluorographic images may then be selected to determine the proper surgical site, and then archived. Endoscopic images can likewise be taken continuously during the surgical procedure. A surgeon can select to archive in existing storage **511** a sequence of images periodically. Thus, intraoperative data **241** may be sent through a preexisting interface and stored in existing storage.

In certain embodiments, intraoperative data **241** can be retrieved from storage **511** and converted from analog to digital format **512**, if necessary, and sent to an interface/communication channel **513**. The interface/communication channel can then send the data for manual selection **514** by the physician, such as by using a foot pedal **515**, or automatically for acquisition **517** and storage in ePR archive **223**, such as by using a large cache memory **516** as an intermediary. The foot pedal **515** can be used when a surgeon decides to keep a certain fluorographic image, or a sequence of endoscopic images during the surgery. The foot pedal may feature several selection-button groups. One group of buttons can allow images to be archived, and another group of buttons can control the currently displayed single camera endoscopic video with split screen for adjusting the probe location, as described in further detail with reference to FIG. **5**G. Another group of buttons can be used for display functions, such as zooming, scroll, changing between a static mode and dynamic mode. In certain embodiments, a hand panel may be used instead of a foot pedal. In certain other embodiments, other input devices may be used.

FIG. **5**D illustrates a data workflow for acquiring and storing intraoperative waveform data using the intraoperative data acquisition hardware **501** of FIG. **5**A according to one embodiment of the invention. Intraoperative waveform data **302**, which are substantially continuously displayed on intraoperative data display **120**, are automatically captured at predefined intervals set by a default timer **526**. Additional sets of waveforms can be captured using a foot pedal **515** or other input device, which is configured using timer override **525** to override the default time interval mechanism. The system also features a rule-based alert system **504** to provide alerts if the acquired waveforms **302** fall within the bounds set by the rule-based alert system **504**. For example, if a heart rate waveform exceeds a certain threshold predefined by the rule-based alert system **524**, an alert is issued, as discussed above. The alert functionality is provided by splitting **523** the acquired waveform into separate signals. Although the waveforms are illustrated as being received using an eight channel

mixer **522** and then split **523** into separate eight channel signals, other numbers of channels and types of signals, signal mixers, and splitters can be used. The output intraoperative waveform data from the timer then passes to audio-to-digital converter **512**, if necessary, and then goes through memory **516** and through to the input gateway **210**. The intraoperative waveform data is then sent from the input gateway **210** to ePR server **221**, and then sent to postoperative authoring module **701**, discussed in further detail below with reference to FIG. **7**A.

FIG. **5**E illustrates a data workflow for acquiring and storing intraoperative videos and images using the intraoperative data acquisition hardware **501** of FIG. **5**A according to one embodiment of the invention. In the illustrated configuration, a first video feed including endoscopic images **136** and C-arm video **134** are mixed in a two channel signal mixer **531** and then split in a splitter **532**, such that the first of the two split video feeds can be displayed on a intraoperative data display **120** along with surgical video **132**. The second, remaining video feed from the splitter **532** is then automatically captured on predefined intervals set by a default timer **536**. Additional sets of images from the video feed can be captured using foot pedals **533** and **535** or other input devices configured using timer override **534** to override the default time interval mechanism **536**, such that each input device designated to manually capture an image from a portion of the video feed. Although the waveforms are illustrated as being received using a two channel mixer **531** and then split **532** into separate two channel signals, other numbers of channels and types of signals, signal mixers, and splitters can be used. The output intraoperative video and image data from the timer **536** then passes to audio-to-digital converter **512**, if necessary, and then goes through memory **538** and through to the input gateway **210**. The intraoperative video and image data is then sent from the input gateway **210** to ePR server **221**, and then sent to postoperative authoring module **701**.

FIG. **5**F illustrates a data workflow for integrating the features of FIGS. **5**D and **5**E according to one embodiment of the invention. FIG. **5**F illustrates only one possible integrated configuration of the two system; other integrations of the two systems can also be configured.

During an endoscope-assisted surgical procedure, a surgeon may need to change the currently inserted endoscopic probe for a different operation, for example, from a coarse abrasion to a finer abrasion. When the new probe is replacing the existing probe, the surgeon may need to assure the position of the new probe is the same as that of the removed probe. FIG. **5**G illustrates the method of using a single camera endoscopic system and/or other acquisition device with a playback mechanism for interactive endoscopic probe position correction during surgery according to one embodiment of the invention. In certain embodiments, endoscopic image data is displayed using two displays, such as two independent monitors or a split screen monitor, while in other embodiments, a single display is used. The endoscopic image provided from the endoscopic probe that was removed is frozen on one side of the screen and the live endoscopic image from the newly inserted probe is displayed on another side of the screen.

The method begins by powering a first endoscope camera **555** and manually positioning the first endoscope camera **554** in a target location. At the target location, the image from the first endoscope camera is frozen **557** using a switch **556**. The frozen image remains displayed on the screen. Next, a second endoscope camera is powered on **551** and its data is converted from analog to digital format **552**. The digital data is stored in existing archiving **553**, and also displayed on screen **558** alongside the frozen image. The digital data from the second endoscope camera is then subtracted from the frozen image **559**. In certain embodiments, digital subtraction is used. Digital subtraction between both images is performed in real-time by a customized digital subtraction circuit board chip integrated with the single camera endoscopic video (CCD). In certain embodiments, digital subtraction can be performed at a rate of thirty frames per second. A built-in root-mean-square error (RMS) measurement of the subtracted image chip can compute and displays the RMS number continuously during each subtraction. The smallest RMS error in the sequence is depicted adjacent to the continuous changing sequential numbers on the monitor, and recorded. After a predetermined time, the second probe position with the smallest RMS error is chosen by the surgeon as the position of the second probe. The surgeon can either guide the second probe to the registered position by matching the RMS error manually or the probe can be guided through a six-degree-of-freedom robot arm.

This method has many advantageous features. A surgeon may continue to adjust or otherwise move an endoscopic camera while the image feed from the camera is displayed on the remaining portion of the display, near the captured image of the target location. Should the surgeon desire to move the endoscopic camera back to the target location, the surgeon may compare the live feed on the display screen with the captured image, and determine that when those two images match, the endoscopic camera has returned to the target location. The surgeon may be assisted in his comparison by the use of various image subtraction algorithms that assist in determining a match between the captured image and the image from the live feed, as discussed above.

FIG. **6** illustrates a data workflow for preoperative and intraoperative data according to one embodiment of the invention. Input gateway **210** can be configured to receive preoperative data from local sources, such as from PACS server **170**, as well as remote sources, such as remote imaging modalities **206**. The input gateway **210** can be configured to receive intraoperative data such as surgical video **132**, endoscopic video images **136**, C-arm fluoroscopic images **134**, and waveform data (e.g., EEG **138**, vital signs **139**, EMG **140**, EKG **141**, and output from a laser generator **142**). Input gateway **210** is configured to transmit data to ePR module **220**, which can also receive preoperative data directly.

It is important that a surgeon has access to preoperative data, intraoperative data, and postoperative data of the patient after a surgical procedure in order to assess the procedure's outcome. Preoperative, intraoperative, and postoperative data are organized in the ePR module **220**, which can be configured for any type of surgical operation using corresponding computer algorithms. For example, a surgeon may summarize and dictate a surgical procedure in detail using preoperative and postoperative patient condition outcomes. A surgeon may also want to evaluate, quantify, and record acute and chronic pain as quantitative parameters in order to measure the success of a surgical procedure. Consequently, a post-processing module is helpful for organizing preoperative, intraoperative, and postoperative data and information into a data and analysis module, such as ePR module **220**, accessible to a surgeon and other healthcare practitioner in a patient care area.

In certain embodiments, postoperative processing includes collecting postoperative data **244**, postoperative input gateway **243**, and postoperative display module **130**, which may send or receive information to or from ePR module **220**. In certain embodiments, there are three postoperative time phases wherein pertinent data are collected.

A first time phase is immediately after the surgery, or immediate postoperative outcome, such as for example in a recovery room, where clinical information is collected, such as, for example, vital sign information, neurological status, immediate postoperative outcome (e.g. pain response and neurological function, both motor and sensory, questionnaires), and MRI scans. A second time phase is the intermediate postoperative outcome, which is a time period of up to two months after the completion of the surgical procedure. During this second time phrase, information from questionnaires and MRI scans may be collected. The third time phase is the long term patient outcome, which is a time period of up to six months after the completion of the surgical procedure, wherein information from questionnaires and MRI scans may also be collected. Questionnaires may prompt a patient for information related to nursing and patient status forms. In certain embodiments, many types of questionnaires may be used, such as, but not limited to, questionnaires for medical record/history summation, preoperative take home questions (such as a patient diagnosis diagram), history and physical form, pre-anesthesia evaluation form, preoperative assessment/surgical checklist, post-anesthesia nursing record, the Oswestry disability index for back pain, and quadruple visual analogue scale.

Pain is an important parameter in measuring the success of a surgical procedure, and therefore is also an important source of postoperative data. In certain embodiments, two methods of evaluating chronic and acute pain are configured in the postoperative data display **130**. A first method is to use MRI information to measure the volume of protrusion of a lesion, which indicates the impingement on a nerve as a means to determine chronic pain arising from a surgical area. Mathematics and computer algorithms using three-dimensional MRI images can also be used to analyze lesions on MRI images. Quantitative comparison between pre-surgical and post-surgical MRI scans is then used as input data to determine a level of pain. In certain embodiment, heart rate variability can also be used to measure a degree of acute pain. Real-time heart rate during preoperative, intraoperative, immediate postoperative, intermediate postoperative, and long-term postoperative periods can be collected and organized in the ePR module **220** to compute differences in heart rate at different times. Variability can be correlated with acute pain of the patient. Algorithms for measuring the variability are configured in the surgical data monitoring and display system.

FIG. **7**A illustrates a postoperative workflow according to one embodiment of the invention. Input gateway **210** receives postoperative notes **702**, postoperative forms **703**, and optionally CT data **314** and MRI data **312**. Input gateway **210** may also receive C-arm images **134**, endoscopic video **136**, waveform data **302**, patient evaluation data, and other intraoperative surgical video and data. Input gateway **210** transmits data to ePR module **220**, which includes a postoperative authoring toolkit configured to create postoperative reports which may include text, sampled waveforms, and images.

FIG. **7**B illustrates a block diagram of the postoperative display module **130**, including an authoring tool kit for generating a surgical procedure report, according to one embodiment of the invention. In certain embodiments, the postoperative display module **130** consists of three systems: a postoperative data analysis module **707**, a display and/or graphical user interface **708**, and surgical procedure report information system **705**. The data display **708** is configured to display any combination of preoperative data, intraoperative data, and postoperative data, such as, but not limited to, temperature, systolic pressure, diastolic pressure, heart rate, pulse oximeter, partial pressure of carbon dioxide, bispectral index (BIS) readings, respiratory rate, C-arm images, endoscopic images, preoperative key images, patient demographic data, pain forms, and endoscopic video clips. A BIS monitor is a neurophysiological monitoring device which continually analyses a patient's electroencephalograms during general anesthesia to assess the level of consciousness during anesthesia. Waveform and image data can be acquired automatically and/or simultaneously with or without a timestamp, and may also be displayed synchronously. The postoperative data analysis module **707** is configured to process any combination of preoperative data, intraoperative data, and postoperative data. In certain embodiments, surgical procedure report information system **705** is configured for the generation of surgical reports **706**, such as by a surgeon, which may include patient information, key images selected from preoperative data, intraoperative data, and postoperative data. In certain embodiments, the output format can be portable document format or Microsoft Word format, while in other embodiments, other output formats may be used.

FIG. **7**C illustrates a sample screenshot from a postoperative data display **130** according to one embodiment of the invention. In certain embodiments, postoperative data display **130** displays data such as a cine display of endoscopic images **711**, postoperative annotation of endoscopic images in DICOM format **712**, postoperative authored surgical report **713**, display of C-arm images in DICOM format **714**, time synchronized display of images together with waveform data **715**, a surgical procedure report **706** with images and waveform and key image data selected from preoperative data, intraoperative data, and postoperative data, display of preoperative key images with annotations in DICOM format **717**, display of waveform data from an intraoperative workflow in DICOM format **718**, and display of endoscopic video clips **719** which may, for example, be in MPEG format.

While certain aspects and embodiments of the invention have been described, these have been presented by way of example only, and are not intended to limit the scope of the invention. Indeed, the novel methods and systems described herein may be embodied in a variety of other forms without departing from the spirit thereof. The accompanying claims and their equivalents are intended to cover such forms or modifications as would fall within the scope and spirit of the invention.

What is claimed is:

1. A surgical data monitoring and display system for use in an operating room or another patient care room, comprising:

a data storage module that stores retrospective data and real-time data concerning a patient;

a first processing module that receives the retrospective data, processes the retrospective data into processed retrospective data, and transmits the processed retrospective data to a first display module before or during performance of a medical or surgical procedure on the patient by a healthcare provider;

the first display module, which displays the processed retrospective data;

a first gateway that receives the retrospective data from a server and transmits the retrospective data to the data storage module;

a second processing module that receives the real-time data, processes the real-time data into processed real-time data, and transmits the processed real-time data to a second display module before or during performance of the medical or surgical procedure on the patient by the healthcare provider; and

the second display module, which displays the processed real-time data;

wherein the real-time data concerning the patient comprises at least two of the following: electrocardiographic data, electroencephalographic data, pulse oximetry data, videoscopic data, and vital sign data;

wherein the retrospective data comprises at least one of imaging data, patient identification information, past medical history information, physical examination information, data concerning a past procedure performed on the patient, or data concerning another patient or a teaching case;

wherein the real-time data is acquired during performance of the medical or surgical procedure on the patient;

wherein the first display module and the second display module are positionable in the operating room or another patient care room such that they are viewable by the healthcare provider during the performance by the healthcare provider of the medical or surgical procedure on the patient;

a third processing module configured to receive postoperative data, the retrospective data, and the real-time data, and further configured to process at least one of the postoperative data, the retrospective data, or the real-time data into report data; and

a third display module, which displays the report data; and

an alert module, coupled to the second processing module and configured to provide, on a single display, a visible alert when a predetermined threshold of the real-time data is exceeded; wherein the visible alert comprises at least one of:

moving displayed real-time data from a first location, less prominent on a display of the second display module to the healthcare provider, to a second location, more prominent on the display of the second display module to the healthcare provider while maintaining display of the processed retrospective data on the first display module to be visible to the health care provider; and

enlarging a display of a first set of the processed real-time data, displayed at a first, smaller size on a display of the second display module, to a second, larger size on the display of the second display module while maintaining display of the processed retrospective data on the first display module to be visible to the health care provider;

wherein the first set of the processed real-time data comprises at least one of electrocardiographic data, electroencephalographic data, pulse oximetry data, videoscopic data, or vital sign data; and

wherein the display of the second display module further displays a second set of the processed real-time data adjacent to the display of the first set of the processed real-time data, the second set of the processed real-time data comprising at least one of electrocardiographic data, electroencephalographic data, pulse oximetry data, videoscopic data, or vital sign data.

2. The system of claim **1**, wherein,

when the display of the first set of the processed real-time data is enlarged to the second, larger size on the display of the second display module, (i) the display of the first set of the processed real-time data overlaps the display of the second set of the processed real-time data, and/or (ii) the display of the second set of the processed real-time data is reduced in size.

3. The system of claim **1**, wherein the visible alert further comprises changing a color of displayed real-time data on a display of the second display module.

4. The system of claim **1**, wherein at least one of the first display module, the second display module, and or the third display module comprises a plasma display, liquid crystal display (LCD), nanocrystal display, three-dimensional (3D) display, cathode ray tube (CRT) display, light emitting diode (LED) display, nano-emissive display, or projection display.

5. The system of claim **1**, further comprising an alert module, coupled to the second processing module and configured to provide a visible alert when a predetermined threshold of the real-time data is exceeded, wherein the visible alert comprises changing a color of displayed real-time data on a display of the second display module.

6. The system of claim **1**, wherein the first gateway is configured to receive and transmit the retrospective data according to a predefined priority configuration.

7. The system of claim **1**, wherein the first processing module and the second processing module comprise the same hardware or software processor.

8. The system of claim **1**, wherein at least two of the first processing module, the second processing module, and third processing module provide fault tolerance for each other.

9. The system of claim **1**, further comprising a fourth display module configured to provide fault tolerance for each of the first display module, the second display module, and third display module.

10. The system of claim **1**, wherein the report data comprises a patient surgery record.

11. The system of claim **1**, wherein the vital sign data comprises at least one of a heart rate, a respiratory rate, a blood pressure, and or a body temperature.

12. The system of claim **1**, further comprising:

a second gateway that receives the real-time data from a server and transmits the real-time data to the data storage module; and

a third gateway that receives the postoperative data and transmits the postoperative data to the data storage module.

13. The system of claim **12**, wherein each of the first gateway, the second gateway, and the third gateway provide fault tolerance for each other.

14. The system of claim **12**, wherein the first gateway, the second gateway, and the third gateway constitute the same node on a computer network.

15. The system of claim **1**, further comprising:

an imaging server;

wherein the first processing module receives the retrospective data from the imaging server; and

wherein the retrospective data comprises imaging data.

16. The system of claim **15**, wherein the imaging server comprises a picture archiving and communications system (PACS) server.

17. The system of claim **1**, wherein the real-time data further comprises at least one of electromyogram (EMG) data, imaging data, computed tomography (CT), magnetic resonance image (MRI) data, ultrasound data, C-Arm image data, fluoroscopy data, or X-Ray data.

18. A surgical data monitoring and display system for use in an operating room or another patient care room, comprising:

a data storage module that stores real-time data concerning a patient;

a first processing module that receives the real-time data, processes the real-time data into processed real-time data, and transmits the processed real-time data to a first

display module before or during performance of a medical or surgical procedure on the patient by a healthcare provider; and

the first display module, which displays the processed real-time data;

wherein the real-time data concerning the patient comprises at least two of the following: electrocardiographic data, electroencephalographic data, pulse oximetry data videoscopic data, and vital sign data;

wherein the real-time data is acquired during performance of the medical or surgical procedure on the patient; and

wherein the first display module is positionable in the operating room or another patient care room such that they are viewable by the healthcare provider during the performance by the healthcare provider of the medical or surgical procedure on the patient;

a second processing module configured to receive postoperative data,

retrospective data, and the real-time data, and further configured to process at least one of the postoperative data, the retrospective data, and or the real-time data into report data; and

a second display module, which displays the report data;

an alert module, coupled to the first processing module and configured to provide, on a single display, a visible alert when a predetermined threshold of the real-time data is exceeded;

wherein the visible alert comprises at least one of:

moving displayed real-time data from a first location, less prominent on a display of the first display module to the healthcare provider, to a second location, more prominent on the display of the first display module to the healthcare provider while maintaining display of the report data on the second display module to be visible to the health care provider; and

enlarging a display of a first set of the processed real-time data, displayed at a first, smaller size on a display of the first display module, to a second, larger size on the display of the first display module while maintaining display of the report data on the second display module to be visible to the health care provider;

wherein the first set of the processed real-time data comprises at least one of electrocardiographic data, electroencephalographic data, pulse oximetry data, videoscopic data, and or vital sign data;

wherein the display of the first display module further displays a second set of the processed real-time data adjacent to the display of the first set of the processed real-time data, the second set of the processed real-time data comprising at least one of electrocardiographic data, electroencephalographic data, pulse oximetry data, videoscopic data, and or vital sign data; and

wherein when the display of the first set of the processed real-time data is enlarged to the second, larger size on the display of the first display module, (i) the display of the first set of the processed real-time data overlaps the display of the second set of the processed real-time data, and/or (ii) the display of the second set of the processed real-time data is reduced in size.

19. The system of claim **18**, further comprising:

a third processing module that receives the retrospective data, processes the retrospective data into processed retrospective data, and transmits the processed retrospective data to a third display module before or during performance of the medical or surgical procedure on the patient by the healthcare provider;

the third display module, which displays the processed retrospective data; and

a third gateway that receives the retrospective data from a server and transmits the retrospective data to the data storage module.

20. The system of claim **19**, wherein at least one of the first display module, the second display module, or the third display module comprises a plasma display, liquid crystal display (LCD), nanocrystal display, three-dimensional (3D) display, cathode ray tube (CRT) display, light emitting diode (LED) display, nano-emissive display, and projection display.

21. The system of claim **19**, wherein the third gateway is configured to receive and transmit the retrospective data according to a predefined priority configuration.

22. The system of claim **19**, wherein the first processing module, the second processing module, and the third processing module comprise the same hardware or software processor.

23. The system of claim **19**, wherein at least two of the first processing module, the second processing module, and third processing module provide fault tolerance for each other.

24. The system of claim **19**, further comprising a fourth display module configured to provide fault tolerance for each of the first display module, the second display module, and third display module.

25. The system of claim **19**, wherein the report data comprises a patient surgery record.

26. The system of claim **18**, wherein the vital sign data comprises at least one of a heart rate, a respiratory rate, a blood pressure, or a body temperature.

27. The system of claim **19**, further comprising:

a second gateway that receives the postoperative data and transmits the postoperative data to the data storage module; and

a third gateway that receives the real-time data from a server and transmits the real-time data to the data storage module.

28. The system of claim **27**, wherein each of the first gateway, the second gateway, and the third gateway provide fault tolerance for each other.

29. The system of claim **27**, wherein the first gateway, the second gateway, and the third gateway constitute the same node on a computer network.

30. The system of claim **19**, further comprising:

an imaging server;

wherein the third processing module receives the retrospective data from the imaging server; and

wherein the retrospective data comprises imaging data.

31. The system of claim **30**, wherein the imaging server comprises a picture archiving and communications system (PACS) server.

32. The system of claim **18**, wherein the real-time data further comprises at least one of electromyogram (EMG) data, imaging data, computed tomography (CT), magnetic resonance image (MRI) data, ultrasound data, C-Arm image data, fluoroscopy data, or X-Ray data.

* * * * *